

**Aus dem Institut für Molekularbiologie und Tumorforschung
Leiter: Prof. Dr. R. Müller**

des Fachbereichs Medizin der Philipps-Universität Marburg

**in Zusammenarbeit mit dem Max-Planck-Institut für biophysikalische Chemie in Göttingen
Geschäftsführender Direktor: Prof. Dr. Christian Griesinger**

Investigating the Assembly of Ribonucleoprotein complexes (RNPs)

Inaugural Dissertation

zur Erlangung des Doktorgrades der Humanbiologie
dem Fachbereich Medizin der Philipps-Universität Marburg
vorgelegt von

Annemarie Schultz
aus Bremen

Marburg 2007

Angenommen vom Fachbereich Medizin der Philipps-Universität
Marburg am: 20.07.2007

Gedruckt mit Genehmigung des Fachbereichs.

Dekan: Prof. Dr. B. Maisch

Referent: Prof. Dr. R. Lührmann

1. Korreferent: PD Dr. Heike Krebber

Für Lenie und Christopher

I. Table of Contents

I.	TABLE OF CONTENTS	I
II.	TABLE OF FIGURES.....	IV
III.	INDEX OF TABLES	VI
1.	SUMMARY	1
1.1.	Summary	1
1.2.	Zusammenfassung	2
2.	INTRODUCTION	5
2.1.	Spliceosomal snRNPs	5
2.1.1.	The spliceosome cycle	7
2.1.2.	The spliceosomal U4/U6.U5 tri-snRNP	10
2.1.3.	Assembly of the tri-snRNP	15
2.1.4.	U4/U6.U5 tri-snRNP proteins and retinitis pigmentosa	16
2.2.	Small nucleolar RNPs (snoRNPs)	17
2.2.1.	Pre-rRNA processing	17
2.2.2.	Small nucleolar RNP are involved in pre-rRNA processing	19
2.2.3.	Structure and function of the box C/D snoRNPs	20
2.3.	Similarities between the U4/U6 snRNP and box C/D snoRNPs	23
2.4.	Aim of the work presented in this dissertation.....	28
3.	MATERIALS AND METHODS	30
3.1.	Materials	30
3.1.1.	Fine Chemicals.....	30
3.1.2.	Markers	32
3.1.3.	Radio Chemicals	32
3.1.4.	Enzymes und Inhibitors	32
3.1.5.	Used Organisms.....	33
3.1.6.	Plasmids and Vectors.....	33
3.1.7.	Antibodies.....	34
3.1.8.	Reaction Sets (Kits).....	35
3.1.9.	Chromatography Columns und Column Materials	35
3.1.10.	Antibiotics	36
3.1.11.	Miscellaneous Material	36
3.1.12.	Devices.....	36
3.1.13.	DNA Oligonucleotides	38
3.1.14.	RNA Oligonucleotides	40

3.1.15.	siRNAs	41
3.1.16.	Peptide sequences.....	42
3.1.17.	Common Buffers	42
3.2.	Methods	43
3.2.1.	Standard Molecular Biological Methods.....	43
3.2.2.	Protein Biochemical Methods.....	55
3.2.3.	Immunological Methods	59
3.2.4.	Microbiological Methods.....	62
3.2.5.	Cell Culture	65
3.2.6.	Microscopic Methods	68
3.2.7.	Special Methods.....	72
4.	RESULTS	78
4.1.	Protein-protein and protein-RNA contacts both contribute to the 15.5K protein-mediated assembly of the U4/U6 snRNP and the box C/D snoRNPs	78
4.1.1.	Mutation of conserved amino acids on the surface of protein 15.5K not involved in RNA binding	78
4.1.2.	Conserved amino acids on the surface of protein 15.5K are required for hPrp31 association with the U4 snRNA.....	82
4.1.3.	Numerous mutations on the surface of protein 15.5K disrupt the binding of the CYPH/hPrp4/hPrp3 complex to U4/U6 snRNA	83
4.1.4.	Box C/D snoRNP assembly requires multiple regions on the surface of protein 15.5K.....	85
4.1.5.	Alpha helix 4 of protein 15.5K is required for hU3–55K binding to the U3 snoRNA	87
4.1.6.	A direct interaction between proteins hU3–55K and 15.5K.....	88
4.2.	Protein 15.5K is located in nucleoplasmic foci and is associated with the U4/U6 di–snRNP and the U3 snoRNA <i>in vivo</i>	90
4.2.1.	The U4/U6 di–snRNP and box C/D snoRNP-associated protein 15.5K localises to nucleoplasmic foci	90
4.2.2.	EYFP–15.5K fusion protein <i>in vivo</i> is complexed specifically with the same RNA targets that protein 15.5K was shown to bind directly <i>in vitro</i>	96
4.3.	Association of the spliceosomal hPrp31 protein with the U4 snRNP: Requirement for U4 snRNA's kink-turn stem II and the Nop domain	99
4.3.1.	Hydroxyl-radical footprinting reveals direct contact of protein hPrp31 with various regions of the U4 snRNA	99
4.3.2.	Protein hPrp31 requires stem I and stem II of the 5' stem-loop of U4 for binding	102
4.3.3.	The Nop domain is necessary and sufficient for 15.5K-dependent hPrp31 binding to U4 snRNA	108
4.4.	Mutations associated with retinitis pigmentosa in the U4/U6-specific protein hPrp31.....	111
4.4.1.	Cellular localisation of wild-type and mutant hPrp31 in transfected HeLa cells.....	111
4.4.2.	Mutant hPrp31 A216P is incorporated into the tri–snRNP and interacts with the U5 snRNP-specific hPrp6 protein	116
5.	DISCUSSION.....	119
5.1.	Regions on the 15.5K protein surface are required for complete U4/U6 di–snRNP and box C/D snoRNP assembly.....	119
5.1.1.	Observed effects on complex assembly are specific, due to changes on the 15.5K surface	119
5.1.2.	Differential recognition of the distinct RNAs and protein 15.5K	120

5.1.3.	Influence of conserved amino acids on the 15.5K surface on the association of the U4/U6di–snRNP specific proteins hPrp31 and CypH/hPrp4/hPrp3	120
5.1.4.	Two or more components are involved in box C/D snoRNP assembly on the 15.5K protein–box C/D snoRNA complex	121
5.1.5.	Direct protein–protein interactions are involved in RNP complex formation in the box B/C snoRNP	122
5.1.6.	The eukaryotic proteins L7a, 15.5K, and NHP2 are probably derived from a common ancestor	123
5.2.	The U4/U6 di–snRNP and box C/D snoRNP-associated protein 15.5K localise to nucleoplasmic foci	124
5.3.	Requirement for U4 snRNA's kink-turn stem II and the Nop domain for the association of the spliceosomal hPrp31 protein with the U4 snRNP	125
5.3.1.	Global RNA shielding by hPrp31 of the U4 snRNA in the ternary hPrp31-15.5K-U4 snRNA complex	126
5.3.2.	RNA structural requirements for binding of hPrp31 to the 15.5K protein–U4 snRNA binary complex	128
5.3.3.	Different and shared binding requirements between hPrp31 and the box C/D snoRNP proteins NOP56 and NOP58	132
5.3.4.	The hPrp31 Nop domain is necessary and sufficient for hPrp31 binding to the U4 snRNA-15.5K binary complex	133
5.4.	Analysis of retinitis pigmentosa causing mutations in the U4/U6 specific hPrp31 protein on cellular localisation and tri-snRNP formation	134
5.5.	Future Prospects	136
6.	REFERENCES	138

II. Table of Figures

Figure 2-1 Schematic depiction of the two-step transesterification splicing reaction.	6
Figure 2-2 Schematic depiction of the spliceosome assembly.	8
Figure 2-3 Proposed mechanism for disruption of U4/U6 di–snRNA base-pairing during activation of the spliceosome.	9
Figure 2-4 Postulated secondary structure of the single U4 and U6 snRNA and the base-paired U4/U6 di–snRNA.	11
Figure 2-5 Schematic representation of hPrp31 and the box C/D snoRNP-core proteins NOP56 and NOP58.	13
Figure 2-6 Schematic representation of the assembly of the U4/U6.U5 tri-snRNP.	16
Figure 2-7 Schematic representation of hPrp31 mutations A194E and A216P.	17
Figure 2-8 Schematic representation of pre-rRNA processing in human.	18
Figure 2-9 Structure and function of the box C/D snoRNAs.	21
Figure 2-10 Crystal structure of the kink-turn motif present in the 5' stem-loop of the U4 snRNA.	23
Figure 2-11 Crystal structure of the 15.5K protein bound to the 5' stem-loop of the U4 snRNA.	24
Figure 2-12 The box C/D and box B/C motifs of snoRNAs.	26
Figure 2-13 Schematic representation of box C/D and box B/C snoRNP assembly.	27
Figure 4-1 Sequence alignment of the human 15.5K protein with highly homologous proteins.	78
Figure 4-2 Conserved amino acids present at the surface of the protein were identified and mutated.	79
Figure 4-3 Mutations indicated in the 15.5K-U4 crystal structure.	80
Figure 4-4 RNA-binding by soluble mutants of protein 15.5K.	81
Figure 4-5 Binding of hPrp31 to the U4 snRNA requires residues in alpha helix 3 of 15.5K.	83
Figure 4-6 Association of CypH/hPrp4/hPrp3 to the U4/U6 snRNA requires several regions on the surface of 15.5K.	85
Figure 4-7 Several regions on the surface of protein 15.5K are required for box C/D snoRNP assembly.	86
Figure 4-8. hU3–55K binding to the U3 box B/C motif requires a distinct region on the surface of protein 15.5K.	88
Figure 4-9 Mutant 15.5K-3 inhibits the binding of hU3–55K to the U3 box B/C in the absence of the corresponding RNA.	89
Figure 4-10 The 15.5K protein is localised in nucleoli, Cajal bodies and splicing speckles.	91
Figure 4-11 Cellular localisation of YFP-tagged 15.5K mutants analysed by co-staining of splicing factor SC35.	93
Figure 4-12 Cellular localisation of YFP-tagged 15.5K mutants analysed by co-staining of protein NOP56.	94
Figure 4-13 Cellular localisation of YFP-tagged 15.5K mutants analysed by co-staining Cajal body marker protein coilin.	95
Figure 4-14 Western blot analysing the expression level of YFP-15.5K-1 to 15.5K-5 in HeLa cells.	96
Figure 4-15 HeLa cell line stably expressing EYFP–15.5K.	97
Figure 4-16 <i>In vivo</i> RNA-binding by EYFP–15.5K.	98
Figure 4-17 <i>In vivo</i> RNP-binding of EYFP–15.5K.	99
Figure 4-18 Protein hPrp31 binds directly to U4 snRNA.	101
Figure 4-19 Binding of hPrp31 to the U4 snRNP requires the complete stems I and II of the 5' stem-loop of the U4 snRNA.	104
Figure 4-20 Binding of hPrp31 to the U4 snRNP does not depend on sequence and structure of the terminal penta-loop.	105
Figure 4-21 Elongation of stem II is critical for hPrp31 binding to the U4 snRNP.	106
Figure 4-22 Delineation of hPrp31 Nop domain.	110
Figure 4-23 The Nop domain is necessary and sufficient for binding of hPrp31 to the U4 snRNP.	111
Figure 4-24 Knock-down of spliceosomal hPrp31 protein by siRNAs.	113
Figure 4-25 Expression of HA-hPrp31 (wild-type and mutants) in HeLa cells depleted of the endogenous hPrp31.	115
Figure 4-26 hPrp31 A216P is incorporated into the tri-snRNP and interacts with the U5 protein hPrp6.	118
Figure 5-1 Model summarizing required sites in the U14 Box C/D snoRNA–15.5K binary complex.	122
Figure 5-2 Sequence alignment of the eukaryotic 15.5K protein with the archaeal ribosomal L7a protein.	123

Figure 5-3 Model demonstrating contacted sites of hPrp31 in the U4 snRNA-15.5K binary complex.	128
Figure 5-4 Secondary structure of the U4 or U4atac snRNA 5' stem-loops for selected organisms.	131
Figure 5-5 Schematic representation of the U4/U6 snRNA and U14 box C/D snoRNA.	132

III. Index of Tables

Table 2-1 Protein composition of the U4/U6.U5 tri-snRNP (modified from Kastner (1998))	12
Table 2-2 Proteins associating with the box C/D and Box B/C RNPs.	22

1. Summary

1.1. Summary

Eukaryotic cells contain numerous small nuclear ribonucleoproteins (RNPs) that function in different RNA-processing events in the nucleus. The spliceosomal U1, U2, U5 and U4/U6 snRNPs (small nuclear RNPs) make up one class of complexes that are catalysing a well defined process called pre-mRNA splicing. Pre-mRNA splicing is the process by which non-coding regions (introns) are removed from pre-mRNA transcripts and the protein coding elements (exons) assembled into mature mRNAs before the RNA leaves the nucleus. Another class comprises the box C/D snoRNPs (small nucleolar RNPs) that are involved in processing of the ribosomal RNA (rRNA) in the nucleolus. These complexes function as guides in the site-specific 2'-O-methylation of riboses in the precursor rRNA as well as assisting in rRNA biogenesis.

Though the above-named U4/U6 snRNP and the box C/D snoRNP complexes are distinct in both composition and function, they share a similar RNA component and protein composition. Their RNA component can form a so called kink-turn (k-turn) motif (in the U4 5' stem-loop and box C/D and B/C motif in box C/D snoRNAs), which is bound by a 15.5 kilodalton protein (15.5K).

Besides protein 15.5K, the U4/U6 snRNP and the box C/D snoRNP complexes possess several complex-specific proteins. In addition to seven Sm and seven LSm proteins that bind the Sm site of the U4 snRNA and the 3' end of U6 snRNA respectively, four proteins have been found to be associated with the human U4/U6 snRNP. These include the hPrp31 protein (also called 61K) and three proteins with molecular weights of 20, 60 and 90 kDa that form a biochemically stable, hCypH/hPrp4/hPrp3 (also 20/60/90K) protein complex. As well the box C/D snoRNPs are associated with a number of complex-specific proteins, which practically perform processing of the rRNA. The box C/D snoRNPs, like the U8 and U14 box C/D snoRNA, have been shown to bind proteins NOP56, NOP58, TIP48, TIP49 and fibrillarin. Lastly, the 15.5K protein and the hU3-55K protein belong to the complex assembled on the U3-box B/C motif of the U3 box C/D snoRNA.

The assembly of the RNP complexes is a multiple-stage process that is initiated by 15.5K protein binding to the respective k-turn motif. Protein 15.5K is unique in that it is essential for the hierarchical assembly of the above-named three RNP complexes. Protein 15.5K interacts with the cognate RNAs via an induced-fit mechanism, which results in the folding of the surrounding RNA to create binding site(s) for the RNP-specific proteins. It has been shown that protein-RNA interactions are essential for the binding of complex-specific proteins to the U4/U6 snRNP, C/D snoRNP, and the RNP complex assembled on the U3-box B/C motif. However, at the beginning of this work it was unknown whether protein 15.5K also mediates RNP formation through direct protein-protein

1 Summary

interactions with the complex-specific proteins. To investigate this possibility, a series of protein 15.5K mutations were created in which the surface properties of the protein had been changed. Within the scope of this work, their ability to support the formation of the three distinct RNP complexes was assessed and the formation of each RNP was found to require a distinct set of regions on the surface of the 15.5K protein. This implies that protein-protein contacts are essential for RNP formation in each complex. Further supporting this idea, direct protein-protein interaction was observed between hU3-55K and 15.5K. In conclusion, the data obtained suggest that the formation of each RNP involves the direct recognition of specific elements in both 15.5K protein and the specific RNA.

The U4/U6 snRNP-specific protein hPrp31 and the box C/D snoRNP-specific proteins NOP56 and NOP58 have been shown to be homologous, sharing a conserved domain, the so-called Nop domain. At the beginning of this work, it was unclear how protein hPrp31 and proteins NOP56/NOP58 assemble specifically onto the U4/U6 snRNP and box C/D snoRNPs, respectively. To address this question, structural requirements for the association of protein hPrp31 with the U4 snRNP *in vitro* were analysed. By employing point and deletion mutants of the U4 snRNA, structural features within the U4 snRNA necessary for binding of protein hPrp31 to the U4/U6 snRNP were determined. The findings indicate that the specificity of hPrp31 binding is provided by stems I and II of the U4 snRNA and suggest a way in which protein hPrp31 and proteins NOP56/NOP58 may specifically assemble onto the U4/U6 snRNP and box C/D snoRNPs, respectively. Furthermore, the results presented here provide evidence that the Nop domain on its own is necessary and sufficient for hPrp31 binding to the U4 snRNP, thus suggesting that this domain may be a novel RNA-binding domain.

Recently it has been shown that protein hPrp31 is also of clinical interest. Two mutations (A194E, A216P) in the human hPrp31 gene (PRPF31) are correlated with the autosomal dominant form of retinitis pigmentosa, a disorder that leads to degeneration of the photoreceptors in the retina of the eye. It has been shown that hPrp31 plays a key role in U4/U6.U5 tri-snRNP formation, which is assumed to take place in Cajal bodies (CBs), subnuclear organelles of animal and plant cells. Nevertheless, it is so far unknown whether the mutations in protein hPrp31 affect the stability of the tri-snRNP. Using fluorescence microscopy and biochemical methods it has been shown here how hPrp31 mutations influence the localisation of protein hPrp31 *in vivo* and how they influence U4/U6.U5 tri-snRNP formation.

1.2. Zusammenfassung

Eukaryotische Zellen enthalten eine Vielzahl kleiner Ribonukleoproteinkomplexe (engl. Ribonucleoproteins, RNPs), die an verschiedenen RNA-Prozessierungsereignissen im Zellkern teilnehmen. Die spleißosomalen U1, U2, U5 und U4/U6 snRNP (engl. small nuclear RNPs) Partikel stellen hierbei eine Gruppe dar und katalysieren in einem definierten und dynamischen Prozess die Spleißreaktion. Bei dieser Reaktion werden die nichtcodierenden Bereiche (Introns) aus der Prä-

mRNA herausgeschnitten und die codierenden Bereiche, die so genannten Exons, zu einer reifen mRNA verknüpft. Eine andere Gruppe wird von den C/D Box snoRNPs (engl. small nucleolar RNPs) des Nukleolus gebildet. Diese steuern die Prozessierung der ribosomalen RNA (rRNA) und sind an der ortsspezifischen 2'-O-Methylierung von Ribosen beteiligt. Obwohl der U4/U6 snRNP Partikel und die C/D Box snoRNPs an unterschiedlichen Prozessen in der Zelle beteiligt sind, teilen sie sowohl eine ähnlich RNA Komponente als auch identische und ähnliche Proteine. Ihre RNA Komponente kann ein so genanntes kink-turn (k-turn) Motiv bilden (in der U4 5' stem-loop; C/D und B/C Box Motiv in den C/D Box snoRNAs), das von dem allen RNPs gemeinsamen 15.5K Protein gebunden wird.

Zusätzlich zu dem 15.5K Protein besitzt der U4/U6 snRNP Partikel und die C/D Box snoRNPs partikelspezifische Proteine. Der spleißosomale U4/U6 snRNP Partikel enthält neben sieben Sm- und sieben Lsm-Proteine, die jeweils mit der Sm-Bindungsstelle der U4 snRNA und dem 3' Ende der U6 snRNA assoziiert sind, vier weitere Proteine. Hierzu zählen das Protein hPrp31 (auch 61K) und drei weitere Proteine mit einem Molekulargewicht von 20, 60 und 90 kDa, welche den heteromeren hCypH/hPrp4/hPrp3 (auch 20/60/90K) Proteinkomplex bilden. Die C/D Box snoRNPs sind ebenfalls mit unterschiedlichen Proteinen assoziiert, welche die eigentliche rRNA Modifikationsreaktion durchführen. Sie besitzen sie die Proteine NOP56, NOP58, TIP48, TIP49 und Fibrillarin, die z.B. an die U8 und U14 C/D Box snoRNA binden. Die Proteine 15.5K und hU3-55K bilden den RNP-Komplex, der sich auf dem U3 C/D Box snoRNA-spezifischen B/C Box Motiv zusammenlagert.

Die Zusammenlagerung der RNPs ist ein mehrstufiger Prozess, der von der Bindung des 15.5K Proteins an das jeweilige kink-turn Motiv initiiert wird. Das 15.5K Protein ist einzigartig in seiner Funktion als Komplexbildner für die hierarchische Zusammenlagerung der drei RNP Komplexe. Es interagiert mit dem verwandten k-turn Motiv über einen „induced-fit“ Mechanismus, der in einer Faltung der umliegenden RNA und der Bildung von Bindungsstellen für die RNP-spezifischen Proteine resultiert. Folglich spielen Protein-RNA Interaktionen, für die Bindung der assoziierten Proteine an den U4/U6 snRNP, den C/D Box snoRNP und den Partikel, der sich auf dem U3-spezifischen B/C Box Motiv zusammenlagert, eine wesentliche Rolle. Ob das 15.5K die RNP Bildung jedoch auch durch direkte Protein-Protein Wechselwirkungen mit den komplexspezifischen Proteinen vermittelt, war zu Beginn der vorliegenden Arbeit unklar. Um dieser Möglichkeit nachzugehen, wurde eine Reihe von Mutationen generiert, bei denen die Oberflächeneigenschaften des 15.5K Proteins verändert wurden. Im Rahmen dieser Arbeit wurde der Effekt der Mutationen auf die Zusammenlagerung der RNPs hin untersucht. Es zeigte sich, dass die Zusammenlagerung der drei untersuchten RNP Partikel eine Reihe verschiedener Regionen auf der 15.5K Oberfläche benötigt. Die dargestellten Ergebnisse legen daher nahe, dass direkte Protein-Protein-Interaktionen zwischen 15.5K und den verschiedenen komplexspezifischen Proteinen von Bedeutung sind. Diese Theorie wird ferner dadurch unterstützt, dass in den Studien eine direkte Interaktion zwischen dem 15.5K Protein und dem B/C Box-assozierten Protein hU3-55K beobachtet werden konnte. Zusammenfassend legen die

1 Summary

gewonnenen Daten nahe, dass die Zusammenlagerung der jeweiligen RNP Partikel eine direkte Erkennung von spezifischen Elementen – sowohl auf der 15.5K Proteinoberfläche als auch spezifischer RNA Elemente –einbezieht.

Bei dem U4/U6-spezifischen Protein hPrp31 und den C/D Box-spezifischen Proteinen NOP56 und NOP58 handelt es sich um homologe Proteine, welche eine konservierte Domäne – die sogenannte Nop-Domäne – gemeinsam haben. Zu Beginn dieser Arbeit war nicht bekannt wie hPrp31 und NOP56/NOP58 spezifisch jeweils an den U4/U6 snRNP und die C/D Box snoRNP Partikel binden können. Um diese Fragestellung zu behandeln, wurden die strukturellen Anforderungen für die Assoziation von Protein hPrp31 an den U4 snRNP Partikel untersucht. Unter Verwendung von U4 snRNA Punkt- und Deletionsmutanten wurden strukturelle Merkmale in der U4 snRNA bestimmt, welche für die Bindung des Proteins hPrp31 and den U4/U6 snRNP Partikel essentiell sind. Die Ergebnisse zeigen, dass die spezifische Bindung von hPrp31 an den U4 snRNP Partikel durch die RNA-Elemente „stem I“ und „stem II“ der U4 snRNA bestimmt wird, und legen einen Weg nahe, durch den hPrp31 und NOP56/NOP58 jeweils spezifisch an den U4/U6 snRNP und C/D Box snoRNP Partikel binden könnten. Die Ergebnisse erbrachten ferner den Nachweis, dass die Nop-Domäne für sich notwendig und darüber hinaus ausreichend für die Bindung des Proteins hPrp31 an den U4 snRNP Partikel ist. Sie legen zudem nahe, dass es sich bei dieser Domäne um eine neuartige RNA-bindende Domäne handelt.

Es konnte kürzlich gezeigt werden, dass das Protein hPrp31 auch von klinischem Interesse ist, da zwei Mutationen (A194E, A216P) im humanen hPrp31 Gen (PRPF31) mit der autosomal dominanten Form der Retinitis Pigmentosa in Zusammenhang gebracht werden konnten. Die Retinitis Pigmentosa ist eine Erkrankung, welche zu einer Degeneration der Photorezeptoren in der Netzhaut (Retina) des Auges führt. Es wurde kürzlich gezeigt, dass Protein hPrp31 eine Schlüsselrolle bei der U4/U6.U5 tri-snRNP Assemblierung spielt, welche vermutlich in den Cajal Bodies (sphärischen Unterorganellen des Nukleus) stattfindet. Dennoch ist bis jetzt unklar, ob die hPrp31 Mutationen die Stabilität des tri-snRNP beeinträchtigen. Unter Verwendung von Fluoreszenzmikroskopie und biochemischen Methoden wird in der vorliegenden Arbeit gezeigt, wie die hPrp31 Mutationen sowohl die *in vivo* Lokalisierung als auch die U4/U6.U5 tri-snRNP Assemblierung beeinflussen.

2. Introduction

Eukaryotic cells contain many types of ribonucleoproteins (RNPs) which are complexes formed by RNA molecules associated with proteins. The majority of these RNPs are in the nucleus and can be classified in two groups, the small nuclear RNPs (snRNPs) that function in the maturation of messenger RNAs (pre-mRNA splicing), and the small nucleolar RNPs (snoRNPs) that reside in the cell nucleolus and are required for maturation of the ribosomal RNAs. Although both types of RNPs function in two different processes it was shown, that the complex assembly of some members of the snRNP and snoRNP family requires similar protein components. The assembly of multiprotein RNPs is complex and commonly involves a hierarchical assembly pathway. As the assembly of spliceosomal snRNPs and that of the snoRNPs are the objects of the work presented here. Current state of knowledge on their function, composition and assembly are reviewed in the following sections.

2.1. Spliceosomal snRNPs

Eukaryotic pre-mRNAs must undergo several post-transcriptional modifications before their export to the cytoplasm as functional mRNAs. Most pre-mRNAs have intervening non-coding sequences (introns) that must be removed, in order to connect precisely the coding sequences (exons), to generate a mature and functional mRNA. The mechanism of this critical processing event – called pre-mRNA splicing – has been studied in detail (reviewed in Brow, 2002). It has now been known for a long time that intron removal and ligation of exons occur through two sequential transesterification steps (Figure 2-1) that are carried out by a megaDalton RNP enzyme known as the spliceosome. Most introns have common consensus sequences near their 5' and 3' ends that are recognized by spliceosomal components and are required for spliceosome formation (5' and 3' splice site). The 5' splice site in higher eukaryotes is represented by the eight-nucleotide long consensus sequence AG/GURAGU. The nucleotides GU on the left always correspond to the beginning of the intron. The area of the 3' splice site is defined by the following three sequence elements (Reed, 1989): (i) the branch point, comprising the consensus sequence YNYURAC in which the adenosine represents the highly conserved branch-point adenosine; (ii) the polypyrimidine tract (Yn), consisting of 10-15 pyrimidines; (iii) the 3' splice site, consisting of the consensus sequence YAG/G. The nucleotides AG represent in this context the end of the intron.

2 Introduction

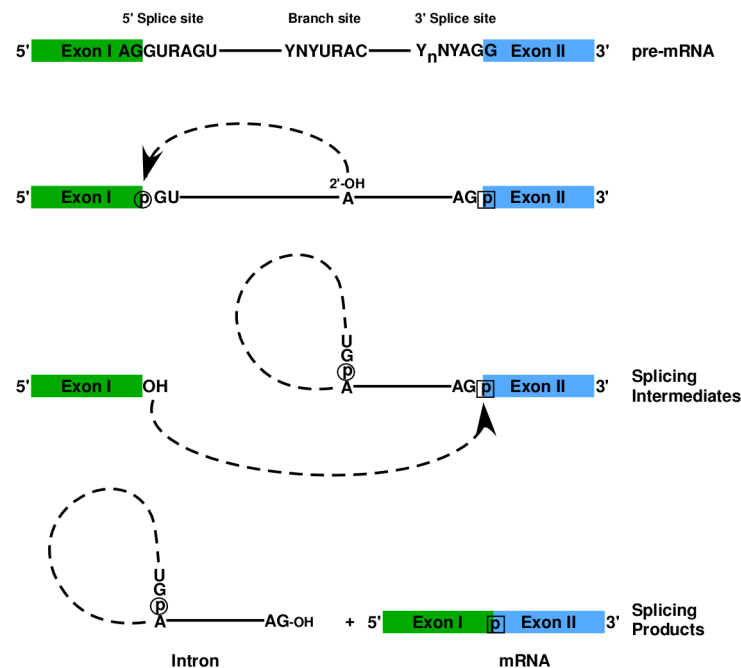


Figure 2-1 Schematic depiction of the two-step transesterification splicing reaction.

In the first step, the 2' hydroxyl group of the conserved adenosine within the branch site attacks the conserved guanine of the 5' splice site at the exon I-intron junction. A 2'-5' phosphodiester bond is made between the two residues, and the junction between exon I and the intron is cleaved. The products are a 2'-5' phosphodiester RNA lariat structure and a free 3'-OH that arises from the upstream exon. In the second step, the 3'-OH end of the released exon I then attacks the phosphodiester bond of the conserved guanine of the 3' splice site at the intron-exon II junction. This reaction liberates the 3'-OH of the intron, resulting in a free lariat and spliced exons. The two-exon sequences are joined together, while the intron sequence is released as a lariat structure. The intron RNA is later degraded in the nucleus.

The assembly of a spliceosome onto a pre-mRNA is an ordered process that involves five uridine-rich RNA molecules, the so-called U snRNAs. U snRNAs are characterized by their small size (between 106 and 187 nucleotides). These are associated with proteins forming small nuclear ribonucleoprotein particles (snRNPs) (Burge, 1999; Brow, 2002; Jurica and Moore, 2003).

These snRNPs associate dynamically with each other and with pre-mRNA substrates through a multitude of RNA-RNA, RNA-protein and protein-protein interactions during spliceosome assembly and splicing catalysis to excise each intron precisely and to join the exons in the correct order in a concerted action.

At present, two distinct spliceosomes have been identified (reviewed by Padgett and Shukla (2002) and Will and Lührmann (2005)). The large majority of introns are called U2-dependent introns and are spliced by the U1, U2, U4, U5 and U6 snRNPs, which form the major spliceosome. A further, minor class of introns has been identified in eukaryotes, including *Arabidopsis*, *Drosophila*, *Xenopus*, mouse and humans (Burge, 1999). This class of

introns was initially identified by their unusual intron termini which consisted of dinucleotides AT–AC at their 5' and 3' ends. For this reason, they were originally referred to as ATAC introns. These introns were later found to be spliced by a group of less abundant snRNPs including U11, U12, U5 and U4atac/U6atac, which form the minor spliceosome, and an unknown number of non–snRNP proteins (Hall and Padgett, 1996; Tarn and Steitz, 1996; Tarn and Steitz, 1996). Thus, of the main spliceosomal subunits (i.e. the snRNPs), only the U5 snRNP is common to the two spliceosomes.

As the major spliceosomal snRNPs, the minor spliceosomal snRNPs interact stepwise and in a highly ordered manner with the pre–mRNA.

2.1.1. The spliceosome cycle

The splicing reaction is a co-ordinated, dynamic process including the stepwise assembly of a spliceosome on the pre–mRNA, the splicing catalysis as well as the subsequent dissociation and recycling of splicing factors (Nilsen, 1998; Staley and Guthrie, 1998; Burge, 1999). The stepwise assembly of the spliceosome involves the co-ordinated binding of pre-assembled U snRNPs and numerous non–U snRNP splice factors onto the pre–mRNA (Figure 2-2).

The first step includes the recognition of the 5' splice site by the 5' end of the U1 snRNP through base pairing with the intronic sequences of the pre–mRNA, initiating thus the early (E) complex formation. This initial step does not require energy (ATP) for formation. U1 is the only component that can bind in the absence of ATP, and its interaction with the pre–mRNA is in general required for the other snRNPs to bind. After the association of the U1 snRNP with the 5' splice site, the U2 snRNP recognizes and binds to the branch point to form complex A. Addition of the U2 snRNP is the first energy-dependent step in the splicing pathway. Binding of U2 snRNP is mediated in part by U1 snRNP, as well as additional non–snRNP factors that bridge the two components. The U4/U6 di–snRNP, in turn, associates with the U5 snRNP and thus the 25S U4/U6·U5 tri–snRNP is formed, which is then integrated into the spliceosome to form complex B. In the subsequent steps, a base-paired region is formed between the U6 snRNA and the U2 snRNA, which leads to the formation of the catalytically active centre (Staley and Guthrie, 1998; Brow, 2002; Nilsen, 2003) (Figure 2-3). During the rearrangement of the fully assembled spliceosome to a catalytically active machine, the intermolecular base pairing between the U4 and U6 snRNAs becomes disrupted and the U4 snRNP particle is released from the spliceosome. Subsequently, the catalytically active

2 Introduction

spliceosome catalyses the first transesterification reaction which leads to the generation of complex C.

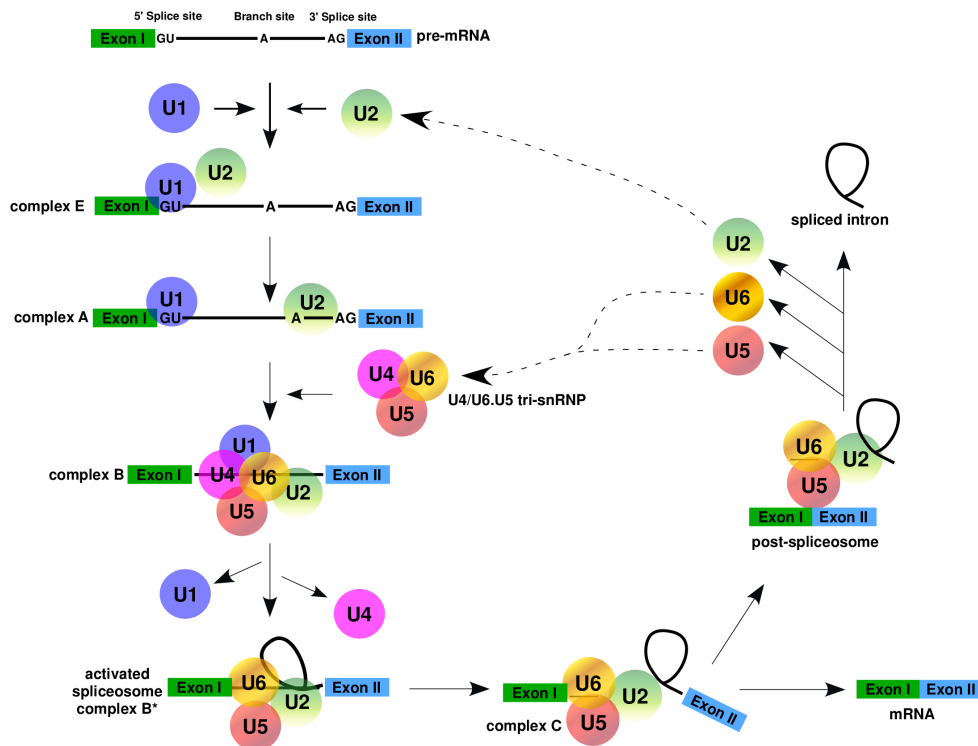


Figure 2-2 Schematic depiction of the spliceosome assembly.

The first step of spliceosome assembly includes the ATP-independent recognition of the 5' splice site by U1 snRNP (E complex). Subsequently, U2 snRNA base pairs with the branch site (A complex). The U4/U6.U5 tri-snRNP binds, giving rise to the B complex. After major RNA-RNA rearrangements, the catalytically activated spliceosome is formed (complex B*). During these rearrangements, the U4 and U6 snRNAs dissociate and the 5' end of U2 enters into base-pairing interactions with U6, forming part of the spliceosomes catalytic core. The activated spliceosome catalyses the first transesterification step of splicing and complex C is formed. After the second step of splicing, the mRNA is released and the post-spliceosomal complex, containing the excised intron and the U2, U5, and U6 snRNPs, dissociates and the snRNPs are then recycled for a new round of splicing (modified from Staley and Guthrie, 1998).

In the course of the splicing reaction, exon I and exon II are linked, generating a mature mRNA, and the intron lariat is released. Following the processing of the pre-mRNA, the spliceosome dissociates, and the snRNPs are recycled for new rounds of splicing (Nilsen, 1998; Staley and Guthrie, 1998).

The U4 and U6 snRNP form a heterodimer through intermolecular base-pairing between the U4 and the U6 snRNA (Bringmann *et al.*, 1984; Hashimoto and Steitz, 1984; Rinke *et al.*, 1985; Brow and Guthrie, 1988). This 13S U4/U6 di-snRNP associates with the 20S U5 snRNP to generate the 25S U4/U6.U5 tri-snRNP particle, which is then integrated into the spliceosome (Black and Pinto, 1989). As the U4/U6 di-snRNP and the U4/U6.U5

tri-snRNP particle are in part object of the presented work, I will focus on this particle in the following sections.

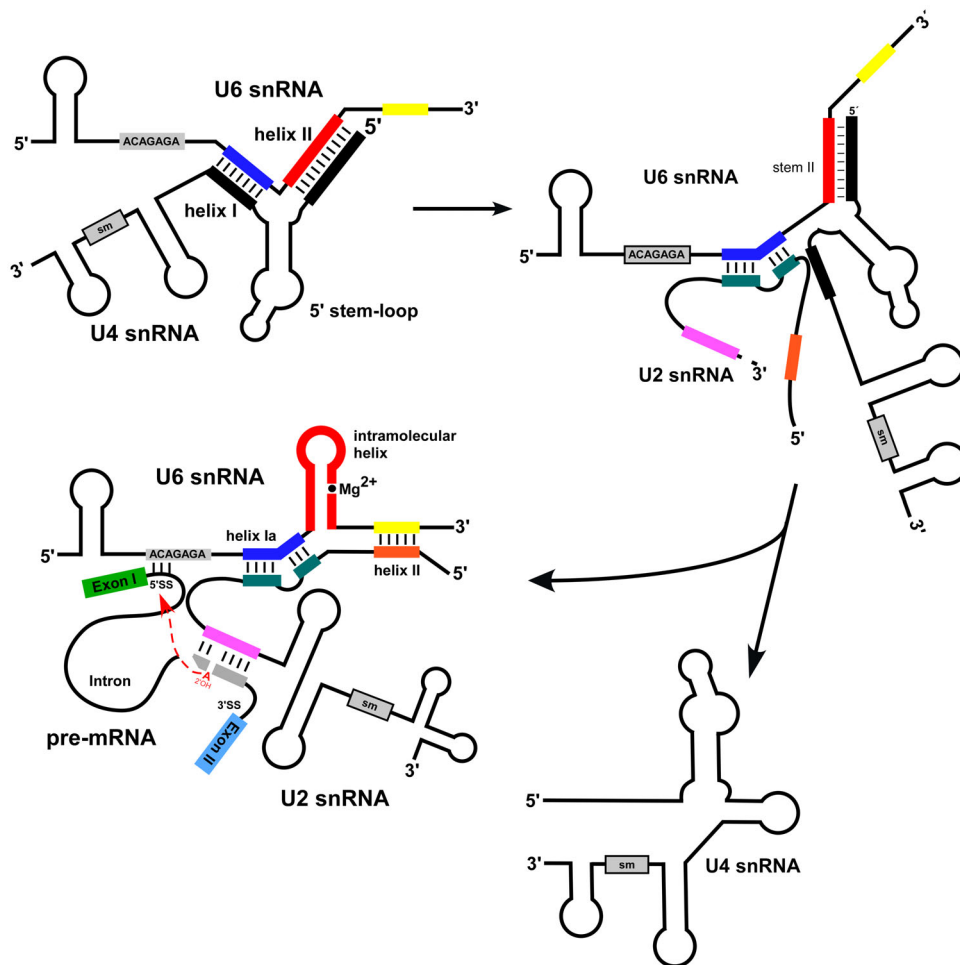


Figure 2-3 Proposed mechanism for disruption of U4/U6 di-snRNA base-pairing during activation of the spliceosome.

Before activation of the spliceosome, the U6 snRNA base-pairs with the U4 snRNA, forming helices I and II of the U4/U6 snRNA duplex. Spliceosome activation is accompanied by the dissociation of U4 snRNA from the U4/U6 duplex, allowing U6 snRNA to pair with U2 snRNA, forming helix Ia, Ib and II. The intramolecular hairpin loop of the U6 snRNA co-ordinates the magnesium ion essential for the first step of splicing catalysis. The pre-mRNA 5' splice site is recognised by the ACAGA box of U6 snRNA before catalysis. The first transesterification step is indicated by the dashed red arrow. The formed network is essential for the structure formation of the catalytically active centre of the spliceosome (Datta and Weiner, 1991; Hausner, 1992; Madhani and Guthrie, 1992; Sun and Manley, 1995). The interaction of the U5 snRNA with the pre-mRNA in the catalytically active centre of the spliceosome is not depicted here for clarity. The U5 snRNP is essentially involved in structural rearrangements of the RNA-RNA network within the spliceosome during its activation.

2.1.2. The spliceosomal U4/U6.U5 tri-snRNP

2.1.2.1. The RNA components of the U4/U6.U5 tri-snRNP

Like the U1 and the U2 snRNA the U4, U5 and the U6 snRNA are characterized by a high content of uracil bases, small size and a phylogenetically conserved primary and secondary structure. The U6 snRNA shows the strongest conservation in sequence and size.

The U4 and U5 snRNA are – like the U1 and U2 snRNA – transcribed by RNA polymerase II and modified at their 5' end by a N⁷-methylguanosine (m⁷G) cap. In the course of U snRNP assembly, which occurs in the cytoplasm, this cap is transformed by hypermethylation into a 2,2,7-trimethyl guanosine (m₃G) cap. The U6 snRNA is an exception: it is transcribed by RNA Polymerase III and carries a γ -monomethylphosphate at its 5' end (Kunkel *et al.*, 1986; Reddy *et al.*, 1987; Brow and Guthrie, 1988; Guthrie and Patterson, 1988; Singh and Reddy, 1989; Tarn and Steitz, 1996).

A group of less abundant snRNPs, U11, U12, U4atac, and U6atac, together with U5, are subunits of the so-called minor spliceosome which catalyses the removal of an untypical class of spliceosomal introns (U12-type) from eukaryotic messenger RNAs in plant, insects, vertebrates and some fungi. The U11, U12 and U4atac/U6atac snRNPs are orthologs of the U1, U2 and U4/U6 snRNPs in the major spliceosome (Hall and Padgett, 1996; Tarn and Steitz, 1996; Kolossova and Padgett, 1997; Yu and Steitz, 1997; Incorvaia and Padgett, 1998). Even though the minor U4atac and U6atac snRNAs are orthologs of U4 and U6, respectively, they share limited sequence homology (~40%). In addition, the sequence of U11 in comparison with U1, as well as U12 compared with U2, are completely unrelated. Even so, the minor U11, U12, U4atac and U6atac snRNAs can be folded into structures similar to U1, U2, U4 and U6, respectively (Tarn and Steitz, 1996).

Moreover, spliceosomal U snRNAs contain post-transcriptionally modified nucleotides that are 2'-O-methylated or pseudouridylated (reviewed in Massenet (1998)). These modifications are made by the small nucleolar RNPs (snoRNPs), the function and composition of which are described in section 2.2. While the U6 snRNA transiently cycles through the nucleolus, the U4 and U5 snRNA are modified like the U1 and U2 snRNA in so-called Cajal bodies, which are located in the nucleoplasm (Ganot *et al.*, 1999; Lange and Gerbi, 2000; Kiss, 2001; Filipowicz and Pogacic, 2002).

Spliceosomal U snRNAs form extensive secondary structures characterised by numerous single- and double-stranded regions and stem-loop structures. Postulated secondary structures are represented in Figure 2-4.

Except for the U6 snRNA, all U snRNAs contain the uridine-rich Sm binding-site (consensus sequence RAU₃₋₆GR), which is essential for the association of the common Sm proteins (Branlant *et al.*, 1982; Jones and Guthrie, 1990; Jarmolowski and Mattaj, 1993; Raker *et al.*, 1996; Raker *et al.*, 1999).

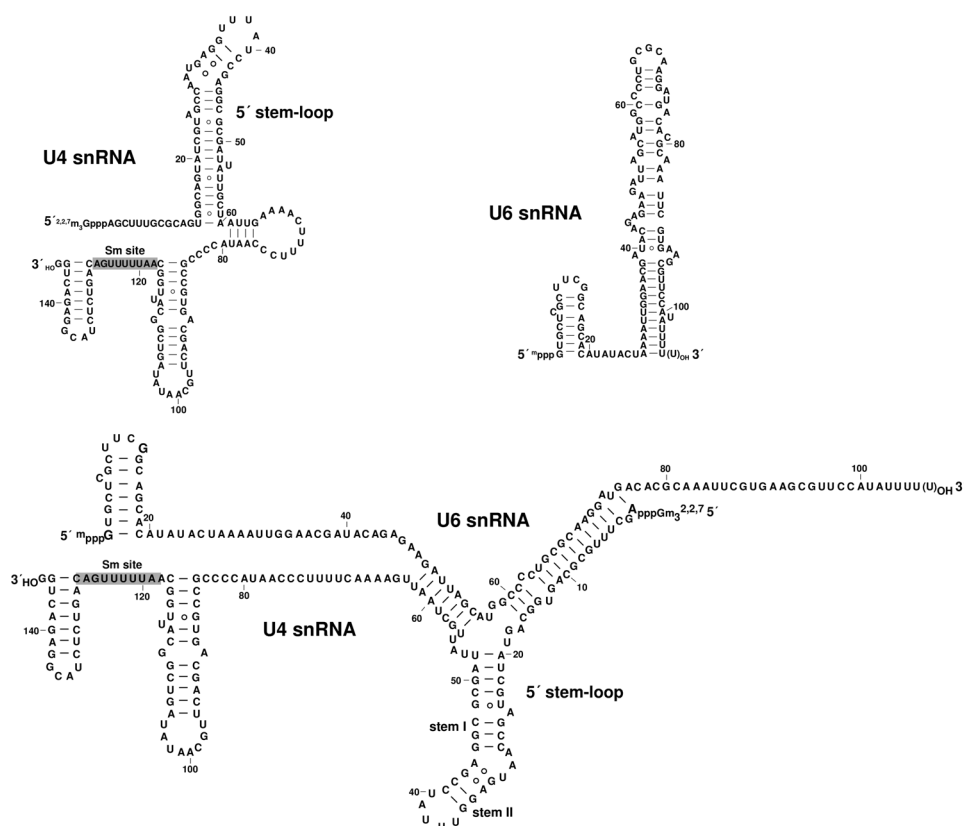


Figure 2-4 Postulated secondary structure of the single U4 and U6 snRNA and the base-paired U4/U6 di-snRNA.

The Sm protein-binding site is depicted by grey shaded capitals. In the U6 snRNA, the Sm consensus sequence is absent (modified from Myslinski and Branlant (1991) and Achsel *et al.* (1999)).

At the beginning of the splicing cycle, (see Figure 2-2) the U4 snRNA and the U6 snRNA are associated firmly with one another by two extended stretches of RNA-RNA base pairs (Figure 2-4). Two intermolecular helices (helix I and helix II) of the U4/U6 snRNA are separated by an intramolecular 5'-terminal hairpin loop (5' stem-loop) of the U4 snRNA (Bringmann *et al.*, 1984; Hashimoto and Steitz, 1984; Rinke *et al.*, 1985; Brow and Guthrie, 1988). Mutational analysis of U4 snRNA in *Xenopus* oocytes and in the HeLa *in vitro* splicing system demonstrated that the 5' stem-loop is essential for spliceosome assembly and pre-mRNA splicing (Vankan *et al.*, 1992; Wersig and Bindereif, 1992). Since the U4 snRNA

2 Introduction

5' stem-loop is not needed for U4/U6 base pairing *in vitro*, it was suggested that it functions in spliceosome assembly at a stage subsequent to U4/U6 snRNP formation (Wersig *et al.*, 1992). The 5' stem-loop of the U4 snRNP can form a conserved stem-internal loop-stem structure (Vidovic *et al.*, 2000). This element is found repeatedly in the high-resolution structures of large and small ribosomal subunits, as well as in the box C/D snoRNAs (see section 2.2.3) and is described in more detail in section 2.3.

2.1.2.2. The protein composition of the U4/U6.U5 tri-snRNP

The protein composition of the major spliceosomal snRNPs has been best characterized in HeLa cells and yeast. Proteins associated with the snRNPs can be subdivided into two classes. The first class consists of the so-called common or Sm proteins, which are tightly associated with all snRNP particles. The second class comprises the particle-specific proteins, which associate with a particular snRNP particle or complex. The protein composition of the U4/U6 di-snRNP, the U5 snRNP, and the U4/U6.U5 tri-snRNP is summarised in Table 2-1 Protein composition of the U4/U6.U5 tri-snRNP (modified from Kastner (1998)).

U snRNP proteins			App. Mw in kDa	13S U4/U6	20S U5	25S U4/U6.U5	Sequence motif
Common proteins	B'/B	Lsm8	29/28	●	●	●	
	D1	Lsm2	16	●	●	●	
	D2	Lsm3	16.5	●	●	●	
	D3	Lsm4	18	●	●	●	
	E	Lsm5	12	●	●	●	
	F	Lsm6	11	●	●	●	
	G	Lsm7	9	●	●	●	
	Specific proteins	U5 snRNP	hPrp8	220		●	●
U5-200K			200		●	●	2 DExH
hSnu114			116		●	●	G-domain
hPrp6			102		●	●	TPR repeat
hPrp28			100		●	●	DEAD/RS
U5-52K			52		●	●	GYF domain
U5-40K			40		●	●	WD40
U5-15K			15		●	●	Thioredoxin fold
U4/U6 snRNP		hPrp3	90	●		●	PWI, DSRM
		hPrp31	61	●		●	Nop domain
		hPrp4	60	●		●	WD40
		CypH	20	●		●	PPlase
		15.5K	15.5	●		●	RNA binding domain
U4/U6.U5 tri-snRNP		110K	110			●	RS
		65K	65			●	RS
	27K	27			●	RS	

Table 2-1 Protein composition of the U4/U6.U5 tri-snRNP (modified from Kastner (1998))

In addition to seven Sm proteins that bind the Sm site of the U4 snRNA, and seven LSm proteins, which are associated with U6 snRNA the 13S U4/U6 snRNP contains five

particle-specific proteins, namely 15.5K, hPrp31 (61K), hPrp3, hPrp4, and hCypH (reviewed in Will and Lührmann (2001)).

The highly conserved protein 15.5K possesses a RNA-binding domain and binds directly to U4 snRNA (Nottrott *et al.*, 1999). It is the first U4/U6-specific protein identified as interacting directly with the U4 snRNA. Protein 15.5K has been shown to be associated with the box C/D snoRNPs. It is unique in its function, as it is essential for the hierarchical assembly of these RNP complexes, which are different in both composition and function. The structure and function of 15.5K within the U4/U6 snRNP and the box C/D snoRNPs is described in more detail in section 2.3.

Protein hPrp31 (*hPrp31*; human pre-mRNA processing factor 31) possesses a so-called Nop domain in its central region, which shows clear homology to a domain of the box C/D snoRNP-associated proteins NOP56 and NOP58 (Gautier *et al.*, 1997; Vithana *et al.*, 2001; Makarova *et al.*, 2002) (see section 2.3 for more detail).

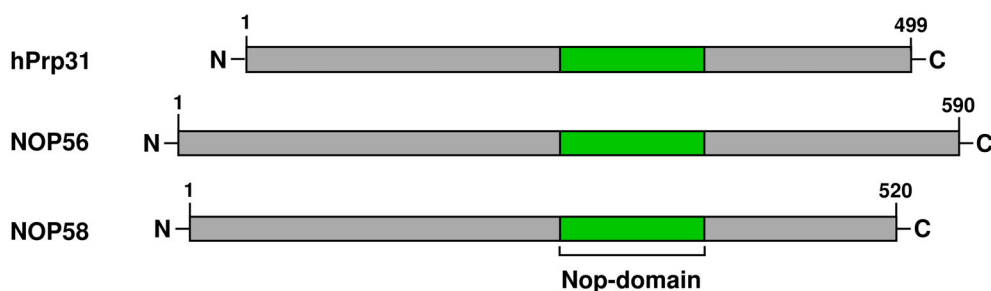


Figure 2-5 Schematic representation of hPrp31 and the box C/D snoRNP-core proteins NOP56 and NOP58.

The homologous Nop domain is indicated in green.

The proteins hCypH, hPrp4, and hPrp3 (or, in the “human” nomenclature, 20K, 60K and 90K) form a biochemically stable, heteromeric complex (Horowitz *et al.*, 1997; Teigelkamp *et al.*, 1998). Protein hCypH belongs to the cyclophilin family of peptidyl-prolyl isomerases, termed cyclophilin H (CypH) (Horowitz *et al.*, 1997; Teigelkamp *et al.*, 1998). The crystal structure of CypH shows a typical cyclophilin fold (Reidt *et al.*, 2000).

Except for the hCypH protein, orthologous proteins termed Snu13p (15.5K in human), Prp4, Prp3 and hPrp31 are also associated with the yeast U4/U6 snRNP particle (Banroques and Abelson, 1989; Petersen-Bjorn *et al.*, 1989; Anthony *et al.*, 1997; Weidenhammer *et al.*, 1997; Gottschalk *et al.*, 1999; Stevens and Abelson, 1999). Like their human counterparts, Prp4 and Prp3 bind directly to each other (Wang *et al.*, 1997; Ayadi *et al.*, 1998; Gonzalez-Santos *et al.*, 2002). The p110 (SART3) protein is required for recycling of the U4/U6 snRNP

2 Introduction

from single U4 and U6 snRNPs and associates only transiently with U6 and U4/U6 (Bell *et al.*, 2002).

Interestingly, recent biochemical evidence has indicated that the U4/U6 snRNP-specific proteins are also associated with the HeLa U4atac/U6atac snRNP of the minor spliceosome (Schneider *et al.*, 2002). The part played by the U4/U6 snRNP-specific proteins in spliceosome assembly and activation is not yet entirely understood. Therefore, further analysis of the function of each protein is required.

One part of the tri-snRNP is the U5 snRNP which is essentially involved in structural rearrangements of the RNA-RNA network within the spliceosome during its activation (see Figure 2-2). The 20S U5 snRNP possesses, in addition to the seven common Sm proteins, a total of eight particle-specific proteins, referred to as U5-15K, U5-40K, U5-52K, hPrp28 (100K), hPrp6 (102K), hSnu114 (116K), U5-200K and hPrp8 (220K) proteins (Bach *et al.*, 1989; Will *et al.*, 1993).

Most of the U5-specific proteins display significant domain features, and play central roles in the splicing machinery (reviewed in Will and Lührmann (1997)). For example, protein U5-200K (in yeast Brr2p) and hPrp28 (in yeast Prp28p) contain the RNA helicase domain (Lauber *et al.*, 1996; Teigelkamp *et al.*, 1997). Protein hSnu114 (in yeast Snu114p) is the sole GTPase identified in the spliceosome to date and is related to translation elongation factor EF-2 (Fabrizio *et al.*, 1997; Stevens *et al.*, 2001; Jurica and Moore, 2003).

By cross-linking experiments it has been demonstrated that only a few proteins are in direct contact with the U5 snRNA in the reconstituted yeast U5 snRNP (Dix *et al.*, 1998). Some additional data further support the observation that U5 snRNP formation is mainly based upon protein-protein interactions. For example, the U5-hPrp6 protein does not bind to either U5 snRNA or the U5 core snRNP when this contains only U5 snRNA and Sm proteins; instead, it binds stably to the 20S U5 snRNP. This result suggested that one or more of the U5-specific proteins are required for the association of the protein hPrp6 (Makarov *et al.*, 2000). Protein hPrp6 contains several 34-amino-acid TPR motifs. TPR domains supply a structural unit of two antiparallel α -helices, building a platform for specific protein-protein interactions (reviewed in Blatch and Lassle (1999)). Interestingly, it was demonstrated by yeast two-hybrid studies that hPrp6 interacts directly with the U4/U6 di-snRNP-specific hPrp31 protein and, through this, connects the U4/U6 di-snRNP and the U5 snRNP (Makarova *et al.*, 2002).

2.1.3. Assembly of the tri-snRNP

Assembly studies *in vitro* have shown that both the U4/U6-specific hPrp31 protein and the heterotrimeric hCypH/hPrp4/hPrp3 protein complex do not bind on their own to the U4/U6 di-snRNP (Nottrott *et al.*, 2002). In both cases, the 15.5K protein must bind first to the k-turn motif of the 5' stem-loop of the U4 snRNA. Protein 15.5K thus functions as a nucleation factor, inducing a hierarchical assembly of the U4/U6 di-snRNP (Figure 2-6). However, hPrp31 and hCypH/hPrp4/hPrp3 bind independently of one another. The situation just described for the U4/U6 di-snRNP particle is the same for the binding of hPrp31 to the alternative U4atac/U6atac snRNAs (Schneider *et al.*, 2002).

A key part in maintaining the stability of the tri-snRNP and in its formation from the U4/U6 di-snRNP and the U5 snRNP is played by the U4/U6-specific protein hPrp31, as demonstrated *in vitro*. Studies with HeLa nuclear extract depleted of hPrp31 showed that hPrp31 is essential for the splicing of pre-mRNA and for the formation of the human tri-snRNP particle (Makarova *et al.*, 2002). Protein hPrp31 performs a dual function in the tri-snRNP particle. On the one hand, hPrp31 binds to the U4 snRNP in the U4/U6 di-snRNP (Nottrott *et al.*, 2002). On the other hand, hPrp31 forms a bridge between the U4/U6 di-snRNP and the U5 snRNP by binding to the U5-specific protein hPrp6 (Makarova *et al.*, 2002). The importance of the bridging function of hPrp31 between the U4/U6 di-snRNP and the U5 snRNP particle is also supported by the observation that, in the course of the catalytic activation of the spliceosome, the association of the U4 snRNP with the U6 snRNP on the one hand and the U5 snRNP on the other hand is weakened and the hPrp31 dissociates along with the U4 snRNP (Makarov *et al.*, 2002).

In order to restore the tri-snRNP so that it can participate in another round of splicing, the U4/U6 duplex must be reformed (Raghuathan and Guthrie, 1998). The human protein p110 (hPrp24 in yeast) has been found to be a U4/U6-recycling factor and a specific component of the U4/U6 di-snRNP (see Table 2-1) (Bell *et al.*, 2002).

The assembly of the tri-snRNP probably takes place in the Cajal bodies, which are subnuclear organelles of animal and plant cells, and which have been proposed to be involved in the assembly and maturation of snRNPs. It has been shown that after knock-down of the U4/U6-specific hPrp31 or the U5-specific hPrp6 protein in HeLa cells, tri-snRNP formation is inhibited, U4/U6 di-snRNPs containing U4/U6 proteins accumulate in Cajal bodies and the U5 snRNPs remained largely in nucleoplasmic speckles (Schaffert *et al.*, 2004).

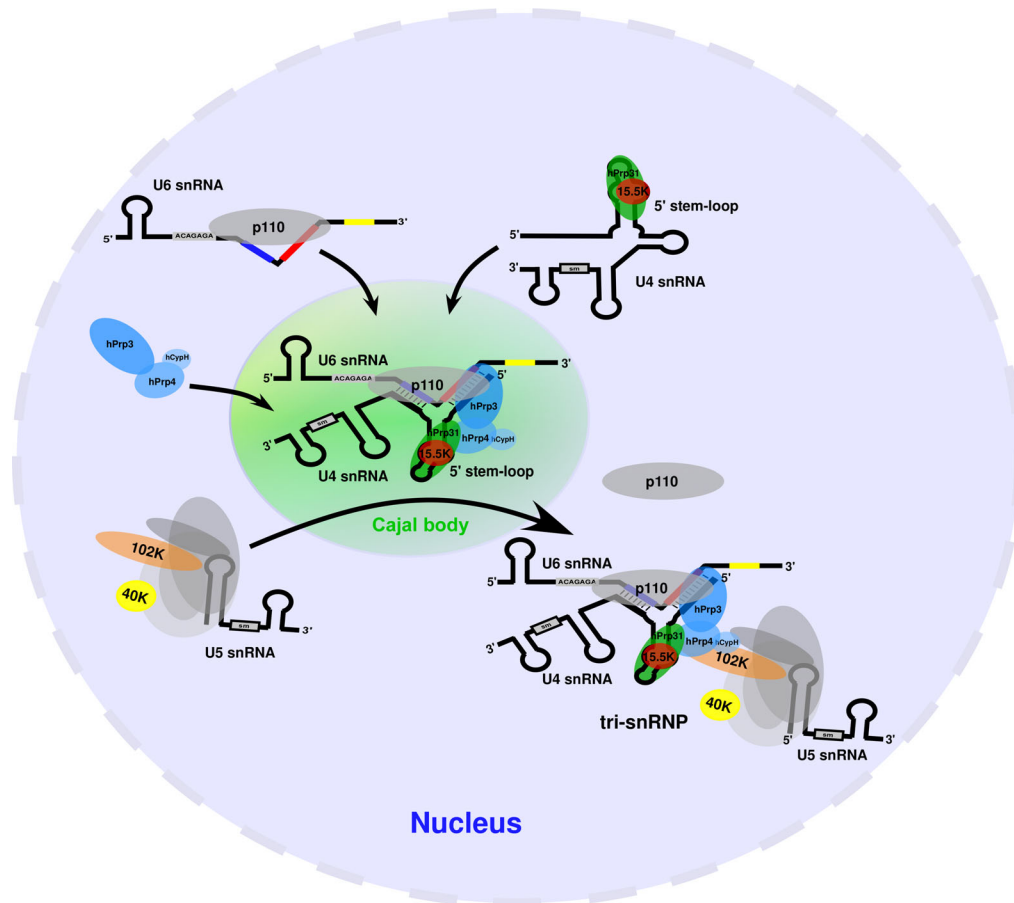


Figure 2-6 Schematic representation of the assembly of the U4/U6.U5 tri-snRNP.

The hierarchical assembly pathway of the U4/U6.U5 tri-snRNP is initiated by the 15.5K protein. The 15.5K protein binds to the kink-turn motif of the U4 5' stem-loop and induces the association of the U4/U6-specific hPrp31 protein and the heterotrimeric hCypH/hPrp4/hPrp3 protein complex. The U4/U6-specific protein p110 plays an important role in U4/U6 di-snRNP recycling. However, p110 leaves the complex upon, or after, association of the U5 snRNP with the di-snRNP. The U4/U6 di-snRNP and the U5 snRNP are bridged by proteins hPrp31 and hPrp6. The U4/U6.U5 tri-snRNP formation is believed to take place in the Cajal bodies, within the nucleus (Schaffert *et al.*, 2004).

2.1.4. U4/U6.U5 tri-snRNP proteins and retinitis pigmentosa

Recently it was shown that the tri-snRNP is also of clinical interest (McKie *et al.*, 2001; Vithana *et al.*, 2001; Chakarova *et al.*, 2002). It was demonstrated that two missense mutations (A194E, A216P) in the human hPrp31 gene (*PRPF31*) are correlated with the autosomal dominant form of retinitis pigmentosa (adRP), a disorder that leads to degeneration of the photoreceptors of the eye (Vithana *et al.*, 2001). The mutations are located within (A216P) and adjacent (A194E) to the Nop domain (see Figure 2-7) shared with box C/D snoRNP-core proteins NOP56 and NOP58 (see Table 2-2). It is so far unknown whether the mutations in hPrp31 affect the stability of the tri-snRNP.

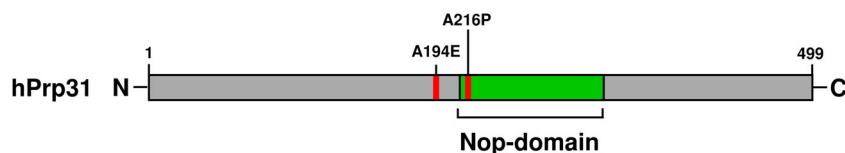


Figure 2-7 Schematic representation of hPrp31 mutations A194E and A216P.

The Nop domain shared with NOP56 and NOP58 is indicated in green.

However, a splicing defect of A216P was demonstrated in yeast by the finding that the expression of yeast hPrp31 with the corresponding A216P mutation failed to complement hPrp31 function in a temperature-sensitive Prp31-deficient yeast strain at the high restrictive temperature (Deery *et al.*, 2002). Mutations in hPrp31 may indirectly affect splicing by inhibiting the translocation of hPrp31 protein into the nucleus (Deery *et al.*, 2002). Furthermore, mutations of several highly conserved residues in the C-terminal part of U5-specific hPrp8p (McKie *et al.*, 2001) and mutations of the gene encoding the U4/U6-specific hPrp3 (Chakarova *et al.*, 2002) are associated with adRP.

It has been suggested that the rod photoreceptors present in the retina have a high demand for splicing of important molecules such as opsin mRNA. Defects in splicing due to loss of function of proteins hPrp31, hPrp3 and hPrp8p may cause a disease in this system. However, the molecular mechanism of adRP associated with mutations in these three tri-snRNP proteins is unclear at present.

2.2. Small nucleolar RNPs (snoRNPs)

2.2.1. Pre-rRNA processing

To satisfy the demand for transcription of large numbers of ribosomal RNA (rRNA) molecules, all cells contain multiple copies of the rRNA genes. Ribosomal RNA –rRNA– genes are arranged in large clusters of, usually, many hundreds of genes. For instance, the human genome contains 150-300 copies of genes that encode the 5.8S, 18S and 28S rRNAs. The genes coding for the 5.8S, 18S, and 28S rRNAs, which are clustered in tandem arrays on five different human chromosomes (chromosomes 13, 14, 15, 21, and 22); the 5S rRNA genes are present in a single tandem array on chromosome 1 (Henderson *et al.*, 1972; Worton *et al.*, 1988).

2 Introduction

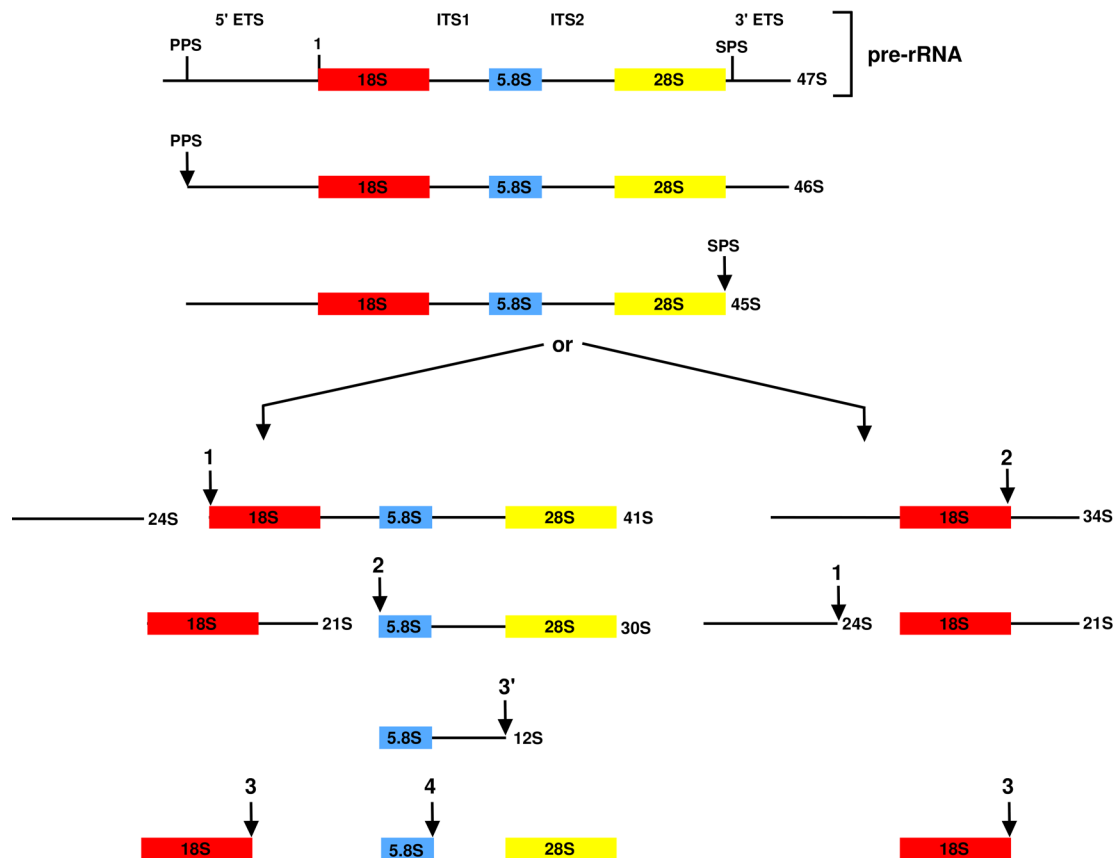


Figure 2-8 Schematic representation of pre-rRNA processing in human.

The 18S (S = sedimentation coefficient), 5.8S, and 28S rRNAs are transcribed as a single precursor (47S), which is cleaved at the primary processing site (PPS) in the 5' external transcribed spacers (ETS) and the second processing site (SPS) in the 3' external transcribed spacers, generating the 45S pre-rRNA. For further processing steps, the pathway depends on the chronological order of the cleavages at sites 1 and 2. Cleavage events result in the generation of the 18S, 5.8S, and 28S rRNAs, which are further modified by of base modifications. The schematic representation was modified from Bowman *et al.* (1981) and Hadjiolova *et al.* (1993).

Each gene unit containing the gene for the 18S, 5.8S and 28S rRNAs is transcribed within the nucleolus by RNA polymerase I as a single 47S precursor rRNA (pre-rRNA) containing external transcribed spacers (ETS) at the 5' and 3' ends, and internal transcribed spacers (ITSs) separating the genes (see Figure 2-8). The 47S pre-rRNA is processed to give the 18S rRNA of the 40S (small) ribosomal subunit and to the 5.8S and 28S rRNAs of the 60S (large) ribosomal subunit. Transcription of the 5S rRNA, which is also found in the large ribosomal subunit, occurs outside the nucleolus and is catalysed by RNA polymerase III (reviewed in Granneman and Baserga (2004)).

The first processing step of the 47S pre-rRNA is a cleavage event within the 5' ETS of the pre-rRNA during the early stages of transcription (Figure 2-8). Moreover, the processing of pre-rRNA involves an extensive amount of base modifications, resulting in the addition of methyl groups to specific bases and ribose residues and also in the conversion of uridine to pseudouridine. In human cells, pre-rRNA processing involves the methylation of about a hundred ribose residues and ten bases, as well as the formation of about a hundred

pseudouridines (Maden, 1998; McCloskey and Crain, 1998). Most of these modifications occur during or soon after synthesis of the pre-rRNA, even if a few take place at later stages of pre-rRNA processing.

2.2.2. Small nucleolar RNP are involved in pre-rRNA processing

The processing of pre-rRNA requires the action of proteins and RNAs in the nucleolus. Nucleoli contain a large number (approximately 200) of small nucleolar RNAs (snoRNAs) which function in pre-rRNA processing (Kiss-Laszlo *et al.*, 1996) (Figure 2-8). SnoRNAs contain a conserved sequence motifs ('boxes') termed C, D, H and ACA, respectively, and they are classified, according to which boxes are present, as C/D-type or H/ACA-type. Like the spliceosomal snRNAs, the snoRNAs are complexed with proteins, forming snoRNPs. Individual snoRNPs consist of single snoRNAs associated with eight to ten proteins. The snoRNPs then assemble on the pre-rRNA to form processing complexes in a manner analogous to the formation of the spliceosome on the pre-mRNA (see section 2.1.1). Most C/D-type snoRNPs direct the methylation of the ribose 2'-O-hydroxyl group, and most H/ACA-type snoRNPs direct the conversion of uridines into pseudouridines. A few snoRNPs of both types are necessary for certain cleavage events of pre-rRNAs, probably because they assist the folding of these RNAs in a crucial way. Like the spliceosomal snRNAs, the snoRNAs are complexed with proteins, forming snoRNPs. Individual snoRNPs consist of single snoRNAs associated with eight to ten proteins. The snoRNPs then assemble on the pre-rRNA to form processing complexes in a manner analogous to the formation of the spliceosome on the pre-mRNA (see section 2.1.1).

A small number of both H/ACA-type and box C/D-type snoRNPs are necessary for the cleavage of pre-rRNAs into 18S, 5.8S, and 28S products (Tycowski *et al.*, 1994; Liang and Fournier, 1995; Peculis, 1997; Borovjagin and Gerbi, 1999). This is probably because they assist the folding of these RNAs in a critical way. For instance, the most abundant nucleolar snoRNA is U3, which is present in about 200,000 copies per cell and is required for the initial cleavage of pre-rRNA within the 5' ETS sequences (see 2.2.1). Likewise, the U8 snoRNA is responsible for cleavage of pre-rRNA to the 5.8S and 28S rRNAs, while the U22 snoRNA is responsible for cleavage of the pre-rRNA to the 18S rRNA.

However, the majority of snoRNAs function in directing the base modifications of pre-rRNA. Most of the snoRNAs contain short sequences of about 15 nucleotides that are

2 Introduction

complementary to 18S or 28S rRNA (Figure 2-9) (Ganot *et al.*, 1997; Ni *et al.*, 1997; Kiss-Laszlo *et al.*, 1998). These complementary regions contain the sites of base modification in the rRNA. By base-pairing with specific regions of the pre-rRNA, snoRNAs act as guide RNAs, targeting the enzymes responsible for ribose methylation or pseudouridylation to the exact site on the pre-rRNA molecule.

Interestingly, the spliceosomal snRNAs contain many post-transcriptionally modified nucleotides (Reddy and Busch, 1988). The U6 snRNA, for example, contains eight 2'-*O*-methyl groups and three pseudouridines, whose generation is directed by snoRNAs (Tycowski *et al.*, 1998; Ganot *et al.*, 1999). The snoRNAs that guide the modification of U6 snRNA are structurally and functionally indistinguishable from snoRNAs that direct the modification of the 18S, 5.8S and 28S rRNAs (Kiss, 2001; Filipowicz and Pogacic, 2002; Terns and Terns, 2002).

As the box C/D snoRNPs are among the objects of the investigation presented in this dissertation, they will be described in more detail in the following two sections.

2.2.3. Structure and function of the box C/D snoRNPs.

The RNA component of each box C/D snoRNP particle directing the 2'-*O*-methylation of the ribose in the pre-rRNA is central to RNP formation, trafficking, and function. It provides binding sites for specific proteins and contains one or several sequences that base-pair with the substrate RNA. The RNA component has no catalytic function on its own, but it assists in accurately positioning the putative methylase relative to the RNA substrate for modification of the sugar (see Figure 2-9).

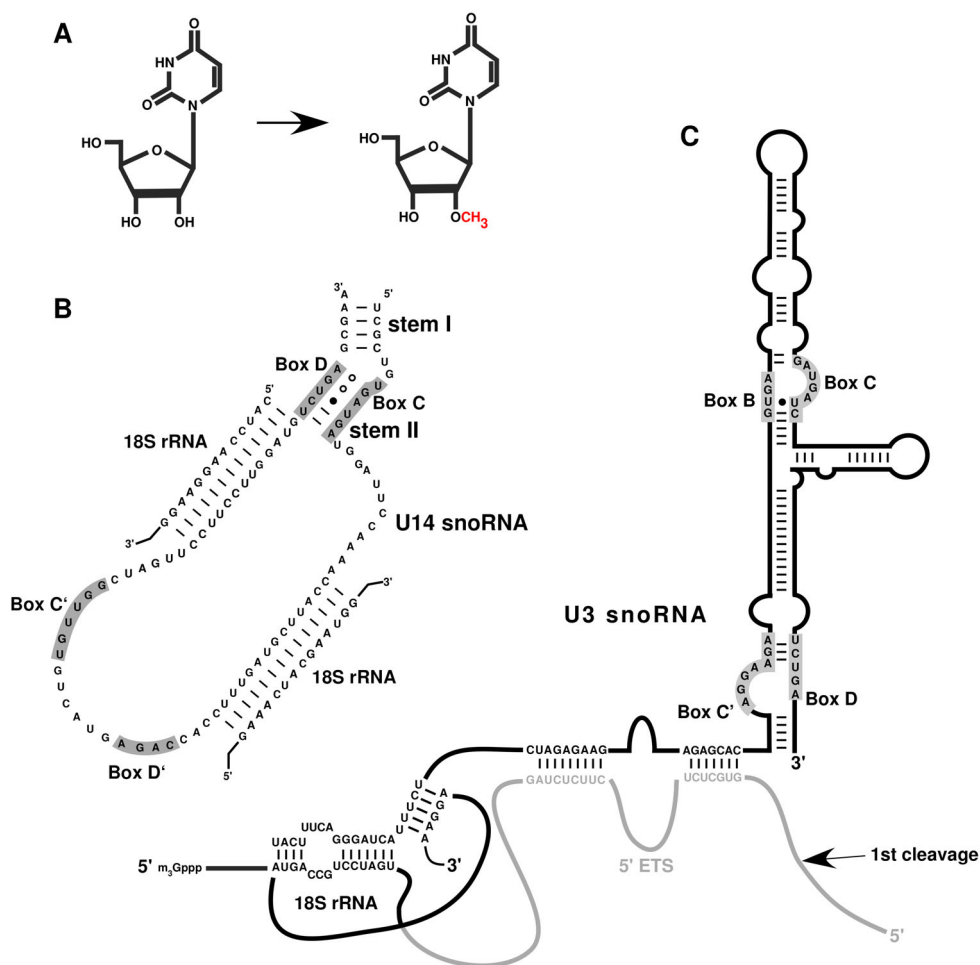


Figure 2-9 Structure and function of the box C/D snoRNAs.

A. Methylation of the 2'-hydroxyl in the ribose moiety according to Lafontaine and Tollervey (1998). B. Secondary-structure model for the U14 box C/D snoRNA base-paired with the 18S pre-rRNA (according to Kiss (2001)). The consensus sequences for boxes C, C', D, and D' are indicated by grey shading. The box C/D interaction with the pre-rRNA generates a conserved structure in which the box D is positioned five nucleotides from the ribose moiety to be 2'-O-methylated. The C'/D' motif does not direct nucleotide methylation, but functions in pre-rRNA processing and 18S rRNA production. C. Schematic representation of the human U3 snoRNA secondary structure (according to Parker and Steitz (1987), Jeppesen *et al.* (1988), Mereau *et al.* (1997), Borovjagin and Gerbi (1999) and Watkins *et al.* (2000)) base-paired with the 18S pre-rRNA. The consensus sequences for boxes C'/D, and B/C are indicated by the grey shading. The 5' external transcribed spacer (5' ETS) is indicated in grey.

Canonical box C/D snoRNAs possess conserved boxes C (consensus sequence 5'-PuUGAUGA-3') and D (consensus sequence 5'-CUGA-3') close to the 5' and 3' termini of the RNA, respectively. The box C/D snoRNAs contain next to the conserved box C/D motif often a less clearly homologous copy of this element termed the box C'/D' motif (Kiss-Laszlo *et al.*, 1998; Gaspin *et al.*, 2000; Omer *et al.*, 2000; Henras *et al.*, 2004). Both motifs direct 2'-O-methylation of the target nucleotide positioned within the guide RNA:substrate RNA duplex and situated five nucleotides upstream from the D or D' box (Box D-plus five-selection rule) (Kiss-Laszlo *et al.*, 1996). In some eukaryotic snoRNAs such as U14 box C/D snoRNA (see), the C'/D' motif does not direct nucleotide methylation but functions in pre-rRNA processing and 18S rRNA production (Liang and Fournier, 1995). The complete secondary structure of

2 Introduction

box C/D snoRNA is still not entirely known. However, it has been shown that boxes C and D form a k-turn motif (Caffarelli *et al.*, 1996; Cavaille and Bachellerie, 1996; Watkins *et al.*, 1996; Xia *et al.*, 1997; Darzacq and Kiss, 2000; Villa *et al.*, 2000), which is described in more detail in section 2.3. This box C/D motif is crucial for box C/D snoRNP assembly and function (Caffarelli *et al.*, 1996; Cavaille and Bachellerie, 1996; Watkins *et al.*, 1996; Lange *et al.*, 1998; Samarsky *et al.*, 1998).

The box C/D snoRNPs are associated with four core proteins, namely 15.5K, NOP56, NOP58 and fibrillarin (see Table 2-2; Schimmang *et al.*, 1989; Wu *et al.*, 1998; Lafontaine and Tollervey, 1999; Lafontaine and Tollervey, 2000; Watkins *et al.*, 2000). It was shown recently that the assembly of the box C/D snoRNP follows a hierarchical pathway. The binding of protein 15.5K to the k-turn motif in the box C/D motif is essential for the subsequent association of the box C/D snoRNP-specific proteins NOP56, NOP58 and fibrillarin, as well as for the binding of the two assembly factors TIP48 and TIP49 (Watkins *et al.*, 2002) (see section 2.3 for more detail).

	Protein	App. MW in kDa	Sequence motif	Known or predicted function
Box C/D	fibrillarin	34	SAM-Methylase	Putative 2'-O-Methylase rRNA-processing
	NOP56	66	Nop domain	rRNA-processing
	NOP58	59.6	Nop domain	rRNA-processing snoRNA stability
	TIP48	51	Walker A/B	Putative RNA-Helicase snoRNP Biogenesis putative Chaperone function
	TIP49	50	Walker A/B	Putative RNA-Helicase snoRNP Biogenesis putative Chaperone function
	15.5K	15.5	RNA binding domain	Nucleation factor Box C/D snoRNP assembly
	U3 Box B/C	hU3-55K	55	WD40
15.5K		15.5	RNA binding domain	Nucleation factor Box C/D snoRNP assembly

Table 2-2 Proteins associating with the box C/D and Box B/C RNPs.

The 2'-O-Methylation of the ribosomal RNA is catalysed by fibrillarin, which shares structural features with methyltransferases, and is guided by the associated snoRNAs (Tollervey *et al.*, 1993; Niewmierzycka and Clarke, 1999). The box C/D motif probably plays

a key role in the correct positioning of fibrillar, in such a way that it methylates the correct ribose of the substrate RNA nucleotide (see 2.2.2).

The U3 box C/D snoRNA, which functions in processing and not in modification, contains a U3-specific k-turn motif, termed the box B/C motif, which also binds protein 15.5K (Watkins *et al.*, 2000). Binding of 15.5K to the B/C motif (see section 2.3 for more detail) are also essential for the recruitment of the U3-specific hU3–55K (see Figure 2-13) (Granneman *et al.*, 2002). The box B/C motif, and therefore probably the 15.5K and hU3–55K, is essential for the formation of the 80S *SSU* (small subunit) processome and consequently for processing of the 18S rRNA and production of the small subunit of the ribosome (Granneman *et al.*, 2004).

2.3. Similarities between the U4/U6 snRNP and box C/D snoRNPs

The U4/U6 snRNP and the box C/D snoRNPs are though distinct in both composition and function, are sharing a similar RNA component and protein composition. Their RNA component can form a so called kink-turn motif (in the U4 5' stem-loop and box C/D and B/C motif in box C/D snoRNAs), which is bound by the 15.5K protein.

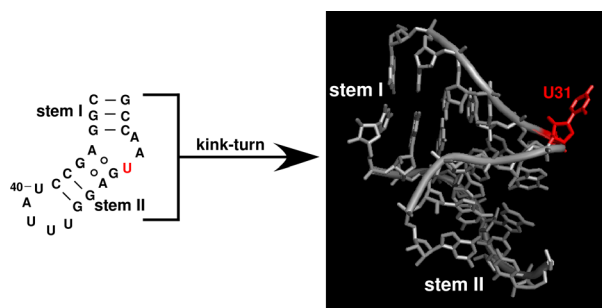


Figure 2-10 Crystal structure of the kink-turn motif present in the 5' stem-loop of the U4 snRNA.

The kink in the phosphate-sugar backbone culminates with the flipped out U31 nucleotide, which is highlighted in red. Sheared G-A base pairs are indicated by the open circles. The conformation of the terminal penta-loop of the 5' stem-loop shown here was not resolved in the crystal structure (modified from Vidovic *et al.*, 2000).

This RNA motif has a kink in its phosphodiester backbone that causes a sharp turn in the RNA helix. Therefore, it has been initially called kink-turn (k-turn) motif (see Figure 2-10) (Klein *et al.*, 2001). In the 5' stem-loop of the U4 snRNA, two stems – stem I and stem II – are connected by an internal asymmetric loop. In the 5' stem-loop of the U4 snRNA, stem I consists of three Watson-Crick G-C base pairs and stem II consists of two Watson-Crick G-C base pairs. Two tandem-sheared G-A base pairs are formed in the internal loop. A terminal

2 Introduction

penta-loop is attached to stem II. The flipped-out uridine (U31), the unpaired adenines (A29, A30), and the guanine (G32) are involved in hydrogen bonds and hydrophobic interactions. Unpaired nucleotides and the tandem-sheared G-A base pairs are critical for binding of the 15.5K protein to the U4 snRNA (Nottrott *et al.*, 1999; Vidovic *et al.*, 2000).

The highly conserved protein 15.5K possesses a RNA-binding domain and binds directly to U4 snRNA (Nottrott *et al.*, 1999), to the box C/D and B/C motif of the box C/D snoRNPs (Watkins *et al.*, 2000, Granneman *et al.*, 2002). It belongs to a family of homologous RNA-binding proteins that includes the ribosomal proteins S12, L7a, L30 as well as the H/ACA snoRNP protein NHP2 (Koonin *et al.*, 1994). A common feature of these proteins is that they all recognise a k-turn motif (Figure 2-10). Members of this family of proteins have been shown to bind the k-turn motif using an induced fit interaction with changes in the structure of both the RNA and protein components (Nottrott *et al.*, 1999; Reidt *et al.*, 2000; Williamson, 2000; Turner *et al.*, 2005; Wozniak *et al.*, 2005). Protein 15.5K is the first U4/U6-specific protein identified as interacting directly with the U4 snRNA.

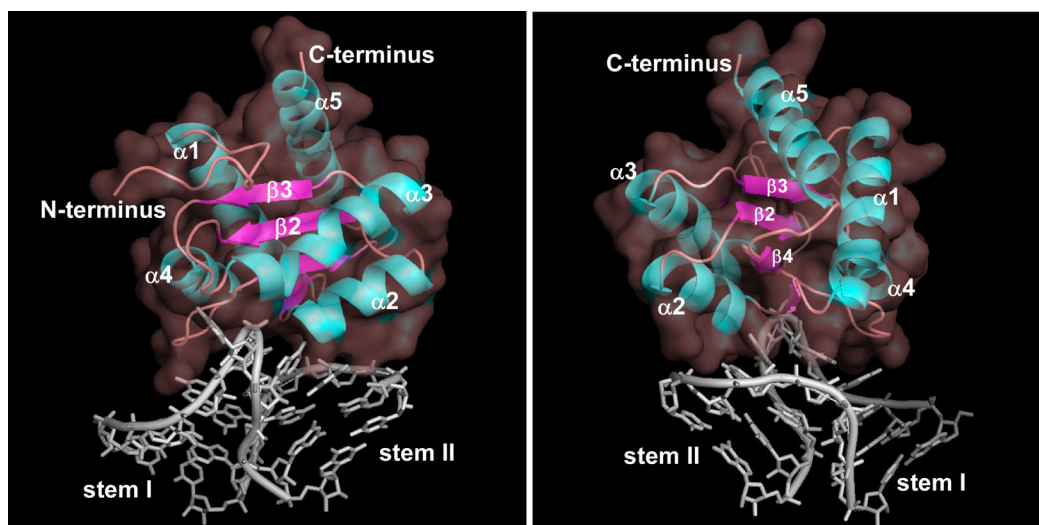


Figure 2-11 Crystal structure of the 15.5K protein bound to the 5' stem-loop of the U4 snRNA.

The crystal structure of the 15.5K protein displays a protein folds into a compact globular domain consisting of alternating α -helices and β -sheets (a so-called α - β - α sandwich). The flipped out U31 of the kink-turn motif locates in a binding pocket of the 15.5K.

The structure of protein 15.5K in complex with the 5' stem-loop of U4 snRNA was determined by X-ray crystallography to a resolution of 2.9 Å (Vidovic *et al.*, 2000) (see Figure 2-11 15.5K crystal structure). The 128 amino acid residues of the 15.5K protein fold into a single, compact globular domain of alternating α -helices and β -strands that form a α - β - α sandwich structure. In the 15.5K protein, the RNA binding surface consists of amino acid residues located in two α -helices (α 2 and α 4), one β -strand (β 1), and three different loops (β

1- α 2, β 2- α 3, and α 4- β 4). These residues interact predominantly with the nucleotides of the U4 snRNA k-turn motif, whose nucleotide U31 is tightly bound in a pocket of the protein.

The 15.5K protein has been found to perform a similar function in the minor spliceosome (Nottrott *et al.*, 1999), the RNA-binding site adopting a structural organisation similar to that observed in the major spliceosome. Interestingly, a recent study has shown that the 15.5K protein is, in addition, a component of both the box C/D snoRNPs and the U3-specific box B/C motif, providing thus a link between the pre-mRNA and pre-rRNA processing machineries (Watkins *et al.*, 2000). These findings raised the interesting possibility that the U4/U6 snRNP and the box C/D RNPs share a common ancestral snRNP.

The box C/D motif is a two-part protein-binding element with internal loop nucleotides, forming a k-turn motif, that is essential for binding protein 15.5K, while the strongly conserved sequence of stem II is required for the binding of the remaining box C/D snoRNA-associated proteins (Szewczak *et al.*, 2002; Watkins *et al.*, 2002) (See Figure 2-13). This suggests that the stem II nucleotides form part of a binding site for proteins other than 15.5K. Consistent with this idea, substitutions of stem II nucleotides that establish or preserve Watson-Crick base-pairing do not inhibit the binding of protein 15.5K. On the other hand, these stem II substitutions restrain the association of the remaining C/D RNP core proteins with the C/D box motif (Watkins *et al.*, 2002). Recently, it was shown by cross-linking experiments that the NOP58 protein can be cross-linked to the 3' uridine residue in stem II of the C box, whereas fibrillarlin can be cross-linked to the 5' uridine residue of the D box in stem II (Cahill *et al.*, 2002).

The U3 box C/D snoRNA, which functions in processing and not in modification, contains a U3-specific k-turn motif, termed the box B/C motif, which also binds protein 15.5K (Watkins *et al.*, 2000). Interestingly, the sheared G-A base pairs do not form in an isolated B/C motif, suggesting that protein 15.5K induces k-turn formation upon binding the B/C motif (induced fit; see also section 2.3). Binding of 15.5K and the small internal loop adjacent to stem I in B/C motif also essential for the recruitment of the U3-specific hU3-55K (see Figure 2-13) (Granneman *et al.*, 2002). The box B/C motif, and therefore probably the 15.5K and hU3-55K, is essential for the formation of the 80S *SSU* (small subunit) processome and consequently for processing of the 18S rRNA and production of the small subunit of the ribosome (Granneman *et al.*, 2004).

2 Introduction

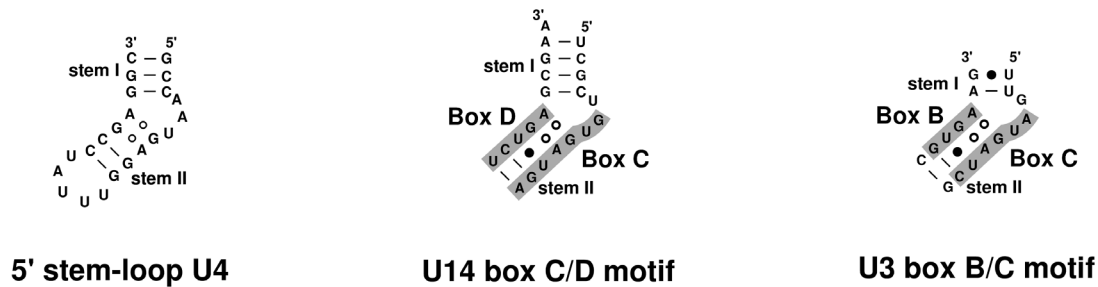


Figure 2-12 The box C/D and box B/C motifs of snoRNAs.

The box C/D and box B/C motifs present in the U14 and U3 snoRNA, respectively, can be folded into a structure similar to that of the 15.5K binding site within the U4 snRNA 5' stem-loop. Sheared G-A base pairs are indicated by the open circles. Remaining non-Watson-Crick base pairs are indicated by black dots. The consensus sequences for boxes C/D, and B/C are indicated by grey shading.

Similarly as described for binding of the box C/D snoRNP-specific proteins, protein hPrp31 and the hCypH/hPrp4/hPrp3 complex do not only require the presence of 15.5K for interaction with U4/U6 snRNA, but as well certain RNA elements within the U4 and U6 snRNA. The hCypH/hPrp4/hPrp3 heteromer requires helix II but not helix I of the U4/U6 duplex for binding (see Figure 2-13), and this interaction involves a direct contact between protein 90K and U6 also requires the U4 5' stem-loop, and is observed only when stem II of the U4/U6 duplex is formed. Protein hPrp31 directly contacts the 5' portion of U4 snRNA via a novel RNA-binding domain and requires at least the U4 snRNA 5' stem-loop for interaction with the U4/U5 snRNP (Nottrott *et al.*, 2002).

Protein hPrp31 (*hPrp31*; human pre-mRNA processing factor 31) possesses a so-called Nop domain in its central region, which shows clear homology to a domain of the box C/D snoRNP-associated proteins NOP56 and NOP58 (Gautier *et al.*, 1997; Vithana *et al.*, 2001; Makarova *et al.*, 2002) (see also 2.2.3 and 2.3). The structure of this domain was recently determined by X-ray crystallography for the archaeal NOP56/58 homologue Nop5p (Aittaleb *et al.*, 2003). Interestingly, hPrp31 also shows functional homology to NOP56 and NOP58. Here too, the binding of protein 15.5K to the k-turn motif is a requirement for the binding of NOP56 und NOP58 to the box C/D snoRNA (Watkins *et al.*, 2000).

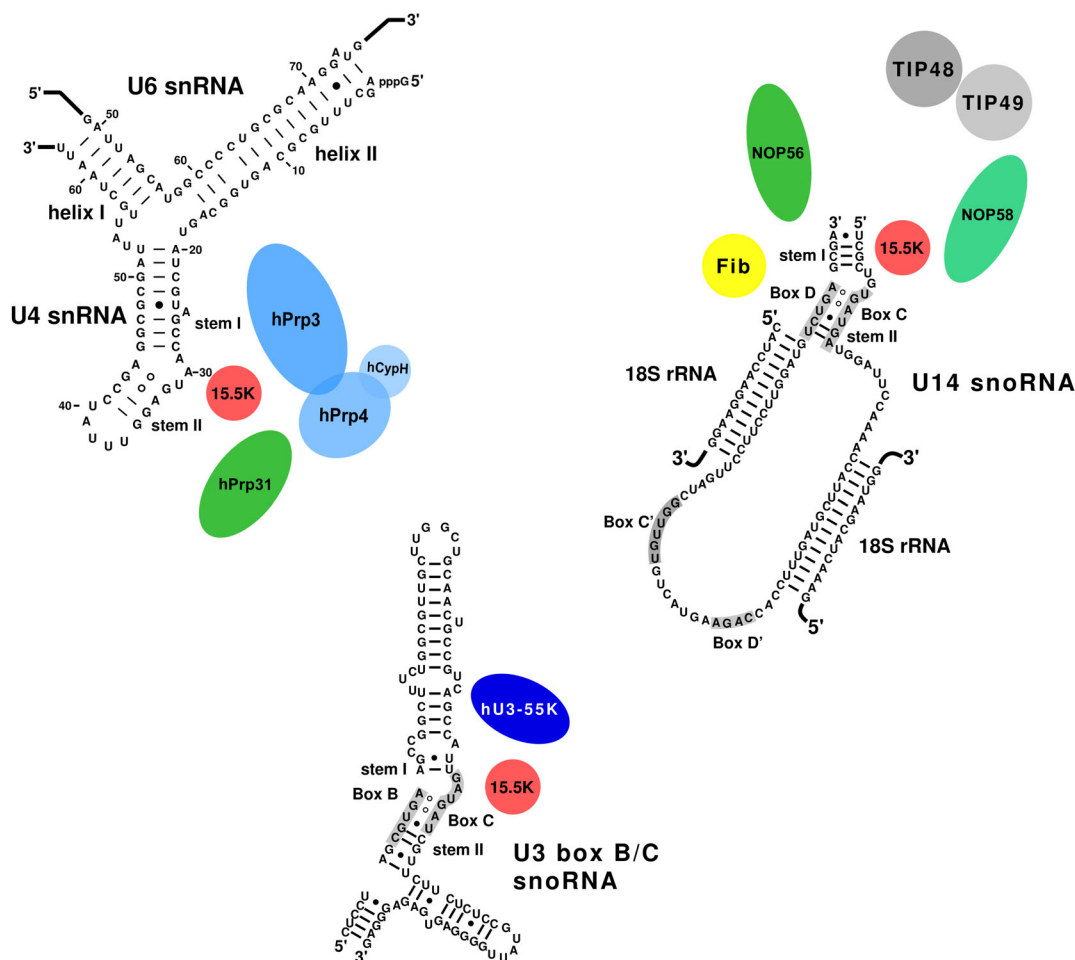


Figure 2-13 Schematic representation of box C/D and box B/C snoRNP assembly.

The U4/U6 snRNP, the box C/D and box B/C snoRNA are shown here schematically with the conserved nucleotides of the box C/D and box B/C motif indicated by grey shading. As the primary snoRNA binding protein, 15.5K binds to the kink-turn, while the remaining U4/U6 snRNP proteins hPrp31, hCypH/hPrp4/hPrp3, the box C/D snoRNP proteins NOP56, NOP58, fibrillarin, TIP48 and TIP49 and the box B/C-specific hU3-55K protein bind the 15.5K-snoRNA complex. Box C/D snoRNP and box B/C-specific proteins specifically recognize the conserved sequence of stem II and the small internal loop adjacent to stem I respectively.

Interestingly, an identified cross-link between the U4atac snRNA and protein hPrp31, which mapped to an amino acid within the Nop homology domain (see Figure 2-5), indicates that this could function as an RNA-binding motif (Nottrott *et al.*, 2002; Kühn-Hölsken *et al.*, 2005). By ultraviolet irradiation of the U4atac snRNP and the native purified U4/U6-U5 tri-snRNP particle, hPrp31 was cross-linked to single-stranded nucleotide regions at the three-way junction and the terminal penta-loop of the U4atac and the U4 snRNA (Nottrott *et al.*, 2002; Kühn-Hölsken *et al.*, 2005). This argues for the existence of direct contacts between hPrp31 and the U4 snRNA. The formation of the U4-15.5K complex suffices for the stable binding of hPrp31. However, it remains unclear which regions of the U4 snRNA are required for this stable binding, and what factors determine its specificity. The corresponding determinants in hPrp31 are likewise unknown.

2.4. Aim of the work presented in this dissertation

The k-turn-binding protein 15.5K is unique in that it is essential for the hierarchical assembly of three RNP complexes distinct in both composition and function, namely the U4/U6 snRNP, the box C/D snoRNP, and the RNP complex assembled on the U3-box B/C motif. The assembly of each of these complexes requires unique sequence elements found in the cognate RNA. Furthermore, changes in the RNA structure mediated by the binding of protein 15.5K are proposed to create the binding site for the complex-specific proteins. However, it is possible that protein 15.5K also mediates RNP formation by protein-protein interactions with the complex-specific proteins. The 15.5K protein is evolutionarily highly conserved throughout its entire sequence. However, only ~10% of its surface is directly involved in RNA-binding. This suggests that protein 15.5K may perform tasks other than just RNA-binding in either the assembly and/or the function of one or more of the different complexes. In addition, the close proximity of the binding sites for the box C/D proteins and hPrp31 to the 15.5K binding site makes it highly likely that protein-protein contacts exist between these components. To broaden our understanding of RNP complex formation, one aim of the work presented here was therefore to find out whether protein 15.5K nucleates complex assembly, entirely or in part, through direct protein-protein interactions. In order to test this possibility, the published crystal structure of protein 15.5K bound to the U4 5' stem-loop was used to identify conserved amino acids on the surface of protein 15.5K for subsequent mutagenesis. The mutants generated were to be tested for their ability to support the formation of the U4/U6 snRNP, the box C/D snoRNP, and the U3 box B/C complex.

It was already known that the 15.5K protein associates with the U4 snRNA *in vitro*. Therefore, the examination of its nuclear localisation pattern and its association *in vivo* with the U4 snRNA and the box C/D snoRNAs were of further interest to gain more information about the site of U4/U6 di-snRNP and box C/D snoRNP assembly. In addition, it was of interest whether the conserved 15.5K surface has any influence on complex assembly and localisation of the U4/U6 snRNP and the box C/D snoRNPs *in vivo*.

The U4/U6-specific protein hPrp31 plays a key part in the stability of the tri-snRNP and in its formation from the U4/U6 di-snRNP and the U5 snRNP. As mentioned above, the association of the hPrp31 protein requires not only the binding of the 15.5K protein to the U4 snRNA, but also elements located within the U4snRNA. Recently, by ultraviolet irradiation of the U4atac snRNP and the native purified U4/U6.U5 tri-snRNP particle, hPrp31 was cross-linked to single-stranded nucleotide regions at the three-way junction and the terminal penta-

loop of the U4atac and the U4. Furthermore, by hydroxyl-radical footprinting analysis, nucleotides within the U4 snRNA specifically contacted by protein hPrp31 have been identified. However, at the beginning of this work, structural requirements within the U4 snRNA necessary for binding of protein hPrp31 to the U4/U6 snRNP were unknown. Therefore, it was of major interest to identify RNA elements within the U4 snRNA required for its binding and to learn more about the molecular interactions involved in binding of protein hPrp31 to the U4/U6 snRNP.

The corresponding determinants in the hPrp31 protein are likewise unknown. Clues to structural requirements for the association of the hPrp31 protein were the more interesting as hPrp31 shows functional and structural homology with NOP56 and NOP58. Protein hPrp31 possesses a so-called Nop domain in its central region, which shows clear homology with a domain of the box C/D snoRNP-associated proteins NOP56 and NOP58. This raises the question of how the specificity of the binding of hPrp31 to the U4 snRNA (i.e., and not to the box C/D snoRNA) is achieved. Interestingly, a cross-link (see above) identified between the U4atac snRNA and protein hPrp31, which mapped to an amino acid within the Nop homology domain, indicates that this could function as an RNA-binding motif (Nottrott *et al.*, 2002; Kühn-Hölsken *et al.*, 2005). However, at the beginning of this work it was unclear whether this Nop homology domain is sufficient for the binding to the U4 snRNP. Therefore, the minimal requirements on the side of the hPrp31 protein for binding to the U4 snRNP were to be analysed by using a number of protein hPrp31 deletion mutants.

As described before, Prp31 is also of clinical interest. Mutations in its gene (PRPF31), located in and around the conserved hPrp31 Nop domain, are correlated with the autosomal dominant form of retinitis pigmentosa (Vithana *et al.*, 2001). However, the molecular mechanisms underlying this disease are so far unknown. Thus, it was of interest to investigate the molecular effect of these mutations on stability of the U4/U6.U5 tri-snRNP and to analyse their influence on hPrp31 localisation *in vivo*.

3. Materials and Methods

3.1. Materials

3.1.1. Fine Chemicals

Standard chemicals, organic substances, and solvents used in this work were obtained from Merck (Darmstadt) or Serva (Heidelberg). Their degree of purity is „pro analysis“. The best supplier has been chosen respectively.

Product	Manufacturer
Acrylamide 30% (0.8% Bis–Acrylamide)	Roth, Karlsruhe
Agarose (Type II)	Sigma, Deisenhofen
Amplify™	Amersham Biosciences, Freiburg
APS (Ammonium persulfate)	Merck, Darmstadt
Bio–Rad Protein Assay	Bio–Rad, Munich
Bromophenol Blue	Bio–Rad Lab., USA
Bovine Serum Albumin (BSA)	Sigma, Taufkirchen
CASYton (isotonic sodium chloride solution)	Schaerfe System, Reutlingen
Calcium chloride	Merck, Darmstadt
Coomassie Brilliant Blue R250	Serva, Heidelberg
Coomassie Brilliant Blue G250	Serva, Heidelberg
Denhardt’s reagent	Invitrogen, Karlsruhe
ddH ₂ O	Millipore
DTT (Dithiothreitol)	Roth, Karlsruhe
DMSO (Dimethyl sulfoxide)	Merck, Darmstadt
Dulbecco’s modified eagle medium (DMEM)	Gibco RBL, Eggenstein
EDTA (Ethylene–diamine–tetraacetic acid)	Roth, Karlsruhe
Ethanol	Merck, Darmstadt
Ethidium bromide	Roche, Switzerland
Fetal Calf Serum (FCS)	GibcoBRL, Karlsruhe
Ficoll 400	Amersham Pharmacia, Freiburg
Formaldehyde	Riedel-de Haën, Seelze
Glucose	Sigma, Taufkirche
Glutathion (reduced)	Sigma, Deisenhofen
Glycerol (bonded to Tridodecylmethylammonium chloride)	Merck, Darmstadt
Glycogen	Roche, Switzerland
Glycine	Roth, Karlsruhe
Heparin	Sigma, Deisenhofen
HEPES (N-2-hydroxyethylpiperazine-N -2-	Calbiochem, USA

Product	Manufacturer
ethanesulfonic acid)	
Imidazol	Merck, Darmstadt
Isopropyl- β -D-thiogalactoside (IPTG)	Sigma, Deisenhofen
LB medium (capsules)	Bio 101, USA
LB agarose media (capsules)	Bio 101, USA
Potassium phosphate	Sigma, Deisenhofen
Milk powder	Naturaflor, Dietmannsried
Magnesium chloride	J.T. Baker, Holland
2'-Mercaptoethanol	Roth, Karlsruhe
Mowiol 4-88	Calbiochem, USA
OptiMEM 1	GIBCO, New Zealand
Paraformaldehyde	Merck, Darmstadt
PMSF (Phenyl methane sulfonyl fluoride)	Roche, Mannheim
Polyvinyl pyrrolidon	Merck, Darmstadt
Ponceau S	Serva, Heidelberg
Protein-A-Sepharose CL-4B	Amersham Pharmacia, Freiburg
Roti-Phenol/Chloroform	Roth, Karlsruhe
Salmon Sperm DNA (10 mg/ml)	Stratagene, USA
Sodium acetate	Sigma, Deisenhofen
Sodium-carbonate	J.T. Baker, Holland
Sodium-chloride	Roth, Karlsruhe
Sodium dehydrogenate phosphate	Merck, Darmstadt
Sodium dodecyl sulfate (SDS)	Serva, Heidelberg
Poly(vinylidene difluoride) membrane, Hybond-P	Amersham Pharmacia Biotech, Freiburg
Phenol-Chloroform-Isoamylalcohol (PCA)	Roth, Karlsruhe
Bovine serum albumin (BSA)	Roche, Switzerland
TEMED (N,N,N',N'-Tetra methyl ethylendiamine)	Sigma, Deisenhofen
Tris-(hydroxymethyl)amino methane	Roth, Karlsruhe
Triton X-100	Sigma, Deisenhofen
tRNA, E. Coli MRE 600	Boehringer, Mannheim
Tween20	Sigma, Deisenhofen
Urea	Roth, Karlsruhe
Xylencyanol FF	Fluka, Switzerland

3 Materials and Methods

3.1.2. Markers

Product	Source
Mark 12, protein marker (range 2.5-200 kDa)	Invitrogen, Netherlands
DNA-molecular weight marker III (sizes DNA fragments between 0.12 and 21.2 kbp)	Roche Applied Science, Mannheim
DNA-molecular weight marker VI (sizes DNA fragments between 0.15 and 2.1 kbp)	Roche Applied Science, Mannheim
Rainbow Prestained Protein standard (range 10-250 kDa)	Bio-Rad, Munich
Precision Unstained protein standard (range 10-250 kDa)	Bio-Rad, Munich

3.1.3. Radio Chemicals

Product	Manufacturer
[α - ³² P] pCp; 3000 Ci/mmol	Amersham Pharmacia Biotech, Freiburg
[³⁵ S] Methionine; 1000 Ci/mmol	Amersham Pharmacia Biotech, Freiburg
[α - ³² P] UTP; 3000 Ci/mmol	Amersham Pharmacia Biotech, Freiburg
[γ - ³² P] ATP; 6000 Ci/mmol	Amersham Pharmacia Biotech, Freiburg
[α - ³² P] dATP; 3000 Ci/mmol	Amersham Pharmacia Biotech, Freiburg

3.1.4. Enzymes und Inhibitors

Product	Manufacturer
Alkaline Shrimp Phosphatase	Roche, Switzerland
Restriction Endonucleases	New England Biolabs, Schwalbach
<i>Pfu</i> DNA Polymerase (2.5 U/ μ l)	Stratagene, Heidelberg
T7 RNA Polymerase	New England Biolabs, Schwalbach
SP6 RNA Polymerase	Promega, USA
T4 DNA Ligase	New England Biolabs, Schwalbach
T4 Polynucleotide kinase	New England Biolabs, Schwalbach
T4 RNA Ligase	New England Biolabs, Schwalbach
Thrombin	Amersham Pharmacia Biotech, Freiburg
PreScission Protease	Amersham Pharmacia Biotech, Freiburg
complete™ EDTAfree Protease Inhibitor tablets	Roche, Switzerland
DNase I	Roche, Switzerland
Proteinase K (10 mg/ml)	Sigma, Deisenhofen
RNase A (1 mg/ml)	Ambion, USA
RNasin (40 U/ μ l)	Promega, USA
RQ DNase I (1 U/ μ l)	Promega, USA
Taq DNA Polymerase (5U/ μ l)	Promega, USA
Trypsin-EDTA	GIBCO, New Zealand

3.1.5. Used Organisms

Product	Manufacturer
Epicuran Codon Plus <i>E.coli</i> BL21(DE3)– RIL	Stratagene, Heidelberg
Epicuran Codon Plus <i>E.coli</i> BL21–RIL	Stratagene, Heidelberg
Epicuran Codon Plus <i>E.coli</i> BL21(DE3)– RP	Stratagene, Heidelberg
Epicuran Codon Plus <i>E.coli</i> BL21–RP	Stratagene, Heidelberg
Epicuran Codon Plus <i>E.coli</i> BL21(DE3)– LysS	Stratagene, Heidelberg
XL1–blue <i>E. coli</i>	Stratagene, USA
HMS 174 (DE3) <i>E. Coli</i>	Novagen, USA
XL1–blue super competent <i>E.coli</i>	Stratagene, USA
One Shot DH5a–T1	Invitrogen, Netherlands
HeLa SS6 cells (human cervix carcinoma cells)	Shooter and Grey, 1952
YFP–Fibrillarin expressing stable cell line (HeLa)	Lamond Lab, UK (Leung and Lamond, 2002)

3.1.6. Plasmids and Vectors

Plasmid	Description	Source, Reference
pGex–hPrp31	pGex–6–P–1 vector expressing the human hPrp31 protein with a GST–tag; AmpR; restriction sites BamHI → XhoI	Nottrott <i>et al.</i> , 2002
pGex–15.5K	pGex–4–T–2 vector expressing the human 15.5K protein with a GST–tag at the N–terminus; AmpR; restriction sites BamHI → Sall	Nottrott <i>et al.</i> , 1999
pGex–15.5K–1, –2, –3, –4 and –5	pGex–4–T–2 vector expressing mutant 15.5K proteins with a GST–tag at the N–terminus; AmpR; restriction sites BamHI → Sall	This study
pET–hPrp31	pET–28a vector expressing the human hPrp31 protein with a His–tag at the C–terminus; T7 promoter; restriction sites EcoRI → HindII	Makarova <i>et al.</i> , 2002
pGEM–3Zf(+)-hU3–55K	pGEM–3Zf(+) vector containing the sequence of the U3-specific hU3–55K protein, subcloned in the EcoRI site of the vector; T7 promoter	Pluk <i>et al.</i> , 1998
phU4	pUC13 vector containing the sequence of the human U4 snRNA; SP6 promoter; AmpR; linearized with DraI	Wersig und Bindereif, 1990
phU5	pEMBL 8(+) vector containing the sequence of the human U5 snRNA; T7 promoter; AmpR; linearized with HindIII	Wersig und Bindereif, 1990
phU6	pUC13 vector containing the sequence of the human U6 snRNA; SP6 promoter; AmpR; linearized with BamHI	Wersig und Bindereif, 1990
pEYFP–15.5K	Mammalian expression vector pEYFP–C1 expressing the human 15.5K protein with a YFP–tag at the N–terminus; CMV promoter; KanR/NeoR	Dierk Ingelfinger, AG Lührmann
pEYFP–15.5K–1, –2, –3, –4 and –5	Mammalian expression vector pEYFP expressing mutant 15.5K proteins with a YFP–	This study

3 Materials and Methods

Plasmid	Description	Source, Reference
	tag; CMV promoter; KanR/NeoR	
pcDNA–Flag15.5K	Mammalian expression vector pcDNA3.1 expressing the human 15.5K protein with a Flag–tag at the N–terminus; CMV promoter; AmpR/NeoR	This study
pcDNA–Flag15.5K–1, –2, –3, –4 and –5	pcDNA3.1 vector expressing the human 15.5K protein with a Flag–tag at the N–terminus; CMV promoter; AmpR/NeoR	This study
pETM–hPrp31	Mammalian expression vector pETM–41 expressing the hPrp31 with an MBP–tag at the N–terminus; T7 promoter; KanR	Sunbin Liu, AG Lührmann
pETM–hPrp31 Nop–domain	Mammalian expression vector pETM–41 expressing the hPrp31 deletion mutant with an MBP–tag at the N–terminus; T7 promoter; KanR	This study
pETM–hPrp31 Nop Δ C	Mammalian expression vector pETM–41 expressing the hPrp31 deletion mutant with an MBP–tag at the N–terminus; T7 promoter; KanR	This study
pTA2–hPrp31	Mammalian expression vector pTA2 expressing the human hPrp31 wild–type with an HA–tag at the N–terminus; T7 and CMV promoter; AmpR/NeoR	Sunbin Liu, AG Lührmann
pTA2–hPrp31–A194E	Mammalian expression vector pTA2 expressing the human hPrp31 retinitis pigmentosa mutant A194E with an HA–tag at the N–terminus; T7 and CMV promoter; AmpR/NeoR	This study
pTA2–hPrp31–A216P	Mammalian expression vector pTA2 expressing the human hPrp31 retinitis pigmentosa mutant A216P with an HA–tag at the N–terminus; T7 and CMV promoter; AmpR/NeoR	This study
pCS2–Lamin A	pCS2+ vector containing a Flag–tag coding sequence, expresses 2.1 TOPO cloning vector	Bechert <i>et al.</i> , 2003; AG Weber (MPI, Göttingen)

3.1.7. Antibodies

Antibody	Source, Reference
α –Fibrillarin antibody	AG Lührmann (Watkins <i>et al.</i> 2002)
α –NOP56 antibody	AG Lührmann (Watkins <i>et al.</i> 2002)
α –NOP58 antibody	AG Lührmann (Watkins <i>et al.</i> 2002)
α –TIP48 antibody	AG Lührmann (Watkins <i>et al.</i> 2002)
α –TIP49 antibody	AG Lührmann (Watkins <i>et al.</i> 2002)
α –15.5K antibody rabbit serum	AG Lührmann (Nottrott <i>et al.</i> 1999)
α –hU3–55K	Granneman <i>et al.</i> , 2002
α –GST antibody	Roche, USA
α –H20 antibody	AG Lührmann (Bochnig <i>et al.</i> , 1987)
Monoclonal α –coilin–antibody (5P10 π)	M. Carmo–Fonseca, Portugal

Antibody	Source, Reference
Monoclonal α -SC35-antibody	Sigma, Taufkirchen
α -hPrp4 (60K) rabbit serum („Roy“)	AG Lührmann (Lauber <i>et al.</i> , 1997)
α -hPrp31 (61K) rabbit serum („4825“)	AG Lührmann (Makarova <i>et al.</i> 2002)
α -40K rabbit serum („Paul“)	AG Lührmann (Achsel <i>et al.</i> 1998)
α -HA antibody	Roche, USA
α -GFP-Antibody	Roche, USA
Goat- α -rabbit antibody, coupled Texas Red	Molecular Probes, USA
Goat- α -mouse antibody, coupled Alexa 488	Molecular Probes, USA
Goat- α -rabbit antibody, coupled Alexa 647	Molecular Probes, USA

3.1.8. Reaction Sets (Kits)

Kit	Manufacturer
ABI PRISM™ Dye Deoxy Cycle Sequencing Kit	Applied Biosystems, Weiterstadt
Cell Line Nucleofector Kit R	Amaxa, Cologne
ECL Western Blot Detection Kit	Amersham Biosciences, Freiburg
Lipofectamine 2000	Invitrogen, Netherlands
QIAquick PCR Purification Kit	Qiagen, Hilden
QIAprep Spin Miniprep Kit	Qiagen, Hilden
QIAquick Gel Extraction Kit	Qiagen, Hilden
QIAquick nucleotide removal kit	Qiagen, Hilden
HiSpeed Plasmid Midi Kit	Qiagen, Hilden
Rabbit Reticulocyte Lysate System	Promega, USA
pCR T7/CT TOPO™ TA Cloning Kit	Invitrogen, Netherlands
Quick Change™ Site-Directed Mutagenesis Kit	Stratagene, Heidelberg
BigDye Terminator Sequencing Kit	Perkin Elmer, USA
Prime it II Random Prime Labelling Kit	Stratagene, USA
TNT T7 Coupled Reticulocyte Lysate System	Promega, USA

3.1.9. Chromatography Columns und Column Materials

Product	Manufacturer
Amylose Resin	New England Biolabs, France
Glutathion-Sephacrose 4B	Amersham Pharmacia Biotech, Freiburg
Talon resin	Clontech, USA
Protein-A-Sephacrose CL – 4B	Amersham Pharmacia Biotech, Freiburg
p-Aminobenzamidine Agarose	Sigma, Steinheim
ProbeQuant G-50 and G-20 columns	Amersham Pharmacia Biotech, Freiburg
SulfoLink coupling gel	Pierce, USA

3 Materials and Methods

3.1.10. Antibiotics

Antibiotic	Manufacturer
Ampicillin	Sigma, Deisenhofen
Kanamycin	Sigma, Deisenhofen
Chloramphenicol	Sigma, Deisenhofen
Penicillin/Streptomycin	Biochrom, Berlin
Gentamycin (G418)	Invitrogen, Netherlands

3.1.11. Miscellaneous Material

Product	Manufacturer
Ultrafilter (0.2 and 0.45 µm)	Millipore, USA
Microcon	Millipore, USA
Centriplus	Millipore, USA
Cryo freezing container	Nalgene, USA
Slide-A-Lyser dialysis cassette (MWCO, 0.5 – 3 ml)	Pierce, USA
Glassware	Merck, Darmstadt
Reaction Tubes (0.5 ml, 1.5 ml, 2.0 ml)	Eppendorf, Hamburg
Reaction Tubes (15 ml, 50 ml)	Falcon, Germany
Electroporation Cuvettes	Bio-Rad, Munich
Cassettes for exposing X-ray films	Kodak, Augsburg
X-ray film BioMax MR	Kodak, Augsburg
Parafilm	American National Can, USA
Pipettes (adjustable)	Eppendorf, Hamburg
Whatman 3MM paper	Whatmen, England
Centrifuge Tubes, different sizes	Sorvall, USA
Centrifuge cups (1l, 450 ml)	Sorvall, USA
Nylon membrane Hybond XL	Amersham Pharmacia Biotech, Freiburg
PVDF (Polyvinylidene difluoride) membrane	Bio-Rad, Munich
Sterican needles	Braun, Melsungen
Spinocan Luer Lock needles	Braun, Melsungen
Syringes, different sizes	Braun, Melsungen
Cell culture flasks, different sizes	Sarstedt, Nürnberg
Cell culture dishes, different sizes	Greiner, Frickenhausen
Cell scraper (Rubber policeman)	Sarstedt, Nürnberg

3.1.12. Devices

Device	Manufacturer
Amata nucleofector	Amata, Cologne
Autoclave, Varioklav	H+P, Oberschleißheim
CASY Counter TT	Schärfe System, Reutlingen

Device	Manufacturer
Electroporator, Gene Pulser Xcell	Bio–Rad, Munich
Roll Incubator	Karl Hecht, Staufen
Chambers for gelelectrophoresis	Manufactured in the institute, Bio–Rad Munich
Gel documentation system (Geldoc)	Bio–Rad, Munich
Geldryer Modell 583	Bio–Rad, Munich
„head–over–tail”–Rotor	Fröbel, Lindau
Heatblock Unitek HB–30	Grand Instruments, UK
High–voltage transformer	Amersham Pharmacia Biotech, Freiburg
Hybridization oven	Hybaid Biometra, UK
Inverse microscope Axiovert 25	Zeiss, Jena
Inverse Zeiss LSM 510 META Laser Scanning microscope	Zeiss, Jena
CO ₂ Incubator BBD 6220	Kendro, USA
Incubator with and without shaker	New Brunswick Science, Nürtingen
Magnetic stirrer KMO 213	KiKA Labortechnik, Staufen
Megafuge 1.0R	Kendro, USA
Pipette Aid Akkujet	Hirschmann
pH Meter MI 229	Mettler Toledo, Switzerland
Phosphoimager screens, different sizes	Molecular Dynamics
Phosphoimager Typhoon 8600	Molecular Dynamics
Rotation Shaker	Karl Hecht, Staufen
X–ray film processor X–Omat	Kodak, USA
Sequencer ABI Prism 310	Perkin Elmer, USA
Sonifier	Bransdon, USA
Thermocycler	Hybaid, Netherlands
Centrifuges (Sorvall, Heraeus)	Kendro, Osterode
Sorvall SA–600 rotor	Kendro, Osterode
Sorvall SLA–1500 rotor	Kendro, Osterode
Sorvall SS–34 rotor	Kendro, Osterode
Sorvall SLA–6000 rotor	Kendro, Osterode
SpeedVac concentrator	Eppendorf, Hamburg
Spectrophotometer Ultrospec 3000pro	Amersham Pharmacia Biotech, Freiburg
Scintillationcounter Tro–Carb 2100TR	Packard, Dreieich
Table centrifuge with and without cooling unit	Kendro, Osterode
Trans–Blot cell	Bio–Rad, Munich
UV lamp, 254 nm	Herolab, Wiesloch
Vortex	Scientific Industries, USA
Waterbath 1012	Gesellschaft für Labortechnik, Burgwedel
Waterbath HBR4 digital	Janke & Kunkel, Staufen i. Br.

3 Materials and Methods

3.1.13. DNA Oligonucleotides

Listed DNA oligonucleotides were produced by MWG–Biotech AG. Nucleotides changed with respect to the wild–type sequence were indicated by bold capitals.

Oligonucleotide	Sequence
	Primers used for introducing point mutations into the 15.5K sequence
15.5K-1A	5'–GTTCTTCGATGACCTGGAGCAAG CGTTT AGT TTTCTTTCGCCG GTTCGAAGCCTTTCCTCGGTTAC-3'
15.5K-1B	3'–GTTCTTCGATGACCTGGAGCAAG CGTTT AGT TTTCTTTCGCCG GTTCGAAGCCTTTCCTCGGTTAC-5'
15.5K-2A	5'–CTGCAACTGCCGCTGCTGTGT CGCAAAAT GAATGTGCCCTACGTGTTTGTG-3'
15.5K-2B	3'–GACGTGGACGGCGACGACACAG CGTTT TACTTACACGGGATGCACAAACAC-5'
15.5K-3A	5'–GTGTTTGTGCGCTCCAAGCAG GAT CTGGGG GAA GCCTGTGGGGTCTCCAGG-3'
15.5K-3B	3'–CACAAACACGGGAGGTTTCGT CCTAG ACCC CTT CGGACACCCAGAGGTCC-5'
15.5K-4A	5'–GAAGGCTCGCAGCTGAACAG AAAATCAAAT CCATT CAGAGC TCCATGAAAGGCTCTTAG-3'
15.5K-4B	3'–CTTCCGAGCGTCGACTTTGT CAATACTTT AGGTAAGT CTCG AGGTAAC TTTCC GAGAATC-5'
15.5K-5A	5'–TCCAATCCATT CAGCAGT CCATT AGCAGC CTCTAGTCTAAACCTGTGGC-3'
15.5K-5B	3'–AGGTTAGGTAAGTCGT CAGGTAAT TCGTCG GAGAATCAGATTTGGACACCG-5'
15.5K-6A	5'–GGATCCATGACTGAGGCTGAT AAAGCGAGCTATGTGAAATTTGAAGT GCCGCCACCTCACCAGAAGCTA-3'
15.5K-6B	3'–CCTAGGTACTGACTCCGACT ATTT CGCT CGATACACTTTAAACTTCACGGC CGGGTGGAGTGGTTCTTCGAT-5'
15.5K-7A	5'–GAGCCACTGGAGATCATTTCT GCG CTGCCGCTGCTGTGTGAAGAC-3'
15.5K-7B	3'–CTCGGTGACCTCTAGTAAGAC CGC GACGGCGACGACACACTTCTG-5'
15.5K-8A	5'–GACAAGAATGTGCCCTACGT GATT GTGCGCTCCAAGCAGGCC-3'
15.5K-8B	3'–CTGTTCTTACACGGGATGCAC TAA ACACGCGAGGTTTCGTCCGGG-5'
15.5K-9A	5'–GCCTGTCTGTACCATCAA AGCGAAGATAAAGGTGCG CAGCAGATCCAATCCATT CAG -3'
15.5K-9B	3'–CGGACAAGACAGTGGTAGTTTT TCGCTTCTATTTCCACGGC TCGTCTAGGTTAGGTAAGTC-5'
15.5K-10A	5'–TCCAATCCATT CAGCAGT CC CGCG AAAGGG GCGT TAGTCTAAACCTGTGGCCTC-3'
15.5K-10B	3'–AGGTTAGGTAAGTCGT CAGGCGCTTT CC CGCAAT CAGATTTGGACACCGGAG-5'
15.5K-11A	5'–TCCAATCCATT CAGCAGT CCATT AACGAACTCAAAGGT TAAACCTGTGGCCTCTGCC-3'
15.5K-11B	3'–AGGTTAGGTAAGTCGT CAGGTAATTTGCTT GAG TTTCCA ATTTGGACACCGGAGACGG-5'
15.5K-12A	5'–CCATGACTGAGGCTGATGT GTGCC CAG AGGCCAG CCCCCTTGCC CGCGCC ACCTCACCAGAAGCTA-3'
15.5K-12B	3'–GGTACTGACTCCGACTACAC ACGGGTATA CG TCGGGG AAACGG GCG CGGGTGGAGTGGTTCTTCGAT-5'
15.5K-13A	5'–CCATGACTGAGGCTGATGT GTGCC CAG AGGCC ATCCCTTGCCGATGCC-3'
15.5K-13B	3'–GGTACTGACTCCGACTACAC ACGGGTATA CGGATAGGGGAACGGCTACGGG-5'
15.5K-14A	5'–GGCTGATGTGAATCCAAAGGCC AGC CCCCCTTGCC CGCGCC ACCTCACCAGAAGCTA-3'
15.5K-14B	3'–CCGACTACACTTAGGTTTCCGG TCGGGG AAACGG GCG CGGGTGGAGTGGTTCTTCGAT-5'
15.5K-15A	5'–CAAGAAGCTACTGGACCTCGTT CGCAAAT CATGT GAA TATAAGCAGCTTCGGAAAGG-3'
15.5K-15B	3'–GTTCTTCGATGACCTGGAGCAAG CGTTT AGTAC CTT TATATTCGTCGAAGCCTTCC-5'
15.5K-16A	5'–GCCTGTCTGTACCATCAA AGCGG TC GAAA CTGG GCG CAGCAGATCCAATCCATT CAG -3'
15.5K-16B	3'–CGGACAAGACAGTGGTAGTTTT TCGCC GAG TTT GAC CGC GTCTAGGTTAGGTAAGTC-5'
15.5K-CYS1A	5'–CTGGACCTCGTT CAGCAGTCA GCGA ACTATAAGCAGCTTCGGAAAG-3'
15.5K-CYS1B	3'–GACCTGGAGCAAGTCGT CAGT CGC TTGATATTCGTCGAAGCCTTTC-5'
15.5K-CYS2A	5'–TTCTGCACCTGCCGCTGCT GCGG AAGACAAGAATGTGCCCTAC-3'
15.5K-CYS2B	3'–AAGACGTGGACGGCGAC CGCCTT CTGTTCTTACACGGGATG-5'

Oligonucleotide	Sequence
15.5K-CYS3A	5'-CAAGCAGGCCCTGGGGAGAGCC CGCGGGGT TCCAGGCCTGCATC-3'
15.5K-CYS3B	3'-GTTTCGTCGGGACCCCTCTCGG CGCCCC CAGAGGTCCGGACAGTAG-5'
15.5K-CYS4A	5'-GTCTCCAGGCTGTTCATCGCC CGCT TGTCCACCATCAAAGAAGG-3'
15.5K-CYS4B	3'-CAGAGGTCCGGACAGTAGCGG CGCAGACAGTGGTAGTTT CTTC-5'
15.5K-CYS5A	5'-CTGGACCTCGTTCAGCAGTCA AGCAACTATA AGCAGCTTCGGAAAG-3'
15.5K-CYS5B	3'-GACCTGGAGCAAGTCGTCA GTTCGTTGATATTCGTCGAAGCCTTT C-5'
pEYFP-15.5K-4A	5'-CCATCAAAGAAGGCTCGCAGCTGAAACAGAAAATCAAATCCATTCCAGAGCTCCATTGAAAGGC TCTTAGTCTGAATTCTGC-3'
pEYFP-15.5K-4B	5'-GCAGAATTCAGACTAAGAGCCTTTCAATGGAGCTCTGAATGGATTGATTTCTGTTCAGCT GCGAGCCTTCTTTGATGG-3'
pEYFP-15.5-4B	5'-GCAGAATTCAGACTAAGAGCCTTTCAATGGAGCTCTGAATGGATTGATTTCTGTTCAGCT GCGAGCCTTCTTTGATGG-3'
pEYFP-15.5K-5A	5'-CCAATCCATTCCAGCAGTCCATTAGCAGCCTCTTAGTCTGAATTCTGCAGTCG-3'
pEYFP-15.5K-5B	5'-CGACTGCAGAATTCAGACTAAGAGGCTGCTAATGGACTGCTGAATGGATTGG-3'
pEYFP-15.5-5B	5'-CGACTGCAGAATTCAGACTAAGAGGCTGCTAATGGACTGCTGAATGGATTGG-3'
Primers used for introducing point mutations into the hPrp31 sequence	
hPrp31 RP-A194Ea	5'-GGCCTGCGACATGGAGCTGGAGCTGAACGC-3'
hPrp31 RP-A194Eb	5'-GCGTTCAGCTCCAGCTCCATGTCGCAGGCC-3'
hPrp31 RP-A216Pa	5'-CGGATGTCCTTCATCCCACCCAACCTGTCC-3'
hPrp31 RP-A216Pb	5'-GGACAGGTTGGGTGGGATGAAGACATCCG-3'
hPrp31 RP-A216Paa215-335a	5'-GGGCGCCATGATCCCACCCAACCTGTCC-3'
hPrp31 RP-A216Paa215-335b	5'-GGACAGGTTGGGTGGGATCATGGCGCCC-3'
Primers used for the generation of hPrp31 deletion mutants	
hPrp31-aa59	5'-ATGTTTGCTGAGATTATG-3'
hPrp31-aa92	5'-GTCATCGTGGATGCCAAC-3'
hPrp31-aa215	5'-ATCGCACCCAACCTGTC-3'
hPrp31-aa310	5'-CTCGTGAAACTGTCCAC-3'
hPrp31-aa335	5'-CGGCGGCTCCTGCCACTT-3'
Miscellaneous primers used for cloning and sequencing	
15.5NFlagpcDNA3a	5'-CACCATGGACTACAAGGACGATGATGACAAGCCCGGGATGACTGAGGCTGATGTGAATCC-3'
15.5NFlagpcDNA3b	5'-GCCACAGGTTTAGACTAAGAGCCTTTCAATGG-3'
15.5CFlagpcDNA3a	5'-CACCATGACTGAGGCTGATGTGAATCC-3'
15.5CFlagpcDNA3b	5'-TTACTTGTTCATCATCGTCCTTGTAGTCCATCCCGGGGACTAAGAGCCTTTCAATGGACTGC-3'
61K-TOPO_rev	5'-TCAGGTGGACATAAGGCCACTCTT-3'
5'-YFP	5'-GCCACCATGGTGAAGCAAGGGCGAGGAGCTGTTACCGGGGTG-3'
3'-YFP	5'-GCTGCTTCATGTGGTCCGGGTAGCGGGCGAAGCACTGCAGGC-3'

3 Materials and Methods

3.1.14. RNA Oligonucleotides

All listed RNA oligonucleotides were obtained from Dharmacon Research Inc., USA. Nucleotides changed according to the wild-type sequence were indicated by bold capitals.

Oligonucleotide	Description	Sequence
U4-1	U4 5' end, nucleotides A1-U52	5'-AGCUUUGCGCAGUGGCAGUAUCGUAGCCAAUGAGG UUUAUCCGAGGCGCGAU-3'
U4-2	U4 5' stem-loop, nucleotides A20-U52	5'-AUCGUAGCCAAUGAGGUUUU <u>A</u> UCCGAGGCGCGAU-3'
U4-3	U4 5' stem-loop with terminal GAAAC penta-loop	5'-AUCGUAGCCAAUGAGGGAAACUCCGAGGCGCGAU-3'
U4-4	U4-5' stem-loop with terminal ribosomal GNRA tetra-loop	5'-AUCGUAGCCAAUGAGGGCAACCGAGGCGCGAU-3'
U4-5	U4-5' stem-loop with terminal AAGU tetra-loop	5'-AUCGUAGCCAAUGAGGAAGUCCGAGGCGCGAU-3'
U4-7	U4 5' stem-loop with an elongated stem II by one additional base pair	5'-AUCGUAGCCAAUGAGGCUUU <u>A</u> UGCCGAGGCGCGAU-3'
U4-8	U4 5' stem-loop with an elongated stem II by three additional base pairs	5'-AUCGUAGCCAAUGAGGUCGUUU <u>AUCGACCGAGGCGCG</u> <u>AU</u> -3'
U4-9	U4 5' stem-loop with an elongated stem II by five additional base pairs	5'-AUCGUAGCCAAUGAGGUCGACUUU <u>AUGUCGACCGAGGC</u> <u>GCGAU</u> -3'
U4-10	U4 5' stem-loop deletion mutant, nucleotides A20-U52	5'-GGCCAAUGAGGUUU <u>AUCGAGGCC</u> -3'
U4-11	U4-5' stem-loop with terminal ribosomal U ^{NCG} tetra-loop	5'-AUCGUAGCCAAUGAGGUUCGCGAGGCGCGAU-3'
U4-12	U4-5' stem-loop with terminal UUU tri-loop	5'-AUCGUAGCCAAUGAGGUUUCCGAGGCGCGAU-3'
U4-13	U4-5' stem-loop with an elongated stem II by an additional A-U base pair	5'-AUCGUAGCCAAUGAGGUUU <u>AU</u> CCGAGGCGCGAU-3'
U4-15A	U4-5' stem-loop containing a methylation at position U38	5'-AUCGUAGCCAAUGAGGU <u>m</u> UUUAUCCGAGGCGCGAU-3'
U4-15B	U4-5' stem-loop containing a methylation at position A39	5'-AUCGUAGCCAAUGAGGUUU <u>m</u> AUCCGAGGCGCGAU-3'
U4-15C	U4-5' stem-loop containing a methylation at position U40	5'-AUCGUAGCCAAUGAGGUUU <u>m</u> UCCGAGGCGCGAU-3'
U4-15D	U4-5' stem-loop containing a methylation at position C41	5'-AUCGUAGCCAAUGAGGUUU <u>m</u> CCGAGGCGCGAU-3'
U4-16	U4-5' stem-loop containing a deoxy-Uridine at position 38	5'-AUCGUAGCCAAUGAGGU <u>d</u> UUUAUCCGAGGCGCGAU-3'
U4-16B	U4-5' stem-loop containing a deoxy-Adenosin at position 39	5'-AUCGUAGCCAAUGAGGUUU <u>d</u> AUCCGAGGCGCGAU-3'
U4-16C	U4-5' stem-loop containing a deoxy-Uridine at position 40	5'-AUCGUAGCCAAUGAGGUUU <u>d</u> AUCCGAGGCGCGAU-3'
U4-16D	U4-5' stem-loop containing a deoxy-Cytosin at position 41	5'-AUCGUAGCCAAUGAGGUUU <u>d</u> CCGAGGCGCGAU-3'
U4-ol-a	U4-2, open loop, 5' fragment, hybridizes with U4-ol-a	5'-AUCGUAGCCAAUGAGGUU-3'
U4-ol-b	U4-2, open loop, 3' fragment, hybridizes with	5'-UAUCCGAGGCGCGAU-3'

Oligonucleotide	Description	Sequence
	U4-ol-b	
U4-A1	U4-2, open loop with point mutation, hybridizes with U4-A2, 5' fragment	5'-AUCGUAGCCAAUGAGGGU-3'
U4-A2	hybridizes with U4-A1, 3' fragment	5'-UAACCGAGGCGCGAU-3'
U4-A3	hybridizes with U4-13, 3' fragment	5'-UAGCCGAGGCGCGAU-3'
U4-A4	U4-2 without A-bulge, same number of bases	5'-GCCGCGCCAAUGAGGUUUAUCCGAGGCGCGC-3'
U4-A5	U4-2 with A-bulge and elongated stem I	5'-GCAUCGUAGCCAAUGAGGUUUAUCCGAGGCGCGAUGC-3'
U4-A6	U4-7 open loop with point mutations, 5' fragment, hybridizes with U4-A7	5'-AUCGUAGCCAAUGAGGCUU-3'
U4-A7	oligo 7 open loop, 3' fragment, hybridizes with U4-A6	5'-UAUGCCGAGGCGCGAU-3'
U4-A8	U4-2 without loop, 5' fragment, hybridizes with U4-A9	5'-AUCGUAGCCAAUGAGG -3'
U4-A9	U4-2 without loop, 3' fragment, hybridizes with U4-A8	5'-CCGAGGCGCGAU-3'
U4-tetra-loop	U4-5' stem-loop with terminal tetra-loop; (Cojocarú et al., 2005)	5'-AUCGUAGCCAAUGAGGUGAACCGAGGCGCGAU-3'
U4-A10	U4-2 without loop, 5' fragment, hybridizes with U4-A11	5'-AUCGUAGCCAAUGAGGU-3'
U4-A11	U4-2 without loop, 3' fragment, hybridizes with U4-A10	5'-ACCGAGGCGCGAU-3'
U4-A12	U4-2 without loop, 5' fragment, hybridizes with U4-A13	5'-AUCGUAGCCAAUGAGGC-3'
U4-A13	U4-2 without loop, 3' fragment, hybridizes with U4-A12	5'-GCCGAGGCGCGAU-3'

3.1.15. siRNAs

siRNA	Description	Sequence
BB1/Firefly luciferase	siRNA against the mRNA of the firefly luciferase (<i>Photinus pyralis</i>); position 153-173 in the ORF (Elbashir et al., 2001)	5'-CACGUACGCGGAAUACUUCGAAA-3'
EA2/hPrp31	siRNA against the mRNA of protein hPrp31; position 1648-1706 within the 3' UTR (Schaffert et al., 2004)	5'-CAGUAUGGGCUAGAGCAGGUCUU-3'

3.1.16. Peptide sequences

Peptide	Sequence
15.5K	CTEADVNPkAYPLAD
Fibrillarin	CRGNQSGKNV-MVEPH
NOP56	CTVNDPEEAGHRSRSK
TIP48	CTTKVPEIRDVTRIER
TIP49	DAKSSAKILADQQDKYC
hPrp31	AEFLKVKGEKSGLM

3.1.17. Common Buffers

10× PBS (pH 7.4)
1.37 M NaCl
20.7 mM KCl
80 mM Na ₂ HPO ₄ *7H ₂ O
20 mM KH ₂ PO ₄

CE-Buffer
10 mM Cacodylsäure/KOH pH 7.0
0.2 mM EDTA pH 8.0

10× PBS (pH 8.0)
1.3 M NaCl
20 mM K ₂ PO ₄ pH 8.0

TE-Buffer
10 mM Tris/HCL pH 7.5
1 mM EDTA-(Na) ₂

10× TBE
0.89 M Tris
0.89 M Boric Acid
25 mM EDTA pH 8.0

All buffers have been filter sterilized before usage.

3.2. Methods

3.2.1. Standard Molecular Biological Methods

3.2.1.1. Concentration determination of nucleic acids

Concentration of DNA and RNA in solution was determined with a spectral photometer by measuring the extinction at 260 nm against a reference value (Sambrook *et al.*, 1989).

Conversion is done by using the following parameters:

$$\begin{array}{l} 1 \text{ OD}_{260} = 50 \text{ } \mu\text{g/ml double-stranded DNA} \\ 1 \text{ OD}_{260} = 33 \text{ } \mu\text{g/ml single-stranded DNA} \\ 1 \text{ OD}_{260} = 40 \text{ } \mu\text{g/ml single-stranded RNA} \end{array}$$

Measuring the absorption spectra between 210 nm and 310 nm allows determining the purity of the DNA. The absorption maximum should be at 260 nm and the ratio of the absorption at 260 nm and 280 nm should be between 1.8 and 2.0.

3.2.1.2. Phenol–Chloroform–Isoamylalcohol extraction (PCA)

To remove proteins from nucleic acid containing solutions samples have to be extracted with phenol–chloroform–isoamylalcohol. After adding phenol-chloroform-isoamylalcohol and mixing, proteins will enter the organic phase, while nucleic acid will stay in the aqueous phase.

Phenol-chloroform-isoamylalcohol is added to the nucleic acid containing solution at the ratio of 1:1 and the mixture is then vortexed for 10 seconds. Subsequently a 2 minutes centrifugation step is performed. The upper water-layer is transferred into a new tube and ethanol-precipitated (see 3.2.1.3).

PCA–Solution

50% (v/v) Phenol
2% (v/v) Isoamylalcohol,
48% (v/v) Chloroform
saturated with TE buffer
(3.2.1.2)

3 Materials and Methods

3.2.1.3. Ethanol precipitation

Usually, 2.5 - 3 volumes of an 100% ethanol/0.12 M acetate solution is added to the DNA or RNA sample in a microcentrifuge tube, which is then placed at -80°C for 30 minutes. Frequently, this precipitation is performed by incubation at -20°C overnight. To recover the precipitated DNA/RNA, the tube is centrifuged at $12.000 \times g$ for 15 minutes at 4°C in a microcentrifuge, the supernatant is discarded. The DNA/RNA pellet is rinsed with 70% ethanol (v/v) solution and centrifuged again for 5 minutes, the supernatant is decanted and the tube is drained. After a second centrifugation, the residual supernatant is again discarded, and the DNA/RNA pellet is dried using a Speed-Vac concentrator. The dried DNA is dissolved in ddH₂O or TE buffer (3.2.1.2), and dried RNA in ddH₂O or CE buffer (3.2.1.17).

3.2.1.4. Isopropanol precipitation

For desalting of samples, DNA is precipitated with isopropanol. Subsequently to the PCA extraction (3.2.1.2), 0.7 volumes isopropanol is added and mixed.

To recover the precipitated DNA, the tube is centrifuged at $12.000 \times g$ for 15 minutes at 4°C in a microcentrifuge. The supernatant is discarded and the DNA pellet is rinsed with 70% (v/v) ethanol solution. After a 5 minutes centrifugation the supernatant is decanted. The pellet is dried as described above and dissolved in ddH₂O or TE buffer (3.2.1.2).

3.2.1.5. Agarose gel electrophoresis of nucleic acids

Agarose gel electrophoresis is employed to check the progression of a restriction enzyme digestion, to determine the yield and purity of a DNA isolation or PCR reaction, and to fractionate DNA molecules by size, which can then be eluted from the gel. Prior to gel casting, dried agarose is dissolved in buffer by heating in a microwave oven and the warm gel solution then is poured into a mould, which is fitted with a well-forming comb. The percentage of agarose in the gel varied. Although 0.7% agarose gels typically are used, in cases where accurate size fractionation of DNA molecules smaller than 1 kb is required, a 1, 1.5, or 2% agarose gel is prepared, depending on the expected size(s) of the fragment(s). Ethidium bromide is included in the gel matrix to enable fluorescent visualization of the DNA fragments under UV light. Agarose gels are submerged in electrophoresis buffer in a horizontal electrophoresis apparatus. DNA samples are mixed with agarose gel loading dye and loaded into the sample wells. Electrophoresis usually is at 150-200 mA for 0.5 to 1 hour at room temperature, depending on the desired separation. Size markers are co-

electrophoresed with DNA samples, when appropriate for fragment size determination. After electrophoresis, the gel is placed on a UV light box and a picture of the fluorescent ethidium bromide-stained DNA separation pattern is taken with a camera (Bio-Rad Gel documentation system).

Agarose gel loading dye (5×)

0.25% (w/v) Bromophenol blue
0.25% (w/v) Xylencyanol FF
30% (v/v) Glycerine

3.2.1.6. Denaturing Gel electrophoresis of nucleic acids

The denaturing gel electrophoresis of nucleic acids according to (Maxam and Gilbert, 1986) provides a method for the separation RNA molecules. Secondary structures within the RNA molecules are dissolved before separation by the use of polyacrylamide gels containing Urea, which has denaturing characteristics.

According to the size of the fragments to be separated, polyacrylamide concentrations of 8 to 20% were used (Sambrook *et al.*, 1989). The RNA sample was dissolved in RNA loading dye solution and was denatured at 95°C for 5 minutes before loading on the gel. Gel electrophoretic separation of the RNA was performed in 1× TBE at 20 mA.

If denaturing gel electrophoresis was performed with the aim to purify *in vitro* translated RNAs or RNA oligonucleotides separated RNAs were visualized by UV shadowing (see section 3.2.1.7).

Urea polyacrylamide gel

8M Urea
8%-20% Polyacrylamide/Bisacrylamide (40%)
1× TBE
ad 100 ml H₂O
500 µl APS (10%)
50 µl TEMED

RNA loading dye solution

80% Formamide TBE
1 mM EDTA pH 8.0
0.025% (w/v) Bromophenol Blue
0.025% (w/v) Xylencyanol FF

3.2.1.7. UV shadowing

UV shadowing is a technique for visualizing nucleic acids separated on acrylamide/urea gels. The technique utilizes shortwave UV light (254 nm) and a fluor-coated TLC plate. The detection limit of UV shadowing is approximately 0.3 µg of nucleic acid. RNA oligonucleotides and RNA transcripts prepared for *in vitro* binding assays were purified by electrophoretic separation and elution from gel fragments.

3 Materials and Methods

After electrophoresis, the glass plates and cover of the gel with plastic wrap are removed. The gel is wrapped with a plastic sheet. In a darkened room, the plastic-wrapped gel is placed on top of the fluor-coated TLC plate. The nucleic acid bands are visualized by shining a hand-held UV light source (254 nm) on the surface of the gel. Nucleic acid appears as dark purple shadow while the TLC plate will appear green. Care must be taken since the xylencyanol and bromophenol blue dyes present in most gel loading buffers also appear as dark shadows during UV shadowing and maybe mistaken for nucleic acid. The band of interest is marked, and cut out with a clean scalpel, and the gel piece is further cut into tiny pieces which are then transferred into a tube. The RNA is eluted from the gel in elution buffer at 4°C over night. Additionally the eluted sample is PCA extracted (see 3.2.1.2) and ethanol precipitated (see 3.2.1.3).

Elution Buffer

0.5 M NH ₄ OAc
1 mM EDTA
0.1% SDS

3.2.1.8. „Polymerase Chain Reaction“ (PCR)

The Polymerase chain reaction (PCR) was mainly used for cDNA cloning and plasmid construction in the presented work (e.g. YFP-15.5K-5, Flag-15.5K-1 to 15.5K-5, and hPrp31 deletion mutants). To specifically amplify DNA sequences, to introduce compatible restriction enzyme sites and to introduce sequence elements (e.g. Flag-tag), 20 to 30 base pairs long nucleotides forward and reverse primers were designed. These were complementary to the beginning and end of the DNA fragment to be amplified. To allow the efficient digestion by restriction enzymes at the 5' and 3' end of the PCR product several additional nucleotides (3 to 6) were added at the 5' ends of the primers (3.1.13) adjacent to the restriction site.

The PCR process usually consists of a series of twenty to thirty-five cycles. Each cycle consists of three steps. In the first step, the double-stranded DNA is heated to 95°C in order to separate the strands. This step is called *denaturing*; it breaks apart the hydrogen bonds that connect the two DNA strands. After separating the DNA strands, the temperature is lowered so the primers can attach themselves to the single DNA strands. Prior to the first cycle, the DNA is normally denatured for an extended time to ensure that the template DNA is single-strand. The second step is called *annealing*. The temperature of this stage depends on the primers and is usually 5°C below their melting temperature (45-60°C). The third step is called

elongation and the DNA-Polymerase has to copy the DNA strands. This step is called. The elongation temperature depends on the DNA polymerase. The optimal temperature for the *Taq*- or *Pfu* DNA polymerase enzyme to work is 72°C.

The main difference between *Pfu* and the *Taq* DNA polymerase is that *Pfu* possesses a superior thermostability and 'proofreading' properties. This means that *Pfu* DNA polymerase-generated PCR fragments will have fewer errors than *Taq*-generated PCR fragments. As a result, *Pfu* is more commonly used for molecular cloning of PCR fragments than the historically popular *Taq*.

The time for this step depends both on the DNA polymerase itself and on the length of the DNA fragment to be amplified (about 1 minute per 1 kbp). A *final elongation* step is used after the last cycle to ensure that any remaining single stranded DNA is completely copied.

PCR-reaction	Stock
10 µl <i>Pfu</i> Polymerase buffer	10×
10 µl DMSO	
2.5 µl dNTP-Mix	10 mM
2.5 µl 5' primer	10 mM
2.5 µl 3' primer	10 mM
0.5 µg DNA	
1 µl <i>Taq</i> or <i>Pfu</i> DNA Polymerase	
Ad 100 µl ddH ₂ O.	

Typical parameters for a PCR-reaction used in this work:

Step	Temperature	Time
Denaturing	95°C	1 minute
Number of cycles	1	
2.		
1. Denaturing	95°C	45 seconds
2. Annealing	62°C	45 seconds
3. Elongation	72°C	2 minutes
Number of cycles	25	
3.		
3. Elongation	72°C	10 minutes
Number of cycles	1	

3.2.1.9. Restriction digest using restriction Endonucleases

The restriction digest was used to prepare DNA for analysis or other processing like molecular cloning. Restriction enzymes cut DNA segments within a specific nucleotide sequence, and always make its incisions in the same way. These recognition sequences are

3 Materials and Methods

typically only four to twelve nucleotides long. For the ligation of the vector DNA and the insert DNA both have to be prepared by digesting with suitable restriction enzymes and purified after digest (QIAquick PCR Purification Kit (Qiagen)).

All restriction digest was performed according to the manufacturer's manual (New England Biolabs).

3.2.1.10. Elution of DNA-fragments from agarose gels

This method is used to quickly extract and purify DNA fragments of 70 bp to 10 kb length from standard or low-melt agarose gels for use in subsequent reactions like e.g. restriction digests, ligations or PCR reactions. For this procedure, a gel extraction kit was used and the purification was performed according to the manufacturer instructions (QIAquick gel extraction kit, Qiagen).

3.2.1.11. Ligation of vector and insert DNA

For ligation, vector and insert DNA are first prepared by digesting with appropriate restriction enzymes. Then they are purified with the QIAquick PCR Purification Kit (Qiagen) according to the manufacturer's instructions.

The ligation reaction was as follows. For the optimal ligation efficiency, two DNA molecules in the range of 3:1 to 5:1 molar ratio of insert to vector were prepared for the ligation reaction (see below). This reaction mixture was incubated at 16°C for 3 to 16 hours. Next, the reaction was incubated at 65°C for 15 minutes to inactivate the enzyme. Then, 2 µl of the ligation reaction were used for transformation of *E.coli* (see 3.2.4.6).

Ligation reaction	Stock
2 µl T4 DNA-Ligase buffer	10×
50 ng linearized vector	
150 ng dephosphorylated insert	
1 µl T4 DNA-Ligase	400 U/µl
ad 20 µl dH ₂ O	

3.2.1.12. Preparation of endotoxin-free plasmid DNA

Isolation and preparation of endotoxin-free plasmid DNA from *E. coli* was performed using the QIAGEN Hi Speed Plasmid Midi Kit and the QIAprep Spin Miniprep Kit (see

3.1.8). The extraction and purification procedure was performed according to the manufacturer instructions.

3.2.1.13. Sequencing of recombinant DNA by Dye Deoxy Sequencing

Sequencing of recombinant DNA was performed using the ABI PRISM Dye Deoxy Cycle Sequencing Kit (Applied Biosystems). This sequencing method, also called Taq–Cycle–sequencing was developed by Manoni *et al.* (1992) according to Sanger *et al.* (1977). Copies of the DNA-template are synthesized in a sequencing PCR by the Taq DNA–Polymerase in the presence of an oligonucleotide primer, dNTPs and dideoxynucleotides (ddNTPs), terminator bases, which are labeled with high-sensitivity dyes (see below). The incorporation of the labeled ddNTPs causes termination of the chain. The essence of the technique is the creation of a set of DNA fragments that match the chain to be sequenced. Each fragment is one nucleotide longer than the last. By determining the identity of the final nucleotide in each fragment, the sequence of the whole chain can be determined. The generated DNA fragments are separated by capillary electrophoresis. As the fragments electrophoresed, the beam of the laser focused at the bottom of the gel made the dye-labeled fragments glow as they passed. The colour of each dye-labeled fragment was then interpreted by the computer as a specific base.

The ABI PRISM Model 377 Sequencer is equipped with an argon laser for exciting the dyes and is able to read at maximum capacity, over 400.000 bases in a day. The purity and quality of the DNA template are of most importance for a successful sequencing reaction.

3 Materials and Methods

Sequencing PCR-reaction:

Sequencing reaction
100 to 300 ng DNA
1 pmol 3' or 5' primer
4 μ l BigDye Terminator Mix
0.5 μ l DMSO
ad 10 μ l ddH ₂ O

Cycling Parameters used for sequencing:

Step	Temperature	Time	Cycles
Denaturing	95°C	4 minutes	1
Denaturing	95°C	30 seconds	
Annealing	55°C	30 seconds	
Elongation	60°C	4 minutes	25

Following the PCR reaction, synthesized DNA is purified by Ethanol-precipitation (3.2.1.3) or using the Qiagen DyeEx and dried using a SpeedVac concentrator. Before loading the samples onto the sequencer, dried DNA is resuspended in 20 μ l ABI PRISM buffer and incubated 3 minutes at 90°C.

3.2.1.14. Northern-Blot

For the analysis of RNAs associated *in vivo* with YFP-tagged protein 15.5K (4.2) and HA-tagged protein hPrp31 (4.4) immunoprecipitation experiments were performed (3.2.3.2). After separating co-precipitated RNA molecules on a denaturing gel (see 3.2.1.6), RNA molecules in the gel were transferred to a nylon membrane. The RNAs of interest can then be identified by hybridisation to radioactive probes and visualised by autoradiography. The described protocol is adapted from Sambrook *et al.* (1989).

RNA molecules in the gel were transferred to the nylon membrane by wet transfer at 17V over night at 4°C in transfer buffer (see below). RNAs were covalently bound to the nylon membrane by UV cross-linking (120 mJ/cm²). The blot could be stored for several days at 4°C or -20°C wrapped in plastic wrap. Before hybridization with the radioactive probes, unspecific binding is saturated with salmon sperm DNA by the incubation with prehybridization buffer for 2 hours at 42°C. Membranes are then incubated for 48-72 hours at 42°C with a radioactive DNA probe (3.2.1.15) specific for the RNA of interest.

After that, the membrane is washed 2 times for 5 minutes with 2 \times SSC/0.5% SDS (w/v), 2 times for 5 minutes with 2 \times SSC/0.1% SDS (w/v) at room temperature and finally with 2 \times SSC/0.1% SDS (w/v) at 50°C. Next the radioactive signals are visualized by

autoradiography. The membrane can be re-blotted with another probe after removal of the bound probe by cooking the membrane in a solution consisting of 1× SSC and 0.1% SDS (w/v).

<p>Prehybridization Buffer</p> <p>20× SSC 25 mM Sodium phosphate, pH 6.5 6× SSC 5× Denhardt's 0.5% SDS 50% Formamide 0.2 mg/ml salmon sperm DNA 2% (w/v)</p>	<p>Hybridization Buffer</p> <p>Same buffer as prehybridization buffer, plus 2 – 3×10^7 cpm of each radioactive probe</p>
<p>100 x Denhardt's</p> <p>2% (w/v) Polyvinylpyrrolidon 2% (w/v) BSA 2% (w/v) Ficoll 400</p>	<p>Transfer Buffer</p> <p>25 mM Sodium phosphate, pH 6.5</p>
<p>20 x SSC</p> <p>3 M NaCl 0.3 M Sodium citrate pH 7.0</p>	

3.2.1.15. Preparation of the radioactive DNA probe

For detection of the U snRNAs and snoRNAs by northern blotting a radioactive probe was prepared using the Prime It II Random Primer Labelling Kit (Stratagene) according to the supplier's protocol. In this procedure, DNA is radioactively labelled using a Klenow fragment which exhibits 5' → 3' polymerase activity and the 3' → 5' exonuclease activity.

As a template 25-50 ng of plasmid DNA or PCR fragment containing the coding region for the according U snRNA and snoRNAs were used.

At the beginning the DNA template is denatured. Next, normally 6 nucleotides long random prime oligonucleotides are added and anneal to the DNA template. The Klenow fragment uses these primers for synthesising the DNA probe incorporating [α - 32 P]-dATP (3000Ci/mmol). Then, unbound nucleotides were removed by gel-filtration (ProbeQuant G-50 column). Before hybridisation, the radioactive probe was denatured for 10 minutes at 70°C. For one northern analysis 2-3× 10⁷ cpm were used.

3 Materials and Methods

3.2.1.16. *In vitro* Transcription

The radio-labeled U4 snRNA, U14 box C/D and U3 box B/C snoRNA used in this work were generated by run-off transcription (Melton *et al.*, 1984). This method is based on the observation that the transcription complex will fall off from a DNA template if complex reaches the end of the template. A restriction enzyme site within the gene can therefore be chosen to generate run-off transcripts of the desired length.

First, plasmids containing the sequence coding for the designated RNA is linearized using the appropriate restriction enzyme (see below). Complete digest was checked by agarose gel electrophoresis (see 3.2.1.5). Linearized DNA was purified by phenol-chloroform-isoamylalcohol extraction and ethanol precipitation. The dried pellet was resuspended to a final concentration of 0.5-1 $\mu\text{g}/\mu\text{l}$.

RNA	Restriction enzyme	Promoter
U4 snRNA	DraI	SP6
U14 box C/D snoRNA	BamHI	T7
U3 box B/C RNA	BamHI	T7

Transcription reaction is set as described below using either SP6 or T7 RNA polymerases with respect to the promoter sequence of the DNA template (see table above). The set reaction is incubated for 4 hours at 37°C. Subsequently, the DNA template is digested by the addition of RQ DNase (1U/ μg DNA–template) incubating for another 15 minutes at 37°C.

The RNA transcript is then purified by phenol-chloroform-isoamylalcohol and ethanol precipitation. After drying the pelleted RNA transcript, RNA is resuspended in 10-30 μl ddH₂O. When there was too much background from aberrant premature stops, the RNA transcript was additionally purified by UV-shadowing and elution from gel-fragments (see 3.2.1.7).

1. SP6-controlled <i>in vitro</i> transcription reaction	
5 μg linearized DNA 20 μl 5 \times Transcription Buffer 20 μl rNTPs (each 25mM ATP, CTP, GTP) 1 μl Enzyme Mix Sp 6 ad 100 μl with ddH ₂ O	Transcription Buffer (5\times) 400 mM HEPES–KOH, pH 7,5 160 mM MgCl ₂ 10 mM Spermidine 200 mM DTT

2. T7-controlled *in vitro* transcription reaction

5 µg linearized DNA
 20 µl 5× Transcription Buffer
 30 µl rNTPs (each 25mM ATP,
 CTP, GTP)
 1 µl Enzyme Mix T7
 ad 100 µl with ddH₂O

Transcription Buffer (5×)

400 mM HEPES –KOH, pH 7,5
 120 mM MgCl₂
 10 mM Spermidine
 200 mM DTT

3.2.1.17. *In vitro* Transcription of radio-labeled RNA

For the preparation of radio-labeled U4 snRNA, U14 snoRNA and U3 box B/C RNA transcripts, the *in vitro* transcription reaction described above was performed in the presence of [α -³²P]-UTP.

***In vitro* transcription reaction**

1 µg linearized DNA
 2 µl 5× Transcription Buffer
 1 µl rNTP mix
 2 µl [α -³²P]-UTP (3000 Ci/mmol)
 0.5 µl RNasin (40 U/µl)
 1 µl Enzyme Mix T7 or SP6
 ad 10 µl with ddH₂O

Transcription Buffer (5×)

400 mM HEPES –KOH, pH 7,5
 120 mM MgCl₂
 10 mM Spermidine
 200 mM DTT

10× rNTP mix

5 mM ATP, GTP and CTP
 1 mM UTP

Transcription reaction is incubated for 2 hours at 37°C. Subsequently, the DNA template is digested by the addition of RQ DNase (1U/µg DNA–template) incubating for another 15 minutes at 37°C.

The RNA transcript is then purified by phenol-chloroform-isoamylalcohol and ethanol precipitation. After drying the pelleted RNA transcript, RNA is resuspended in 10-30 µl ddH₂O. The RNA transcript can be additionally purified by denaturing gel electrophoresis (3.2.1.6) and subsequent elution from gel-fragments (see 3.2.1.7).

3.2.1.18. 5'-end-labeling of RNA

RNA oligonucleotides were labeled with [³²P] γ ATP (6000 Ci/mmol) by phosphorylation of the 5'-end using the T4 polynucleotide kinase (New England Biolabs, Schwalbach) according to the instructions by the manufacturer.

3 Materials and Methods

Kinase labelling reaction	
1 µl RNA oligonucleotide	PNK Buffer (10×) 0.7 M Tris-HCl 0.1 M MgCl ₂ 50 mM Dithiothreitol pH 7.6
1 µl 10× PNK buffer	
5 µl [³² P] γATP (6000 Ci/mmol)	
1 µl T4 polynucleotide kinase	
ad 10 µl with ddH ₂ O	

The reaction was incubated for 1 hour at 37°C. Next, 40 µl of buffer CE were added and the reaction was transferred to a G-20 or G-50 spin column (Probe Quant G-20/G-50 micro columns) for removal of remaining radionucleotides. Labeled RNAs were then purified by PCA extraction (3.2.1.2) and ethanol precipitation (3.2.1.3) and the dried pellet was resuspended in ddH₂O or CE buffer.

Labeled RNA oligonucleotides can be additionally purified by denaturing gel electrophoresis (3.2.1.6) and subsequent elution from gel-fragments (see 3.2.1.7).

3.2.1.19. Coupled *in vitro* Transcription and Translation

For analysing protein-protein interaction of GST-15.5K and the U3 box B/C RNA-specific protein hU3-55K, protein hU3-55K was radio-labeled with ³⁵S-Methionine using the TNT Coupled Reticulocyte Lysate Systems from Promega according to instructions by the manufacturer.

In vitro transcription and translation was performed with T7 RNA polymerase and full-length hU3-55k cDNA cloned in vector pGEM-3Zf(+) essentially as described by Pluk *et al.* (1998).

The reaction components were assembled following the example below. After addition of all the components, the lysate was gently mixed by pipetting the reaction up and down. All handling of the lysate components has been performed on ice.

Example of TNT Lysate Reactions	
TNT® Rabbit Reticulocyte Lysate	25 µl
TNT® Reaction Buffer	2 µl
TNT® RNA Polymerase (SP6, T3 or T7)	1 µl
Amino Acid Mixture, Minus Methionine	1 µl (1mM)
[³⁵ S]Methionine (1,000 Ci/mmol)	
RNasin® Ribonuclease Inhibitor (40u/µl)	1 µl
DNA template(s) (0.5 µg/µl)	2 µl
Nuclease-Free Water to a final volume of	50 µl

The reaction was incubated for 2 hours at 30°C. Subsequently 2 µl are analysed via SDS-PAGE and autoradiography. Translates can be stored at -80°C and were used in GST-pull-down assays (see 3.2.7.2).

3.2.2. Protein Biochemical Methods

3.2.2.1. Bradford Assay

The Bradford assay is a convenient and very fast method to determine protein concentrations in aqueous solutions. The procedure is performed according to the manufacturer's instructions (Bio-Rad).

The assay is based on the fact that the absorbance maximum of the Coomassie Brilliant Blue G-250 shifts from 465 nm to 595 nm when binding to protein occurs. Both, the hydrophobic and ionic interactions stabilize the anionic form of the dye, are causing the visible colour change.

To 20 μ l of a protein solution are added 980 μ l dilute Bio-Rad protein assay solution (diluted 1:5, v/v; 1 mg/ml Coomassie Brilliant Blue G 250 in 85% H_3PO_4). After 5 minutes incubation time the absorbance is measured at 595 nm and calibrated against a blank value, set up with ddH₂O. The protein concentration is then determined by calibration against BSA standards. In parallel protein standards (1, 2, 3, 4, 5 and 6 mg/ml) are measured, which are then used to determine the concentration of the protein solution.

3.2.2.2. SDS-PAGE (SDS-Poly Acrylamide Gel Electrophoresis)

The SDS-Poly Acrylamide Gel Electrophoresis was used to separate proteins by size and was performed according to (Laemmli, 1970). The purpose of this method is to separate proteins according to their size, independent of other physical feature. The solution of proteins to be analyzed is first mixed with SDS (Sodium dodecyl sulfate), an anionic detergent, which denatures secondary and non-disulfide-linked tertiary structures, and applies a negative charge to each protein in proportion to its mass.

The denatured proteins are then applied to one end of a layer of polyacrylamide gel. An electric current is applied across the gel, causing the negatively-charged proteins to migrate across the gel. Depending on their size, each protein will move in a different way through the gel matrix.

Two glass plates were cleaned once with ddH₂O and once with absolute ethanol, before the plates are used to assemble a gel chamber with the help of 1.2 mm spacers. The separating gel was cast using either 8 or 12% polyacrylamide gel solutions (see table below) to separate proteins in the molecular-weight range of interest. Polymerization was started by

3 Materials and Methods

addition of TEMED and 10% ammonium-persulfate. The gel was poured immediately up to $\frac{3}{4}$ of the height of the glass plates and the acrylamide- solution was overlaid with a few ml of H₂O in order to prevent air-exposure and allow the acrylamide solution polymerize evenly. The gel was allowed to polymerize for 1 hour at room temperature. After polymerization, the H₂O covering the gel was removed and the stacking gel was prepared and poured immediately, a comb was inserted, and the gel was allowed to polymerize for 1 hour at room temperature. After complete polymerization of the polyacrylamide, the gel was associated with a gel chamber submerged with electrophoresis buffer. Protein samples are mixed with 100 μ l SDS sample buffer and heated to 95°C for 10 minutes and 40 μ l of each were loaded into a sample well of the gel. Proteins are focused while moving through the stacking gel at 15-25 mA and separated in the separating gel at 35 mA.

12% Separating gel solution		8 % Separating gel solution		5% Stacking gel solution	
Acrylamide 30% (0.8% Bis–Acrylamide)	12 ml	Acrylamide 30% (0.8% Bis–Acrylamide)	8 ml	Acrylamide 30% (0.8% Bis–Acrylamide)	1.66 ml
Separating gel buffer (4 \times)	7.5 ml	Separating gel buffer (4 \times)	7.5 ml	Stacking gel buffer (4 \times)	2.5 ml
H ₂ O	10,5 ml	H ₂ O	14.5	H ₂ O	5.89
APS 10%	100 μ l	APS 10%	100 μ l	APS 10%	50 μ l
TEMED	100 μ l	TEMED	100 μ l	TEMED	50 μ l

Separating Gel Buffer (4 \times)
1.6 M Tris/HCl pH 8,8 0.4% (w/v) SDS

Stacking Gel Buffer (4 \times)
500 mM Tris/HCl pH 6.8 0.4% (w/v) SDS

Electrophoresis Buffer
192 mM Glycine 25 mM Tris/HCl pH 8.8 0.1% (w/v) SDS

SDS Sample Buffer
60 mM Tris/HCl pH 6.8 1 mM EDTA 2% (w/v) SDS 16% (v/v) Glycine 0.1% (w/v) Bromphenol blue 0.05% (v/v) β -Mercaptoethanol

3.2.2.3. Staining of proteins with Coomassie Brilliant Blue

Coomassie Blue staining is based on the non-specific binding of the dye Coomassie Brilliant Blue R 250 and G250 to basic and aromatic amino acid side chains.

The gel is soaked in a solution of the dye for about 1 hour. During the subsequent destaining procedure, only the dye bound to the protein is retained in the gel. The gel is then fixed in the fixing solution for about 1 hour and dried. Coomassie Blue binds to proteins approximately stoichiometrical, so this staining method is useful when relative amounts of protein need to be determined by densitometry. The detection is limited to 0.1–0.5 μg of protein.

Staining solution
0.25% (w/v) Coomassie Brilliant Blue R 250
0.1% (w/v) Coomassie Brilliant Blue G 250
40% (v/v) Methanol
10% (v/v) Acetic acid

Destaining solution
40% (v/v) Methanol
10% (v/v) Acetic acid

Fixing solution
3% Glycerol (v/v)
30% Methanol

3.2.2.4. Affinity purification of MBP-fusion proteins

The hPrp31 cDNA was subcloned into pETM–41 (EMBL, Heidelberg) to produce MBP-fusion proteins. *E. coli* strain HMS174 was transformed with pETM–41–hPrp31 and grown at 20°C with shaking (200 rpm) to an OD_{600} of 0.8 in LB media in the presence of Kanamycin (see table below). IPTG was added to a concentration of 1 mM to induce protein expression. After further incubation for 3 hours at 20°C with shaking, cells were pelleted. Cells were resuspended in 25 ml buffer B and incubated for 1 hour at 4°C in the presence of 1 mg/ml lysozyme (Sigma Aldrich) and one tablet of complete protease inhibitor (Roche, Mannheim). Cells were then subjected to sonication with a microtip (Branson) with three 20 second bursts at an amplitude of 40%. Insoluble material was pelleted by centrifugation at 10.000 g for 30 min, and the MBP–hPrp31–containing lysate was loaded directly onto 2 ml of Amylose Sepharose slurry (Amersham Pharmacia Biotech). Bound MBP–hPrp31 was washed once with 20 ml buffer C and twice with buffer B. Bound MBP–hPrp31 was eluted then with buffer B containing 10 mM maltose and finally fractions of 500 μl each (usually 3-4 fractions) were collected. Protein content of the fractions was detected by Bradford (see 3.2.2.1). The peak fractions were pooled and dialysed against buffer B.

3 Materials and Methods

Buffer B	Buffer C	Elution Buffer
50 mM Tris pH 8.0 150 mM NaCl 1 mM EDTA 1 mM DTT	50 mM Tris/HCl pH 8.0 300 mM NaCl 1 mM EDTA 1 mM DTT	50 mM Tris pH 8.0 150 mM NaCl 1 mM EDTA 1 mM DTT 10 mM maltose

Expressed proteins and transformed *E.coli* strains are listed:

Recombinant protein	vector	Resistance	Strain for expression
MBP-hPrp31 wt and deletion mutants	pETM-41	Kanamycin	<i>E.coli</i> HMS174

3.2.2.5. Affinity purification of GST–fusion proteins

The glutathione S-transferase (GST) affinity tag allows for rapid, near homogeneous purification of proteins expressed from GST expression systems. GST-15.5K and GST–hPrp31 are expressed in *E.coli* and isolated from bacteria in a similar procedure as described above in section 3.2.2.4.

2 ml of GST resin are washed with 20 ml of buffer 2 in a 50 ml Falcon tube and the protein-rich supernatant from a 1 litre *E.coli* culture is added. GST resin and supernatant are incubated for 1 hour at room temperature shaking gently. Supernatant is removed after spinning down the beads at 2000 rmp and GST-sepharose washed two times with 20 ml buffer 2. During the last washing step, the slurry of beads is poured into an empty column (Bio-Rad) and the wash buffer is released by gravity flow. GST-fusion proteins can be released from the GST resin keeping the GST-tag. In this case, 6 ml of elution buffer are added to the GST resin and the eluate collected in 500 µl fractions by gravity flow.

Another possibility is to cleave the GST-tag while the protein is still bound to the GST-sepharose. The GST-tag remains on the beads while the protein is released to the supernatant. To perform this cleavage reaction, 6 ml of buffer 2 and 75U Thrombin or PreScission protease are added to the slurry and incubated over night shaking gently at room temperature. The supernatant is released by gravity flow from the empty column and collected in 500 µl fractions. The beads are washed two times with 2 ml buffer 2 and the wash is collected. Protein concentration is determined by Bradford (see 3.2.2.1).

To remove the Thrombin protease from the eluate after cleavage, 50 µl P-Aminobenzamidine Agarose (binding capacity 10-20 mg/ml), which binds the Thrombin protease are added, and incubated for 30 minutes at 30°C shaking gently. P-

Aminobenzamidine Agarose is removed from the eluate by centrifugation and filtration. Without loss of activity, eluates can be stored at -80°C for prolonged periods of time.

Buffer 2	Elution Buffer
50 mM Tris pH 7.9	50 mM Tris/HCl pH 7.9
100 mM NaCl	100 mM NaCl
2.5 mM MgCl_2	2.5 mM MgCl_2
2 mM DTT	2 mM DTT
0.1% Triton X-100	15 mM reduced Glutathion

Recombinant protein	vector	Resistance	Strain for expression
GST-15.5K	pGex-4-T-2	Ampicillin	<i>E.coli</i> BL21 pLysS
GST-hPrp31	pGex-6-P-1	Ampicillin	<i>E.coli</i> BL21 RP

3.2.3. Immunological Methods

3.2.3.1. Western-Blot

For Western-Blot analysis proteins were first separated by SDS-PAGE (3.2.2.2). Next, separated proteins were transferred from the SDS-gel to a PVDF (Polyvinylidene difluoride) membrane (Bio-Rad) using a wet transfer apparatus (Bio-Rad). A pre-stained molecular weight marker, which was applied before SDS-gel electrophoresis, was used as an indication for a successful transfer. The gel, membrane and sheets of Whatman paper 3MM were soaked in transfer buffer (see table below), and the sandwich containing the gel and membrane was placed between sheets of 3MM Whatman paper. The transfer was performed for 1 hour at 350 mA in the presence of an ice cooling unit in the transfer chamber. Upon completion of the transfer, the blotting sandwich was disassembled and the membrane then used for Western-blotting.

To decrease non-specific binding of antibodies, non-specific binding sites on the membrane were blocked in TBS-Triton X-100 buffer (see table below) containing 5% non-fat dry milk (w/v) for two hours at room temperature or at 4°C overnight on a rocking platform. All further steps were carried out in TBS-Triton X-100 buffer containing 1% non-fat dry milk (w/v). After blocking, the membrane was washed 3 times, and then incubated with primary antibody against the protein of interest for one hour at room temperature on a rocking platform. The optimum dilution of primary antibodies used in this work, were determined by titration and are listed in the table below.

3 Materials and Methods

The membrane was washed three times for 15 minutes each and then incubated with a secondary antibody. Depending on the origin of the first antibody, this was either anti-mouse or anti-rabbit, both of the IgG class with a coupled peroxidase. They were used at a dilution of 1:50000 (anti-rabbit) or 1:30000 (anti-mouse) respectively.

The membrane was washed three times and developed with enhanced chemiluminescence (ECL) detection reagents (Amersham Biosciences) as follows. An appropriate amount of equal volumes of Amersham detection reagents 1 and 2 were first mixed and then applied to the membrane. After incubation for 60-90 seconds at room temperature, the membrane was drained, wrapped in plastic film and exposed to X-ray film for 10 seconds to 5 minutes depending on the intensity of the signal. The membrane could be re-probed with a different antibody after stripping it of the previous antibody. For this purpose, the membrane was incubated in stripping buffer (see table below) at 50°C for 30 minutes on a rocking platform.

Transfer Buffer 1.5 l SLAB 4 0.6 l Methanol 0.9 l ddH ₂ O	SLAB 4 50 mM Tris/HCl pH 8.5 380 mM Glycine 0.1% (w/v) SDS
TBS-Triton X-100 20 mM Tris/HCl pH 7.5 150 mM NaCl 2% (w/v) 0.05% (v/v) Triton X-100	Stripping Buffer 100 mM 2-Mercaptoethanol 2% (w/v) SDS 62.5 mM Tris/HCl pH 6.7

Dilution of used antibodies	Origin	Dilution
α -hPrp4 ("Roy")	Rabbit serum	1: 500
α -hPrp31 „4825”	Rabbit serum	1: 100
α -GFP	Mouse monoclonal antibody	1:2000
α -40K ("Paul")	Rabbit serum	1:500
α -HA antibody	Mouse monoclonal antibody	1:2000

3.2.3.2. Radio-immunoprecipitation (RIPA)

For the analysis of protein-protein interactions within the U4/U6 snRNP or the box C/D snoRNP complexes described in this work, radio-immunoprecipitation was used throughout. In this procedure

In this procedure, the antibody against the bait protein was immobilized on protein-A-sepharose beads. For this purpose, 20 μ l protein-A-sepharose beads per reaction were first washed three times with. Subsequently, 5-20 μ l affinity purified antibodies or antiserum were added per 20 μ l beads aliquot, and after an addition of five volumes PBS (pH 8.0), incubation was performed for 1h at 4°C. Unbound antibodies were then removed from the beads by washing three times with PBS. Next, beads were used in the assay by adding the different samples to be analysed (see below).

After adjusting the volume to 300 μ l with reconstitution buffer (see table below), CypH/hPrp4/hPrp3 binding to U4/U6 snRNA was performed according to Nottrott *et al*, (2002) by incubating ~60 fmoles U4/U6 duplex, containing ³²P-labeled minimal U6 snRNA with 40 pmoles purified CypH/hPrp4/hPrp3 complex in the presence or absence of 30 pmoles recombinant, purified 15.5K or mutant 15.5K (see below). Immunoprecipitation was with anti-hPRP4. Protein-A-sepharose beads were washed four times with 500 μ l of reconstitution buffer and the associated U4/U6 snRNA was extracted by PCA extraction (3.2.1.2) and ethanol precipitation (3.2.1.3), and then analysed by PAGE and autoradiography.

In vitro box C/D snoRNP assembly using nuclear extracts was performed as described by Watkins *et al*, (2002). Briefly, 800 pmoles of SL1 oligonucleotide was added to 10 μ l HeLa nuclear extract to block the endogenous 15.5K. *In vitro* transcribed ³²P-labeled U14 snRNA, pre-incubated in the absence or presence of recombinant 15.5K (or mutant protein), was added to the nuclear extract and incubated for 30 minutes at 30°C in 300 μ l reconstitution buffer (see below). Immunoprecipitation was with antibodies specific for the core box C/D snoRNP proteins and the two assembly factors TIP48 and TIP49. RNA was recovered as described above.

In vitro assembly of the U3 box using nuclear extracts was performed essentially similar except that ³²P-labeled U3 box B/C RNA was used and the precipitation was with anti-hU3-55K antibodies.

Radio-immunoprecipitation using α -GFP, α -40K and α -HA was performed similarly as described for the box C/D snoRNP. However, nuclear extracts used here derived from a small scale extract preparation as described in section 3.2.5.4. Following the final washing procedure, RNAs were extracted by phenol-chloroform-isoamylalcohol extraction and ethanol precipitation. Proteins were directly eluted from a separate bead aliquot by adding one volume of protein loading dye to the protein-A-sepharose.

3 Materials and Methods

RNA was analysed by denaturing PAGE followed by northern blotting and proteins by PAGE and western blot analysis.

Antibodies	Complex type	Reconstitution Buffer
α -hPrp4 ("Roy")	U4/U6 snRNP	20 mM Tris/HCl pH 7.4, 150 mM NaCl, 0.1% Triton X-100
α -NOP56, α -NOP58, α -TIP48, α -TIP49, α -fibrillarin	Box C/D snoRNP	20 mM Hepes/KOH pH 7.9, 150 mM NaCl, 3 mM MgCl ₂ , 0.1% Triton X-100, 0.5 mM DTT, 10% Glycerol (v/v)
α -hU3-55K	U3 Box B/C RNP	20 mM Hepes KOH pH 7.9, 150 mM NaCl, 3 mM MgCl ₂ , 0.1% Triton X-100, 0.5 mM DTT, 10% Glycerol (v/v)
α -GFP	U4/U6 snRNP and Box C/D snoRNP	20 mM Tris/HCl pH 7.4, 150 mM NaCl, 0.1% Triton X-100
α -40K ("Paul")	U4/U6 snRNP	20 mM Tris/HCl pH 7.4, 150 mM NaCl, 0.1% Triton X-100
α -HA antibody	U4/U6 snRNP	20 mM Tris/HCl pH 7.4, 150 mM NaCl, 0.1% Triton X-100

3.2.3.3. Affinity purification of antibodies

Peptides (2 mg; 3.1.16) were coupled to SulfoLink coupling gel as described by the manufacturer. 1/10 volume of PBS (pH 8.0) was added to 5 ml of crude serum. Next, the serum was filtered (0.45 μ m aseptic filter), loaded on the peptide column and the column was rotated for 2 hours at room temperature. The column was washed with 30 volumes of PBS and the antibodies were eluted with 100 mM Glycine (pH 2.9). The collected 500 μ l fractions were immediately neutralized by adding 100 μ l of 1M Tris. The amount of purified antibody was determined by the Bradford assay (3.2.2.1). Fractions with an OD₅₉₅ > 0.25 were pooled, BSA was added to a final concentration of 50 μ g/ml and the antibodies were dialysed over night against PBS. The affinity purified antibodies were stored in aliquots at -80°C.

3.2.4. Microbiological Methods

3.2.4.1. Cultivation of E.coli

Bacterial strains carrying plasmids or genes with antibiotic selection marker were cultured in liquid or on solid medium containing the selective agent. Stock solutions of antibiotics were sterilised by filtration and aliquots stored at -20°C. Antibiotics were added to freshly autoclaved medium (cooled to below 50°C); concentrations of stocks and working solutions of the antibiotics are listed below.

LB Medium (capsules, BIO 101)

10 g Tryptone
5 g Yeast extract
0.5 g NaCl

Antibiotic	Stock solution	Working solution
Ampicillin	50 mg/ml in water, -20°C	100 µg/ml, 1/500
Tetracycline	5 mg/ml in ethanol, -20°C	50 µg/ml, 1/100
Streptomycin	10 mg/ml in water, -20°C	50 µg/ml, 1/200
Chloramphenicol	34 mg/ml in ethanol, -20°C	170 µg/ml, 1/200

3.2.4.2. Plates

E.coli strains can be streaked and stored on LB plates containing 1.5% agar and the appropriate antibiotic. With a flamed and cooled wire loop an inoculum of bacteria from a glycerol stock was streaked on top of a fresh agar plate, and incubated upside down at 37°C for 12-14 hours until colonies developed.

LB Agar Medium (capsules, BIO 101)

10g Tryptone
5g Yeast extract
0.5g NaCl
15g Agar

3.2.4.3. Liquid cultures

Bacterial liquid cultures for small scale plasmid preparations were grown as follows. A culture of 1–5 ml LB medium containing the appropriate selective antibiotic is inoculated by a single colony from a freshly streaked selective plate. The solution is incubated for 12–16 h at 37°C with vigorous shaking (240 rpm). Bacterial cells are harvested by centrifugation at > 8000 rpm (6800 x g) in a conventional, table-top microcentrifuge for 3 min at room temperature (15–25°C). Plasmid preparation is performed as described in 3.2.1.12.

Bacterial liquid cultures for big scale plasmid preparations were grown as described below. A starter culture was prepared by inoculating 10 ml LB medium containing the appropriate antibiotic with a single colony from a freshly streaked selective plate. The culture was grown for 4–6 h hours at 37°C with vigorous shaking (~240 rpm) until $OD_{600} = 0.8-1.2$. The starter culture was diluted 1/500 to 1/1000 into a larger volume of selective LB medium and grown overnight (12-16 h) at 37°C with shaking (~250 rpm). Cells were harvested by

3 Materials and Methods

centrifugation at $6.000 \times g$ for 15 min. The cell pellet was then ready for the plasmid purification protocol (see 3.2.1.12). Plasmid preparation is performed as described in 3.2.1.12.

3.2.4.4. Preparation of competent *E. coli* cells

Competent *E. coli* cells are prepared according to the procedure described by Dagert and Ehrlich (1979). For the preparation 5 ml of the *E. coli* strain BL21 codon plus RIL/RP cells or XL1 cells were grown in LB medium in an Erlenmeyer flask at 37°C over night. The flask is chosen at least five times the volume of the culture (>25 ml) to allow good aeration of the cells. *E. coli* codon plus RIL cells contain extra copies of the *E. coli argU*, *ileY*, and *leuW* tRNA genes while the BL21-CodonPlus RP strains contain the *argU* and *proL* tRNA genes which are selected by Chloramphenicol. To keep the extra plasmids BL21-CodonPlus cells have to be grown in the presence of Chloramphenicol whereas *E. coli* XL1 cells are grown without antibiotic. 2.5 ml of the over night culture are transferred into 50 ml LB media. Cells are grown to the early log phase at a density of $OD_{600} = 0.5-0.7$ and are collected by centrifugation at $5.000 \times g$ at 4°C for 5 minutes. Cells have to be kept ice cold in all further steps. Cells are resuspended in 1/2 culture volume of 0.1M ice-cold $CaCl_2$. Cells are collected again by centrifugation (see above) and then are gently resuspended in 1/10 culture volume 0.1M ice-cold $CaCl_2$. Ice-cold sterile glycerol (87%, v/v) is added to a final concentration of 10% (v/v). After gently mixing, the cells are left on ice for 30 minutes. Aliquots of 50 μ l of the cell suspension are flash frozen and then stored at -80°C

3.2.4.5. Glycerol *E.coli* stocks

E.coli strains can be stored for many years at -80°C in 15% glycerol (v/v). For this purpose, 0.15 ml glycerol were first placed into a 2 ml screw-cap vial and sterilised by autoclaving. 0.85 ml of the *E.coli* culture were then added and mixed to ensure even distribution of the bacterial culture and the glycerol. Cultures were flash frozen in liquid nitrogen and stored at -80°C.

3.2.4.6. Transformation of *E.coli*

Competent cells were removed from the -80°C freezer and allowed to thaw on ice. 100 μ l cells aliquots were placed into pre-chilled 12 ml polypropylene tubes. Then, 1 μ l from the ligation reaction or plasmid preparation (1-10 ng DNA) were added to the cells, moving the pipette through the cells while dispensing. Cells were incubated for 30 minutes on ice and

heat-shocked for 45 seconds to 2 minutes at 42°C. Then, cells were placed on ice for 2 minutes, and 0.9 ml of room temperature LB medium was added. The culture was incubated for 1 hour at 37°C with shaking (225 rpm). Following, cells were centrifuged at $10.000 \times g$ for 2 minutes and resuspended in 100 μ l LB medium. Of this suspension, 90 and 10 μ l were plated on separate LB plates containing the required antibiotic and incubated overnight upside-down at 37°C. Bacterial colonies can then be used for plasmid preparation (see 3.2.4.3 and 3.2.1.12).

3.2.5. Cell Culture

3.2.5.1. Cultivation of HeLa cells

HeLa SS6 were grown in a CO₂ Incubator at 37°C and 5% CO₂ with saturating humidity (95%) in cell culture growth medium (see below).

Cell Culture Growth Medium Dulbecco's modified eagle medium (DMEM) 10% (v/v) Fetal Calf Serum (FCS) 100 U/ml Penicillin/Streptomycin
--

3.2.5.2. Passaging HeLa cells

Cells were split routinely three times a week and for this they were harvested by trypsinisation. For trypsinisation, the medium was removed from the flask and cells were washed carefully with PBS (pH 7.4) to remove residual medium. 1-2 ml of pre-warmed Trypsin-EDTA solution was added to the flask (75 cm²) and incubated at 37°C until cells were detached (1-2 minutes). Trypsinisation was stopped by adding a 2 ml of growth medium. Following, cells were resuspended in an appropriate volume of pre-warmed growth medium. Appropriate dilutions of HeLa SS6 cells were transferred to a fresh cell culture flask (75 cm²) containing 10 ml medium. Typically, confluent HeLa SS6 cells were split in a 1:10 ratio, confluency was then reached again after 2-3 days.

3.2.5.3. Freezing and thawing of HeLa cells

The cells were trypsinized, resuspended in medium containing serum, centrifuged at $1.000 \times g$ for 5 minutes, and then resuspended in freezing medium (see below). 1 ml of the cell suspension (approximately $3-5 \times 10^6$ cells) was transferred into each freezing vial.

3 Materials and Methods

Freezing vials were placed into a Cryo freezing container (Nalgene) and stored in a -80°C freezer overnight. This allowed freezing of the cells at a rate of $1^{\circ}\text{C}/\text{minute}$. The following day vials were transferred to a liquid nitrogen chamber. For thawing, a vial of frozen cells was removed from liquid nitrogen and placed in a 37°C water bath until thawed. To remove DMSO from the freezing medium, the cell suspension was pipetted into a centrifuge tube containing pre-warmed medium, and centrifuged at $1.000 \times g$ for 5 minutes. The supernatant was discarded; cells were resuspended in fresh growth medium and transferred to the cell culture flask. Cells were incubated overnight under their usual growth conditions, and the medium was replaced the next day.

Freezing Medium
Dulbecco's modified eagle medium (DMEM)
10% (v/v) Fetal Calf Serum (FCS)
7.5% DMSO

3.2.5.4. Small-scale procedure for preparation of nuclear and nucleolar extracts

For the biochemical analysis of HeLa cells either expressing YFP-15.5K (see section 4.2) or HA-hPrp31 Retinitis Pigmentosa mutants after hPrp31 knock-down (see section 4.4) nuclear extract was prepared using a small scale procedure modified from (Lee and Green, 1990).

Cells of four cell culture plates (Ø 14.5 cm; $\sim 0.5\text{-}1 \times 10^8$ cells) were washed once with cold PBS (pH 7.4) and were harvested by scraping carefully using a cell scraper. Cells were resuspended in 10 ml of cold PBS and were transferred to a 50 ml Falcon tube. Tubes were filled up to 50 ml with PBS. Next, cells were pelleted by centrifugation for 5 minutes at $1.000 \times g$ without brake at 4°C . Then, cells were resuspended in about 1 ml of PBS, transferred to an Eppendorf tube and the packed cell volume was determined after pelleting cells for 5 minutes at $1.000 \times g$ by either using the calibration on the Eppendorf tube or comparing against known volumes. The packed cells were resuspended in one packed cell volume of buffer A (see below) and allowed to swell on ice for 15 minutes. Next, cells were lysed by rapidly pushing them through a narrow-gauge needle (25g 5/8; 15.9 mm) as follows. A 1 ml hypodermic syringe with needle attached is filled with buffer A and the syringe plunger was used to displace the buffer as fully as possible to remove air bubbles. The cell suspension was drawn slowly into the syringe from a 1.5-ml Eppendorf tube and then ejected with a single

rapid stroke. Seven rapid strokes are usually sufficient to break more than 95% of the cells. The homogenate was centrifuged for 60 seconds at $12.000 \times g$ and 4°C . The nuclear pellet is resuspended in two thirds of one packed cell volume (determined above) of buffer C. Next, a 30 minutes incubation step on ice at 4°C with stirring using a mini-magnet followed. The suspension was then centrifuged for 5 minutes at $12.000 \times g$ to pellet cell debris and nucleoli. The supernatant (nuclear extract) is dialyzed against buffer D for 2 hours at 4°C . For preparation of nucleolar extract, the pelleted nucleoli were then resuspended in five packed cell volumes of buffer D' and then sonicated by 3×5 pulses (Output control: 4; Duty cycle: 30%) using a microtip (Branson). To recover the snoRNPs from the nucleoli the suspension was centrifuged for 30 minutes at $16.000 \times g$.

The nuclear and nucleolar extracts can be used directly or quick-frozen in liquid nitrogen and stored at -80°C . Frozen extracts should be centrifuged 1 minute at $12.000 \times g$ before use to remove precipitates. To an approximation, two 75 cm^2 cell culture flasks of cells at 80% confluence yield about $150 \mu\text{l}$ of nuclear extract with a protein concentration of $\sim 5\text{mg/ml}$.

Buffer A
10 mM HEPES-NaOH [pH 7.9]
1.5 mM MgCl_2
10 mM KCl
1.0 mM DTT

Buffer D
20 mM HEPES-NaOH [pH 7.9]
10% Glycerol (v/v)
100 mM KCl
0.2 mM EDTA
0.5 mM PMSF
1.0 mM DTT

Buffer C
20mM HEPES-NaOH [pH 7.9]
25% Glycerol (v/v)
420 mM NaCl
1.5 mM MgCl_2
0.2 mM EDTA
0.5 mM Phenylmethylsulfonyl fluoride (PMSF)
1.0 mM DTT

Buffer D'
20 mM HEPES-NaOH [pH 7.9]
150 mM NaCl
0.2 mM EDTA
0.5 mM DTT
10% Glycerol (v/v)

3 Materials and Methods

Stocks
100 mM PMSF
1M DTT in H ₂ O

3.2.5.5. Generation of a stable EYFP-15.5K expressing HeLa cell line

To set up the selection for the stable EYFP-15.5K expressing cell line (HeLa^{EYFP-15.5K}, 4.2), freshly split cells were transfected (see 3.2.6.3) with the pEYFP-C1-15.5K. The following day, the standard media was replaced with media containing Gentamycin (G418; 400 µg/ml). This will select for cells that have stably incorporated the GFP plasmid into their genomic DNA. Selection for colonies expressing EYFP-15.5K was carried out for three weeks. The Gentamycin containing media in the dish was changed every day, taking care to wash dead cells off the bottom of the dish, and leaving only colonies of stable cells behind.

Colonies were picked and transferred to a 24-well dish with 1 ml media containing Gentamycin in each well. The colonies were picked blind as there was no inverted light microscope available under sterile conditions. Cells were rinsed with PBS (pH 7.4) and then colonies were dispersed by incubating with PBS containing 5% Trypsin. Using a Gilson pipette with a sterile yellow tip, colonies of interest were scraped and sucked gently into the tip. The colonies were then transferred to a well in the 24-well plate.

Always when grown to confluency level, cells were split and transferred to a 6-well plate with a coverslip on the bottom of each well that would allow screening the colonies. Colonies were selected according to their expression level of EYFP-15.5K. Colonies of interest were passaged from the 6-well plate into the next bigger dish. Cells were grown under selection conditions until a sufficient number of cells for the maintenance of the cell line was reached (about 20% confluency). Half of the cells were frozen and stored in a liquid nitrogen container (see 3.2.5.3), the other half was cultivated for small scale nuclear extract preparation (see 3.2.5.4) and biochemical analysis (4.2).

3.2.6. Microscopic Methods

3.2.6.1. Fluorescence microscopy

After performing indirect immuno-fluorescence staining (3.2.6.2), images were acquired with a Zeiss LSM 510 META confocal microscope. Proteins to be detected and the

used fluorophores are listed below. YFP and Alexa 488 were excited with Argon laser lines at 488 nm and by using a dichroic beam splitter (HFT 488). Texas Red was excited with Helium Neon laser lines at 543 nm and by using a dichroic beam splitter (HFT 488/532). Alexa 647 was excited with Helium Neon laser lines at 633 nm by using a dichroic beam splitter (HFT 514/633). The pinhole diameter was set to 106 μm - 1.12 Airy units according to a layer thickness of 0.8 μm . Fluorescence was recorded with a Plan Apochromat 63x/1.4 oil immersion objective.

Background levels were obtained by measuring the mean intensity of each stain outside the cells. Bleedthrough was checked by taking images of cells with a single transfection (e.g. YFP-15.5K) or no transfection and acquiring dual channel images with the same setup used for the co-transfected cells.

Protein	First antibody	Secondary antibody/Fluorophore	Wavelength	Complex or Foci
15.5K	α -15.5K	Goat- α -rabbit antibody, coupled Texas Red	532 nm	U4/U6 snRNP, Box C/D and B/C snoRNPs
SC35	α -SC35	Goat- α -rabbit antibody, coupled Texas Red	532 nm	Splicing speckle marker
SC35	α -SC35	Goat- α -mouse antibody, coupled Alexa 488	488 nm	Splicing speckle marker
15.5K		EYFP	488 nm	U4/U6 snRNP, Box C/D and B/C snoRNPs
Coilin	α -Coilin	Goat- α -rabbit antibody, coupled Alexa 647	633 nm	Cajal Body marker
hPrp31	α -hPrp31	Goat- α -mouse antibody, coupled Alexa 488	488 nm	U4/U6 snRNP
hPrp4	α -hPrp4	Goat- α -rabbit antibody, coupled Alexa 647	633 nm	U4/U6 snRNP

3.2.6.2. Indirect immuno-fluorescence staining

For immuno-fluorescence studies, HeLa cells were grown on multi-well slides. For analysing the localisation of the 15.5K protein (section 4.2), HeLa cells were grown overnight, fixed and stained as described below. For studying the influence of hPrp31 Retinitis Pigmentosa mutations on the localisation of protein hPrp31 and protein hPrp4 (section 4.4), HeLa cells were fixed and stained 48 hours after transfection of HA-hPrp31 and siRNAs against either protein hPrp31 (EA2) or the firefly luciferase (control, GL2) as described in the following procedure.

HeLa cells were washed once PBS (pH 7.4) and then fixed by incubating for 20 minutes in PBS containing 4% (w/v) paraformaldehyde (PFA) at room temperature.

3 Materials and Methods

Subsequently, cells were again washed once PBS. The cells can be stored like this until needed. For long term storage, cells can be covered with PBS containing 0.05% (v/v) sodium azide and 0.2% (w/v) PFA.

Following the paraformaldehyde fixation, cells were permeabilized by incubating them in PBS containing 0.2% Triton X-100 for 15 minutes at room temperature. To remove the detergent, cells were washed four times with PBS and unspecific binding sites were saturated by incubating with PBS containing 10% FCS (v/v) for 1 hour at room temperature or overnight at 4°C. The solution was removed and the slides were dried carefully in air; the usage of a Kleenex which sucks the liquid of the slide is very useful and careful. Next, 50µl of the first antibody in PBS containing 10% FCS were pipetted onto the cells and incubation was for 1 to 2 hours at room temperature. The first antibody was then removed by quickly washing three times and then three times for 10 minutes with PBS. The liquid was removed from the slides as described above and then, 50 µl of second antibody in PBS containing 10% FCS were pipetted onto the cells and incubated 1 to 2 hours at room temperature. Following further extensive washings exactly as described above, cells were finally mounted on glass slides with Mowiol 4-88 (Calbiochem, USA) and were dried for at least one hour before the confocal microscopy examination.

First Antibody	Type/Species	Dilution	Comment
α-15.5K	Polyclonal rabbit	1:200	Stains 15.5K
α-NOP56 antibody	Polyclonal rabbit	1:500	Stains NOP56
P80 (coilin)	Polyclonal rabbit	1:1000	Stains Cajal bodies
α-HA antibody	Mouse monoclonal antibody	1:2000	Stains HA-tagged proteins
α-hPrp4 ("Roy")	Rabbit serum	1: 500	Stains hPrp4
α-SC35	Mouse monoclonal antibody	1:1000	Stains splicing factor SC35

Secondary Antibody	Type/Species	Dilution
Alexa 488-coupled antibody	Monoclonal, goat-anti-mouse	1:500
Alexa 647-coupled antibody	Monoclonal, goat-anti-mouse	1:500
Texas Red-coupled antibody	Monoclonal, goat-anti-rabbit	1:500

3.2.6.3. Transient transfection of mammalian cells

For analysing the localisation of the EYFP-15.5K protein (4.2), HeLa cells were grown over night, fixed and stained as described above. For transfection, HeLa (SS6) cells were cultured in 24-well plates and grown on coverslips overnight until 40-80% confluency and the transfection was performed using the Lipofectamine 2000 reagent (Invitrogen, Netherlands) according to the supplier's protocol.

The day before transfection, cells were trypsinized, counted, and plated the in 24-well plates at 2×10^5 cells per well so that they would be 80-90% confluent on the following day for the transfection. Cells were plated in their normal growth medium containing serum and antibiotics (Penicillin/Streptomycin). For each well of cells to be transfected, 1-5 μg of plasmid DNA were diluted into 50 μl of OptiMEM 1 medium. In addition, for each well of cells, 1.5 μl of Lipofectamine 2000 reagent were diluted into 50 μl OptiMEM 1 medium and the mixture was incubated for 5 minutes at room temperature. Once the Lipofectamine 2000 reagent was diluted, it had to be combined with the plasmid DNA within 30 minutes. This dilution was prepared as a master mix for multiple wells.

The diluted DNA was combined with the diluted Lipofectamine 2000, and the mixture was incubated at room temperature for 20 minutes to allow DNA- Lipofectamine complexes to form. Growth medium was then removed from cells and 0.5 ml of serum-free medium were added to each well. Next, the DNA- Lipofectamine complexes (100 μl) were added directly to each well and mixed gently by rocking the plate back and forth.

Transfected cells were incubated at 37°C in a CO₂ incubator for 4-5 hours. Then, 0.5 ml of growth medium containing 10% FCS, were added. Cells were incubated ~16 hours post-transfection and the expression and co-localisation of the product of the transfected gene analysed by immuno-fluorescence microscopy (3.2.6.1). For the preparation of small-scale nuclear extracts (3.2.5.4) the protocol was scaled up. The scale-up requirements were determined by estimating the expression efficiency and the needed amount of extract.

3.2.7. Special Methods

3.2.7.1. Electrophoretic Mobility Shift Assay (EMSA)

Binding specificity of the 15.5K protein mutants with the U4 snRNA and the U14 snoRNA (see 4.1.1), and the interaction of the U4/U6 snRNP-specific protein hPrp31 with the U4 snRNA were investigated by Electrophoretic Mobility Shift Assay (EMSA) (see 4.3.2).

The Electrophoretic Mobility Shift Assay, variously also called Gel Shift, or Band Shift Assay, is a technique for studying protein:RNA interactions. The assay is based on the fact that complexes of protein and RNA migrate through a non-denaturing polyacrylamide gel more slowly than free RNA fragments or oligonucleotides.

Approximately 0.03 pmol ³²P-labeled U14 or U4 snRNA transcribed RNA or RNA oligonucleotides were incubated with 25 pmol recombinant protein 15.5K and/or 50 pmol MBP-hPrp31 or 250 pmol MBP-hPrp31 deletion mutants in the presence of 10 µg of *E. coli* tRNA (Boehringer, Mannheim) for 1 hour at 4°C in a final volume of 20 µl buffer B. Subsequently, RNA and RNA-protein complexes were resolved on a 6% (80:1) native polyacrylamide gel containing 0.5× TBE and visualised by autoradiography as described (Reuter *et al.*, 1999). Additionally, quantification was performed on a Phosphoimager.

6% Gel solution

12 ml Gel A (30% Acrylamide)
2,25 ml Gel B (2% Bisacrylamide)
3 ml 10× TBE
ad 60 ml with dH₂O
750 µl APS (10% stock)
37,5 µl TEMED

5× Heparin loading dye

0.5 x TBE
5 µg/µl Heparin
50% Glycerine
0.25% Bromphenol blue

Buffer B

50 mM Tris/HCl pH 8.0
150 mM NaCl
1 mM EDTA
1 mM dithiothreitol (DTT)
2% Triton X-100

3.2.7.2. GST pull-down assay

Protein-protein interactions within the U4/U6 snRNP (see 4.1.2) and the box C/D snoRNP (see 4.1.6) were investigated by GST pull-down. The pull-down assay is a simple

technique to test the interaction between a tagged protein and another interaction partner which can be a protein or an RNA molecule. The GST-tagged bait protein, purified from an appropriate expression system (see 3.2.2.4), is immobilized on a glutathione affinity gel. The bait serves as the secondary affinity support for identifying new protein partners or for confirming a previously suspected protein partner of the bait. Prey protein can be obtained from multiple sources including recombinant purified proteins, nuclear extract or *in vitro* transcription/translation reactions (see 3.2.1.17). Protein-RNA and protein-protein interactions can be visualized by SDS-PAGE and associated detection methods depending on the sensitivity requirements of the interacting proteins. These methods include Western blotting, ³⁵S-radioisotopic detection or the co-precipitation of a ³²P-labeled *in vitro* transcribed RNA which is dependent on the interaction of the bait and prey protein or RNA.

For instance, the binding of hPrp31 to the U4 snRNA was assayed by GST pull-down by incubating purified recombinant GST-hPrp31 with ³²P-labeled *in vitro* transcribed U4 snRNA in the presence or absence of recombinant, purified 15.5K or mutant 15.5K. Complexes were purified using glutathione sepharose and U4 snRNA association analysed by PAGE and autoradiography.

To assay hU3-55K binding to 15.5K, *in vitro* translated ³⁵S-labeled hU3-55K (see 3.2.1.17) was incubated with either GST or GST-15.5K. Complexes were isolated using glutathione sepharose and the co-purifying hU3-55K analysed by SDS-PAGE and autoradiography.

The procedure includes the following steps. Per reaction 20 µl of glutathione sepharose beads were washed three times with 500 µl PBS (pH 8.0) and next incubated for 1 hour at 4°C with blocking buffer (see below). Beads were washed again three times and are equilibrated with reaction buffer (see below).

For assaying the interaction of the GST-tagged U4/U6-specific hPrp31 with the 15.5K protein, protein GST-hPrp31 is pre-bound to the glutathione sepharose by incubating 30 pmoles of GST-hPrp31 with 20 µl glutathione sepharose beads for 1 hour at 4°C in 200 µl of reaction buffer on a head-over-tail rotor. Non-bound protein is removed by washing the beads three times with 500 µl reaction buffer. Next, bound hPrp31 protein is incubated with ³²P-labeled *in vitro*-transcribed U4 snRNA (see 3.2.1.16) in the presence or absence of 15 pmol of recombinant, purified 15.5K or 15.5K mutant. Complexes were purified using glutathione sepharose, and U4 snRNA association was analyzed by polyacrylamide gel electrophoresis (PAGE) and autoradiography.

3 Materials and Methods

To assay hU3-55K binding to 15.5K, *in vitro*-translated ³⁵S-labeled hU3-55K (see 3.2.1.17) was incubated with either GST or GST-15.5K according to Granneman *et al.* (2002). Complexes were isolated using glutathione sepharose, and the co-purifying hU3-55K was analyzed by sodium dodecyl sulfate SDS-PAGE and autoradiography. All data from pull-down experiments were quantified using either a phosphorimager or scanned autoradiographs. Where necessary, the signals were normalized relative to either the input or supernatant for that particular sample.

Blocking Buffer	Reaction Buffer
20 mM Hepes/HCl, pH 7.9	20 mM Tris/HCl, pH 7.5
300 mM KCl	100 mM NaCl
0.01% Triton X-100	0.1% Triton X-100
10 mg/ml tRNA	
0.5 mg/ml BSA	
20 mg/ml Glycogen	

3.2.7.3. Site-directed mutagenesis of proteins

Site-directed mutagenesis was performed using the QuikChange Site-Directed Mutagenesis Kit (Stratagene) according to the manufacturer's instructions. The PCR-based site-directed mutagenesis allows site-specific mutations to be incorporated in double-stranded plasmid DNA.

Synthetic oligonucleotides, or primers, complementary to opposite strands of the vector containing the desired mutation(s) are annealed to the target region. During the PCR reaction the mutant oligonucleotides are extended using a plasmid DNA strand as the template by the PfuTurbo DNA polymerase introducing the desired point mutations. First, oligonucleotides containing the desired point-mutation were designed. Oligonucleotides are favourable between 25 and 45 bases in length and with a melting temperature (T_m) of $\geq 75^\circ\text{C}$. Sense and anti-sense primers should have a similar melting temperature, should have a minimum GC content of 40% and should terminate in one or more C or G bases. The primers designed for introducing point-mutations for studying protein-protein interactions in this work are listed in 3.1.13.

Following, the product is treated with the *DpnI* endonuclease, which is specific for methylated and hemi-methylated DNA and is used to digest the parental DNA template and to select for the mutation-containing synthesized DNA. The DNA isolated from more or less all

E. coli strains is dam methylated and therefore susceptible to *DpnI* digestion. Next, the vector DNA containing the desired mutations is transformed into XL1-Blue supercompetent cells.

Mutant strand synthesis reaction:

Reaction	Stock
5 µl reaction buffer	10×
5–50 ng dsDNA template	
125 ng primer 1	
125 ng primer 2	
1 µl dNTP mix	
ad 50 µl ddH ₂ O	
1 µl PfuTurbo® DNA polymerase	2.5 U/µl

Cycling Parameters used in this work:

Step	Temperature	Time
Denaturing	95°C	30 seconds
Annealing	55°C	1 minute
Elongation	68°C	13 minutes
Cycles:	18	

3.2.7.4. UV cross-linking

For UV cross-linking of *in vitro* reconstituted hPrp31-15.5K-U4 snRNA complexes (4.3.3), complexes containing 0.3 pmol labelled RNA were prepared in a final volume of 20 µl as described in section 3.2.7.1. UV cross-linking of *in vitro* reconstituted hPrp31-15.5K-U4 snRNA complexes was carried out in 96 well microtiter plates using a UV-B light source at 254 nm (4x8W, G8T5, Herolab) at a distance of ~3 cm. Samples were cooled during illumination by putting the 96 well microtiter plates on an ice. To check whether a formed product derived only by the covalent bonding of the protein to the RNA after cross-linking, control samples were either digested by RNase T1/A or Proteinase K using 3 µg RNase A and T1 for 1 hour at 37°C. Then, samples were directly analysed by SDS-PAGE on 10% gels. Proteins cross-linked to the RNA were visualised by autoradiography.

3.2.7.5. Preparation of RNA Duplexes

The U4/U6 snRNA duplexes used for investigating the effect of mutant 15.5K protein on the association of the hCypH/hPrp3/hPrp4 with the U4/U6 snRNP (4.1.3) were formed by annealing 20 nM ³²P-labeled U6 snRNA oligonucleotide (nucleotides 58-87 of the U6 snRNA; see 3.2.1.17) with 200 nM un-labeled U4 snRNA in buffer A (see below) as

3 Materials and Methods

described in Nottrott *et al.* (2002). Samples were incubated at 80°C for 1 min, cooled slowly to 30°C and placed on ice.

Buffer A
50 mM Tris-HCl pH 7.5
150 mM NaCl
5 mM MgCl ₂
1 mM EDTA
1 mM DTT

3.2.7.6. Transient transfection of plasmid DNA and/or double-stranded siRNAs into HeLa cells via nucleofection

The effect of hPrp31 Retinitis Pigmentosa mutations on localisation of protein hPrp31 and protein hPrp4 was analysed by transfecting HeLa cells simultaneously with HA-tagged hPrp31 protein wild type and mutants, and siRNA duplexes against the 3' UTR of protein hPrp31. Attempts to transfect cells only with HA-hPrp31 wild type and mutants lead to a low expression of the protein. The Nucleofector technology offered the possibility of gently transfecting cells with plasmids and siRNAs simultaneously, whereas transfection using the Bio-Rad Electroporator caused high cell mortality and low transfection/expression efficiency.

For the transfection of HeLa cells the Cell Line Nucleofector Kit R was used. Cells for transfection were in the logarithmic phase (~50-60% confluency). Two cell culture flasks (75 cm² growth area) were taken, corresponding to 5-6 × 10⁶ cells. Cells were washed with PBS (pH 7.4) and trypsinized with 3 ml of Trypsin-EDTA. Cells from the two cell culture flasks were combined (2 × 10⁶ cells/ml in 6 ml Trypsin-EDTA) in a Falcon tube and the volume was filled up to 10 ml by the addition of DMEM/10% FCS/Penicillin/Streptomycin to obtain 1.2 × 10⁶ cells/ml. Next, 1 × 10⁶ - 5 × 10⁶ cells were taken for each cuvette to be used and centrifuged at 200 × g for 10 minutes. The supernatant was removed and cells were resuspended in 100 µl Nucleofector solution. 1-5 µg of plasmid DNA (1-5 µl in ddH₂O or TE buffer (3.2.1.2)) and/or 0.5-3 µg siRNA duplexes were added to the 100 µl cell suspension and transferred to the cuvettes supplied. For transfection of HeLa cells with both plasmid DNA and siRNAs, Nucleofector program I-13 was chosen, since it was useful for a high transfection efficiency. Following transfection, 500 µl pre-warmed culture medium were added to the cuvette, and the cell suspension transferred to a 12-well plate (1.5 ml/well). Cells were grown at 37°C under standard conditions for 48 hours till the knock down of hPrp31 and

expression of the HA-hPrp31 were efficient. The knock-down/add-back effect was analysed by immuno-fluorescence microscopy, western blot or immunoprecipitation studies.

4. Results

4.1. Protein-protein and protein-RNA contacts both contribute to the 15.5K protein-mediated assembly of the U4/U6 snRNP and the box C/D snoRNPs

4.1.1. Mutation of conserved amino acids on the surface of protein 15.5K not involved in RNA binding

The high sequence conservation of protein 15.5K suggests that this protein may play additional roles in the function and/or assembly of one or more of the 15.5K-containing RNP complexes. Indeed, conserved amino acids may be important for protein-protein interactions essential for the formation of the RNP complexes.

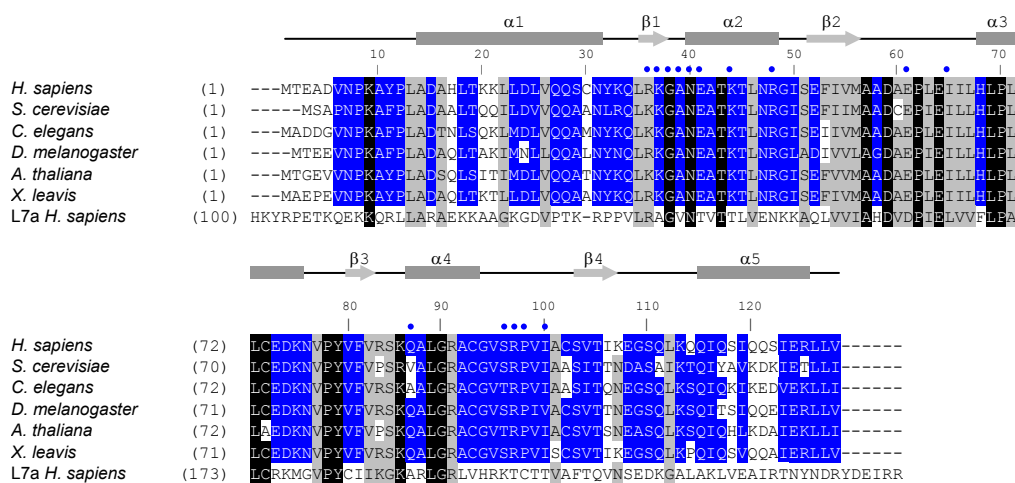


Figure 4-1 Sequence alignment of the human 15.5K protein with highly homologous proteins.

Amino-acid alignment of protein 15.5K from human (*H. sapiens*), *Saccharomyces cerevisiae* (Snu13p), *Caenorhabditis elegans* (Accession no. Q21568), *Drosophila melanogaster* (Accession no. GH03082), *Arabidopsis thaliana* (Accession no. A71421), and *Xenopus laevis* (Accession no. AAH46579) with the human ribosomal protein L7a sequence using the ClustalV program. Conserved residues are indicated by grey boxes and are grouped as described in (Schulz and Schirmer, 1979). Identical and conserved residues are indicated in white on black boxes and in black on grey boxes, respectively. Residues specifically conserved in protein 15.5K are depicted in white on blue boxes. Amino-acid positions are indicated on the left. The secondary structure of the human 15.5K protein (Vidovic *et al.*, 2000) is indicated above the alignment, and amino acids involved in RNA-binding are indicated by blue circles.

In order to test this possibility, conserved amino acids at the surface of protein 15.5K were identified that could be mutated in order to test their function in the assembly of the various RNPs. Conserved amino acids were identified from a sequence alignment using

sequences of homologous, but not functionally related, human L7a ribosomal protein in order to indicate the amino acids that are highly conserved in this family of RNA-binding proteins (Figure 4-1; indicated in black and grey).

The remaining conserved amino acids are therefore specific to protein 15.5K (Figure 4-1; indicated in blue). By using the crystal structure of protein 15.5K bound to the 5' stem-loop of the U4 snRNA (Vidovic *et al.*, 2000) clusters of conserved amino acids present at the surface of the protein were identified and mutated (see Materials and Methods and Figure 4-2).

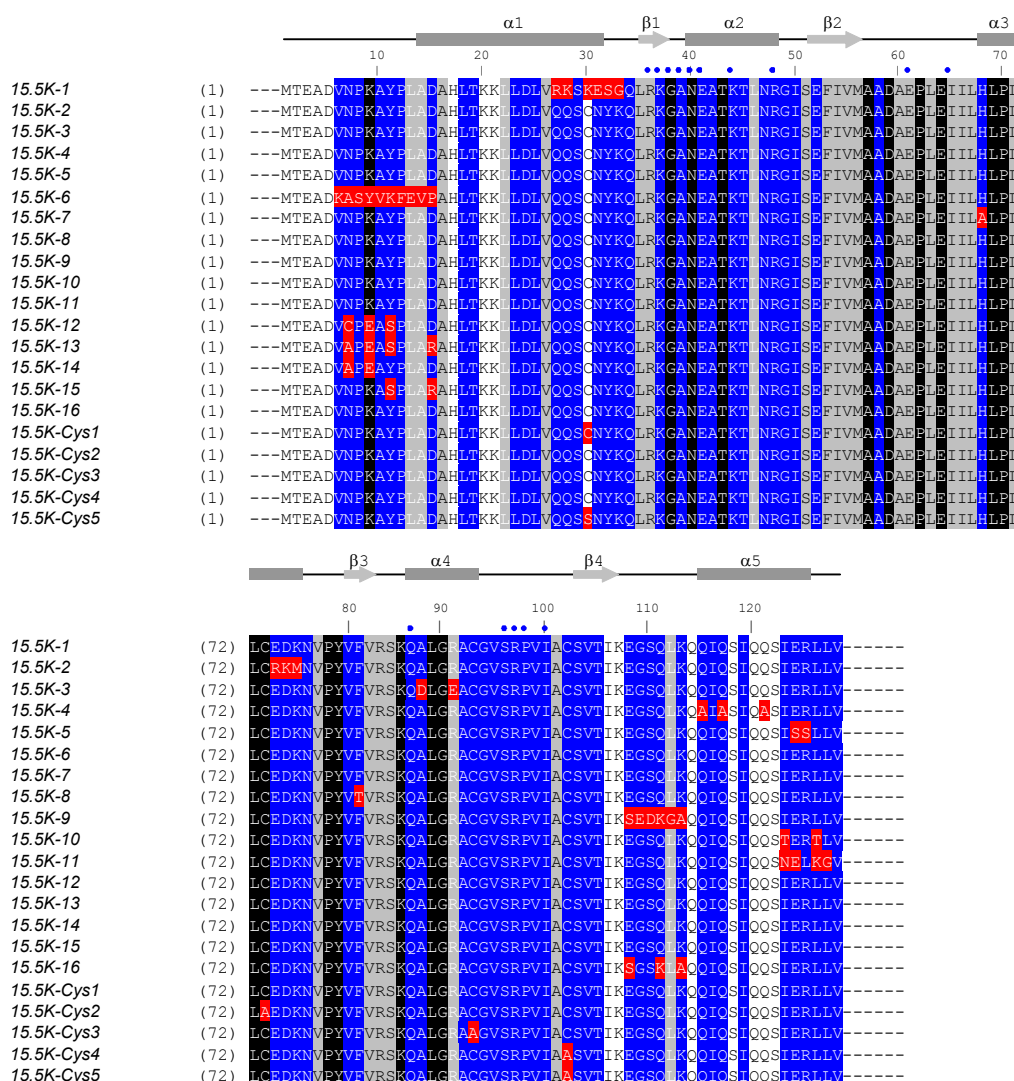


Figure 4-2 Conserved amino acids present at the surface of the protein were identified and mutated. Mutated amino acids were highlighted in red in the sequence alignment. Amino acids are shaded as described in Figure 4-1.

4 Results

Note that mutations were not made in the conserved amino acids known to be involved in RNA binding or to be in close proximity to the RNA-binding pocket (Figure 4-3) (Vidovic *et al.*, 2000). In addition, by replacing the conserved residues with amino acids present at the corresponding positions of structurally similar proteins, such as the human L7a protein, it was hoped that the changes would not disrupt the overall structure of the protein. However, only 5 of the 21 mutants originally constructed (Figure 4-2) were soluble after overexpression in *E. coli*. (Soluble mutants are shown in Figure 4-3 in the 15.5K crystal structure). The insoluble mutants included both single amino-acid changes and larger mutations, and there was no obvious explanation regarding which mutants were soluble and which were not. However, it should be emphasised that the soluble mutants cover the main conserved regions of the protein surface not involved in RNA-binding (see Figure 4-3). The only conserved region not covered in this series of mutations was the N terminus. Unfortunately, proteins containing either point mutations or larger multi-amino-acid changes in this region were completely insoluble.

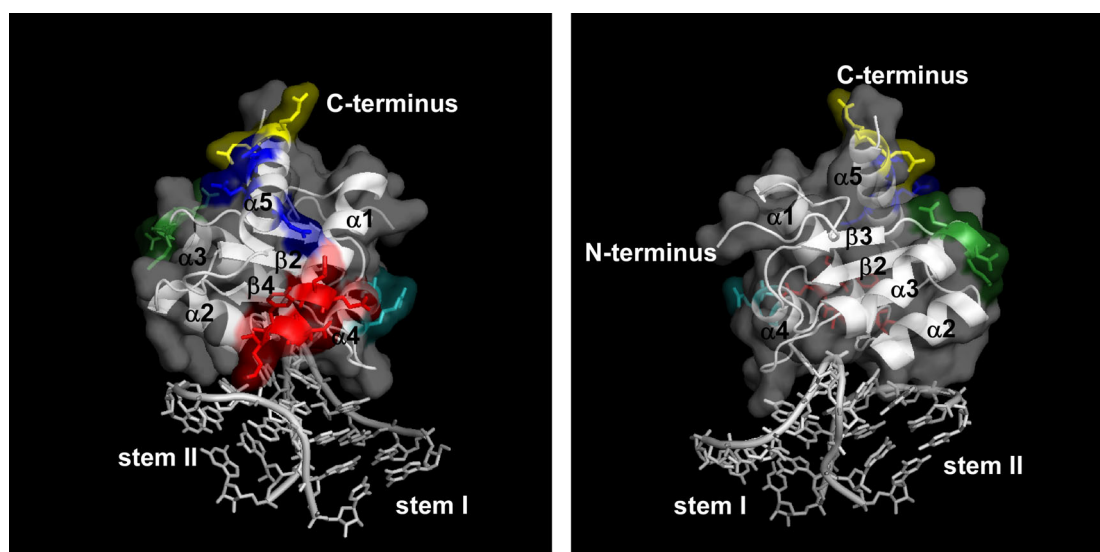


Figure 4-3 Mutations indicated in the 15.5K-U4 crystal structure.

The positions of the residues targeted for mutagenesis on the surface of protein 15.5K are depicted using the crystal structure of protein 15.5K bound to the 5' stem-loop of the U4 snRNA (Vidovic *et al.*, 2000). The surface plot of protein 15.5K is shown in white and the U4 snRNA is shaded grey. The positions of the amino acids targeted for mutagenesis are indicated in red (mutant 15.5K-1), green (15.5K-2), turquoise (15.5K-3), blue (15.5K-4), or yellow (15.5K-5).

One important aspect of this approach is that the mutant proteins should not affect RNA-binding. Even though care was taken to avoid selecting regions close to the RNA-binding domain, it was important for the various snRNP and snoRNP assembly assays that the mutants bind the RNA with an affinity and specificity similar to that of the wild-type protein. In order to test this, purified recombinant proteins were incubated with ^{32}P -labelled U4

(Figure 2-4), U3 box B/C snoRNA (Figure 2-13), U14 box C/D snoRNA (Figure 2-13), or mutant U14 RNAs box C/D snoRNA (Watkins *et al.*, 2000), and the resulting complexes were then resolved on a native polyacrylamide gel. This demonstrated that each of the mutant proteins bound the U4 and U14 RNAs with specificity similar to that seen for the wild-type protein (Figure 4-4 C, and data not shown). Importantly, titration experiments to measure the affinity of U4, U14, and U3-box B/C RNA (Watkins *et al.*, 2000) binding showed that all of the mutant proteins bind these RNAs with a K_d value that is basically the same as that of the wild-type protein (< 2-fold variation; data not shown). Interestingly, the migration behaviour of the 15.5K-RNA complex in the native gel was slightly different for each mutation. It appears likely that this is due to changes to the surface properties of the protein, which in turn affect the migration behaviour in native gels.

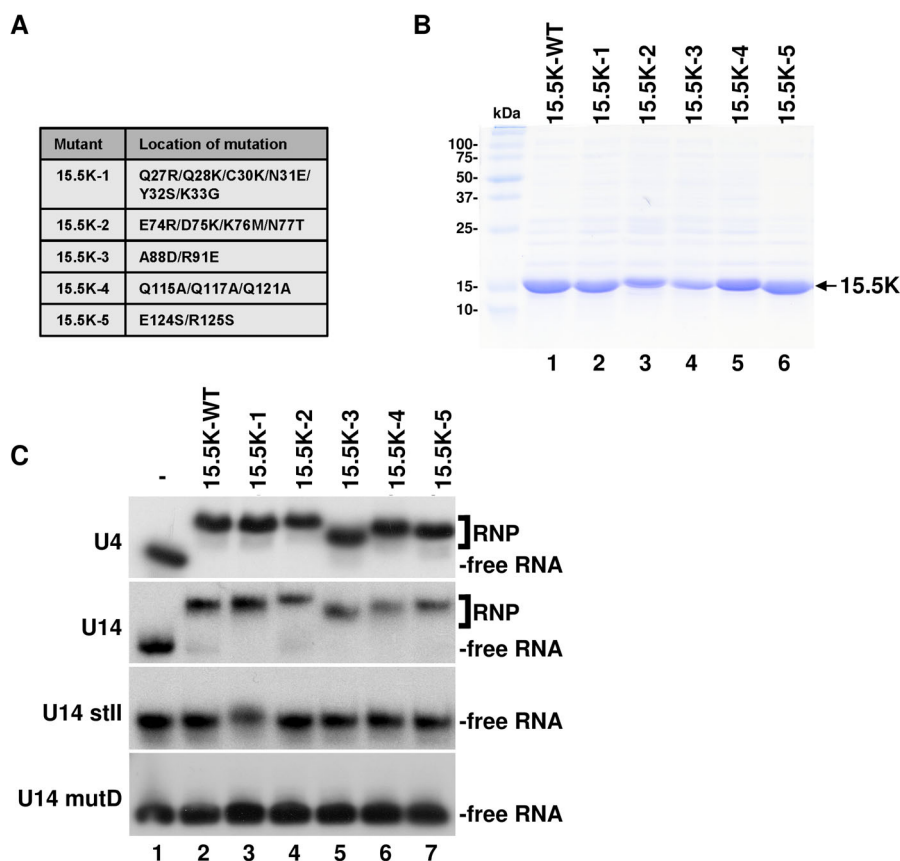


Figure 4-4 RNA-binding by soluble mutants of protein 15.5K.

A. Table of soluble mutants. **B.** SDS PAGE of 15.5K mutants. **C.** Gel mobility-shift analysis of the interaction of recombinant protein 15.5K and its mutants with U4, U14 and U14 mutants. The mutant proteins were incubated with ^{32}P -labelled snRNA prepared by transcription *in vitro* or snoRNA transcripts and the resulting RNA-protein complexes were resolved on a 6% native polyacrylamide gel and visualised by autoradiography. The identity of the protein used is indicated above each lane. The position of the protein-RNA complex (RNP) and the free RNA are indicated on the right. The RNA used is indicated on the left.

Importantly, none of the proteins bound the U14 mutD (GA to GC in the box D) and U14 stII RNAs (stem II: U-U, G-C, A-U changed to U-U, C-C, G-U), in which the conserved

4 Results

GA nucleotides and stem II of the U14 snoRNA box C/D motif have been mutated, respectively (Watkins *et al.*, 2002). Therefore, in creating the mutants neither the affinity nor specificity of RNA-binding was changed; this is consistent with the fact that the changed amino acids are not part of the RNA-binding domain.

4.1.2. Conserved amino acids on the surface of protein 15.5K are required for hPrp31 association with the U4 snRNA

Next, it was of interest to determine whether any of these mutations block the formation of 15.5K-dependent RNP complexes. As a first approach, the ability of these mutants to support hPrp31 binding to the U4 snRNA was investigated. Recombinant 15.5K protein (either wild-type or mutant) was incubated with GST-hPrp31 (Figure 4-5 B) and ³²P-labelled U4 snRNA (Figure 4-5 A). Importantly, for both, wild-type and mutant 15.5K proteins, the amount of protein used, was shown to be in excess of that required to bind fully the RNA in the experiment. After incubation, GST-hPrp31 was isolated using glutathione Sepharose, and bound RNAs were analysed by polyacrylamide gel electrophoresis. Consistent with earlier work (Nottrott *et al.*, 2002), protein 15.5K is required for the co-precipitation of the U4 snRNA with GST-hPrp31 (Figure 4-5 C; cf. lanes 1 and 2). Quantitative measurement revealed that mutants 15.5K-1, 15.5K-3, 15.5K-4 and 15.5K-5 also supported hPrp31 association with the U4 snRNA, and with similar efficiency: only 15.5K-1 showed a slight reduction (85%) compared with the wild-type protein (taken as 100%, Figure 4-5 C; cf. lane 2 with lanes 3, 5, 6, and 7). In contrast, a fourfold reduction of U4 snRNA association with hPrp31 was observed with 15.5K-2 (Figure 4-5 C, lane 4). Importantly, electrophoretic mobility-shift analysis (EMSA) of the binding reactions showed that all mutant proteins bound the U4 snRNA demonstrating (i) that the lack of 15.5K-2-recruitment of hPrp31 is not due to a lack of RNA-binding under these conditions and that (ii) each of the proteins is stable under the reaction conditions used (data not shown).

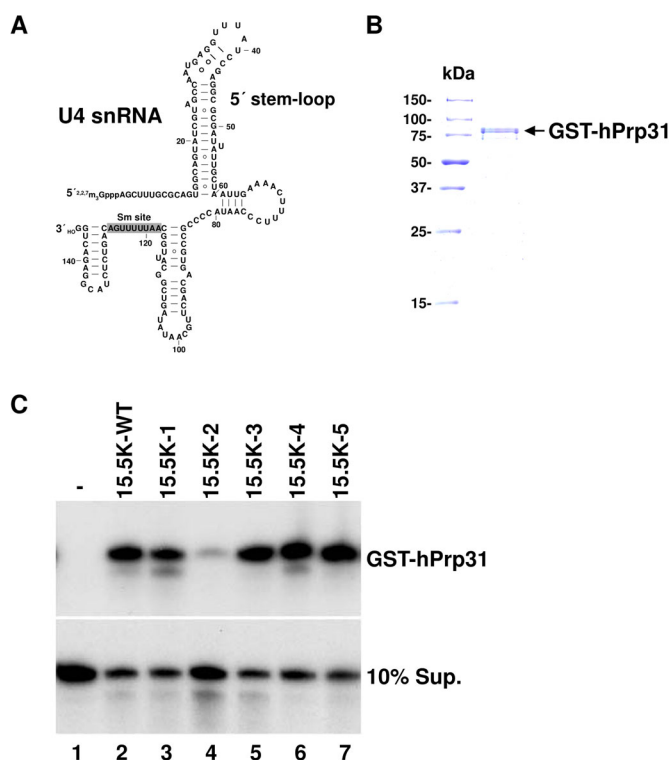


Figure 4-5 Binding of hPrp31 to the U4 snRNA requires residues in alpha helix 3 of 15.5K.

A. Postulated secondary structure of the single U4 snRNA (modified from (Myslinski and Branlant, 1991; Achsel *et al.*, 1999). The Sm protein-binding site is depicted by grey shading. **B.** SDS PAGE of GST-hPrp31. GST-hPrp31 was stained with Coomassie blue. **C.** GST-hPrp31 was incubated with ^{32}P -labelled U4 snRNA in the presence (lanes 2, 3, 4, 5, 6 and 7) or absence (lane 1) of either wild-type or mutant 15.5K. GST-hPrp31 was isolated by using glutathione resin, and the bound RNA was extracted and ethanol-precipitated. The bound RNA (upper panel; GST-hPrp31) and unbound RNA (lower panel; 10% Sup.) was analysed on a denaturing 8% polyacrylamide/7 M urea gel and visualised by autoradiography. The identity of the 15.5K protein used is indicated above each lane.

Since 15.5K-2 bound to the U4 snRNA on its own (see Figure 4-4 C, lane 4) the lack of hPrp31 recruitment must be due to the mutation of surface amino acids in α helix 3 and the adjacent loop $\alpha 3$ – $\beta 3$ (see Figure 4-3). The fact that this region of the protein is important for the recruitment of hPrp31 in this simple three-component system supports the hypothesis that protein 15.5K mediates the assembly of RNP complexes, in part, through protein-protein contacts.

4.1.3. Numerous mutations on the surface of protein 15.5K disrupt the binding of the CYPH/hPrp4/hPrp3 complex to U4/U6 snRNA

After the demonstration that changes in the surface amino acids can affect the binding of hPrp31 to U4 snRNA, the question of whether the mutations would support the binding of the CypH/hPrp4/hPrp3 heteromeric complex to U4/U6 snRNA was investigated. To answer

4 Results

the question, the reconstitution assay developed by Nottrott *et al.* (2002) was used. Briefly, recombinant 15.5K protein was incubated together with (i) radiolabelled U4/U6 snRNA duplex, in which the minimal fragment of U6 snRNA required for CypH/hPrp4/hPrp3 binding was radiolabelled (Figure 4-6 A), and (ii) biochemically purified CypH/hPrp4/hPrp3 protein complex (Figure 4-6 B). The assembled complexes were then immunoprecipitated using anti-hPrp4 antibodies, and the co-precipitated RNAs were analysed by polyacrylamide gel electrophoresis.

Consistent with previous findings (Nottrott *et al.*, 2002), the U4/U6 snRNA duplex was co-precipitated by anti-hPrp4 antibodies when incubated with CypH/hPrp4/hPrp3 and 15.5K, but not when it was incubated with CypH/hPrp4/hPrp3 alone (Figure 4-6; lanes 1 and 2). Analysis of the mutants in this assay revealed that 15.5K-1 supported the U4/U6 snRNA-CypH/hPrp4/hPrp3 interaction to 80% of the level seen with the wild-type protein (Figure 4-6; lane 4). In contrast, a greater than five-fold reduction in complex formation, relative to the wild-type protein, was observed using 15.5K-3 and 15.5K-4 (Figure 4-6; lanes 4 and 7) and the interaction was effectively abolished in the presence of 15.5K-2 and 15.5K-5 (lanes 5 and 8). Therefore, four of the five regions – including α helix 3 and the adjacent loop α 3- β 3, α helix 4 and α helix 5 – are required for the interaction between U4/U6 snRNA and the CypH/hPrp4/hPrp3 complex. This suggests that significant contacts are made between one or more of the proteins in the CypH/hPrp4/hPrp3 complex and protein 15.5K that are important for U4/U6 snRNP formation.

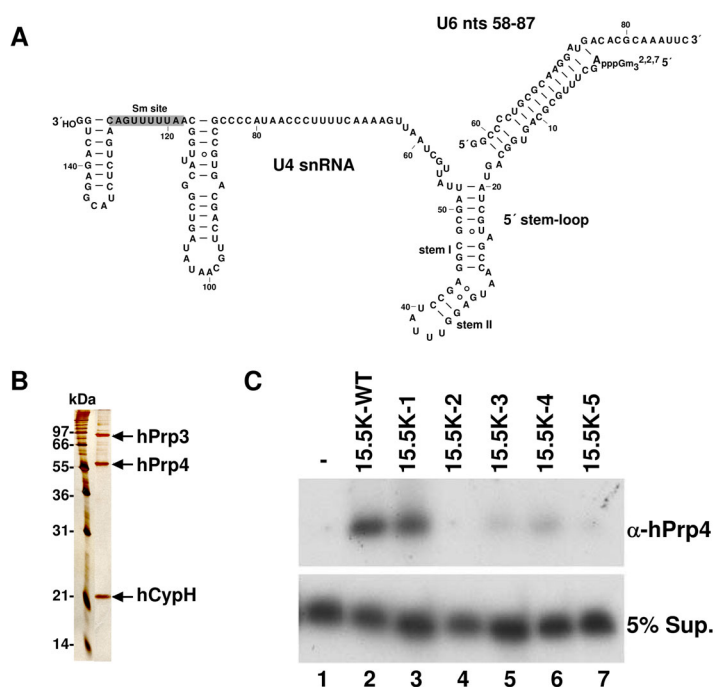


Figure 4-6 Association of CypH/hPrp4/hPrp3 to the U4/U6 snRNA requires several regions on the surface of 15.5K.

A. The secondary structure of the U4 snRNA in complex with the U6 snRNA nucleotides 58-87. The Sm protein-binding site is depicted by grey shaded capitals. (modified from Myslinski and Branlant (1991) and Achsel *et al.* (1999)). **B.** SDS PAGE of the purified, native CypH/hPrp4/hPrp3 protein complex. CypH/hPrp4/hPrp3 complex was visualized by silver staining. **C.** Purified CypH/hPrp4/hPrp3 complex was incubated with U4/U6 snRNA duplex (U4 snRNA base-paired with ^{32}P -labelled U6 nucleotides 58-87) in the presence (lanes 2-7) or absence (lane 1) of wild-type or mutant 15.5K. The CypH/hPrp4/hPrp3 complex was then immunoprecipitated using anti-hPRP4 antibody; the co-precipitated RNA (upper panel; α -hPRP4) and the RNA present in the supernatant (lower panel; 5% Sup.) were analysed on a denaturing 8% polyacrylamide/7 M urea gel and visualized by autoradiography. The identity of the 15.5K protein used is indicated above each lane.

4.1.4. Box C/D snoRNP assembly requires multiple regions on the surface of protein 15.5K

Next, attention was turned to the assembly of the box C/D snoRNP. For this, a system was used that was established earlier to investigate the assembly of the U14 snoRNP (Watkins *et al.*, 2002). Briefly ^{32}P -labelled U14 snoRNA (Figure 4-7 A), prepared by transcription *in vitro*, was incubated with HeLa nuclear extract and snoRNP assembly determined by immunoprecipitation using antibodies specific to the core box C/D proteins and the assembly factors TIP48 and TIP49. In this system, the binding of the endogenous protein 15.5K in the extract could be selectively blocked by introducing an excess of the 5' stem-loop of the U4 snRNA (SL1, Figure 4-7 B) (Watkins *et al.*, 2002). Box C/D snoRNP assembly in the blocked extract was restored by the addition of recombinant protein 15.5K. Therefore, this approach was used to determine the ability of the mutant proteins to support box C/D snoRNP assembly. Protein-binding was subsequently investigated by using anti-fibrillarin, NOP56,

4 Results

NOP58, TIP48, and TIP49 antibodies; the co-precipitated RNAs were analysed by polyacrylamide gel electrophoresis.

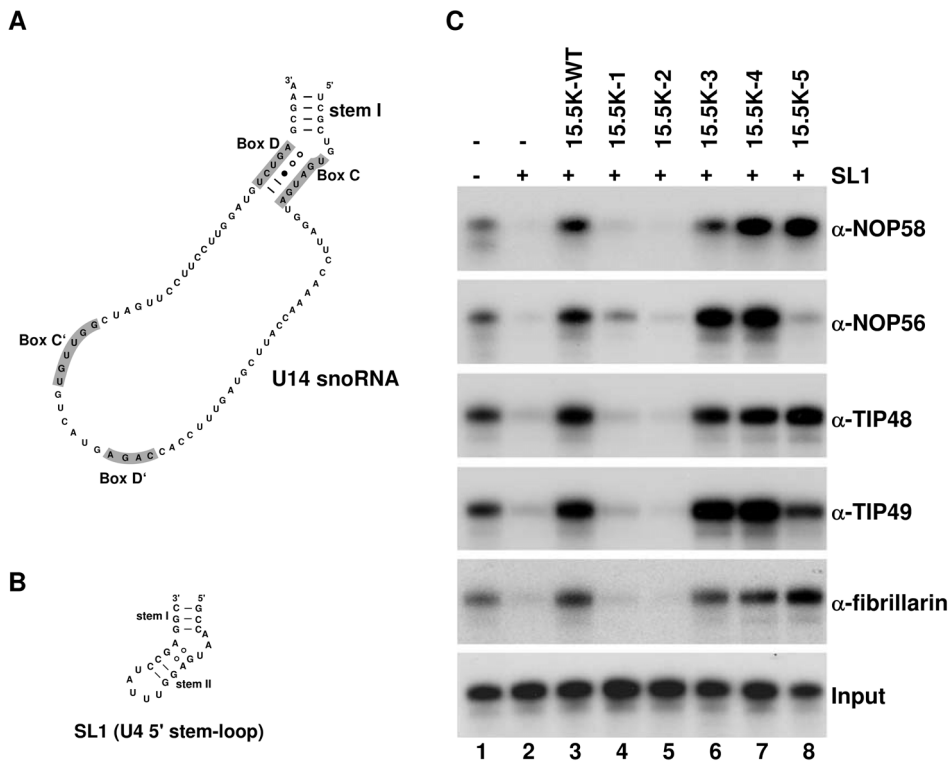


Figure 4-7 Several regions on the surface of protein 15.5K are required for box C/D snoRNP assembly.

A. Secondary-structure model for the U14 box C/D snoRNA base-paired with the 18S pre-rRNA (according to Kiss (2001)). The consensus sequences for boxes C, C', D, and D' are indicated by the grey shading. **B.** U4 snRNA 5' stem-loop RNA oligonucleotide (SL1) used to block the endogenous 15.5K. **C.** HeLa nuclear extract was pre-incubated either with 800 pmol of U4-SL1 RNA oligonucleotide (+) or with buffer (-). Radiolabelled U14 snoRNA was subsequently added in the presence (lanes 2-8) or absence (lane 1) of wild-type or mutant 15.5K. The binding of individual snoRNP proteins was then assayed by immunoprecipitation. Bound RNAs were recovered and then separated on an 8% polyacrylamide/7M urea gel. Antibodies used for immunoprecipitation are indicated on the left. Input: 10% of the RNA after incubation in nuclear extract. The 15.5K protein used is indicated above each lane.

Consistent with previous observations (Watkins *et al.*, 2002), the addition of U4 SL1 RNA inhibited the assembly of box C/D snoRNP, while the binding of all proteins was restored by the addition of recombinant protein 15.5K (Figure 4-7 C, lanes 1-3). Similar levels of association of NOP56, NOP58, fibrillarin, TIP48, and TIP49 with the U14 snoRNA were also observed when the wild-type protein was replaced by either mutant 15.5K-3 or 15.5K-4 (Figure 4-7; lanes 6 and 7). In most cases, the level of precipitation was slightly higher than that seen for the wild-type protein, however, slightly reduced for fibrillarin and NOP58 (90% of wild-type levels) when mutant 15.5K-3 was used. In contrast, the binding of all proteins was either reduced by a factor greater than 20 or effectively abolished when mutants 15.5K-1 and 15.5K-2 were used in this assay (lanes 4 and 5). Interestingly, 15.5K-5 supported the binding of only a subset of the box C/D-associated proteins (lane 8). In the

presence of 15.5K-5, NOP58, TIP48, and fibrillarin, the association observed was equivalent to that seen with the wild-type protein, whereas the binding of TIP49 and NOP56 was either reduced (80% of wild-type levels) or effectively abolished (~2% of wild-type), respectively. These results imply that several regions of the 15.5K protein surface are important for box C/D snoRNP assembly, including amino acids in α helix 1 (15.5K-1), in α helix 3 and in the adjacent loop between α 3 and β 3 (see Figure 4-3) for complete box C/D snoRNP formation, and including amino acids in α helix 5 for the specific association of NOP56 and TIP49.

4.1.5. Alpha helix 4 of protein 15.5K is required for hU3–55K binding to the U3 snoRNA

Following the investigation of the effect of the mutations on the formation of U4 snRNP, U4/U6 snRNP and box C/D snoRNP, the assembly of the U3-specific box B/C RNP complex was addressed. It has already been shown, by using the U4 5' stem-loop as a competitor, that the binding of hU3–55K to the U3 B/C motif in nuclear extract is dependent on exogenous protein 15.5K (Granneman *et al.*, 2002). Therefore, this approach was used to investigate the ability of the 15.5K mutants to support hU3–55K binding. Briefly, ³²P-labelled U3 box B/C RNA (Figure 4-8 A) was incubated with nuclear extract that had been pre-treated with the U4 5' stem-loop RNA SL1 (see Figure 4-7 B), and then the extent of protein binding was determined by immunoprecipitation using anti-hU3–55K antibodies. Co-precipitated RNAs were then analysed by polyacrylamide gel electrophoresis. Consistent with earlier observations (Granneman *et al.*, 2002), addition of SL1 RNA inhibited the co-precipitation of the U3 box B/C snoRNA with anti-hU3–55K antibodies (Granneman *et al.*, 2002).

This interaction was restored by the addition of recombinant protein 15.5K. The ability of the mutant proteins to restore protein binding was then determined. The mutants 15.5K-1, 15.5K-2, 15.5K-4 and 15.5K-5 all effectively restored the association of the hU3–55K with the U3 box B/C RNA, i.e., to 90-100% of the wild-type level (Figure 4-8 B, lane 4, 5, 7, and 8, respectively). In contrast, protein 15.5K-3 resulted in a reduction in the association of the hU3–55K protein by a factor greater than 10 (lane 6). These results show that the conserved region of α helix 4, found on the protein surface, is important for interaction of hU3–55K protein with the U3 box B/C RNP complex.

4 Results

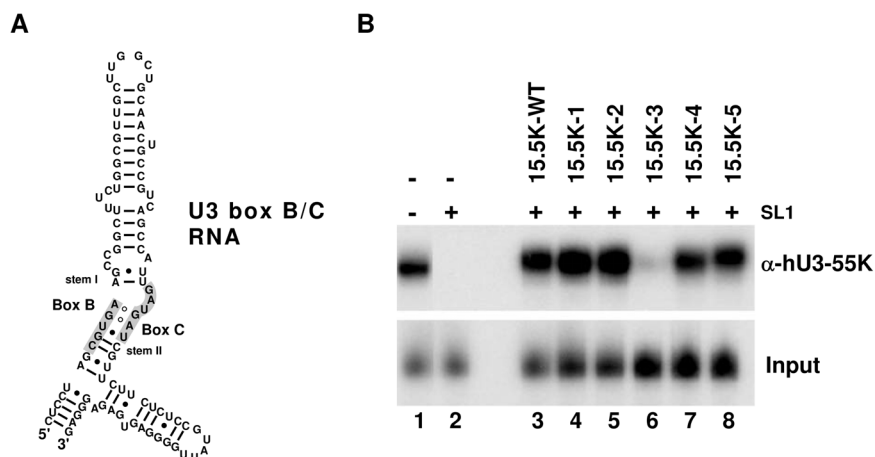


Figure 4-8. hU3-55K binding to the U3 box B/C motif requires a distinct region on the surface of protein 15.5K.

A. Schematic depiction of the U3 B/C RNA. **B.** HeLa nuclear extract was pre-incubated either with 800 pmol U4-SL1 RNA oligonucleotide (+) or with buffer (-). Radiolabelled U3 box B/C motif RNA was subsequently added in the presence (lanes 3-8) or absence (lanes 1 and 2) of recombinant protein 15.5K or mutant 15.5K. The binding of hU3-55K was then assayed by immunoprecipitation. Bound RNAs were recovered and then separated on an 8% polyacrylamide/7M urea gel. Input: 5% of the RNA after incubation in nuclear extract. The 15.5K protein used is indicated above each lane.

4.1.6. A direct interaction between proteins hU3-55K and 15.5K

In earlier work, an *in vitro* assembly system, using recombinant 15.5K and hU3-55K prepared by translation *in vitro*, was developed to analyse the assembly of the box B/C RNP complex (Granneman *et al.*, 2002). This system was used to investigate further the relative importance of the RNA and protein 15.5K in the recruitment of hU3-55K. GST-tagged 15.5K was incubated with ³⁵S-labelled hU3-55K (prepared by translation *in vitro*) in the presence or absence of box B/C RNA. GST-15.5K was isolated by using glutathione Sepharose, and its association with hU3-55K was determined by SDS polyacrylamide gel electrophoresis followed by autoradiography. As described previously (Granneman *et al.*, 2002), when 0.25 pmol GST-15.5K was used, co-purification of the hU3-55K was dependent on the presence of the box B/C RNA (Figure 4-9 A, lane 3 and 5). This amount of protein was also previously shown still to be capable of binding the U3 box B/C snoRNA in the absence of hU3-55K (Granneman *et al.*, 2002), indicating that the protein is stable in the absence of the U3-specific protein. However, increasing the amount of GST-15.5 (25 pmol) resulted in a significant co-precipitation of 15.5K in the absence of the B/C RNA (Figure 4-9 A, lane 6). Interestingly, under these conditions the binding of hU3-55K was stimulated more than 3-fold by the presence of the B/C RNA (Figure 4-9 A, lanes 4 and 6), suggesting that the full interaction is

mediated by both the RNA and 15.5K. The use of 25 pmol of GST alone failed to precipitate hU3–55K, showing that this interaction is specific (lane 2).

The observed interaction between protein 15.5K and protein hU3–55K was not susceptible to RNase A treatment of the translate (data not shown), suggesting that the result was not due to endogenous RNA present in the reticulocyte lysate.

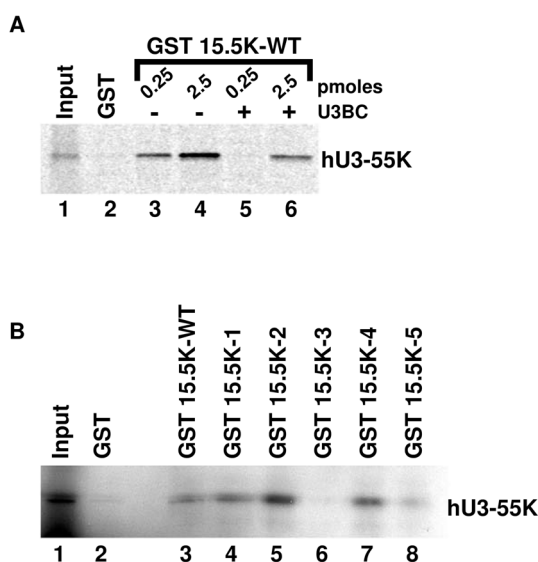


Figure 4-9 Mutant 15.5K-3 inhibits the binding of hU3–55K to the U3 box B/C in the absence of the corresponding RNA.

A. ^{35}S -labelled hU3–55K was incubated either with GST-15.5K (0.25 or 25 pmol) in the absence (-) or presence (+) of U3 box B/C RNA (lanes 3-6), or with 25 pmol GST (lane 2). Bound, radiolabelled proteins were purified using glutathione resin, resolved on a 12% polyacrylamide SDS gel and revealed by autoradiography. The amount of recombinant protein 15.5K used is indicated above each lane. Input; 10% of the input material. **B.** ^{35}S -labelled hU3–55K was incubated with 25 pmol of either wild-type or mutant GST-15.5K (lanes 3-8) or GST (lane 2). Bound, radiolabelled proteins were purified using glutathione resin and resolved on a 12% polyacrylamide SDS gel. Input; 10% of the input material. The identity of the GST-protein used is indicated above each lane.

If the interaction observed with the *in vitro* hU3–55K translate is the same as the proposed interaction, required for hU3–55K recruitment as observed in experiments using nuclear extract (see 4.1.5), then one would predict that 15.5K-3 (mutation in Alpha helix 4) should not bind this protein. Therefore, the ability of the 15.5K mutants to interact with hU3–55K was investigated. Protein hU3–55K (prepared by translation *in vitro*) was allowed to react with 25 pmol of the GST-tagged protein. The experiment showed that GST-15.5K-1, -2, and -4 associated with hU3–55K either to a level equivalent to that of the wild-type protein, or even more efficiently (~2-fold higher for GST-15.5K-2; Figure 4-9 B, cf. lane 2 and lanes 4, 5, and 7). GST-15.5K-5 bound hU3–55K to about 60% of the levels seen for the wild-type protein (Figure 4-9 B, lane 8). This suggests that, although this mutant does not function as efficiently as the wild-type protein, the mutation does not suppress significantly the

4 Results

association between hU3–55K and the 15.5K-box B/C RNA complex. However, GST-15.5K-3 showed a reduction in hU3–55K co-precipitation levels by a factor of ~20 (lane 6). These data therefore provide compelling evidence that a protein-protein interaction with 15.5K is important for the binding of hU3–55K to the U3 snoRNA.

4.2. Protein 15.5K is located in nucleoplasmic foci and is associated with the U4/U6 di–snRNP and the U3 snoRNA *in vivo*

4.2.1. The U4/U6 di–snRNP and box C/D snoRNP-associated protein 15.5K localises to nucleoplasmic foci

The next question was whether the 15.5K mutants show a localisation pattern different from that of the 15.5K protein wild-type and the 15.5K protein mutants affect RNP complex assembly *in vivo*.

To address this question, initially the location of 15.5K protein wild-type was determined. This protein was made visible both by immuno-fluorescence and by expression of protein 15.5K fused to enhanced yellow fluorescent protein (EYFP; Cormack *et al.*, 1996). The distribution of the labelled 15.5K protein was observed by fluorescence microscopy. As the epitope for α -15.5K antibody is likely not accessible in the tri-snRNP as it is probably covered by complex-specific proteins (Nottrott *et al.*, 1999), detection of protein 15.5K without SDS treatment was not possible. It has been shown that pre-treatment with 1% SDS produces a dramatic increase in staining intensity by indirect immuno-fluorescence (Brown *et al.*, 1996). Thus, to allow detection of 15.5K, HeLa cells were treated with SDS after fixation with paraformaldehyde.

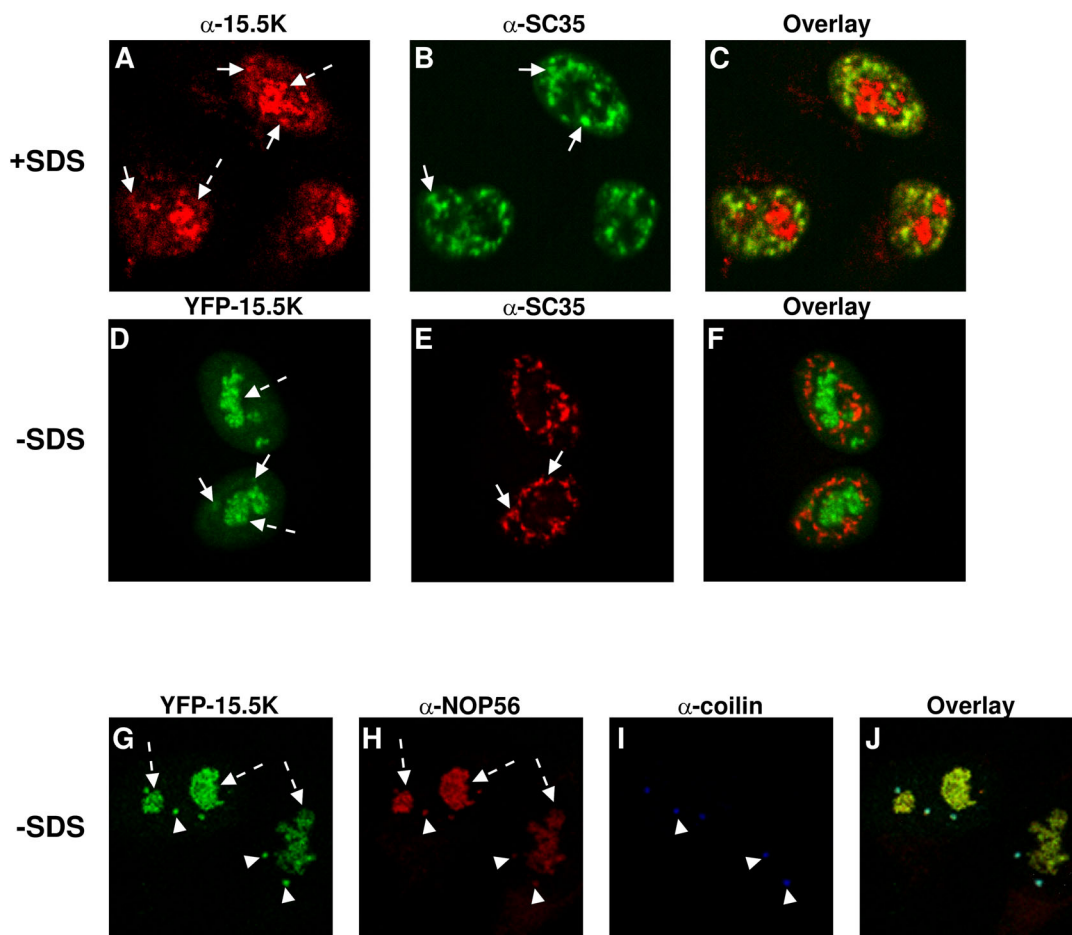


Figure 4-10 The 15.5K protein is localised in nucleoli, Cajal bodies and splicing speckles.

A–F. HeLa cells were fixed and stained with α -15.5K and counterstained with α -SC35 antibodies. In addition, HeLa cells were transiently transfected with pEYFP–15.5K for 16 h, fixed and counterstained with α -SC35 antibody. Cells shown in A–C were treated with SDS before staining. G–J. Cells were transiently transfected with pEYFP–15.5K and treated as described above. Fixed cells were counterstained with α -NOP56 and α -Coilin antibodies. Splicing speckles are indicated by solid arrows. The arrowheads indicate Cajal bodies and dashed arrows indicate nucleoli.

Antibody-labelled protein 15.5K was seen to be confined to the nucleus; it accumulated in large areas (Figure 4-10 A and Figure 4-10 B, dashed arrows) and also in a number of smaller clusters (Figure 4-10 A, solid arrows). The distribution of 15.5K protein fused to EYFP was similar to that of antibody-labelled 15.5K; thus, EYFP–15.5K was also seen to accumulate in large areas. However, in contrast to antibody-labelled 15.5K, the nucleoplasmic distribution of EYFP–15.5K was more homogeneous. The smaller clusters were less obvious (Figure 4-10 D). However, a nucleus expressing EYFP–15.5K showed small foci, adjacent to the nucleoli, where the EYFP-protein 15.5K accumulated (Figure 4-10 G, arrowheads).

As 15.5K protein is a component of splicing active snRNPs and snoRNPs, which specifically localise to splicing speckles, Cajal bodies and/or nucleoli, the distribution of 15.5K was compared with the distributions of (i) antibody-labelled SC35 protein, as a marker

4 Results

for splicing speckles, (ii) NOP56 as a marker for nucleoli, and (iii) coilin as a marker for Cajal bodies (Figure 4-10).

Endogenous 15.5K protein and transiently expressed EYFP–15.5K both co-localised with SC35 in the splicing speckles (Figure 4-10 A–F, indicated by solid arrows), suggesting that 15.5K is a component of the splicing speckles. The small differences in the appearance of the splicing speckle patterns are likely to be due to the SDS treatment of HeLa cells before antibody incubation during the immuno-fluorescence procedure (Figure 4-10 B).

As the reactivity of NOP56, NOP58 and fibrillarin with antibody is impaired in SDS-treated cells, it was not possible to observe the immuno-fluorescence of the box C/D snoRNP-specific proteins or fibrillarin together with antibody-labelled 15.5K protein. Therefore, experiments to show co-localisation of 15.5K with nucleolar proteins and Cajal bodies were performed using EYFP–15.5K fusion protein. Transiently expressed EYFP–15.5K co-localised with NOP56 in the nucleoli (Figure 4-10 G, H, and J) and also in Cajal bodies (Figure 4-10 G, I, and J).

The localisation of 15.5K in nucleoli and Cajal bodies is consistent with earlier results (Leung and Lamond, 2002). However, a permanent localisation of 15.5K in the splicing speckles has not been reported before. Leung and Lamond (2002) demonstrated that newly imported 15.5K transiently co-localises with splicing factors in splicing speckles. At later time points, the signal in speckles was no longer detected and EYFP–15.5K accumulates specifically in nucleoli and Cajal bodies.

The localisation of the 15.5K mutants was determined by using the YFP-tagged mutants 15.5K-1 to 15.5K-5. The 15.5K mutants 15.5K-1, 15.5K-3, 15.5K-4, and 15.5K-5 localised to splicing speckles, nucleoli, and to Cajal bodies similar to the wild-type protein 15.5K (see Figure 4-11, Figure 4-12, and Figure 4-13). However, mutant 15.5K-2, which was only expressed to a very low level (see Figure 4-14, lane 4), was prevented from translocating from its site of synthesis in the cytoplasm to the nucleus (G, H and I in Figure 4-11).

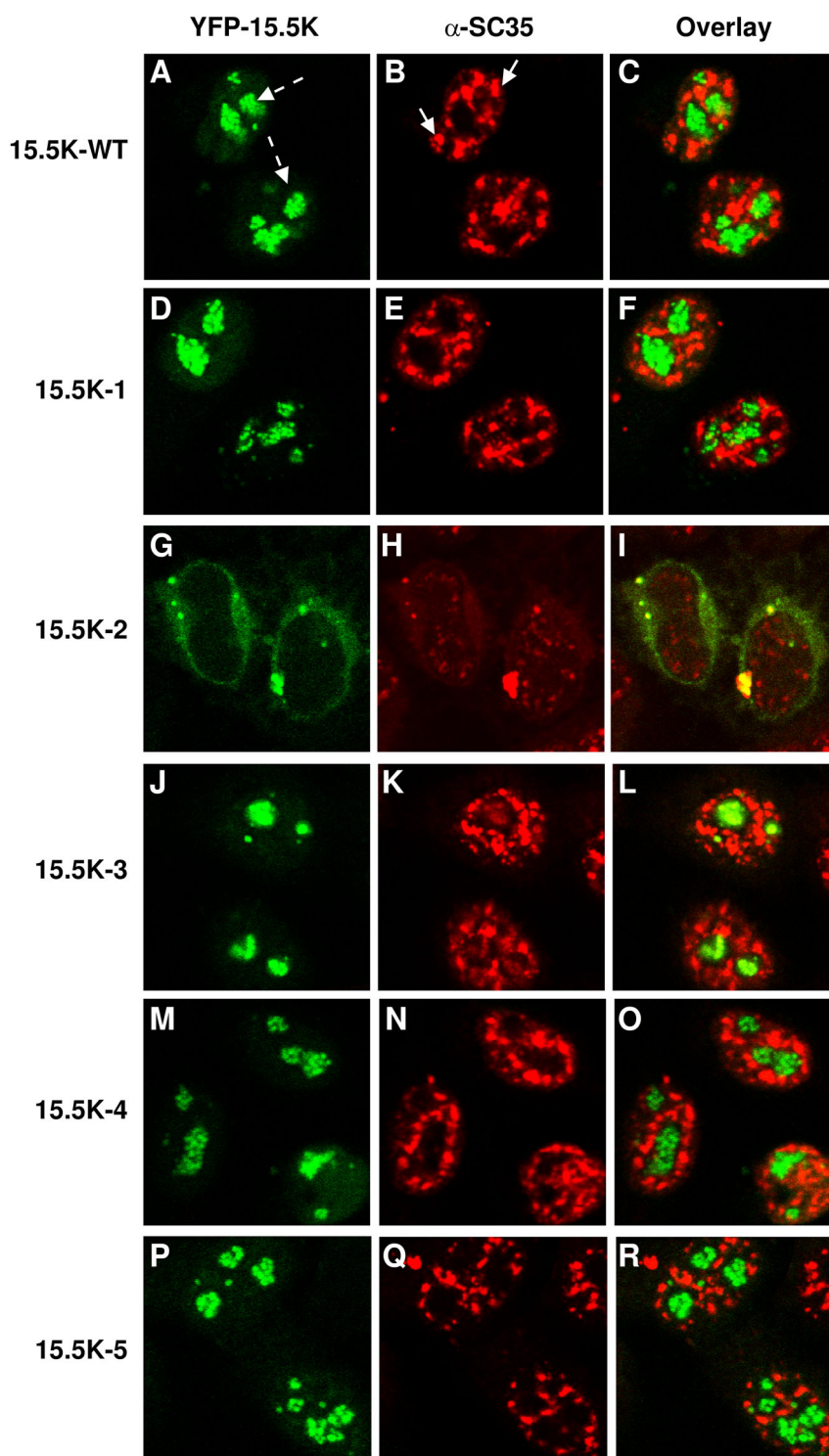


Figure 4-11 Cellular localisation of YFP-tagged 15.5K mutants analysed by co-staining of splicing factor SC35.

HeLa cells were transiently transfected with pEYFP-15.5K and fixed and stained with α -SC35 antibodies 16 h post transfection. Splicing speckles and nucleoli are indicated by solid and dashed arrows respectively.

4 Results

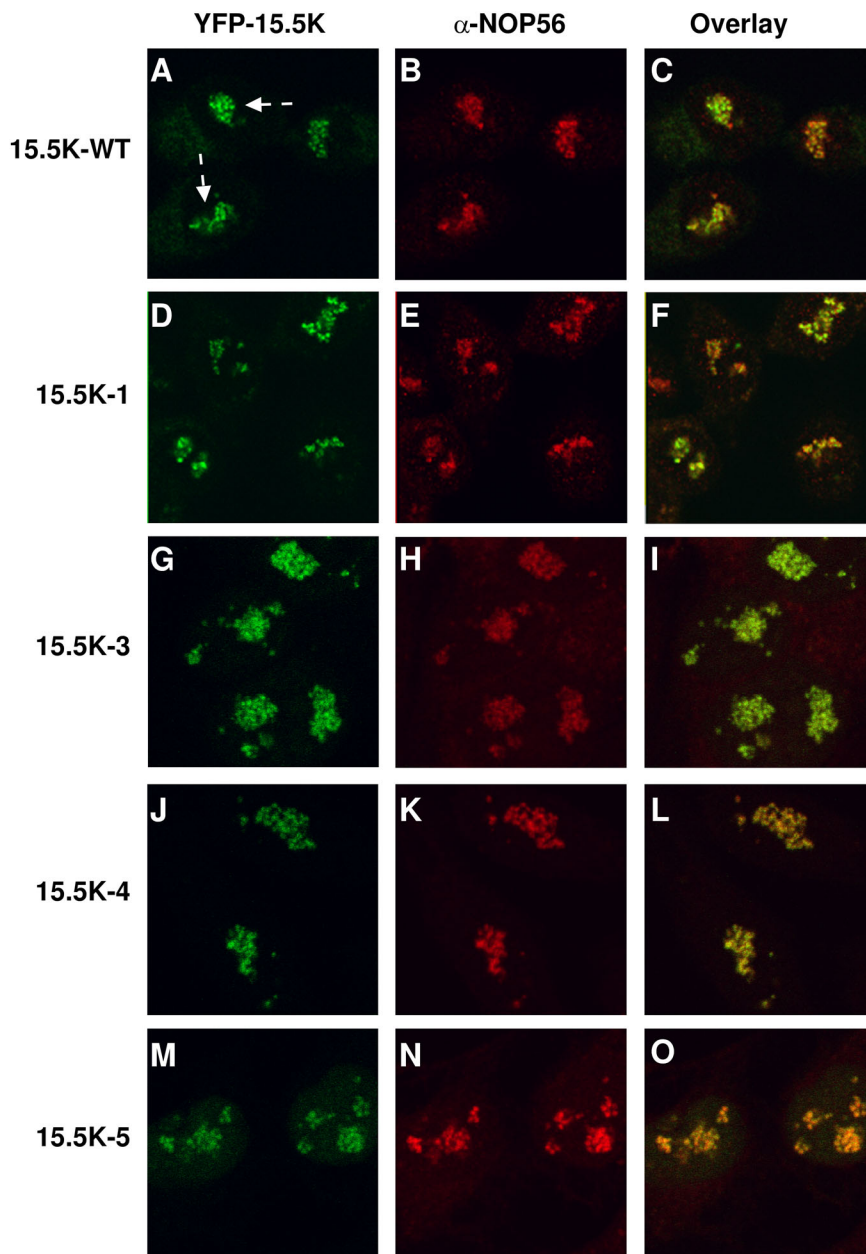


Figure 4-12 Cellular localisation of YFP-tagged 15.5K mutants analysed by co-staining of protein NOP56. HeLa cells were transiently transfected with pEYFP-15.5K and fixed and stained with α -NOP56 antibodies 16 h post transfection. Nucleoli are indicated by the dashed arrows.

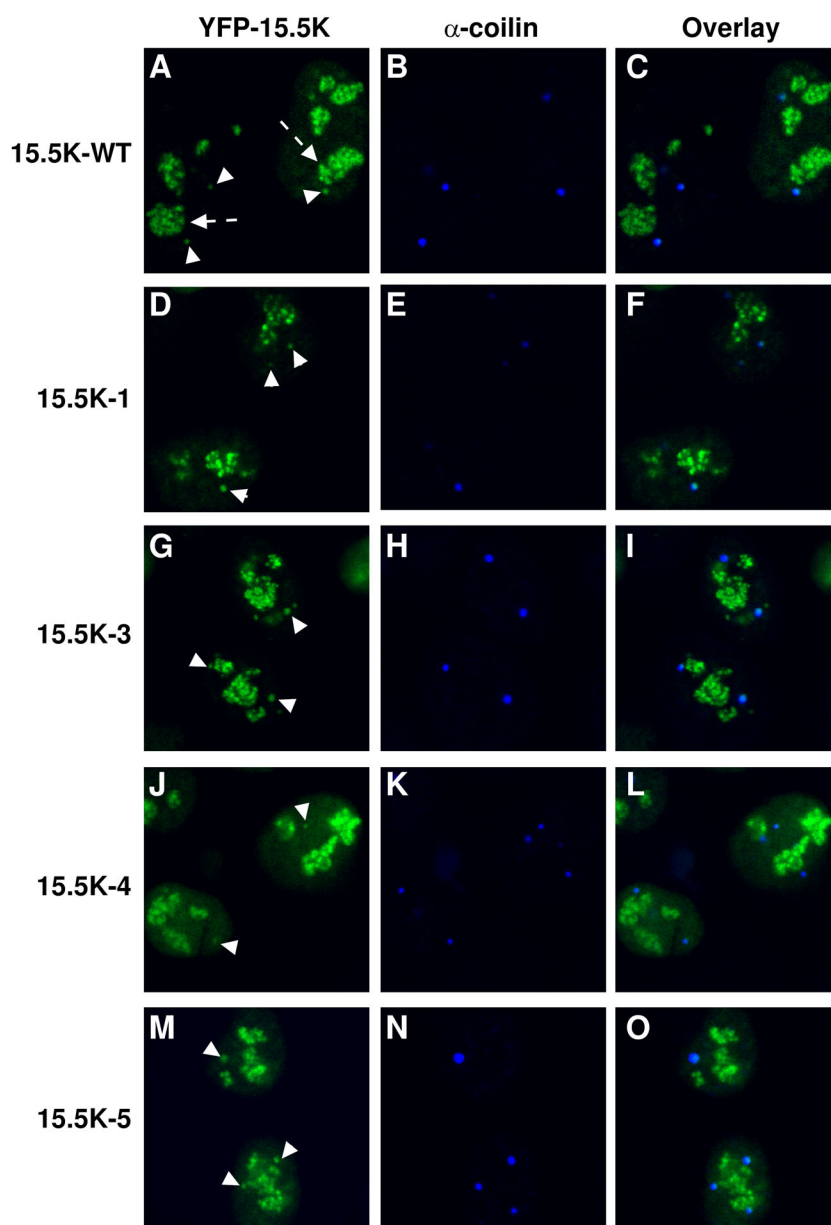


Figure 4-13 Cellular localisation of YFP-tagged 15.5K mutants analysed by co-staining Cajal body marker protein coilin.

HeLa cells were transiently transfected with pEYFP-15.5K and fixed and stained with α -coilin antibodies 16 h post transfection. Cajal bodies and nucleoli are indicated by arrowheads and dashed arrows respectively.

4 Results

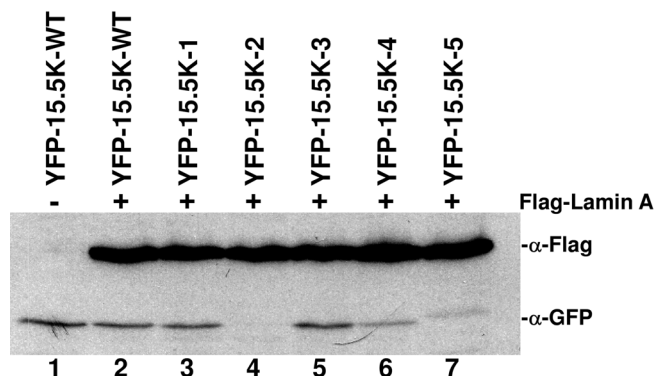


Figure 4-14 Western blot analysing the expression level of YFP-15.5K-1 to 15.5K-5 in HeLa cells.

HeLa cells were transiently transfected with pEYFP-15.5K wild type, mutants and Flag-Lamin A (Bechert *et al.*, 2003; AG Weber), which was used as a transfection, expression and loading control. 16 h post transfection nuclear extracts were prepared and the expression level of EYFP-15.5K wild type and mutants were analysed by western blot using anti-GFP. Loaded amount of extract was normalized by cell number before extract preparation. The level of Flag-Lamin A detected by anti-Flag antibodies demonstrates that equal amounts of extract were loaded.

4.2.2. EYFP-15.5K fusion protein *in vivo* is complexed specifically with the same RNA targets that protein 15.5K was shown to bind directly *in vitro*

As the expression level of the YFP-15.5K wild type and mutants in HeLa cells was very unequal (see Figure 4-14) a biochemical analysis using transiently transfected HeLa cells turned out to be difficult due to problems in normalizing pull down experiments and due to a low yield of nuclear extract. To facilitate investigating the role of protein 15.5K on U4/U6 snRNP and box C/D snoRNP complex assembly *in vivo*, it was tried to generate HeLa cell line stably expressing EYFP-15.5K wild type and mutants (see 3.2.5.5).

Unfortunately, the generation of stable cell lines expressing the 15.5K mutants failed as there could be no YFP-15.5K mutant expressing colonies selected likely due to a cytotoxic effect of the mutants to the cells. Therefore, the biochemical analysis of 15.5K mutants expressed in HeLa cells was not possible. However, experiments were carried out using the stable cell line expressing EYFP-15.5K wild type (HeLa^{EYFP-15.5K}; see 3.2.5.5) identifying RNPs 15.5K is associated with *in vivo*.

The expression level of the exogenous YFP-15.5K protein is about three times lower compared to that of the endogenous 15.5K protein (see Figure 4-15). However, as it was of only of interest to find out which RNAs bind to the 15.5K protein *in vivo*, this fact was of little importance for the present study.

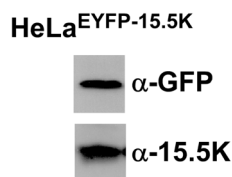


Figure 4-15 HeLa cell line stably expressing EYFP–15.5K.

A western blot was performed using anti-GFP and anti-15.5K antibodies showing expression levels of endogenous 15.5K and EYFP–15.5K in the nuclear extract prepared from a HeLa cell line stably expressing EYFP-15.5K (HeLa^{EYFP-15.5K}). Membrane was blotted twice using first anti-GFP and then anti-15.5K antibodies. The first antibody was removed from the membrane by membrane stripping.

To confirm that the EYFP–15.5K fusion protein expressed in the stable HeLa^{EYFP-15.5K} cell line behaves biochemically in a manner similar to recombinant 15.5K protein and 15.5K protein from HeLa cells, observed in previous *in vitro* binding studies (Nottrott *et al.*, 1999; Watkins *et al.*, 2000), its specificity of RNA-binding *in vivo* was investigated. An extract from HeLa^{EYFP-15.5K} cells was immunoprecipitated with an α -GFP antibody. RNAs in the immunoprecipitate were separated by urea-polyacrylamide gel electrophoresis, transferred to nylon membrane, and hybridised with probes for U2, U4, U5, and U6 snRNAs and U3 snoRNA (Figure 4-16). This showed that U3 snoRNA, U4, U5 and U6 snRNA – but not U2 snRNAs – had been co-precipitated with the α -GFP antibody (Figure 4-16, lane 8). Control experiments, i.e., bead control (Figure 4-16, lanes 2, 4 and 7 respectively) and an HeLa^{EGFP-Fibrillarin} nuclear cell extract (Figure 4-16, lane 5; HeLa^{EGFP-Fibrillarin} cell line provided by the laboratory of Prof. Angus Lamond), showed that although the α -GFP antibody still precipitated the fluorescent fusion protein from these extracts (western blot data not shown), it did not precipitate any of the RNAs tested, whereas the same α -GFP antibody precipitated the U3 snoRNA, but not the U2, U4, U5, and U6 snRNAs, from a HeLa^{EGFP-Fibrillarin} cell extract (Figure 4-16, lane 5).

It is known that U4 and U6 snRNAs usually exist as a duplex inside the nucleus (Bringmann *et al.*, 1984; Hashimoto and Steitz, 1984; Rinke *et al.*, 1985; Brow and Guthrie, 1988). The co-immunoprecipitation of U4 and the U6 snRNA is therefore not surprising. However, the α -GFP antibodies failed to precipitate tri-snRNP particles above the background values, as the U5 snRNA signal does not exceed background level compared to the level co-precipitated by ECFP-fibrillarin (Figure 4-16, compare lane 5 and lane 8). The fraction of 15.5K bound to the U4/U6.U5 tri-snRNP is probably poorly accessible for the α -GFP antibodies. This idea is consistent with the observation that the 15.5K epitope is inaccessible to 15.5K antibodies in the tri-snRNP as it is probably covered by complex-specific proteins (Nottrott *et al.*, 1999). Associated complex-specific proteins could also cover

4 Results

even a tag of the scale of a GFP-tag fused to 15.5K making it inaccessible to the α -GFP antibody.

These results show that the EYFP–15.5K fusion protein is specifically complexed *in vivo* with the same RNA species that protein 15.5K was shown to bind directly to *in vitro* (Nottrott *et al.*, 1999; Watkins *et al.*, 2000).

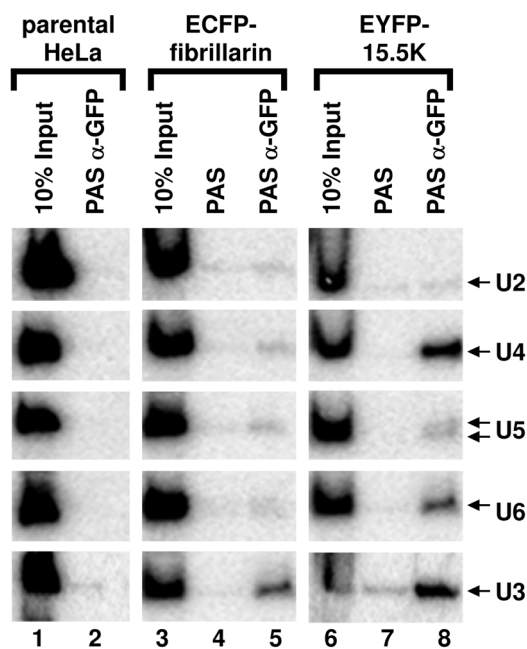


Figure 4-16 *In vivo* RNA-binding by EYFP–15.5K.

The *in vivo* RNA-binding by EYFP–15.5K was assayed by immunoprecipitation, and the binding of snRNAs U2, U4, U5, and U6 as well as of snoRNA U3 was tested by northern hybridisation.

Following the demonstration that EYFP–15.5K is specifically complexed with the same RNA molecules that 15.5K was shown to bind directly *in vitro*, the binding specificity of the U4/U6 di–snRNP and the box C/D snoRNP complex-specific proteins hPrp4 and NOP56 was investigated. The EYFP–15.5K fusion protein was immunoprecipitated by using anti-hPrp4 and anti-NOP56 antibodies, and the co-precipitated EYFP–15.5K fusion protein was investigated by western blotting using α -GFP antibodies.

Briefly, nuclear extract from HeLa^{EYFP-15.5K} cells was incubated with protein-A-Sepharose beads to which α -hPrp4 or α -NOP56 antibodies had previously been coupled. The EYFP–15.5K fusion protein was co-precipitated with anti-hPrp4 and detected with α -GFP antibodies. The results, shown in Figure 4-17, revealed that both α -NOP56 (lane 5) and α -hPrp4 antibodies (lane 5) precipitated the EYFP–15.5K fusion protein. The bead controls (lanes 3 and 4) showed that the EYFP–15.5K fusion protein was specifically precipitated by beads with coupled α -NOP56 and α -hPrp4 antibodies. This experiment shows that *in vivo* the

EYFP–15.5K fusion protein is specifically complexed with U4/U6 snRNP and box C/D snoRNP, containing hPrp4 and NOP56 respectively.

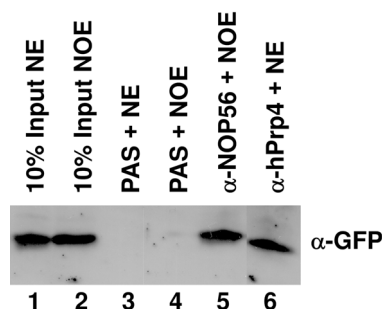


Figure 4-17 *In vivo* RNP-binding of EYFP–15.5K.

The *in vivo* RNP-binding of EYFP–15.5K was assayed by immunoprecipitation with α -hPrp4 and α -NOP56 antibodies and was analysed by western blotting using an α -GFP antibody. NE = nuclear extract, NOE = nucleolar extract.

4.3. Association of the spliceosomal hPrp31 protein with the U4 snRNP: Requirement for U4 snRNA's kink-turn stem II and the Nop domain

4.3.1. Hydroxyl-radical footprinting reveals direct contact of protein hPrp31 with various regions of the U4 snRNA

It was shown earlier that protein hPrp31 only makes direct contact with the U4 snRNA after protein 15.5K binds to the kink-turn motif of U4 snRNA (Nottrott *et al.*, 2002). In order to narrow down the possible locations of this contact in the ternary 15.5K-hPrp31-U4 snRNA complex, hydroxyl-radical footprinting experiments performed by Stephanie Nottrott have been re-examined (see Schultz *et al.*, 2006b). In this method, hydroxyl radicals are produced; these cleave the RNA backbone at the ribose units, and an RNA that is shielded by protein will be protected from such cleavage. Analysis was performed by using primer extension with reverse transcriptase. Through a comparison with cleavage sites on naked RNA, the absence of a transcriptional stop before a particular position is considered as a protection at this position in the complex.

The ternary U4 snRNA–15.5K–hPrp31 complex was assembled by incubating full-length U4 snRNA (prepared by transcription *in vitro*) with an excess of recombinant protein 15.5K and glutathione-S-transferase (GST)-hPrp31 (Nottrott *et al.*, 2002). Under the conditions used, more than 95% of the U4 snRNA was converted into the ternary complex, as assayed by EMSA (data not shown). In order to distinguish nucleotides protected by protein

4 Results

hPrp31 from those protected by protein 15.5K only, a binary 15.5K-U4 snRNA complex was assembled in a parallel sample; naked RNA was used as a reference. These complexes were treated with H₂O₂ in the presence of Fe(II)–EDTA to generate hydroxyl radicals. The RNA was subsequently analysed by primer extension (Figure 4-18 A) of the U4 snRNA.

A comparison of the cleavage pattern of naked RNA (lane 2) with that of a control omitting the reagent Fe(II)–EDTA (lane 1) shows distinct cleavages at all nucleotides (compare lanes 1 and 2). Lane 3 shows the hydroxyl-radical cleavage pattern observed in the binary 15.5K–U4 snRNA complex. Strong protection is found in the kink-turn and in the adjacent stems I (A29–G34) and II (G43–C47) (lanes 2 and 3; compare (Figure 4-18, FP 2 and FP 1, red bars). This is in agreement with the results of earlier studies (Vidovic *et al.*, 2000; Nottrott *et al.*, 2002) in which these nucleotides were identified as the binding site for protein 15.5K. The cleavage pattern of U4 snRNA in the ternary complex revealed a number of additional protection sites arising from the presence of protein hPrp31. One region extended from G35 to C42 (lanes 3 and 4; FP A in (Figure 4-18 A) comprising the penta-loop and nucleotides of stem II not protected by protein 15.5K. Further, protection was observed in stem I next to the kink-turn at positions G26, C27, and C28 (FP B) and at nucleotides C16 and G18 (FP C) (Figure 4-18 A and Figure 4-18 B).

4 Results

In the U4/U6 snRNA duplex, FP C would be located in the U4/U6 helix II, adjacent to the three-way junction of the U4/U6 duplex. Therefore it would be of interest to know whether protein hPrp31 would similarly protect these nucleotides when binding to the 15.5K–U4 snRNA complex in the context of the duplex. To investigate this, first the duplex was created by annealing U6 snRNA to U4 snRNA before addition of proteins 15.5K and hPrp31. Formation of the U4/U6 duplex was quantitative, and the duplex was as efficient as the single-stranded U4 snRNA in ternary complex formation, as determined by EMSA (data not shown). Hydroxyl radical footprinting was then performed as above, on (i) the protein-free U4/U6 duplex (Figure 4-18, lane 6), (ii) the complex formed between the duplex and protein 15.5K (Figure 4-18, lane 7), and (iii) the complex formed between the pre-formed 15.5K–U4/U6 snRNA complex and protein hPrp31 (Figure 4-18 A, lane 8). Duplex formation on its own did not influence the accessibilities of the riboses in U4 snRNA (Figure 4-18 A, lanes 6 and 2), except for a reduced reactivity at A39–G43 in the U4/U6 snRNA duplex. Similarly, the footprint of protein 15.5K on the U4 in the U4/U6 duplex was essentially identical to the one described above (Figure 4-18 A, lanes 7 and 3, FP 1 and FP 2). The addition of protein hPrp31 resulted in protection of nucleotides essentially identical to those seen in the absence of U6 snRNA (Figure 4-18 A, lanes 8 and 4). In particular, the protection of the penta-loop and the adjacent stem II was unchanged (FP A). Protection at the bottom of stem I (FP B), adjacent to the binding site for protein 15.5K, was more extensive in that A25 also showed protection. Somehow more enlarged was FP C, which was found to extend from G14 to G18. Figure 4-18 B depicts the footprints on the secondary structures of U4 snRNA (Myslinski and Branlant, 1991) and the U4/U6 snRNA duplex (Bringmann *et al.*, 1984) respectively. The overall pattern of protection of U4 snRNA by protein hPrp31 was thus comparable in the hPrp31–15.5K–U4 snRNA and the hPrp31–15.5K–U4/U6 snRNA complexes, with only differences observed on the borders of the protected regions in FP B and C. In summary, these data show that *in vitro* protein hPrp31 protects regions of stems I and II, the complete terminal penta-loop, and nucleotides in the helix adjacent to the three-way junction.

4.3.2. Protein hPrp31 requires stem I and stem II of the 5' stem-loop of U4 for binding

The next question investigated was that of which of the structural elements of U4 snRNA that were found to be protected from hydroxyl radical attack by protein hPrp31 in the footprinting experiment were required for stable binding of protein hPrp31 to the

15.5K-U4 snRNA binary complex. For this more detailed analysis, a series of mutant RNA oligonucleotides was prepared, and these were assayed by EMSA for ternary-complex formation. To ease solubilisation of hPrp31, a fusion protein comprising the maltose-binding protein (MBP) fused to hPrp31 was used (Figure 4-19 A). This behaves in a manner identical to non-tagged hPrp31 (data not shown). In all experiments, the binary 15.5K-U4 snRNA complex (B in Figure 4-19 B) was first assembled with recombinant 15.5K protein and radiolabelled RNA oligonucleotide. Formation of the ternary complex (T in Figure 4-19 B) was then initiated by adding MBP-hPrp31 protein. Complexes were then analysed directly by native PAGE at 4 °C.

Since the single-stranded 5' region of the U4 snRNA was protected by the protein, this segment was deleted first (U4-2, Figure 4-19 B). No reduction in the amount of ternary complex formed (Figure 4-19 B; lanes 3 and 7) was observed compared with the longer deletion mutant U4 snRNA (U4-1), which binds in a manner identical to that of the wild-type U4 snRNA (Nottrott *et al.*, 2002). Hence, the contact between the single-stranded 5' end of the U4 snRNA and protein hPrp31 is not required for stable binding. However, the deletion of five base pairs from stem I severely depressed the formation of stable ternary complex (U4-3; Figure 4-19 B, lanes 3 and 11). Residual ternary complexes (in yields of approximately 20% compared with the U4-2 or U4-1 RNA) were unstable, resulting in an ill-defined smear migrating above the binary 15.5K-U4 snRNA complex. Binding activity could not be restored by extending the truncated three-base-pair-long stem I of mutant U4-3 by a C-G base pair (U4-4, SL1 in reference Nottrott *et al.* (2002), Figure 4-19 B). Furthermore, changing the sequence of the upper part of stem I while leaving the number of base pairs intact, or deleting the bulged-out A, did not reduce the yield of ternary complex (oligonucleotides U4-10 and U4-11; data not shown). Therefore, it is possible to reach the conclusion that the length of stem I is critical for stable binding of protein hPrp31 to the binary 15.5K-U4 snRNA complex, and that this double-helical RNA structure, irrespective of sequence, forms part of the binding determinant.

4 Results

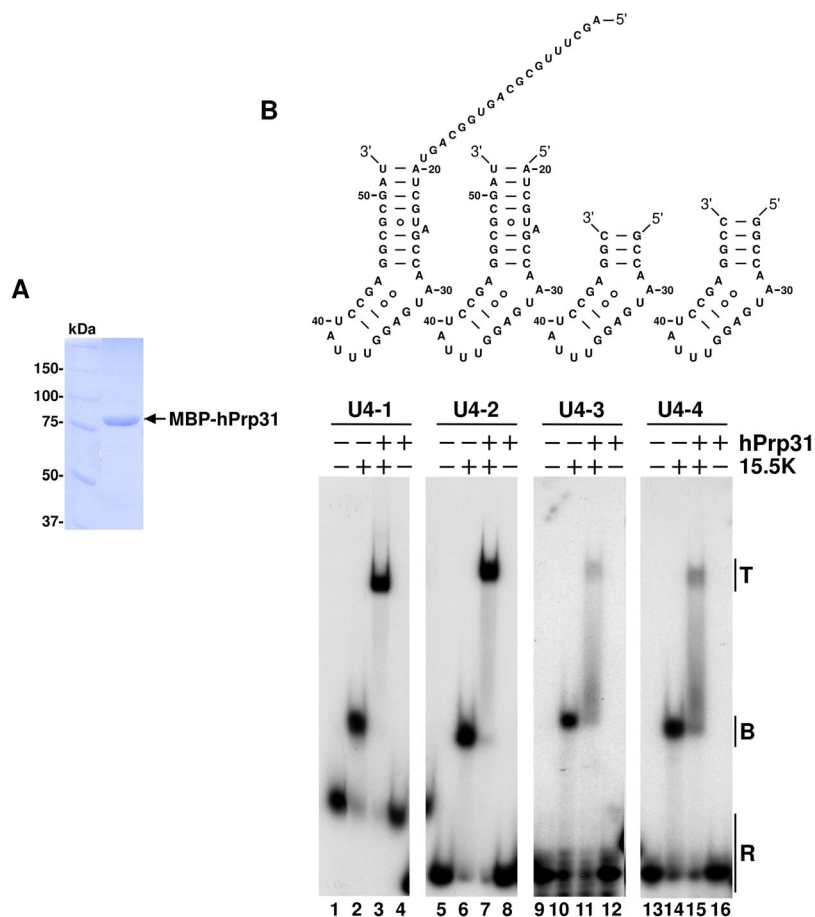


Figure 4-19 Binding of hPrp31 to the U4 snRNP requires the complete stems I and II of the 5' stem-loop of the U4 snRNA.

A. SDS PAGE of MBP-hPrp31. MBP-hPrp31 was stained with Coomassie blue. **B.** The gels show EMSA of the interaction between protein hPrp31 and the 15.5K-U4 snRNA deletion mutant complex. The binary complex was first assembled with protein 15.5K and mutant U4 snRNA s (top panels), and ternary-complex formation was then initiated by adding protein hPrp31. Complexes were separated on a 6% native polyacrylamide gel. The positions of the protein-RNA complexes are indicated on the right: R, free RNA; B, binary complex consisting of the RNA and 15.5K; T, ternary complex, consisting of the RNA, 15.5K and protein hPrp31. The sequence and structure of the respective U4 snRNA deletion mutant used is indicated above each panel.

The hydroxyl-radical footprint showed protection of the entire penta-loop in the ternary complex (Figure 4-18 A and B). Next, a number of different penta-loop mutants were tested, and their effect on stable ternary-complex formation in the experimental system outlined above was assayed. The U4-2 mutant (Figure 4-19 B), which has wild-type properties while being closest in length to the other mutants, was used as a reference with which to compare the mutants. Replacement of the penta-loop by an unrelated sequence did not impair complex formation (U4-5, Figure 4-20).

Its replacement with a tetranucleotide loop (UGAA in U4-6, Figure 4-20; other loops tested were UUCG and GCAA) likewise had no effect (Figure 4-20, lanes 3 and 11 and data not shown). Therefore, a more dramatic change in the penta-loop's backbone was introduced by opening it up. An RNA duplex with dangling ends was created by annealing the 5' (20-37)

and 3' (38–52) halves of the U4 snRNA 5' stem-loop (U4-A, Figure 4-20). Unexpectedly, this duplex still allowed efficient ternary-complex formation (Figure 4-20, lanes 3 and 15). Finally, the penta-loop was simply deleted, by annealing 5' and 3' halves lacking the penta-loop sequence entirely (U4-B, Figure 4-20).

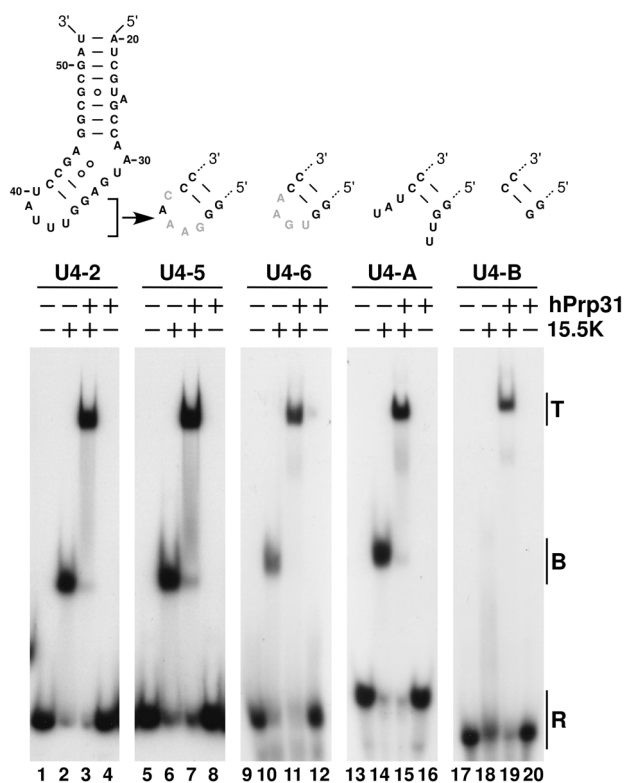


Figure 4-20 Binding of hPrp31 to the U4 snRNP does not depend on sequence and structure of the terminal penta-loop.

EMSA analysis of the interaction between protein hPrp31 and the 15.5K–U4 snRNA complex containing mutant RNAs was performed as described in Figure 4-19. U4-A and U4-B duplexes were generated before the assay by annealing the radiolabelled 5' and the unlabelled 3' half of the 5' stem-loop. A schematic representation of the sequence and the structure of each loop mutation in the U4 5' stem-loop (corresponding to oligonucleotide U4-2) is indicated above the respective panel. Numerous other penta- and tetranucleotide loops were tried out; all with the same result (see text).

This duplex's stability was dramatically impaired (EMSA; data not shown); it no longer supported the formation of significant amounts of stable binary 15.5K–U4 snRNA complex (Figure 4-20, lane 18), as compared with the reference U4-2 (lane 2) and with all other mutants tested (lanes 6, 10, 14). However, this duplex did support the efficient formation of stable ternary complex upon addition of protein hPrp31 to the binary complex assembly mixture (lane 19). Protein hPrp31 therefore appears to stabilise transient interactions of protein 15.5K with U4 snRNA in the ternary complex. Therefore, it may be inferred that the penta-loop *per se* is not essential for protein hPrp31 binding to the 15.5K–U4 snRNA binary complex. In addition to the penta-loop, protein hPrp31 had also been found to be in contact with the adjacent short stem II (Figure 4-18A and B). Since the penta-loop was not

4 Results

required for stable ternary-complex formation, the function of stem II in ternary-complex formation was next investigated.

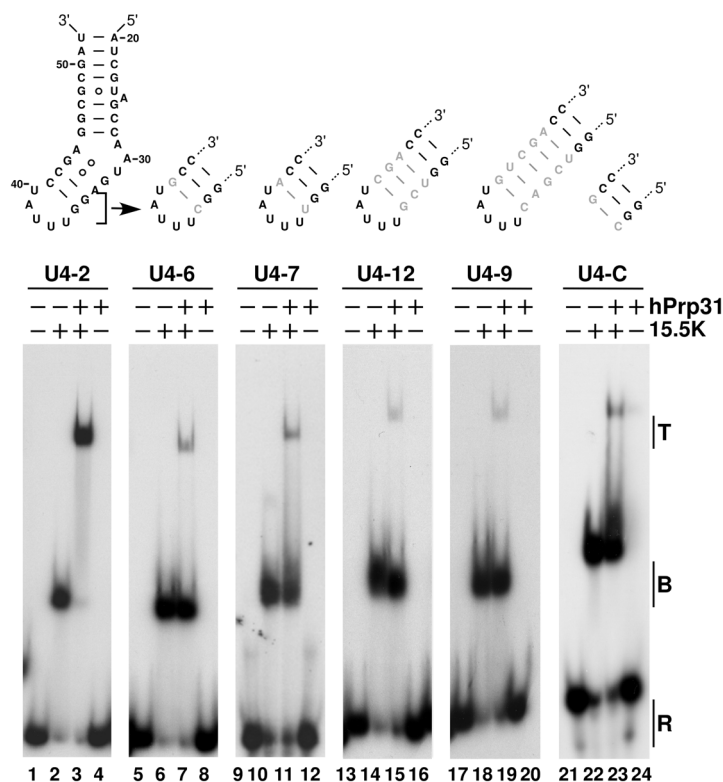


Figure 4-21 Elongation of stem II is critical for hPrp31 binding to the U4 snRNP.

EMSA analysis of the interaction between protein hPrp31 and the 15.5K-U4 snRNA complex containing mutant RNAs was performed as described in Figure 4-19. A schematic representation of the sequence and the structure of each stem II mutation tested is given above the respective panel.

As a first step, stem II was extended by a single C-G base pair (U4-7, Figure 4-21). Strikingly, this mutant no longer supported ternary-complex formation in the assay system used (Figure 4-21, lanes 3 and 7; approximately 90% reduction of ternary complex formation when quantified by Phosphoimager analysis). Extension by a U-A base pair (U4-8, Figure 4-21) had a similar effect (Figure 4-21, lane 11). Not surprisingly, identical results were obtained by increasing the length of the stem to 5 or 7 base pairs (Figure 4-21, U4-12 and U4-9; lane 19 and 15 respectively). Furthermore, deletion of the penta-loop with retention of the three-base-pair-long stem II (U4-C, Figure 4-21) was similarly detrimental to ternary-complex formation (Figure 4-21, lane 23). The inhibitory effect of this additional base pair was thus independent of the presence of the penta-loop. A shortening of stem II was not deemed feasible because the already weak binding of 15.5K to the penta-loop deletion (mutant U4-3) would be further compromised by interfering with the 15.5K binding site (Reuter *et al.*, 1999; Vidovic *et al.*, 2000).

Taken together, these data show that the length of stem II is important for the association of protein hPrp31 with the 15.5K–U4 snRNA binary complex. Since protein hPrp31 is known to interact also with the 15.5K-U4atac snRNA binary complex (Nottrott *et al.*, 2002), while the U4atac snRNA has a different stem II sequence and the same length, the conclusion may be strengthened: the determining factor is apparently the length, and not the sequence.

So far, these results show that both stem I and stem II are required for stable binding of protein hPrp31 to the 15.5K–U4 snRNA binary complex, to form the ternary hPrp31-15.5K–U4 snRNA complex. While stem I could not be shortened without loss of binding activity, stem II – unexpectedly – could not be elongated.

4.3.3. The Nop domain is necessary and sufficient for 15.5K-dependent hPrp31 binding to U4 snRNA

Having established the elements of the U4 snRNA structure required to bind protein hPrp31, it was next investigated whether the so-called Nop domain of protein hPrp31 (see 2.1.2.2 and 2.3) is sufficient for binding U4 snRNA in the 15.5K–U4 snRNA binary complex. Exact demarcation of the Nop domain from sequence alignments is difficult because of ambiguities in locating its boundaries (Gautier *et al.*, 1997; Vithana *et al.*, 2001; Makarova *et al.*, 2002). However, in the crystal structure of the archaeal homologue Nop5p, which has recently become available (Aittaleb *et al.*, 2003), an independent structural domain can be identified at the C terminus of Nop5p (B), indicated by red α -helices and grey loops). This domain corresponds to the conserved central domain in NOP56, NOP58, and hPrp31 (B). On the basis of these structure-based alignments, it may be inferred that the conserved Nop domain of hPrp31 corresponds to α helices 6-12 of Nop5p. Delineation of this domain is fully consistent with secondary-structure prediction (A and C). Therefore, amino acids 215–335 of hPrp31 will hereafter be referred to as the Nop domain. This assignment differs slightly from previously published definitions of the Nop domain (Gautier *et al.*, 1997; Vithana *et al.*, 2001; Makarova *et al.*, 2002; Kühn-Hölsken *et al.*, 2005). However, the Nop domain sequence as identified here is contained in all the published definitions.

The protein fragment corresponding to the hPrp31 Nop domain (E) was expressed as an MBP fusion protein in *E. coli* (Figure 4-23 A). Its activity in ternary-complex formation, with the U4-2 RNA, was compared with that of the full-length protein in the binding assay described above (4.3.2 and Figure 4-19). Remarkably, the Nop domain on its own supported ternary-complex formation (Figure 4-23 B, lane 5) but with a slightly lower affinity compared with that of the full-length protein (lane 3). Deletion of 20 amino acids from the C terminus (amino acids 310–335; E) would be predicted to disrupt the Nop domain (α helix 12 of Nop5p, E). This truncated Nop domain was prepared in the same way as the full-length Nop domain (Figure 4-23 A) and was found to be completely inactive in ternary-complex formation (Figure 4-23 B, lane 4).

4 Results

◀ Figure 4-22 Delineation of hPrp31 Nop domain.

A. Fold Index for protein hPrp31. Putatively folded regions are shown in green and disordered regions are shown in red. **B.** Crystal structure of the archaeal Nop5p protein of *A. fulgidus* according to Aittaleb *et al.* (2003). The position of the homologous central Nop domain is indicated by the red α -helices and grey loops and the disordered loop within the Nop domain of Nop5p protein is indicated by the dashed grey line. **C.** Secondary structure prediction using Predict Protein by Burkhard Rost (EMBL, Heidelberg, Germany; Rost and Sander, 1993). PHD = PHD: Profile network prediction Heidelberg. PHD predicted secondary structure: H=helix, E=extended (sheet), blank=other (loop). Rel_sec: reliability index for PHDsec prediction (0=low to 9=high). SUB_sec: subset of the PHDsec prediction, for all residues with an expected average accuracy > 82%. For this subset the following symbols are used: L is loop. No prediction is made for this residue, as the reliability is < 5 in the reliability index. Secondary-structural elements comprising the Nop domain derived from the archaeal Nop5p crystal structure are indicated above the sequences. **D.** Alignment of the human hPrp31 with the homologous sequences of human NOP56, NOP58 and the archaeal Nop5p; the respective GenBank accession numbers are NP_006383, NP_057018 and NP_070912. Sequence alignments were performed by the Clustal method. Identical and conserved amino-acid residues are indicated in white on a black background and white on a blue background, respectively. Similar amino-acid residues are boxed in grey. Secondary-structural elements comprising the Nop domain derived from the archaeal Nop5p crystal structure are indicated above the sequences. **E.** Schematic representation of the hPrp31 deletion mutants. The light grey box represents the putative Nop domain in hPrp31.

In the absence of protein 15.5K, neither the full-length Nop domain nor the truncated one bound the RNA on its own (lanes 6–8); this resembles the situation for the full-length protein hPrp31. Furthermore, binding of the Nop domain was dependent on the presence of the correct flanking RNA elements, since a U4 mutant with an elongated stem II (U4-9; for details, see above and the legend to Figure 4-23 C) did not support ternary-complex formation (Figure 4-23 C, lane 3). It thus appears that the Nop domain is both necessary and sufficient for binding to the U4 snRNA in the 15.5K–U4 snRNA binary complex.

The band-shift experiments demonstrate that the Nop domain is sufficient for stable ternary-complex formation. However, it was not clear whether this domain is sufficient to induce the direct RNA-protein contacts to the penta-loop that were observed earlier (Nottrott *et al.*, 2002; Kühn-Hölsken *et al.*, 2005). This issue was of particular interest because the penta-loop is not essential for ternary-complex formation (see Figure 4-20). Therefore, RNA-protein contacts in the penta-loop by UV cross-linking in the minimal ternary complex were investigated. For this purpose, this complex was assembled with radiolabelled U4-2 RNA oligonucleotide and the Nop domain, UV cross-linking was performed and the reaction mixture was analysed by SDS-PAGE (Figure 4-23 D, lane 3). As controls, the reaction was performed with the RNA component only (lane 1), with RNA and protein 15.5K but not the Nop domain (lane 2) and with omission of protein 15.5K (lane 4). A prominent cross-linking product of about 65 kDa was detected clearly in the complete assembly mixture only (lane 3). The cross-linked species contained both RNA and protein, since it was sensitive to digestion with Proteinase K or with RNase T1 (data not shown). Further, the apparent molecular weight

is consistent with the sum of the MWs of the hPrp31 Nop domain MBP fusion protein (53.9 kDa) and the U4-2 RNA oligonucleotide (10.6 kDa).

These data demonstrate that the Nop domain is sufficient to induce the RNA-protein contacts between itself and the penta-loop of the RNA.

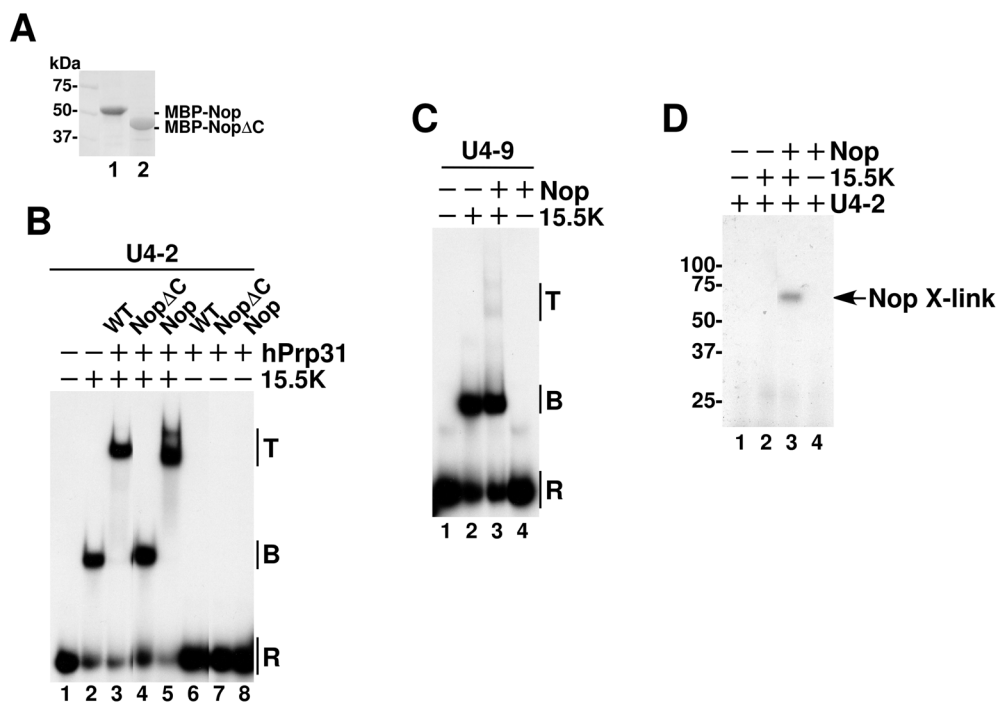


Figure 4-23 The Nop domain is necessary and sufficient for binding of hPrp31 to the U4 snRNP.

A. SDS PAGE of hPrp31 deletion mutants. **B.** EMSA to test the interaction between the hPrp31 deletion mutants and the U4 snRNA 5' stem-loop (U4-2; see Figure 4-19, Figure 4-20, and Figure 4-21) was performed as described in Figure 4-19. **C.** To test the binding specificity of the Nop domain, a binding assay was performed using a U4 snRNA mutant in which stem II was elongated by five additional base pairs (for sequence see Materials and Methods). This mutant did not support binding of wild-type hPrp31 (data not shown). **D.** Recombinant 15.5K and the hPrp31 Nop domain were reconstituted with 5'-end-labelled U4-2 RNA oligonucleotide. The protein-RNA complexes were then UV-irradiated and the irradiation products were resolved on a 12% polyacrylamide-SDS gel. The cross-linking product of about 65 kDa is indicated by the arrow.

4.4. Mutations associated with retinitis pigmentosa in the U4/U6-specific protein hPrp31

4.4.1. Cellular localisation of wild-type and mutant hPrp31 in transfected HeLa cells

In this section, the effects of hPrp31 adRP point mutations A194E and A216P (see section 2.1.4) on the location of protein hPrp31 within human cells and the formation of the tri-snRNP are addressed. Experimentally, this was done by combining RNAi depletion with

4 Results

fluorescence microscopy and biochemical methods. (The mutations associated with adRP are referred to hereinafter as “adRP mutations”; this is not meant to imply an established causal connection.)

To address the question of the location in the cell of hPrp31 adRP mutations and to investigate biochemically the formation of tri-snRNP, wild-type and mutant hPrp31 was subcloned into the pTA2 vector (Invitrogen) and tagged at its NH₂ terminus with an HA-tag. As no antibody against hPrp31 is available, the observation of endogenous hPrp31 was not possible.

To increase the expression level of the ectopically expressed HA-tagged hPrp31 protein and to investigate the effect of the introduced hPrp31 mutant alone, HeLa SS6 cells were depleted of endogenous hPrp31 by RNAi. This depletion raised the expression of the HA-hPrp31 wild-type protein from 20% to 80%. This higher expression level was important for later biochemical studies with nuclear extracts prepared on a small scale. RNAi experiments were performed using 21-nt siRNA duplexes (Elbashir *et al.*, 2001; Elbashir *et al.*, 2002). An siRNA duplex targeting the 3'UTR of the mRNA encoding the hPrp31 was used to “knock down” the endogenous hPrp31 protein; as a control, a non-human protein with no human homologues (firefly luciferase; GL2) was used. The transfection procedure was performed on a millilitre scale, with simultaneous transfection of pTA2-HA-hPrp31 and the siRNA (EA2) by electroporation (Amaxa nucleofector). In this way, enough cells were obtained for a small-scale preparation of nuclear extract that was suitable for subsequent biochemical assays (Lee and Green, 1990).

To demonstrate that the cells had indeed been depleted of the hPrp31 wild-type, western blot analyses with antibodies directed against hPrp31 were performed. As shown in Figure 4-24 B, the level of protein hPrp31 was reduced by about 95% (lane 2). This knock-down was specific, as cells treated with an siRNA against luciferase did not show a knock-down effect (GL2, lane 1).

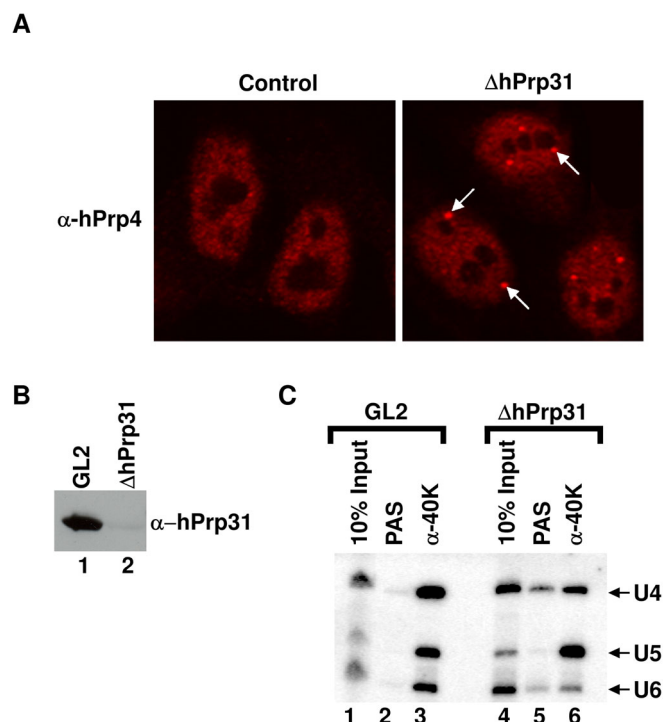


Figure 4-24 Knock-down of spliceosomal hPrp31 protein by siRNAs.

A. HeLa cells transfected with siRNA targeting firefly luciferase (Control, GL2) and the U4/U6 protein hPrp31 (EA2, Δ hPrp31) were examined 48 h after transfection using indirect immunofluorescence. **B.** A western blot showing levels of hPrp31 protein in the nuclear extract prepared from HeLa cells 48 h after transfection with hPrp31-specific siRNA (EA2, Δ hPrp31) and a luciferase siRNA control (GL2). **C.** Anti-40K was used to immunoprecipitate snRNPs from the nuclear extract prepared from HeLa cells 48 h after transfection with siRNAs targeting luciferase and the U4/U6 protein hPrp31 (Δ hPrp31). PAS: Protein A-Sepharose incubated with nuclear extract. RNA was isolated from the immunoprecipitated snRNPs and characterised by northern blotting.

It has been shown that intact tri-snRNP particles require the presence of the hPrp31 protein (Schaffert *et al.*, 2004). Consistent with these earlier studies, antibodies against protein 40K, a protein that is a part of the U5 snRNP, precipitate intact tri-snRNPs from cell extracts transfected with an siRNA against the non-human firefly luciferase (GL2, Figure 4-24 C, lane 3). In extracts of cells that have been depleted of protein hPrp31, the antibody precipitates primarily U5 snRNPs (Figure 4-24 C, lane 6). Therefore, the lack of protein hPrp31 prevents interaction between the U5 snRNP and U4/U6 di-snRNP.

A possible effect of hPrp31 knock-down on the distribution of the U4/U6 di-snRNP-specific proteins hPrp3, hPrp4 and p110 was investigated by fluorescence microscopy with appropriately labelled antibodies. Consistent with the results of Schaffert *et al.* (2004), removal of hPrp31 by RNAi led to a pronounced accumulation of the U4/U6-specific protein hPrp4 in discrete nuclear foci (Figure 4-24 A, Δ hPrp31), so called Cajal bodies (compare Schaffert *et al.* 2004). In all cases, the intensity of the fluorescence signals in the Cajal bodies increased significantly in comparison with cells that had undergone control transfections (Figure 4-24 A, Control).

4 Results

As demonstrated by western blotting with antibodies directed against hPrp31 and the HA-tag (Figure 4-25 B), in cells depleted of the endogenous, hPrp31 (lane 2, lower panel) the exogenous HA-hPrp31 protein wild-type is expressed at a similar level (lane 3, upper and lower panel) as the endogenous hPrp31 wild-type protein in extracts of cells transfected with an siRNA against the non-human firefly luciferase (lane 1, lower panel). There was only minimal expression of the adRP causing hPrp31 mutant A194E detectable by western blotting (Figure 4-25 B, lane 4, upper and lower panel), whereas the expression of hPrp31 mutant A216P was reduced about five times compared to the HA-hPrp31 wild-type protein (Figure 4-25 B, lane 5, upper and lower panel).

To analyse the effect of the mutations on localisation of protein hPrp31 and the U4/U6 di-snRNP, the distribution of the hPrp31 mutants and the U4/U6-specific protein hPrp4 was checked by immunofluorescence. The distribution of the HA-hPrp31 wild-type and mutant fusion protein was investigated by fluorescence microscopy 46 hours after the simultaneous transfection of pTA2-HA-hPrp31 and siRNAs in HeLa cells, and it was compared with the distribution of the U4/U6 di-snRNP specific protein hPrp4 (60K) as detected by immunofluorescence (Figure 4-25 A). Expression of HA-hPrp31 rescues the hPrp31 knock-down phenotype described by Schaffert *et al.* (2004). Hence, cells expressing HA-hPrp31 do not show the pronounced accumulation of protein hPrp4 in Cajal bodies (Figure 4-25 A, a, b, and c). Both HA-hPrp31 and hPrp4 are distributed in a speckle-like pattern. In Figure 4-25 A (a, b, and c) two cells strongly expressing HA-hPrp31 are shown, next to a third cell expressing HA-hPrp31 weakly (a, indicated by the dashed line). These examples show different levels of the rescued knock-down phenotype within the same cell population, as hPrp4 is still localised in intensely labelled foci in the cell that weakly expresses HA-hPrp31, whereas these hPrp4 foci do not appear in cells with high levels of HA-hPrp31 expression. (Note that this demonstration does not represent the general transfection or expression efficiency of the fusion protein within HeLa SS6 cells, as it was conducted with selected cells.)

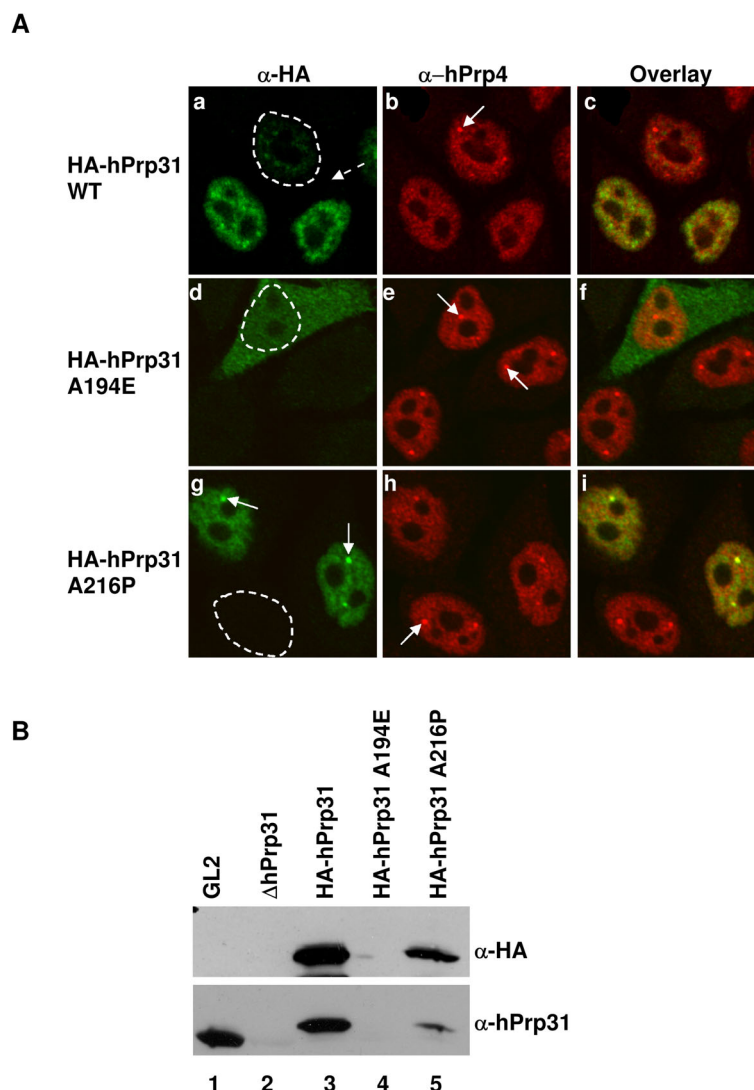


Figure 4-25 Expression of HA-hPrp31 (wild-type and mutants) in HeLa cells depleted of the endogenous hPrp31.

A. HeLa cells transfected with siRNA targeting the U4/U6 protein hPrp31 (EA2, Δ hPrp31) and pTA2-HA-hPrp31 wild-type (a, b, and c) and mutants A194E (d, e, and f) and A216P (g, h, and i) were examined 48 h after transfection as described in Figure 4-24. **B.** A western blot was performed using anti-HA and anti-hPrp31 antibodies showing levels of hPrp31 wild-type and mutants in the nuclear extract prepared from HeLa cells 48 h after transfection with hPrp31-specific siRNA (EA2, Δ hPrp31), a luciferase siRNA control (GL2) and pTA2-HA-hPrp31 wild-type and mutants A194E and A216P. Analyses of the U4/U6.U5 tri-snRNP incorporation of hPrp31 mutant A216P. Membrane was blotted twice using first anti-HA and then anti-hPrp31 antibodies. The first antibody was removed from the membrane by membrane stripping.

As detected previously by western blotting, adRP mutant hPrp31 A194E is expressed very poorly in HeLa cells (Figure 4-25 B, lane 4). The same observation is made by immunofluorescence: in the experiment shown, only every tenth cell expressed the mutant hPrp31 A194E protein (Figure 4-25 A, d). Interestingly, mutant hPrp31 A194E arises in the cytoplasm and only a small fraction is transported to the nucleus. The nucleoli, in which there is no HA-hPrp31 A194E, are visible as black holes in the staining pattern of the cell nucleus (d, indicated by the dashed line). Counterstaining of hPrp4 reveals that hPrp31 A194E does not accumulate in Cajal bodies as hPrp4 and that hPrp4 is still present in these foci. Thus,

4 Results

mutant hPrp31 A194E is not able to reverse the accumulation of hPrp4 in Cajal bodies in hPrp31 knock-down cells (Figure 4-25 A, e, indicated by solid arrows).

In contrast to HA-hPrp31 A194E, mutant HA-hPrp31 A216P is localised in the cell nucleus (Figure 4-25 A, g). The expression of HA-hPrp31 A216P, as detected by western blotting, is reduced by a factor of about 3 compared with the corresponding expression in the wild-type (see above). This fact raises the assumption of lower expression efficiency, which paradoxically was not detectable by fluorescence microscopy. Quantification of the fluorescence signal would be an alternative, and this is discussed below among possible future prospects (Section 5.4). Interestingly, mutant HA-hPrp31 A216P is localised in the nucleus and itself accumulates in the Cajal bodies (Figure 4-25 A, g, indicated by arrows). This accumulation has not been observed for the HA-hPrp31 wild-type. At the same time, HA-hPrp31 A216P is not capable of reversing the accumulation of hPrp4 in Cajal bodies (Figure 4-25 A, h).

Taken together, the presented experiments demonstrate that the phenotype observed upon hPrp31 knock-down can be rescued by HA-tagged hPrp31 wild-type protein. The mutant hPrp31 A194E shows a strong localisation defect. This mutant appears to have a defect in locating to the nucleus, probably because of impaired nuclear import, and remains in the cytoplasm. At the same time, hPrp31 A194E is not capable of reversing the accumulation of hPrp4 in Cajal bodies. In contrast, mutant hPrp31 A216P is capable of migrating to the nucleus. However, this mutant is not able to liberate hPrp4 from the Cajal bodies and itself accumulates in Cajal bodies.

4.4.2. Mutant hPrp31 A216P is incorporated into the tri-snRNP and interacts with the U5 snRNP-specific hPrp6 protein

Previously, it was shown that hPrp31 is required for the formation of the U4/U6.U5 tri-snRNP and functions as a bridge in the tri-snRNP by interacting directly with the U5-specific protein hPrp6 (Makarova *et al.*, 2002).

To analyse the effect of adRP mutants on tri-snRNP formation, immunoprecipitation assays followed by northern blot analysis were performed using nuclear extracts from cells expressing either the HA-tagged hPrp31 wild-type or the mutant hPrp31 A216P protein (Figure 4-26). As the level of expression of mutant hPrp31 A194E was very low, further biochemical analysis of this mutant was not possible. Interestingly, yeast two-hybrid analysis

revealed recently that mutant hPrp31 A194E shows a significantly reduced binding to the U5 snRNP-specific protein hPrp6 (Liu, 2005).

Anti-HA antibodies were used to immunoprecipitate snRNPs from the nuclear extract prepared from cells transfected with siRNAs targeting the U4/U6 protein hPrp31 (Δ hPrp31) and either the wild-type and mutant pTA2-HA-hPrp31. As shown in Figure 4-26 A, lane 3, HA-hPrp31 wild-type precipitates the U4, U6, and U5 snRNP via the anti-HA antibody. This result therefore demonstrates that the HA-tagged hPrp31 protein is incorporated into the U4/U6.U5 tri-snRNP.

The mutant hPrp31 A216E behaved similarly to the wild-type hPrp31 (Figure 4-26 A, lane 6). The HA-tagged mutant hPrp31 A216P was similarly shown to precipitate the U4, U6, and U5 snRNPs via the anti-HA antibody. Therefore, the presence of the mutant hPrp31 A216P did not impair the formation of the U4/U5.U6 tri-snRNP in the nuclear extracts used. Unfortunately, the signal of the U5 snRNA detected by northern blot is very weak. This may be because HA-hPrp31 in the U4/U6.U5 tri-snRNP is poorly accessible for the α -HA antibodies, or it may be because the tag prevents formation of the tri-snRNP. The latter problem might be circumvented by the transfection of non-tagged hPrp31 wild-type and mutant protein. The high efficiency of the hPrp31 knock-down (95%, see Figure 4-25) would allow investigation of the effect of the ectopically expressed proteins, as only a small (and negligible) amount of endogenous hPrp31 protein remains in the cells after hPrp31 knock-down.

To address the effect of the mutation A216P in hPrp31 on the interaction of hPrp31 with hPrp6, immunoprecipitation assays using anti-HA antibodies and nuclear extracts from cells expressing the HA-hPrp31 wild-type and mutant A216P respectively were performed and the precipitated hPrp6 was detected by western blotting. As shown in Figure 4-26 B, lane 4, wild-type HA-hPrp31 precipitates hPrp6 via the anti-HA antibody. This result demonstrates that the HA-tagged hPrp31 protein is in direct contact with hPrp6 and consequently supports the bridging of the U4/U6 di-snRNP and the U5 snRNP. The ability of the mutant hPrp31 A216P to precipitate hPrp6 via the anti-HA antibody was similar to that of the wild-type hPrp31. To normalise the result of the experiment, the protein concentration of the nuclear extracts was taken into account and not the concentration of the ectopically expressed HA-hPrp31 wild-type or mutant hPrp31 A216P. The supernatant shows that the amounts of hPrp6 were equal in all nuclear extracts used (Figure 4-26 B, lower row, lanes 2–5). As expression of hPrp31 A216P was reduced by a factor of 5 compared with the expression of the hPrp31

4 Results

wild-type protein (see Figure 4-25 B), and therefore is consequently only one-fifth as much hPrp31 A216P as hPrp31 wild-type protein in the extract available for the immunoprecipitation, it is not surprising that the amount of precipitated hPrp6 in the western blot appears to be about one-fifth of the amount obtained with the wild-type.

Taken together, these data show that the formation of the tri-snRNP is not affected by the point mutation A216P in hPrp31, and this mutation did not prevent the bridging of the U4/U6 di-snRNP to the U5 snRNP. This bridging was performed via direct interaction of hPrp31 with hPrp6. The pull-down experiments demonstrated that the interaction of hPrp31 with the U5-specific protein hPrp6 is not impaired by the mutation A216P. This result is furthermore supported by yeast two-hybrid analysis, which showed binding of mutant hPrp31 A216P to protein hPrp6 similar to that of the wild-type hPrp31 (Liu, 2005).

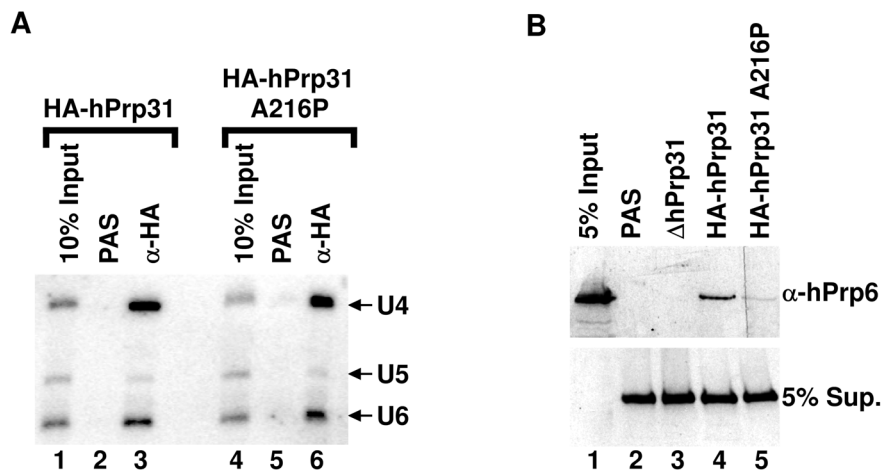


Figure 4-26 hPrp31 A216P is incorporated into the tri-snRNP and interacts with the U5 protein hPrp6.

A. Anti-HA antibodies were used to immunoprecipitate snRNPs from the nuclear extract prepared from HeLa cells 48 h after transfection with siRNAs targeting the U4/U6 protein hPrp31 (Δ hPrp31) and the wild-type and mutant pTA2-HA-hPrp31. PAS: Protein A-Sepharose incubated with nuclear extract. RNA was isolated from the immunoprecipitated snRNPs and characterised by northern blot analysis. **B.** Anti-HA antibody was used to immunoprecipitate proteins from the nuclear extract prepared from HeLa cells 48 h after transfection with siRNAs targeting luciferase, the U4/U6 protein hPrp31 (Δ hPrp31) and the wild-type and mutant pTA2-HA-hPrp31. Proteins were isolated from the immunoprecipitated snRNPs and the U5-specific hPrp6 protein characterised by western blotting. PAS: Protein A-Sepharose incubated with nuclear extract. 5% supernatant, detected by anti-hPrp6 antibodies.

5. Discussion

5.1. Regions on the 15.5K protein surface are required for complete U4/U6 di–snRNP and box C/D snoRNP assembly

One aim of the work presented in this dissertation was to investigate the role that protein–protein interactions play in the 15.5K-mediated assembly of four distinct RNP complexes, namely the U4 snRNP, the U4/U6 di–snRNP, the box C/D and box B/C snoRNP.

It has been noted previously that distinct structures and/or sequences in the RNA are required for the specific assembly of each complex (Granneman *et al.*, 2002; Nottrott *et al.*, 2002; Watkins *et al.*, 2002). The work presented here illustrates the fact that distinct regions of the surface of 15.5K are necessary for the assembly of each complex. This suggests that, in each case, the formation of the RNP requires a complex recognition process involving both protein and RNA.

5.1.1. Observed effects on complex assembly are specific, due to changes on the 15.5K surface

By using the crystal structure of protein 15.5K bound to the 5' stem-loop of U4 snRNA (Vidovic *et al.*, 2000) and sequence alignments, regions of conserved amino acids on the surface of the protein have been identified and mutated. The changes did not alter either the stability or the gross structural organisation of the protein, as each of the mutations supported the formation of at least one RNP complex. Analysis of the ability of these mutants to support RNP formation revealed that different regions on the surface of the protein are required for the assembly of each complex. This implies that, in each of the RNPs, substantial and essential contacts are made between this protein and one or more of the complex-specific proteins. Importantly, these mutations were not in areas of the protein involved RNA-binding, and none of the mutations altered either the affinity or the specificity of protein-binding to the three RNAs - U4 snRNA, the U14 box C/D snoRNA or the U3 box B/C RNA – which represent the RNA component of the three distinct RNPs. In many cases the binding reactions using the mutant 15.5K proteins (Figure 4-5 and Figure 4-6) were analysed by native gel electrophoresis in order to confirm that the proteins were stable and retained their RNA-

5 Discussion

binding ability under the assay conditions used. This therefore implies that the observed effects are the result of specific changes and are not due to non-specific disruption of the overall structure of the protein.

A detailed analysis of the role of the conserved surface amino acids in protein recruitment has been severely hampered by solubility problems observed with a great majority of the mutations constructed during this study. Indeed, 21 mutant constructs were generated during this study, of which only the five mutants used in this study were soluble (see section 4.1.4).

5.1.2. Differential recognition of the distinct RNAs and protein 15.5K

A differential recognition of RNA and 15.5K is not surprising when one considers that the proteins involved in each complex are very different, and that they use distinct domains/structures to mediate complex formation.

The only exception to this is the NOP-domain proteins, namely NOP56, NOP58 and hPrp31 (Gautier *et al.*, 1997). Interestingly, the recruitment of NOP58, NOP56 to U14 snoRNA and the binding of hPrp31 to the U4 snRNA require the highly conserved amino acids present in α helix 3. However, NOP56 and NOP58 binding in HeLa nuclear extract also required other regions of 15.5K, and at this point it is difficult to separate the requirements for binding of the individual snoRNP components.

Therefore, while it is interesting to speculate that NOP58 or NOP56 and hPrp31 may be in contact with the same region of 15.5K, it is at present difficult to draw any conclusions about the nature of the protein-protein interactions in box C/D snoRNPs.

5.1.3. Influence of conserved amino acids on the 15.5K surface on the association of the U4/U6di-snoRNP specific proteins hPrp31 and CypH/hPrp4/hPrp3

It is clear from the data that much of the surface of protein 15.5K is essential for the formation of the U4/U6 snRNP, implying that 15.5K is surrounded by proteins in the U4/U6.U5 tri-snoRNP. This is consistent with earlier observations, in both HeLa and yeast extracts, that 15.5K was not accessible for immunoprecipitation in the tri-snoRNP. Interestingly, 15.5K-2 inhibits the binding of both hPrp31 and the CypH/hPrp4/hPrp3

complex. The binding of these two spliceosomal components has been shown to be independent from one another (Nottrott *et al.*, 2002) and since all of these proteins are present in the U4/U6.U5 tri-snRNP it is likely that this mutation could disrupt two adjacent protein-binding sites on the surface of 15.5K.

5.1.4. Two or more components are involved in box C/D snoRNP assembly on the 15.5K protein–box C/D snoRNA complex

The 15.5K mutations that block box C/D snoRNP assembly either totally abolish the binding of all proteins (mutants 15.5K-1 and 15.5K-2) or inhibit the recruitment of NOP56 and TIP49 (mutant 15.5K-5)(see Figure 5-1). This implies that two or more RNP components directly bind the 15.5K–box C/D snoRNA complex.

Indeed, the data could suggest that the binding of NOP58, TIP48, and fibrillarin is essential for the subsequent recruitment of NOP56 and TIP49. The data show that recruitment of TIP49 and NOP56 are linked as binding of both proteins is disrupted by the same mutation (15.5K-5) on the 15.5K surface.

NOP56 and NOP58, and TIP48 and TIP49 are two pairs of homologous proteins (Newman *et al.*, 2000), respectively. This suggests that TIP48 may be involved in the assembly of NOP58.

NOP56 and NOP58 are proposed to make specific contact with the box C'/D' and C/D motifs respectively, and to interact with one another through a conserved coiled-coil domain (Cahill *et al.*, 2002; Aittaleb *et al.*, 2003). On this basis it can well be imagined that NOP56 recruitment is linked to an interaction with NOP58 bound at the C/D motif. However, the finding that α helix 5 of 15.5K is important for the specific recruitment of NOP56, together with the efficient binding of TIP49 by NOP56, suggests that NOP56 is in direct contact with 15.5K bound to the box C/D motif and that its recruitment is not solely due to contact with NOP58. Further work is required to define the various activities involved in snoRNP assembly.

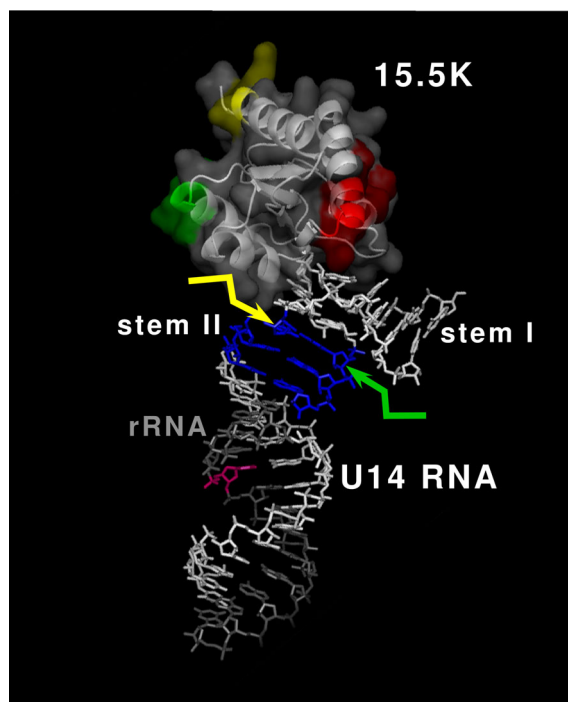


Figure 5-1 Model summarizing required sites in the U14 Box C/D snoRNA–15.5K binary complex.

The 15.5K protein has been resolved by crystallography in complex with the U4 snRNA nucleotides G26–G35 and C41–C47 (Vidovic *et al.*, 2000). For visualisation of regions within the U14 Box C/D snoRNA that are required for Box C/D snoRNP assembly or contacted by Box C/D specific proteins the region of the U14 snoRNA, which hybridizes with the 18S rRNA (indicated in grey, 2[′]-O-methylated nucleotide indicated in purple) was modelled and attached to stem II of 15.5K–U4 kink-turn crystal structure. The essential stem II of the U14 referring to stem II of the U4 kink-turn is highlighted by the blue coloured nucleotides. Nucleotides directly contacted by fibrillarin and NOP58 (Cahill *et al.*, 2002) are indicated by the yellow and green lightnings respectively. The mutations in 15.5K-1 (α helix 1), 15.5K-2 (α helix 3), and 15.5K-5 (α helix 5) of the 15.5K protein, which blocked Box C/D snoRNP assembly (see Figure 4-5) are highlighted in red, green and yellow in the 15.5K crystal respectively.

5.1.5. Direct protein-protein interactions are involved in RNP complex formation in the box B/C snoRNP

The identification of the RNA-independent hU3–55K–15.5K interaction supports the idea that protein–protein interactions within each of the complexes are important. A central feature of the work presented here was the use of a similar approach to detect direct interactions between 15.5K and hPrp31, hPrp3, hPrp4, CypH, NOP56, NOP58, and fibrillarin in the absence of RNA. However, no specific interaction could be detected between 15.5K and these proteins (data not shown). This implies that the interaction between 15.5K and these proteins was not sufficiently stable to allow detection, and that a stable interaction requires the presence of both 15.5K and RNA.

5.1.6. The eukaryotic proteins L7a, 15.5K, and NHP2 are probably derived from a common ancestor

The data imply that protein 15.5K is involved in numerous conserved interactions in the four distinct RNP complexes. The evolutionary pressure required to maintain these interactions therefore explains the high degree of conservation of 15.5K in eukaryotes. In archaea, a homologous protein, namely L7ae, is present in the ribosome, box C/D RNPs, and H/ACA RNPs (Kuhn *et al.*, 2002; Omer *et al.*, 2002; Rozhdestvensky *et al.*, 2003). Therefore, protein L7ae performs three functions. It functions as the eukaryotic L7a in the ribosome, as 15.5K in the box C/D snoRNPs, and as NHP2 in the box H/ACA snoRNPs. This implies that the three eukaryotic proteins are derived from a common ancestor. Interestingly, α helix 3 of the eukaryotic 15.5K, which is required for snoRNP formation, has a similar amino-acid composition in the archaeal L7ae (Figure 5-2), suggesting that this interaction is evolutionarily conserved.

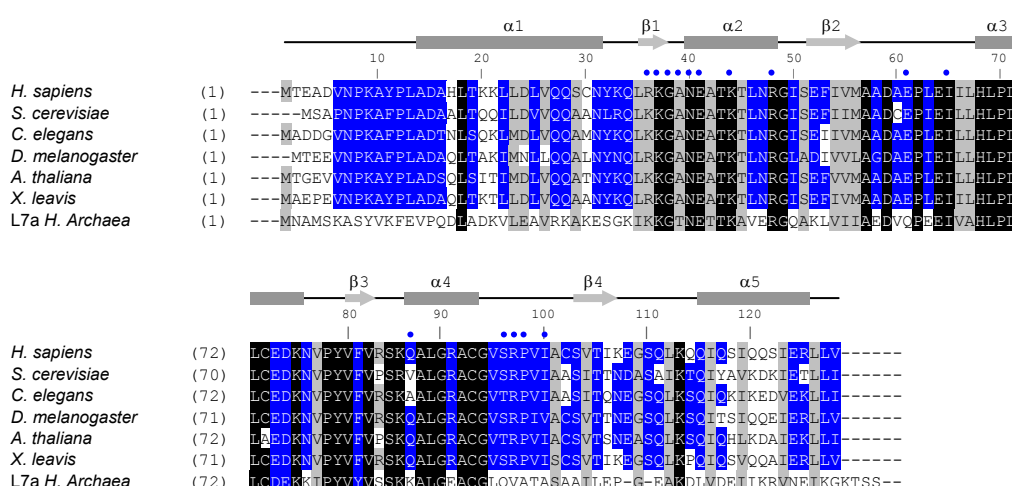


Figure 5-2 Sequence alignment of the eukaryotic 15.5K protein with the archaeal ribosomal L7a protein. Amino-acid alignment of protein 15.5K from human (*H. sapiens*), *Saccharomyces cerevisiae* (Snu13p), *Caenorhabditis elegans* (Accession no. Q21568), *Drosophila melanogaster* (Accession no. GH03082), *Arabidopsis thaliana* (Accession no. A71421), and *Xenopus laevis* (Accession no. AAH46579) with the archaeal (*Sulfolobus*) ribosomal protein L7a sequence using the ClustalV program. Conserved residues are indicated by grey boxes and are grouped as described in (Schulz and Schirmer, 1979). Identical and conserved residues are indicated in white on black boxes and in black on grey boxes, respectively. Residues specifically conserved in protein 15.5K are depicted in white on blue boxes. Amino-acid positions are indicated on the left. The secondary structure of the human 15.5K protein (Vidovic *et al.*, 2000) is indicated above the alignment, and amino acids involved in RNA-binding are indicated by blue circles.

5.2. The U4/U6 di–snRNP and box C/D snoRNP-associated protein 15.5K localise to nucleoplasmic foci

As a part of this study, the *in vivo* localisation pattern of the U4/U6 snRNP- and box C/D-specific protein 15.5K was investigated and the RNAs with which the 15.5K protein is complexed *in situ* were identified. This investigation was performed by using a cultured HeLa cell line. 15.5K was analyzed *in vivo*, either fused to 15.5K antibodies or with an EYFP fluorescent protein tag, and the resulting fusion proteins were shown to have similar localisation patterns. A stably transformed HeLa cell line that expressed EYFP–15.5K was established and used to investigate the specificity of RNA-binding to the endogenous 15.5K.

The analysis has shown that newly expressed 15.5K accumulates in splicing speckles, nucleoli and Cajal Bodies (Figure 4-10). On the basis of the results of previous biochemical studies on the structure and the binding specificity of 15.5K, the U4 snRNA is a possible candidate target for 15.5K in speckles. 15.5K binds U4 snRNA *in vitro* via the 5' stem-loop sequence (Nottrott *et al.*, 1999; Vidovic *et al.*, 2000). Consistent with this idea, hybridisation experiments have shown that the U4 snRNA localised to splicing speckles in HeLa cells; these speckles are thought to be sites of storage of mRNA splicing factors (Carmo-Fonseca *et al.*, 1992; Lamond and Spector, 2003). However, a permanent localisation of 15.5K in the splicing speckles has not been reported before. Leung and Lamond (2002) demonstrated that newly imported 15.5K transiently co-localises with splicing factors in splicing speckles. At later time points, the signal in speckles was no longer detected and EYFP–15.5K accumulates specifically in nucleoli and Cajal bodies.

The binding studies shown in section 4.2.2 demonstrate that EYFP–15.5K interacts *in vivo* with the U4 snRNA. As the U4 snRNA is associated with the U6 snRNA through an extended stretch of RNA base pairs (see 2.1.2.1), the U6 snRNA is co-precipitated with protein 15.5K. Likewise, the U5 snRNA is co-precipitated by 15.5K, as it is connected with the U4/U6 di–snRNP by a bridge made up of the U4/U6-specific protein hPrp31 and the U5-associated protein hPrp6 (Makarova *et al.*, 2002).

Another type of nuclear foci in which protein 15.5K is located are the Cajal bodies, which are involved in snRNP biogenesis and in the trafficking of snoRNPs and snRNPs. SnoRNPs and snRNPs are thought to move through the Cajal body en route to the nucleoli or splicing speckles (Sleeman and Lamond, 1999). Furthermore, there is some evidence that Cajal bodies may play a role in U4/U6.U5 tri-snRNP recycling (Schaffert *et al.*, 2004).

Consistent with this idea the U4 snRNA, which is complexed with protein 15.5K is located in Cajal bodies (Sleeman and Lamond, 1999; Misteli, 2000).

Furthermore, it was shown that 15.5K is located in nucleoli and co-localises with box C/D snoRNP-specific protein NOP56 (Figure 4-10) in nucleoli and Cajal bodies. This result is consistent with immuno-fluorescence results of (Leung and Lamond, 2002). It has been shown by Narayanan *et al.* (1999) that wild-type box C/D snoRNAs associate transiently with Cajal bodies before they localise to nucleoli and that variant RNAs that lack an intact box C/D motif are retained within Cajal bodies.

Additionally, the data show that 15.5K is complexed with the U3 box C/D snoRNA *in vivo*, which also contains a box B/C motif. This result is consistent with the idea that protein 15.5K is associated with the box C/D snoRNAs *in vitro* and *in situ* (Granneman *et al.*, 2002; Leung and Lamond, 2002; Watkins *et al.*, 2002). The protein binds directly the conserved box C/D motif and the U3 specific box B/C motif.

In addition, the *in vivo* localisation pattern of 15.5K mutants and RNAs complexed with 15.5K *in situ* were studied. The effect of these mutants on complex formation of the U4/U6 snRNP and box C/D snoRNPs was investigated *in vitro* (section 4.1). Mutant 15.5K-2 is barely expressed in HeLa cells and was prevented from translocating from its site of synthesis in the cytoplasm to the nucleus (Figure 4-11). However, no significant difference was observed investigating the localisation of the other 15.5K mutants (15.5K-1, 15.5K-3, 15.5K-4, and 15.5K-5), as they localised to the nucleoli, Cajal bodies and splicing speckles in a manner similar to that of the 15.5K wild-type (Figure 4-11, Figure 4-12, and Figure 4-13). This effect is likely to be due to the binding of 15.5K to naked RNAs, in which the protein acts as a nucleation factor for the recruitment of additional U4/U6 snRNP- and box C/D-snoRNP-specific proteins associating with the complex. Therefore, it is possible that the effect on localisation of the fully assembled RNPs is superimposed by 15.5K bound to naked snRNA and box C/D snoRNAs or incompletely assembled RNPs.

5.3. Requirement for U4 snRNA's kink-turn stem II and the Nop domain for the association of the spliceosomal hPrp31 protein with the U4 snRNP

In the next part of this work, the binding of hPrp31 to the U4 snRNA 5' stem-loop complexed with the 15.5K protein was investigated. By using previous hydroxyl-radical

5 Discussion

footprinting analysis (Nottrott, 2002), detailed information on the relevant RNA-protein contacts was obtained. RNA mutational analysis and protein homology comparison revealed some essential features of the RNA-protein interaction, viz (i) the requirements made of the RNA structure and (ii) the role of the hPrp31 Nop domain as a necessary and sufficient factor to mediate stable complex formation. Finally, the results contribute to an understanding of how hPrp31 binds specifically to U4 snRNP and how NOP56/NOP58 to the box C/D snoRNPs. These issues are discussed in turn below.

5.3.1. Global RNA shielding by hPrp31 of the U4 snRNA in the ternary hPrp31-15.5K-U4 snRNA complex

In the quest to understand the interaction of hPrp31 with the U4 snRNA in the ternary complex hydroxyl radical footprinting experiments from the PhD thesis of Stephanie Nottrott (Nottrott, 2002) have been re-examined. In these experiments a direct protein-induced shielding of the RNA by hydroxyl radicals can be observed (Figure 4-18). On both sides of the kink-turn, directly neighbouring the 15.5K binding site (FP 1 and FP 2), discrete footprints were located. First of all, hPrp31 induces protection of the complete penta-loop structure and of all the stem II nucleotides that were not in contact with protein 15.5K (FP A). Secondly, on the other side of the kink-turn, only a few nucleotides of stem I were found protected by hPrp31 (FP B). An additional protection was found between hPrp31 and nucleotides G18 and C16 in the U4 snRNA context (FP C), where this region is part of a helix extending stem I (Myslinski and Branlant, 1991). If one assumes an ideal RNA helix, then the distance of 11 base pairs between FP B and FP C would imply that both footprints are located on the same face of the RNA helix, some 25 Å apart. In the context of the U4/U6 snRNA duplex, FP C is located at almost identical nucleotides, albeit somehow enlarged. In order to obtain a relative placing of FP B and FP C in the U4/U6 snRNA context that would be comparable to its placement in the U4 context, a continuity of stem I with helix II is required. This can only be achieved by a coaxial stacking of stem I onto the U4/U6 helix II. In fact, this has recently been proposed for the U4/U6 three-way junction comprising helix II, stem I and helix I (Lescoute and Westhof, 2006). Satisfyingly, the location of FP C is in good agreement with cross-links that were previously identified between hPrp31 and U4 snRNA nucleotides G18/U19 in the context of the U4/U6.U5 tri-snRNP (Nottrott *et al.*, 2002). These two nucleotides are located directly next to the FP C.

Interestingly, our data are fully compatible with extensive comparison by RNA structure probing of the U4/U6.U5 tri-snRNP (containing hPrp31) and 10S U4/U6 di-snRNP (lacking it) (Mougin *et al.*, 2002). For example, sites of strong cleavage by the double-strand specific nuclease V1 were observed on stem I of U4/U6 snRNAs, irrespective of the presence or absence of hPrp31 (U4-G48 and, to a lesser degree, U4-C49), indicating that hPrp31 makes contact with stem I from one side only. This is further corroborated by discrete V1 cleavages at the 5' end of stem I (U4-U21 and U4-C22), which were only observed in the absence of hPrp31 (Mougin *et al.*, 2002). In sum, these observations suggest that what was observed in the U4/U6 complex is directly applicable to the situation in the tri-snRNP.

Having identified the hPrp31 sites of protection from hydroxyl radicals in the U4 snRNA, next it has been speculated how the experimental binding sites could be arranged in 3D. For this purpose it has been resorted to the crystal structure of the 15.5K-U4 snRNA kink-turn (Vidovic *et al.*, 2000). Through the formation of the kink-turn, stem II would be forced into an angle of about 30° relative to the helix axis of stem I (Vidovic *et al.*, 2000). Stem I of the U4 snRNA 5' stem-loop was now simulated by adding an idealised RNA A-form helix on to the stump of stem I in the crystal structure (Figure 5-3). The experimentally determined protection sites were then mapped onto this model. Clearly, hPrp31 would touch the RNA in two patches, namely FP C and FP B, and at the same time it would bury whatever is exposed of stem II and the penta-loop in FP A (Figure 5-3). From this model it becomes clear that hPrp31 approaches the 15.5K-U4 snRNA complex from one side only.

From the footprint it has been concluded that the relative orientation of hPrp31 to the RNA elements should be topologically equivalent between U4 snRNA and the U4/U6 snRNA duplex. If one would think of the entire helix II and the coaxially stacked stem I as a single idealised RNA helix, then hPrp31 would shield the upper half of this big helix in FP C and FP B. This asymmetric binding would be translated into an asymmetric architecture of the whole particle. Though highly simplified, this model, in conjunction with the three-way junction model (Lescoute and Westhof, 2006), provides readily testable constraints for the relative positioning of helix I of the U4/U6 snRNA duplex. This is currently being done by a variety of different approaches.

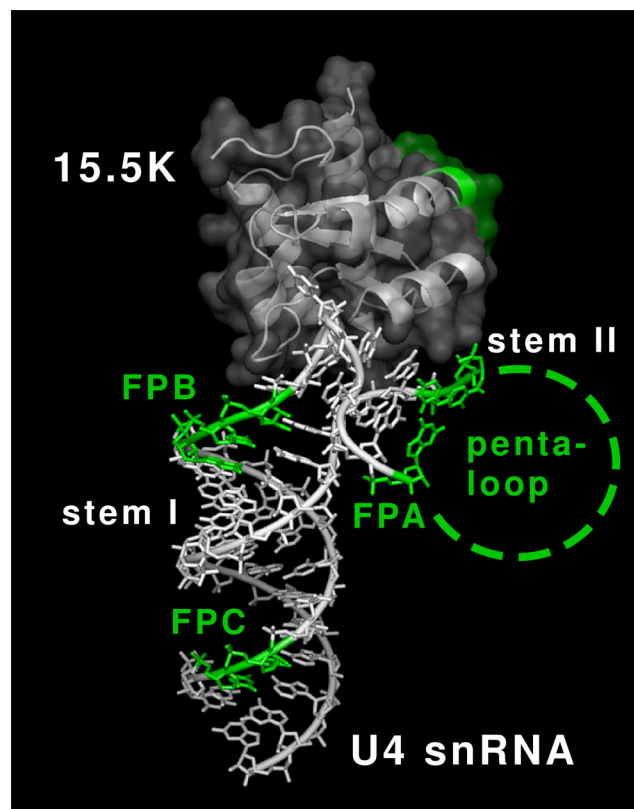


Figure 5-3 Model demonstrating contacted sites of hPrp31 in the U4 snRNA-15.5K binary complex.

The 15.5K protein has been resolved by crystallography in complex with the U4 snRNA nucleotides G26–G35 and C41–C47 (Vidovic *et al.*, 2000). For visualisation of regions within the U4 snRNA that are in contact with protein hPrp31 an ideal A-form helix was attached to stem I of 15.5K-U4 kink-turn crystal structure. The helix sequence used (5' half, 5'-CCUCCUUGGAU-3', 3' half, 5'-AUCCAAGGAAGG-3') differs from the wild-type U4 snRNA sequence. Footprints of hPrp31 in the U4 snRNA are indicated by the green coloured nucleotides and are labelled FP A–C as in the text and in Figure 4-18. The green dashed line indicates the terminal penta-loop which was not resolved in the original crystal structure (Vidovic *et al.*, 2000).

5.3.2. RNA structural requirements for binding of hPrp31 to the 15.5K protein–U4 snRNA binary complex

A systematic mutational analysis revealed a highly differentiated requirement for the various RNA structural elements. A battery of U4 snRNA 5' stem-loop mutants was assayed in an electrophoretic mobility-shift assay (EMSA) for overall kinetic stability in ternary-complex formation.

The complete 5' terminal nucleotides (A1–U19), including those nucleotides that were in contact with U6 snRNA in the ternary complex (FP C), were found to be inessential. Although no binding of the U4–2 had previously been observed (Nottrott *et al.*, 2002), it seems likely that the difference in the assay systems accounts for this discrepancy. The previous pull-down assay involved a wash step at 500 mM salt, whereas in the present study the ternary complex was never subjected to more than 150 mM salt. In addition, the EMSA

may detect kinetically stable complexes, which cannot survive the continuous dilution of a pull-down assay.

Although the region of contact between hPrp31 and the kink-turn is only very short (FP B), the 8-bp stem I was required for efficient hPrp31 binding to the ternary complex. Neither the removal of the upper part (five base pairs and the bulge), nor the removal of a bottom part consisting of four base pairs only, was tolerated (Figure 4-19). The U4atac snRNA, which also supports ternary-complex formation, does not contain the bulged adenosine and has a different stem I sequence, but stem I is of identical length (Figure 5-4). This comparison suggests that the length of eight base pairs, but not the sequence of stem I, is critical for the binding of hPrp31 to the binary complex. This is further corroborated by a phylogenetic analysis, which showed that stem I is, with so far only one exception, exactly 8 bp long (sequences in this region are collated for 13 organisms in Figure 5-4). Consistent with this length requirement, the above-mentioned protection from V1 nuclease cleavage at nucleotides U21 and C22 suggest that hPrp31 protein is in contact with the first base pairs of stem I. This contact does not result in protection of ribose, since the hydroxyl-radical footprint is restricted to the other end of the stem I (FP B). It will be interesting to determine the nature of the RNA-protein contacts involved. This will be particularly interesting in view of the box C/D discrimination discussed below.

Paradoxically, the large penta-loop structure, of which every ribose is in contact with hPrp31, is not required for binding. This is the more surprising because one of the two UV cross-linking sites of hPrp31 on U4 snRNA maps to this region (Nottrott *et al.*, 2002). Further, in the U4atac snRNA penta-loop, which has a different sequence, similar cross-links are observed to hPrp31 (Kühn-Hölsken *et al.*, 2005). These observations suggest that the penta-loop is in close contact with the ribose-phosphate backbone. Various contacts can be detected by UV cross-linking, depending on which base is in contact with the protein surface. Since this RNA-protein interaction pattern is not required for primary recognition in the ternary complex, it is presumably important in one of the dynamic functional states of U4 snRNA during the splicing cycle.

Another interesting feature of the penta-loop deletion mutant (U4-B) is that the binding of protein 15.5K to the truncated U4 5' stem-loop structure was hardly detectable by EMSA, even though ternary-complex formation was unaffected (Figure 4-20, lanes 18 and 19). Thus, it appears that transient and/or weak binding of this protein to the mutant RNA are dramatically stabilised by interaction with hPrp31.

5 Discussion

Since it is known that hPrp31 binds neither the U4 snRNA (Nottrott *et al.*, 2002) nor the 15.5K protein (immunoprecipitation data, not shown) on its own, it appears as if hPrp31 simultaneously recognises the protein and RNA components of the transient binary complex. It is conceivable that hPrp31 simultaneously recognises a composite RNA/protein surface of the binary 15.5K–U4 snRNA complex.

The length of stem II turned out to be of crucial importance for hPrp31 binding to the binary complex. Binding was completely abolished by extending the stem by a single Watson-Crick base pair, irrespective of the presence or absence of the penta-loop (Figure 4-20). These findings imply that hPrp31 can accommodate at most two base pairs of stem II in a binding site; a third base pair interferes sterically with productive binding. This binding site thus contributes significantly to the specificity of the RNA-protein recognition. Interestingly, a phylogenetic comparison of the penta-loops from human, rat, mouse, chicken, and fly U4 snRNA s revealed that in both U4 and U4atac snRNAs no Watson-Crick base pair can be formed at the bottom of the penta-loop. This restricts the length of stem II strictly to two base pairs, lending further support to the model for molecular recognition outlined above. Exceptions are found only in nematode U4 snRNA, which were able to form a C-G pair at the top of the penta-loop, and in yeasts, which have a six-membered loop. The latter may have special requirements, in that the six-membered loop ends with an A-U base pair (Figure 5-4). Alternatively, a specialised loop structure may prevent formation of the A-U base pair in yeast.

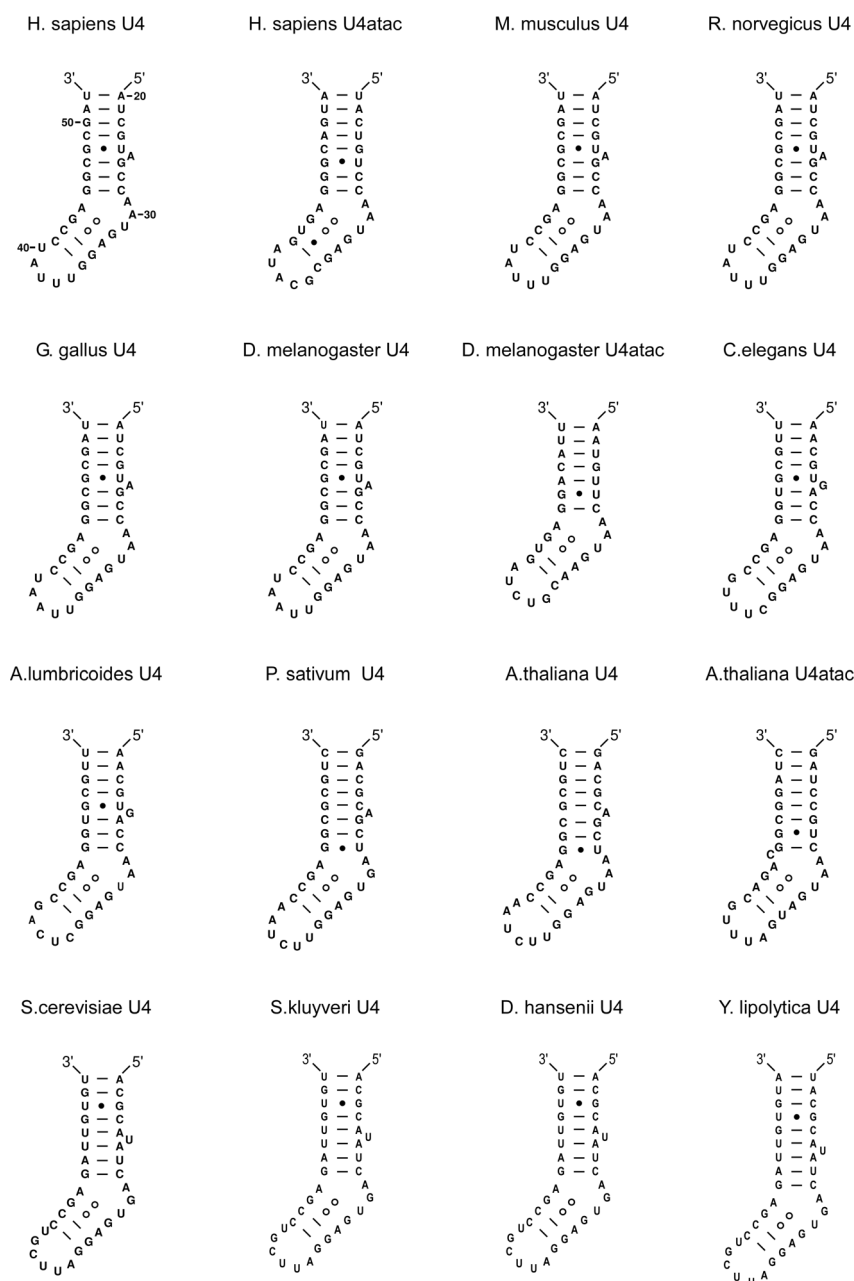


Figure 5-4 Secondary structure of the U4 or U4atac snRNA 5' stem-loops for selected organisms.

Gene bank (<http://www.ncbi.nlm.nih.gov>) accession numbers are given in brackets. *H. sapiens* U4 (NR_002759) and U4atac (U62822), *M. musculus* U4 (M18004), *R. norvegicus* U4 (M26115), *G. gallus* U4 (K00476), *D. melanogaster* U4 (NR_001679) and U4atac (AC007532, positions 155309–155468), *C. elegans* U4 (X07828), *A. lumbricoides* U4 (L22250), *P. sativum* U4 (X15932), *A. thaliana* U4 (X67146) and U4atac (see reference (Wang and Brendel, 2004)), *S. cerevisiae* U4 (M17238). U4 sequences from the yeast strains listed in the bottom row are taken from supplemental reference (Bon *et al.*, 2003). Base pairs are denoted by the following nomenclature: solid lines for W-C base pairs, solid dots for non-canonical base pairs except for sheared G-A base pairs, which are indicated by open circles.

5.3.3. Different and shared binding requirements between hPrp31 and the box C/D snoRNP proteins NOP56 and NOP58

The nucleolar box C/D snoRNPs and the spliceosomal U4 snRNP share a common core RNP structure, consisting of the 15.5K protein bound to an internal RNA loop. hPrp31 selects exclusively U4 snRNA, whereas NOP56/NOP58 selects only the box C/D snoRNP structure, with the ultimate result that two particles with completely different biological properties and functions are produced. The binding requirements of hPrp31 suggest how this discrimination may be achieved on a molecular level. Stems I and II, flanking the 15.5K-induced kink-turn, are undoubtedly the two important RNA structural determinants that are differentially recognised by the different Nop domains (Figure 5-5).

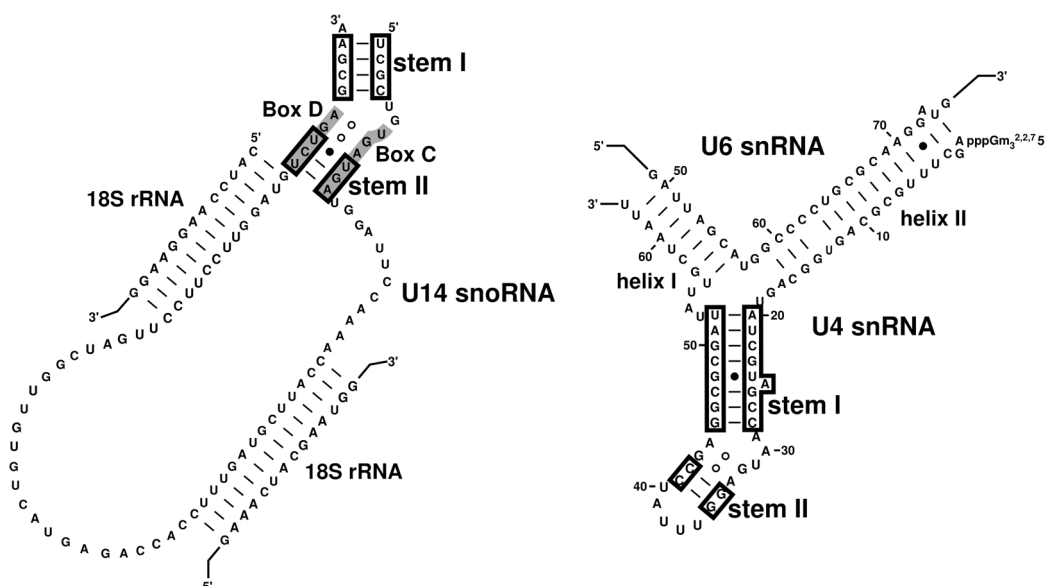


Figure 5-5 Schematic representation of the U4/U6 snRNA and U14 box C/D snoRNA.

The secondary structures of the U4/U6 snRNA (Brow and Guthrie, 1988) and U14 box C/D snoRNA (Watkins *et al.*, 2000; Watkins *et al.*, 2002) are shown on the left and right, respectively. The two flanking stems I and II that together with the internal loop form the k-turn are boxed in black. Conserved boxes C and D of the U14 snoRNA are indicated in black on a grey background. Base pairing interactions are indicated as in Figure 4-18. The two helical structures formed between U14 snoRNA and the 18S rRNA, which are essential for modification and processing are indicated.

As outlined above, the stem II binding site of hPrp31 can only accommodate a two-base-pair-long stem, probably with further restrictions imposed by the closeness of the 15.5K protein. In contrast, in the box C/D snoRNA this stem is a conserved three-base-pair-long stem with a closing A-U pair (Watkins *et al.*, 2002). In fact, the addition of a Watson-Crick base pair to the U4 stem II (mutants U4-7 and U4-8, Figure 4-21) resulted in the loss of hPrp31 binding. Therefore, stem II can be viewed as a major discrimination element.

Moreover, box C/D snoRNAs have strict sequence requirements for stem II, where a central G-C base pair was found to be essential (Watkins *et al.*, 2002). The other discrimination element is probably stem I. A four-base-pair-long stem I on box C/D snoRNAs is sufficient for NOP56/NOP58 binding, while in the U4 snRNA context this is clearly not sufficient.

5.3.4. The hPrp31 Nop domain is necessary and sufficient for hPrp31 binding to the U4 snRNA-15.5K binary complex

The Nop domain, initially identified on the basis of sequence alignment (Makarova *et al.*, 2002) is here defined more precisely by comparing secondary-structure predictions (Figure 4-22) and using the recently published crystal structure of the archaeal Nop5p homologue (Aittaleb *et al.*, 2003). The studies show that this domain on its own is both necessary and sufficient for binding to the binary 15.5K-U4 snRNA complex. In particular, the determinants for recognition of stem II are entirely contained within it. Of the two cross-linking sites of hPrp31 on U4 snRNA, the one mapping to the penta-loop was retained in the RNA construct that could be cross-linked to the Nop domain (Figure 4-23). Therefore, it is reasonable to infer that the Nop domain also contains elements of the binding site that are in contact with the penta-loop. The penta-loop cross-link itself maps to H270 of hPrp31 (Nottrott *et al.*, 2002; Kühn-Hölsken *et al.*, 2005), a residue located in the Nop domain. Interestingly, the homologous position in the archaeal Nop5p crystal structure maps to a flexible loop (cf. Figure 4-22, dashed grey line). While further studies were not attempted, it is tempting to speculate that this unordered loop becomes ordered upon penta-loop binding. On the other hand, the penta-loop, which was found to be unstructured in the binary 15.5K-U4 5' stem-loop structure (Vidovic *et al.*, 2000), may likewise become structured upon ternary-complex formation. This flexibility would be consistent with the above idea that the penta-loop binds in a manner largely independent of sequence.

The observed complex formation suggests that the stem I determinants are likewise contained in the hPrp31 Nop domain. This interesting domain thus recognises three different RNA structural elements, of which stem I and stem II are required for complex formation. In addition, preliminary evidence (Schultz *et al.*, 2006a) indicates that recognition specificity is also influenced by recognition between the proteins hPrp31 and 15.5K in the context of ternary-complex formation, adding a further element of complexity to the process of binding of hPrp31 to the 15.5K-U4 snRNA 5' stem-loop.

5 Discussion

Recently, two mutations responsible for the autosomal form of the disorder retinitis pigmentosa were mapped to the gene encoding the hPrp31 protein (Vithana *et al.*, 2001). While nothing is known about the molecular details of the effect of these mutations, it is important to note that they map onto (mutation A216P) or adjacent to (mutation A194E) the Nop domain that in this work was found necessary and sufficient for hPrp31 binding to the 15.5K–U4 snRNA binary complex. It seems possible that the mutations affect the binding of hPrp31 to U4 snRNP and may thus exert a subtle influence on tri-snRNP stability. Studies are currently under way to investigate these mutations in the assay system.

5.4. Analysis of retinitis pigmentosa causing mutations in the U4/U6 specific hPrp31 protein on cellular localisation and tri-snRNP formation

In this work, the effects of hPrp31 adRP point mutations A194E and A216P causing the autosomal dominant form of retinitis pigmentosa (see 2.1.4) on the localisation of protein hPrp31 within human cells and on tri-snRNP formation have been studied by combining RNAi depletion methods with fluorescence microscopy and biochemical studies using HA-tagged hPrp31, wild-type and mutants.

Recent findings show that when the cells are depleted of hPrp31 protein by RNAi knock-down, the formation of U4/U6.U5 tri-snRNP is inhibited, and stable U4/U6 di-snRNPs and U5 snRNPs accumulate in the cell (Schaffert *et al.*, 2004). This demonstrated for the first time *in vivo* that the U4/U6 protein hPrp31 is essential for the interaction of the U4/U6 di-snRNP with the 20S U5 snRNP, and it is consistent with previous studies performed *in vitro* (Makarova *et al.*, 2002). Interestingly, under conditions where tri-snRNP formation was inhibited, both U4/U6-specific proteins and U4 and U6 snRNAs accumulate in Cajal bodies (Schaffert *et al.*, 2004).

The “rescue” experiments presented here (4.4.2) demonstrate that the wild-type phenotype in HeLa cells depleted of hPrp31 can be restored by expressing HA-tagged hPrp31 wild-type protein (Figure 4-25). The U4/U6 di-snRNP-specific protein hPrp4 is liberated from the Cajal bodies and tri-snRNP formation is restored (see Figure 4-25 and Figure 4-26). This result therefore strengthens the hypothesis (Schaffert *et al.*, 2004) that tri-snRNP formation takes place in Cajal bodies as the expression of exogenous protein hPrp31 is able to restore tri-snRNP formation and wild-type phenotype.

Mutant A194E gave a staining pattern quite different from that of wild-type hPrp31, with signal throughout the cytoplasm and rather less intense staining in the nucleus (Figure 4-25). This might be due to a reduced solubility of the mutant A194E. The sub-cellular localisation shows that A194E mutation interferes with, but does not completely prevent, the translocation of protein from its site of synthesis in the cytoplasm to the nucleus. Interestingly, protein hPrp31 has been shown to interact with importin (β 1) for translocation to the nucleus. However, neither the A194E nor the A216P mutation has any effect on this interaction (Wilkie *et al.*, 2006). Furthermore, hPrp31 A194E is not capable of reversing the accumulation of hPrp4 in Cajal bodies, and the results presented here indicate that mutation A194E results in mis-location of the protein. Some soluble protein does reach the nucleus, as seen from the confocal images. It is possible that the reduced solubility of the mutant protein may result in an insufficiency of splicing activity in cells with a very high metabolic demand, and this remains the most likely explanation for the retinitis pigmentosa disorder. The problem may alternatively lie in the efficiency of the targeting mechanism by which the protein is translocated from its site of synthesis in the cytosol into the nucleus.

This conclusion is supported by the analysis, which showed that fewer mutant than wild-type protein was present in the nucleus (Figure 4-25). It may be that the mutant protein is more susceptible to mis-folding and thus produces insoluble aggregates in the cytosol. This mis-folding may result in a protein with lost function and to an insufficiency of splicing function. This splicing insufficiency might lead to a reduction in the concentrations of certain key proteins and, finally, cause cell photoreceptor degeneration.

In contrast, mutant hPrp31 A216P is capable of migrating to the nucleus. However, this mutant is unable to liberate hPrp4 from the Cajal bodies, and itself accumulates in Cajal bodies (Figure 4-25). As detected by Western blotting the expression of HA-hPrp31 A216P is reduced by a factor of about three compared with the wild-type expression (Figure 4-25). Results furthermore show that the formation of the tri-snRNP is not affected by the point mutation A216P in hPrp31, and the mutation did not prevent the bridging of the U4/U6 di-snRNP to the U5 snRNP (Figure 4-26). Bridging of U4/U6 di-snRNP and the U5 snRNP takes place by direct interaction of hPrp31 with hPrp6. The pull-down experiments presented here demonstrate that the interaction of hPrp31 with the U5-specific protein hPrp6 is not impaired by the mutation A216P (Figure 4-26). This result is furthermore supported by yeast two-hybrid analysis, which showed binding of mutant hPrp31 A216P to protein hPrp6 similar to that of the wild-type hPrp31 (Liu, 2005).

5 Discussion

Taken together, the results presented in section 4.4 suggest a decrease in concentration of functional hPrp31 protein in the nucleus. Such as, inactivation of the Nop domain, could cause an insufficiency of splicing function. The Nop domain has been shown to be necessary for hPrp31 binding to the U4 snRNP (see 4.3.3) and consequently has a key function in tri-snRNP formation (Makarova *et al.*, 2002; Schaffert *et al.*, 2004). One effect of the reduced amount of functional hPrp31 protein in the nucleus may be a reduction in the concentrations of certain key proteins in the cell. Further investigation in the mammalian system will be needed to examine the basic cause of the disorder retinitis pigmentosa.

5.5. Future Prospects

The assembly of the spliceosomal U4/U6 di-snRNP and the box C/D snoRNPs has been shown to be highly complex and to involve a hierarchical assembly pathway (Nottrott *et al.*, 2002; Watkins *et al.*, 2002). This process is initiated by the 15.5K protein, acting as a primary RNA-binding protein. At the beginning of this study it was unknown how 15.5K directs the assembly of the complex. However, the results presented here demonstrate that protein-protein contacts are essential for RNP formation in each complex, and they suggest that the formation of each RNP involves the direct recognition of specific elements in both 15.5K protein and the specific RNA.

The results presented in this work provide a basic idea of the three-dimensional architecture of the U4/U6 di-snRNP and the box C/D snoRNPs (see section 4.1 and 4.3) to which further studies such as X-ray crystallography could fall in line.

In the case of the U4/U6 di-snRNP-specific hCypH/hPrp4/hPrp3 complex, four different regions on the surface of protein 15.5K influenced the assembly (see section 4.1.3). However, it remains unknown which region on the 15.5K surface makes contact with which of the three trimeric-complex proteins. Knowledge of this would provide further essential information about the three-dimensional structure of the U4/U6 di-snRNP and, probably, about the function of each of the proteins in the U4/U6 di-snRNP.

Similar considerations will also apply to the box C/D snoRNP assembly, which is also known to take place in a hierarchical manner (Watkins *et al.*, 2002). Mutants in different regions of the 15.5K surface have been shown to disrupt the association of complex-specific proteins, fibrillarin, NOP56, NOP58, TIP48 and TIP49 (see section 4.1.4). However, it is not known which region on the 15.5K surface makes contact with which of the box C/D-specific proteins. Therefore, the use of recombinant proteins would be helpful in finding out which

box C/D-specific protein is in contact with which region on the 15.5K surface. This could at the same time yield information about the order of events in the formation of the box C/D snoRNP complex, which would improve our understanding about hierarchical complex assembly pathways.

The complex, hierarchical assembly of the U4/U6 di-snoRNP and of the box C/D snoRNPs are probably dynamic processes. The association of a single protein may change the structure of the RNP and at the same time the conformation of the RNA. These dynamic rearrangements within the RNA could be investigated in NMR studies by assembling the complexes in a stepwise manner. Knowledge about RNA-RNA rearrangements within the U4/U6 di-snoRNP and the box C/D snoRNPs is of major interest on understanding of their function in the different processing pathways in which these complexes are involved.

In the work described in this dissertation, structural features of the U4 snRNA and the protein hPrp31 necessary for the binding of hPrp31 to the U4/U6 snRNP were identified (see section 4.3). By employing point and deletion mutants of U4 snRNA and deletion mutants of protein hPrp31, a minimal U4 snRNA–15.5K–hPrp31 trimeric-complex was identified. The results provide a minimal complex that would be suitable for crystallisation; it consists of the U4 5' stem-loop and the hPrp31 Nop domain. Crystallisation of the complex would give further information about the three-dimensional structure of the U4 snRNP. This is a matter of particular interest in comparison with the box C/D snoRNPs as hPrp31 and the box C/D snoRNP-specific proteins NOP56 and NOP58 are homologous proteins sharing the conserved Nop domain. Conserved Nop domains of hPrp31 and NOP56/NOP58 have to recognise on the one hand but have to discriminate on the other hand between the distinct 15.5K-RNA complexes.

Protein hPrp31 is also of clinical interest as two mutations (A194E, A216P) in the human hPrp31 gene (*PRPF31*) are correlated with the autosomal dominant form of retinitis pigmentosa (see section 2.1.4). Using fluorescence microscopy and biochemical methods it has been shown here how hPrp31 mutations influence the localisation of hPrp31 *in vivo* and how they influence U4/U6.U5 tri-snoRNP formation (see section 4.4). However, whether both mutations have any influence on splicing remains unknown. Therefore, an understanding of the effect of mutations A194E and A216P on splicing could be of value in explaining the role(s) of these mutations in autosomal dominant retinitis pigmentosa.

6. References

- Achsel, T., Brahm, H., Kastner, B., Bachi, A., Wilm, M. and Lührmann, R. (1999) A doughnut-shaped heteromer of human Sm-like proteins binds to the 3'-end of U6 snRNA, thereby facilitating U4/U6 duplex formation *in vitro*. *EMBO J.*, **18**, 5789-5802.
- Aittaleb, M., Rashid, R., Chen, Q., Palmer, J.R., Daniels, C.J. and Li, H. (2003) Structure and function of archaeal box C/D sRNP core proteins. *Nat. Struct. Biol.*, **10**, 256-263.
- Anthony, J.G., Weidenhammer, E.M. and Woolford, J.L., Jr. (1997) The yeast Prp3 protein is a U4/U6 snRNP protein necessary for integrity of the U4/U6 snRNP and the U4/U6.U5 tri-snRNP. *RNA*, **3**, 1143-1152.
- Ayadi, L., Callebaut, I., Saguez, C., Villa, T., Moron, J.P. and Banroques, J. (1998) Functional and structural characterization of the prp3 binding domain of the yeast prp4 splicing factor. *J. Mol. Biol.*, **284**, 673-687.
- Bach, M., Winkelmann, G. and Lührmann, R. (1989) 20S small nuclear ribonucleoprotein U5 shows a surprisingly complex protein composition. *Proc. Natl. Acad. Sci. U S A*, **86**, 6038-6042.
- Banroques, J. and Abelson, J.N. (1989) PRP4: a protein of the yeast U4/U6 small nuclear ribonucleoprotein particle. *Mol. Cell. Biol.*, **9**, 3710-3719.
- Bechert, K., Lagos-Quintana, M., Harborth, J., Weber, K. and Osborn, M. (2003) Effects of expressing lamin A mutant protein causing Emery-Dreifuss muscular dystrophy and familial partial lipodystrophy in HeLa cells. *Exp. Cell. Res.*, **286**, 75-86.
- Bell, M., Schreiner, S., Damianov, A., Reddy, R. and Bindereif, A. (2002) p110, a novel human U6 snRNP protein and U4/U6 snRNP recycling factor. *EMBO J.*, **21**, 2724-2735.
- Black, D.L. and Pinto, A.L. (1989) U5 small nuclear ribonucleoprotein: RNA structure analysis and ATP-dependent interaction with U4/U6. *Mol. Cell. Biol.*, **9**, 3350-3359.
- Blatch, G.L. and Lassle, M. (1999) The tetratricopeptide repeat: a structural motif mediating protein-protein interactions. *Bioessays*, **21**, 932-939.
- Bochnig, P., Reuter, R., Bringmann, P. and Lührmann, R. (1987) A monoclonal antibody against 2,2,7-trimethylguanosine that reacts with intact, class U, small nuclear ribonucleoproteins as well as with 7-methylguanosine-capped RNAs. *Eur. J. Biochem.*, **168**, 461-467.
- Bon, E., Casaregola, S., Blandin, G., Llorente, B., Neugeglise, C., Munsterkötter, M., Guldener, U., Mewes, H.W., Van Helden, J., Dujon, B. and Gaillardin, C. (2003) Molecular evolution of eukaryotic genomes: hemiascomycetous yeast spliceosomal introns. *Nucleic Acids Res.*, **31**, 1121-1135.
- Borovjagin, A.V. and Gerbi, S.A. (1999) U3 small nucleolar RNA is essential for cleavage at sites 1, 2 and 3 in pre-rRNA and determines which rRNA processing pathway is taken in *Xenopus* oocytes. *J. Mol. Biol.*, **286**, 1347-1363.
- Bowman, L.H., Rabin, B. and Schlessinger, D. (1981) Multiple ribosomal RNA cleavage pathways in mammalian cells. *Nucleic Acids Res.*, **9**, 4951-4966.

- Branlant, C., Krol, A., Ebel, J.P., Lazar, E., Haendler, B. and Jacob, M. (1982) U2 RNA shares a structural domain with U1, U4, and U5 RNAs. *EMBO J.*, **1**, 1259-1265.
- Bringmann, P., Appel, B., Rinke, J., Reuter, R., Theissen, H. and Lührmann, R. (1984) Evidence for the existence of snRNAs U4 and U6 in a single ribonucleoprotein complex and for their association by intermolecular base pairing. *EMBO J.*, **3**, 1357-1363.
- Brow, D.A. (2002) Allosteric cascade of spliceosome activation. *Annu. Rev. Genet.*, **36**, 333-360.
- Brow, D.A. and Guthrie, C. (1988) Spliceosomal RNA U6 is remarkably conserved from yeast to mammals. *Nature*, **334**, 213-218.
- Brown, D., Lydon, J., McLaughlin, M., Stuart-Tilley, A., Tyszkowski, R. and Alper, S. (1996) Antigen retrieval in cryostat tissue sections and cultured cells by treatment with sodium dodecyl sulfate (SDS). *Histochem. Cell Biol.*, **105**, 261-267.
- Burge, C.B. (1999) *Splicing of precursors to mRNAs by the spliceosome*. Cold Spring Harbor Laboratory Press, Cold Spring Harbor, New York.
- Caffarelli, E., Fatica, A., Prislei, S., De Gregorio, E., Fragapane, P. and Bozzoni, I. (1996) Processing of the intron-encoded U16 and U18 snoRNAs: the conserved C and D boxes control both the processing reaction and the stability of the mature snoRNA. *EMBO J.*, **15**, 1121-1131.
- Cahill, N.M., Friend, K., Speckmann, W., Li, Z.H., Terns, R.M., Terns, M.P. and Steitz, J.A. (2002) Site-specific cross-linking analyses reveal an asymmetric protein distribution for a box C/D snoRNP. *EMBO J.*, **21**, 3816-3828.
- Carmo-Fonseca, M., Pepperkok, R., Carvalho, M.T. and Lamond, A.I. (1992) Transcription-dependent colocalization of the U1, U2, U4/U6, and U5 snRNPs in coiled bodies. *J. Cell Biol.*, **117**, 1-14.
- Cavaille, J. and Bachellerie, J.P. (1996) Processing of fibrillar-associated snoRNAs from pre-mRNA introns: an exonucleolytic process exclusively directed by the common stem-box terminal structure. *Biochimie*, **78**, 443-456.
- Chakarova, C.F., Hims, M.M., Bolz, H., Abu-Safieh, L., Patel, R.J., Papaioannou, M.G., Inglehearn, C.F., Keen, T.J., Willis, C., Moore, A.T., Rosenberg, T., Webster, A.R., Bird, A.C., Gal, A., Hunt, D., Vithana, E.N. and Bhattacharya, S.S. (2002) Mutations in HPRP3, a third member of pre-mRNA splicing factor genes, implicated in autosomal dominant retinitis pigmentosa. *Hum. Mol. Genet.*, **11**, 87-92.
- Cojocar, V., Nottrott, S., Klement, R. and Jovin, T.M. (2005) The snRNP 15.5K protein folds its cognate K-turn RNA: a combined theoretical and biochemical study. *RNA*, **11**, 197-209.
- Cormack, B.P., Valdivia, R.H. and Falkow, S. (1996) FACS-optimized mutants of the green fluorescent protein (GFP). *Gene*, **173**, 33-38.
- Darzacq, X. and Kiss, T. (2000) Processing of intron-encoded box C/D small nucleolar RNAs lacking a 5',3'-terminal stem structure. *Mol. Cell. Biol.*, **20**, 4522-4531.
- Datta, B. and Weiner, A.M. (1991) Genetic evidence for base pairing between U2 and U6 snRNA in mammalian mRNA splicing. *Nature*, **352**, 821-824.
- Deery, E.C., Vithana, E.N., Newbold, R.J., Gallon, V.A., Bhattacharya, S.S., Warren, M.J., Hunt, D.M. and Wilkie, S.E. (2002) Disease mechanism for retinitis pigmentosa

6 References

- (RP11) caused by mutations in the splicing factor gene PRPF31. *Hum. Mol. Genet.*, **11**, 3209-3219.
- Dix, I., Russell, C.S., O'Keefe, R.T., Newman, A.J. and Beggs, J.D. (1998) Protein-RNA interactions in the U5 snRNP of *Saccharomyces cerevisiae*. *RNA*, **4**, 1675-1686.
- Elbashir, S.M., Harborth, J., Lendeckel, W., Yalcin, A., Weber, K. and Tuschl, T. (2001) Duplexes of 21-nucleotide RNAs mediate RNA interference in cultured mammalian cells. *Nature*, **411**, 494-498.
- Elbashir, S.M., Harborth, J., Weber, K. and Tuschl, T. (2002) Analysis of gene function in somatic mammalian cells using small interfering RNAs. *Methods*, **26**, 199-213.
- Fabrizio, P., Laggerbauer, B., Lauber, J., Lane, W.S. and Lührmann, R. (1997) An evolutionarily conserved U5 snRNP-specific protein is a GTP-binding factor closely related to the ribosomal translocase EF-2. *EMBO J.*, **16**, 4092-4106.
- Filipowicz, W. and Pogacic, V. (2002) Biogenesis of small nucleolar ribonucleoproteins. *Curr. Opin. Cell Biol.*, **14**, 319-327.
- Ganot, P., Bortolin, M.L. and Kiss, T. (1997) Site-specific pseudouridine formation in preribosomal RNA is guided by small nucleolar RNAs. *Cell*, **89**, 799-809.
- Ganot, P., Jady, B.E., Bortolin, M.L., Darzacq, X. and Kiss, T. (1999) Nucleolar factors direct the 2'-O-ribose methylation and pseudouridylation of U6 spliceosomal RNA. *Mol. Cell. Biol.*, **19**, 6906-6917.
- Gaspin, C., Cavaille, J., Erauso, G. and Bachellerie, J.P. (2000) Archaeal homologs of eukaryotic methylation guide small nucleolar RNAs: lessons from the *Pyrococcus* genomes. *J. Mol. Biol.*, **297**, 895-906.
- Gautier, T., Berges, T., Tollervy, D. and Hurt, E. (1997) Nucleolar KKE/D repeat proteins Nop56p and Nop58p interact with Nop1p and are required for ribosome biogenesis. *Mol. Cell. Biol.*, **17**, 7088-7098.
- Gonzalez-Santos, J.M., Wang, A., Jones, J., Ushida, C., Liu, J. and Hu, J. (2002) Central region of the human splicing factor Hprp3p interacts with Hprp4p. *J. Biol. Chem.*, **277**, 23764-23772.
- Gottschalk, A., Neubauer, G., Banroques, J., Mann, M., Lührmann, R. and Fabrizio, P. (1999) Identification by mass spectrometry and functional analysis of novel proteins of the yeast [U4/U6.U5] tri-snRNP. *EMBO J.*, **18**, 4535-4548.
- Granneman, S. and Baserga, S.J. (2004) Ribosome biogenesis: of knobs and RNA processing. *Exp. Cell Res.*, **296**, 43-50.
- Granneman, S., Pruijn, G.J., Horstman, W., van Venrooij, W.J., Lührmann, R. and Watkins, N.J. (2002) The hU3-55K protein requires 15.5K binding to the box B/C motif as well as flanking RNA elements for its association with the U3 small nucleolar RNA *in vitro*. *J. Biol. Chem.*, **277**, 48490-48500.
- Granneman, S., Vogelzangs, J., Lührmann, R., van Venrooij, W.J., Pruijn, G.J. and Watkins, N.J. (2004) Role of pre-rRNA base pairing and 80S complex formation in subnucleolar localization of the U3 snoRNP. *Mol. Cell. Biol.*, **24**, 8600-8610.
- Guthrie, C. and Patterson, B. (1988) Spliceosomal snRNAs. *Annu. Rev. Genet.*, **22**, 387-419.
- Hadjiolova, K.V., Nicoloso, M., Mazan, S., Hadjiolov, A.A. and Bachellerie, J.P. (1993) Alternative pre-rRNA processing pathways in human cells and their alteration by cycloheximide inhibition of protein synthesis. *Eur. J. Biochem.*, **212**, 211-215.

- Hall, S.L. and Padgett, R.A. (1996) Requirement of U12 snRNA for *in vivo* splicing of a minor class of eukaryotic nuclear pre-mRNA introns. *Science*, **271**, 1716-1718.
- Hashimoto, C. and Steitz, J.A. (1984) U4 and U6 RNAs coexist in a single small nuclear ribonucleoprotein particle. *Nucleic Acids Res.*, **12**, 3283-3293.
- Hausner, D.S. (1992) Health and ecological dilemmas. Sleeping sickness. *Links*, **9**, 22-23.
- Henderson, A.S., Warburton, D. and Atwood, K.C. (1972) Location of ribosomal DNA in the human chromosome complement. *Proc. Natl. Acad. Sci. U S A*, **69**, 3394-3398.
- Henras, A.K., Dez, C. and Henry, Y. (2004) RNA structure and function in C/D and H/ACA s(no)RNPs. *Curr. Opin. Struct. Biol.*, **14**, 335-343.
- Horowitz, D.S., Kobayashi, R. and Krainer, A.R. (1997) A new cyclophilin and the human homologues of yeast Prp3 and Prp4 form a complex associated with U4/U6 snRNPs. *RNA*, **3**, 1374-1387.
- Incorvaia, R. and Padgett, R.A. (1998) Base pairing with U6atac snRNA is required for 5' splice site activation of U12-dependent introns *in vivo*. *RNA*, **4**, 709-718.
- Jarmolowski, A. and Mattaj, I.W. (1993) The determinants for Sm protein binding to Xenopus U1 and U5 snRNAs are complex and non-identical. *EMBO J.*, **12**, 223-232.
- Jeppesen, C., Stebbins-Boaz, B. and Gerbi, S.A. (1988) Nucleotide sequence determination and secondary structure of Xenopus U3 snRNA. *Nucleic Acids Res.*, **16**, 2127-2148.
- Jones, M.H. and Guthrie, C. (1990) Unexpected flexibility in an evolutionarily conserved protein-RNA interaction: genetic analysis of the Sm binding site. *EMBO J.*, **9**, 2555-2561.
- Jurica, M.S. and Moore, M.J. (2003) Pre-mRNA splicing: awash in a sea of proteins. *Mol. Cell*, **12**, 5-14.
- Kastner, B. (1998) Purification and Electron Microscopy of spliceosomal snRNPs. In Schenkel, J. (ed.), *RNP particles, Splicing and Autoimmune Diseases*. Springer Lab manual. Springer Verlag, Berlin Heidelberg.
- Kiss, T. (2001) Small nucleolar RNA-guided post-transcriptional modification of cellular RNAs. *EMBO J.*, **20**, 3617-3622.
- Kiss-Laszlo, Z., Henry, Y., Bachellerie, J.P., Caizergues-Ferrer, M. and Kiss, T. (1996) Site-specific ribose methylation of preribosomal RNA: a novel function for small nucleolar RNAs. *Cell*, **85**, 1077-1088.
- Kiss-Laszlo, Z., Henry, Y. and Kiss, T. (1998) Sequence and structural elements of methylation guide snoRNAs essential for site-specific ribose methylation of pre-rRNA. *EMBO J.*, **17**, 797-807.
- Klein, D.J., Schmeing, T.M., Moore, P.B. and Steitz, T.A. (2001) The kink-turn: a new RNA secondary structure motif. *EMBO J.*, **20**, 4214-4221.
- Kolosova, I. and Padgett, R.A. (1997) U11 snRNA interacts *in vivo* with the 5' splice site of U12-dependent (AU-AC) pre-mRNA introns. *RNA*, **3**, 227-233.
- Koonin, E.V., Bork, P. and Sander, C. (1994) A novel RNA-binding motif in omnipotent suppressors of translation termination, ribosomal proteins and a ribosome modification enzyme? *Nucleic Acids Res.*, **22**, 2166-2167.

6 References

- Kuhn, J.F., Tran, E.J. and Maxwell, E.S. (2002) Archaeal ribosomal protein L7 is a functional homolog of the eukaryotic 15.5kD/Snu13p snoRNP core protein. *Nucleic Acids Res.*, **30**, 931-941.
- Kühn-Hölsken, E., Lenz, C., Sander, B., Lührmann, R. and Urlaub, H. (2005) Complete MALDI-ToF MS analysis of cross-linked peptide-RNA oligonucleotides derived from nonlabeled UV-irradiated ribonucleoprotein particles. *RNA*, **11**, 1915-1930.
- Kunkel, G.R., Maser, R.L., Calvet, J.P. and Pederson, T. (1986) U6 small nuclear RNA is transcribed by RNA polymerase III. *Proc. Natl. Acad. Sci. U S A*, **83**, 8575-8579.
- Laemmli, U.K. (1970) Cleavage of structural proteins during the assembly of the head of bacteriophage T4. *Nature*, **227**, 680-685.
- Lafontaine, D.L. and Tollervey, D. (1998) Birth of the snoRNPs: the evolution of the modification-guide snoRNAs. *Trends Biochem. Sci.*, **23**, 383-388.
- Lafontaine, D.L. and Tollervey, D. (1999) Nop58p is a common component of the box C+D snoRNPs that is required for snoRNA stability. *RNA*, **5**, 455-467.
- Lafontaine, D.L. and Tollervey, D. (2000) Synthesis and assembly of the box C+D small nucleolar RNPs. *Mol. Cell. Biol.*, **20**, 2650-2659.
- Lamond, A.I. and Spector, D.L. (2003) Nuclear speckles: a model for nuclear organelles. *Nat Rev. Mol. Cell. Biol.*, **4**, 605-612.
- Lange, T.S., Borovjagin, A., Maxwell, E.S. and Gerbi, S.A. (1998) Conserved boxes C and D are essential nucleolar localization elements of U14 and U8 snoRNAs. *EMBO J.*, **17**, 3176-3187.
- Lange, T.S. and Gerbi, S.A. (2000) Transient nucleolar localization Of U6 small nuclear RNA in *Xenopus laevis* oocytes. *Mol. Biol. Cell*, **11**, 2419-2428.
- Lauber, J., Fabrizio, P., Teigelkamp, S., Lane, W.S., Hartmann, E. and Lührmann, R. (1996) The HeLa 200 kDa U5 snRNP-specific protein and its homologue in *Saccharomyces cerevisiae* are members of the DEXH-box protein family of putative RNA helicases. *EMBO J.*, **15**, 4001-4015.
- Lauber, J., Plessel, G., Prehn, S., Will, C.L., Fabrizio, P., Groning, K., Lane, W.S. and Lührmann, R. (1997) The human U4/U6 snRNP contains 60 and 90kD proteins that are structurally homologous to the yeast splicing factors Prp4p and Prp3p. *RNA*, **3**, 926-941.
- Lee, K.A. and Green, M.R. (1990) Small-scale preparation of extracts from radiolabeled cells efficient in pre-mRNA splicing. *Methods Enzymol.*, **181**, 20-30.
- Lescoute, A. and Westhof, E. (2006) Topology of three-way junctions in folded RNAs. *RNA*, **12**, 83-93.
- Leung, A.K. and Lamond, A.I. (2002) *In vivo* analysis of NHPX reveals a novel nucleolar localization pathway involving a transient accumulation in splicing speckles. *J. Cell Biol.*, **157**, 615-629.
- Liang, W.Q. and Fournier, M.J. (1995) U14 base-pairs with 18S rRNA: a novel snoRNA interaction required for rRNA processing. *Genes Dev.* **9**, 2433-2443.
- Liu, S. (2005) Investigation of Protein-protein Interactions within the Human Spliceosomal U4/U6.U5 tri-snRNP Particle. *570 Biowissenschaften, Biologie*. Georg-August-Universität Göttingen, Göttingen, p. 165.

- Maden, B.E. (1998) Eukaryotic rRNA methylation: the calm before the Sno storm. *Trends Biochem. Sci.*, **23**, 447-450.
- Madhani, H.D. and Guthrie, C. (1992) A novel base-pairing interaction between U2 and U6 snRNAs suggests a mechanism for the catalytic activation of the spliceosome. *Cell*, **71**, 803-817.
- Makarov, E.M., Makarova, O.V., Achsel, T. and Lührmann, R. (2000) The human homologue of the yeast splicing factor prp6p contains multiple TPR elements and is stably associated with the U5 snRNP via protein-protein interactions. *J. Mol. Biol.*, **298**, 567-575.
- Makarov, E.M., Makarova, O.V., Urlaub, H., Gentzel, M., Will, C.L., Wilm, M. and Lührmann, R. (2002) Small nuclear ribonucleoprotein remodeling during catalytic activation of the spliceosome. *Science*, **298**, 2205-2208.
- Makarova, O.V., Makarov, E.M., Liu, S., Vornlocher, H.P. and Lührmann, R. (2002) Protein 61K, encoded by a gene (PRPF31) linked to autosomal dominant retinitis pigmentosa, is required for U4/U6.U5 tri-snRNP formation and pre-mRNA splicing. *EMBO J*, **21**, 1148-1157.
- Manoni, M., Pergolizzi, R., Luzzana, M. and De Bellis, G. (1992) Dideoxy linear PCR on a commercial fluorescent automated DNA sequencer. *Biotechniques*, **12**, 48-50, 52-43.
- Massenet, S. (1998) Posttranscriptional modifications in the U small nuclear RNAs. *ASM Press*, 201-227.
- Maxam, A.M. and Gilbert, W. (1986) [A method for determining DNA sequence by labeling the end of the molecule and cleaving at the base. Isolation of DNA fragments, end-labeling, cleavage, electrophoresis in polyacrylamide gel and analysis of results]. *Mol. Biol. (Mosk)*, **20**, 581-638.
- McCloskey, J.A. and Crain, P.F. (1998) The RNA modification database--1998. *Nucleic Acids Res.*, **26**, 196-197.
- McKie, A.B., McHale, J.C., Keen, T.J., Tartelin, E.E., Goliath, R., van Lith-Verhoeven, J.J., Greenberg, J., Ramesar, R.S., Hoyng, C.B., Cremers, F.P., Mackey, D.A., Bhattacharya, S.S., Bird, A.C., Markham, A.F. and Inglehearn, C.F. (2001) Mutations in the pre-mRNA splicing factor gene PRPC8 in autosomal dominant retinitis pigmentosa (RP13). *Hum. Mol. Genet.*, **10**, 1555-1562.
- Melton, D.A., Krieg, P.A., Rebagliati, M.R., Maniatis, T., Zinn, K. and Green, M.R. (1984) Efficient *in vitro* synthesis of biologically active RNA and RNA hybridization probes from plasmids containing a bacteriophage SP6 promoter. *Nucleic Acids Res.*, **12**, 7035-7056.
- Mereau, A., Fournier, R., Gregoire, A., Mouglin, A., Fabrizio, P., Lührmann, R. and Branlant, C. (1997) An *in vivo* and *in vitro* structure-function analysis of the *Saccharomyces cerevisiae* U3A snoRNP: protein-RNA contacts and base-pair interaction with the pre-ribosomal RNA. *J. Mol. Biol.*, **273**, 552-571.
- Misteli, T. (2000) Cell biology of transcription and pre-mRNA splicing: nuclear architecture meets nuclear function. *J. Cell Sci.*, **113 (Pt 11)**, 1841-1849.
- Mouglin, A., Gottschalk, A., Fabrizio, P., Lührmann, R. and Branlant, C. (2002) Direct probing of RNA structure and RNA-protein interactions in purified HeLa cells and yeast spliceosomal U4/U6.U5 tri-snRNP particles. *J. Mol. Biol.*, **317**, 631-649.

6 References

- Myslinski, E. and Branlant, C. (1991) A phylogenetic study of U4 snRNA reveals the existence of an evolutionarily conserved secondary structure corresponding to 'free' U4 snRNA. *Biochimie*, **73**, 17-28.
- Narayanan, A., Speckmann, W., Terns, R. and Terns, M.P. (1999) Role of the box C/D motif in localization of small nucleolar RNAs to coiled bodies and nucleoli. *Mol. Biol. Cell*, **10**, 2131-2147.
- Newman, D.R., Kuhn, J.F., Shanab, G.M. and Maxwell, E.S. (2000) Box C/D snoRNA-associated proteins: two pairs of evolutionarily ancient proteins and possible links to replication and transcription. *RNA*, **6**, 861-879.
- Ni, J., Samarsky, D.A., Liu, B., Ferbeyre, G., Cedergren, R. and Fournier, M.J. (1997) SnoRNAs as tools for RNA cleavage and modification. *Nucleic Acids Symp. Ser.*, 61-63.
- Niewmierzycka, A. and Clarke, S. (1999) S-Adenosylmethionine-dependent methylation in *Saccharomyces cerevisiae*. Identification of a novel protein arginine methyltransferase. *J. Biol. Chem.*, **274**, 814-824.
- Nilsen, T.W. (1998) *RNA-RNA interactions in nuclear pre-mRNA splicing*. Cold Spring Harbor Laboratory Press, Cold Spring Harbor, New York.
- Nilsen, T.W. (2003) The spliceosome: the most complex macromolecular machine in the cell? *Bioessays*, **25**, 1147-1149.
- Nottrott, S. (2002) Strukturelle und funktionelle Charakterisierung der spleißosomalen U4/U6 snRNP-spezifischen Protein-RNA Wechselwirkungen. *Humanmedizin*. Philipps-Universität, Marburg, p. 188.
- Nottrott, S., Hartmuth, K., Fabrizio, P., Urlaub, H., Vidovic, I., Ficner, R. and Lührmann, R. (1999) Functional interaction of a novel 15.5kD [U4/U6.U5] tri-snRNP protein with the 5' stem-loop of U4 snRNA. *EMBO J.*, **18**, 6119-6133.
- Nottrott, S., Urlaub, H. and Lührmann, R. (2002) Hierarchical, clustered protein interactions with U4/U6 snRNA: a biochemical role for U4/U6 proteins. *EMBO J.*, **21**, 5527-5538.
- Omer, A.D., Lowe, T.M., Russell, A.G., Ebhardt, H., Eddy, S.R. and Dennis, P.P. (2000) Homologs of small nucleolar RNAs in Archaea. *Science*, **288**, 517-522.
- Omer, A.D., Ziesche, S., Ebhardt, H. and Dennis, P.P. (2002) *In vitro* reconstitution and activity of a C/D box methylation guide ribonucleoprotein complex. *Proc. Natl. Acad. Sci. U S A*, **99**, 5289-5294.
- Padgett, R.A. and Shukla, G.C. (2002) A revised model for U4atac/U6atac snRNA base pairing. *RNA*, **8**, 125-128.
- Parker, K.A. and Steitz, J.A. (1987) Structural analysis of the human U3 ribonucleoprotein particle reveal a conserved sequence available for base pairing with pre-rRNA. *Mol. Cell. Biol.*, **7**, 2899-2913.
- Peculis, B.A. (1997) The sequence of the 5' end of the U8 small nucleolar RNA is critical for 5.8S and 28S rRNA maturation. *Mol. Cell. Biol.*, **17**, 3702-3713.
- Petersen-Bjorn, S.P., Soltyk, A., Beggs, J.D. and Friesen, J.D. (1989) PRP4 (RNA4) from *Saccharomyces cerevisiae*: its gene product is associated with the U4/U6 small nuclear ribonucleoprotein particle. *Mol. Cell. Biol.*, **9**, 3698-3709.

- Pluk, H., Soffner, J., Lührmann, R. and van Venrooij, W.J. (1998) cDNA cloning and characterization of the human U3 small nucleolar ribonucleoprotein complex-associated 55-kilodalton protein. *Mol. Cell. Biol.*, **18**, 488-498.
- Raghunathan, P.L. and Guthrie, C. (1998) A spliceosomal recycling factor that reanneals U4 and U6 small nuclear ribonucleoprotein particles. *Science*, **279**, 857-860.
- Raker, V.A., Hartmuth, K., Kastner, B. and Lührmann, R. (1999) Spliceosomal U snRNP core assembly: Sm proteins assemble onto an Sm site RNA nonanucleotide in a specific and thermodynamically stable manner. *Mol. Cell. Biol.*, **19**, 6554-6565.
- Raker, V.A., Plessel, G. and Lührmann, R. (1996) The snRNP core assembly pathway: identification of stable core protein heteromeric complexes and an snRNP subcore particle *in vitro*. *EMBO J.*, **15**, 2256-2269.
- Reddy, R. and Busch, H. (1988) Small nuclear RNAs: RNA sequences, structure, and modifications. *Structure and Function of Major and Minor Small Nuclear Ribonucleoprotein Particles.*, **Springer Verlag**.
- Reddy, R., Henning, D., Das, G., Harless, M. and Wright, D. (1987) The capped U6 small nuclear RNA is transcribed by RNA polymerase III. *J. Biol. Chem.*, **262**, 75-81.
- Reed, R. (1989) The organization of 3' splice-site sequences in mammalian introns. *Genes Dev.*, **3**, 2113-2123.
- Reidt, U., Reuter, K., Achsel, T., Ingelfinger, D., Lührmann, R. and Ficner, R. (2000) Crystal structure of the human U4/U6 small nuclear ribonucleoprotein particle-specific SnuCyp-20, a nuclear cyclophilin. *J. Biol. Chem.*, **275**, 7439-7442.
- Reuter, K., Nottrott, S., Fabrizio, P., Lührmann, R. and Ficner, R. (1999) Identification, characterization and crystal structure analysis of the human spliceosomal U5 snRNP-specific 15 kD protein. *J. Mol. Biol.*, **294**, 515-525.
- Rinke, J., Appel, B., Digweed, M. and Lührmann, R. (1985) Localization of a base-paired interaction between small nuclear RNAs U4 and U6 in intact U4/U6 ribonucleoprotein particles by psoralen cross-linking. *J. Mol. Biol.*, **185**, 721-731.
- Rozhdestvensky, T.S., Tang, T.H., Tchirkova, I.V., Brosius, J., Bachellerie, J.P. and Huttenhofer, A. (2003) Binding of L7Ae protein to the K-turn of archaeal snoRNAs: a shared RNA binding motif for C/D and H/ACA box snoRNAs in Archaea. *Nucleic Acids Res.*, **31**, 869-877.
- Samarsky, D.A., Fournier, M.J., Singer, R.H. and Bertrand, E. (1998) The snoRNA box C/D motif directs nucleolar targeting and also couples snoRNA synthesis and localization. *EMBO J.*, **17**, 3747-3757.
- Sambrook, J., Fritsch, E.F. and Maniatis, T. (1989) *Molecular cloning - A Laboratory Manual*, Cold Spring Harbour, New York.
- Sanger, F., Nicklen, S. and Coulson, A.R. (1977) DNA sequencing with chain-terminating inhibitors. *Proc. Natl. Acad. Sci. U S A*, **74**, 5463-5467.
- Schaffert, N., Hossbach, M., Heintzmann, R., Achsel, T. and Lührmann, R. (2004) RNAi knockdown of hPrp31 leads to an accumulation of U4/U6 di-snRNPs in Cajal bodies. *EMBO J.*, **23**, 3000-3009.
- Schimmang, T., Tollervey, D., Kern, H., Frank, R. and Hurt, E.C. (1989) A yeast nucleolar protein related to mammalian fibrillarin is associated with small nucleolar RNA and is essential for viability. *EMBO J.*, **8**, 4015-4024.

6 References

- Schneider, C., Will, C.L., Makarova, O.V., Makarov, E.M. and Lührmann, R. (2002) Human U4/U6.U5 and U4atac/U6atac.U5 tri-snRNPs exhibit similar protein compositions. *Mol. Cell. Biol.*, **22**, 3219-3229.
- Schultz, A., Nottrott, S., Hartmuth, K. and Lührmann, R. (2006) RNA structural requirements for the association of the spliceosomal hPrp31 protein with the U4 and U4atac small nuclear ribonucleoproteins. *J. Biol. Chem.*, **281**, 28278-28286.
- Schultz, A., Nottrott, S., Watkins, N.J. and Lührmann, R. (2006) Protein-protein and protein-RNA contacts both contribute to the 15.5K-mediated assembly of the U4/U6 snRNP and the box C/D snoRNPs. *Mol. Cell. Biol.*, **26**, 5146-5154.
- Schulz, G.E. and Schirmer, R.H. (1979) Amino acids. In Cantor, C.R. (ed.), *Principles of protein structure*. Springer-Verlag, New York, pp. 1-16.
- Singh, R. and Reddy, R. (1989) Gamma-monomethyl phosphate: a cap structure in spliceosomal U6 small nuclear RNA. *Proc. Natl. Acad. Sci. U S A*, **86**, 8280-8283.
- Sleeman, J.E. and Lamond, A.I. (1999) Newly assembled snRNPs associate with coiled bodies before speckles, suggesting a nuclear snRNP maturation pathway. *Curr. Biol.*, **9**, 1065-1074.
- Sleeman, J.E. and Lamond, A.I. (1999) Nuclear organization of pre-mRNA splicing factors. *Curr. Opin. Cell Biol.*, **11**, 372-377.
- Staley, J.P. and Guthrie, C. (1998) Mechanical devices of the spliceosome: motors, clocks, springs, and things. *Cell*, **92**, 315-326.
- Stevens, S.W. and Abelson, J. (1999) Purification of the yeast U4/U6.U5 small nuclear ribonucleoprotein particle and identification of its proteins. *Proc. Natl. Acad. Sci. U S A*, **96**, 7226-7231.
- Stevens, S.W., Barta, I., Ge, H.Y., Moore, R.E., Young, M.K., Lee, T.D. and Abelson, J. (2001) Biochemical and genetic analyses of the U5, U6, and U4/U6 x U5 small nuclear ribonucleoproteins from *Saccharomyces cerevisiae*. *RNA*, **7**, 1543-1553.
- Sun, J.S. and Manley, J.L. (1995) A novel U2-U6 snRNA structure is necessary for mammalian mRNA splicing. *Genes Dev*, **9**, 843-854.
- Szewczak, L.B., DeGregorio, S.J., Strobel, S.A. and Steitz, J.A. (2002) Exclusive interaction of the 15.5 kD protein with the terminal box C/D motif of a methylation guide snoRNP. *Chem. Biol.*, **9**, 1095-1107.
- Tarn, W.Y. and Steitz, J.A. (1996) Highly diverged U4 and U6 small nuclear RNAs required for splicing rare AT-AC introns. *Science*, **273**, 1824-1832.
- Tarn, W.Y. and Steitz, J.A. (1996) A novel spliceosome containing U11, U12, and U5 snRNPs excises a minor class (AT-AC) intron *in vitro*. *Cell*, **84**, 801-811.
- Teigelkamp, S., Achsel, T., Mundt, C., Gotherl, S.F., Cronshagen, U., Lane, W.S., Marahiel, M. and Lührmann, R. (1998) The 20kD protein of human [U4/U6.U5] tri-snRNPs is a novel cyclophilin that forms a complex with the U4/U6-specific 60kD and 90kD proteins. *RNA*, **4**, 127-141.
- Teigelkamp, S., Mundt, C., Achsel, T., Will, C.L. and Lührmann, R. (1997) The human U5 snRNP-specific 100-kD protein is an RS domain-containing, putative RNA helicase with significant homology to the yeast splicing factor Prp28p. *RNA*, **3**, 1313-1326.
- Terns, M.P. and Terns, R.M. (2002) Small nucleolar RNAs: versatile trans-acting molecules of ancient evolutionary origin. *Gene Expr.*, **10**, 17-39.

- Tollervey, D., Lehtonen, H., Jansen, R., Kern, H. and Hurt, E.C. (1993) Temperature-sensitive mutations demonstrate roles for yeast fibrillarin in pre-rRNA processing, pre-rRNA methylation, and ribosome assembly. *Cell*, **72**, 443-457.
- Turner, B., Melcher, S.E., Wilson, T.J., Norman, D.G. and Lilley, D.M. (2005) Induced fit of RNA on binding the L7Ae protein to the kink-turn motif. *RNA*, **11**, 1192-1200.
- Tycowski, K.T., Shu, M.D. and Steitz, J.A. (1994) Requirement for intron-encoded U22 small nucleolar RNA in 18S ribosomal RNA maturation. *Science*, **266**, 1558-1561.
- Tycowski, K.T., You, Z.H., Graham, P.J. and Steitz, J.A. (1998) Modification of U6 spliceosomal RNA is guided by other small RNAs. *Mol. Cell*, **2**, 629-638.
- Vankan, P., McGuigan, C. and Mattaj, I.W. (1992) Roles of U4 and U6 snRNAs in the assembly of splicing complexes. *EMBO J.*, **11**, 335-343.
- Vidovic, I., Nottrott, S., Hartmuth, K., Lührmann, R. and Ficner, R. (2000) Crystal structure of the spliceosomal 15.5kD protein bound to a U4 snRNA fragment. *Mol. Cell*, **6**, 1331-1342.
- Villa, T., Ceradini, F. and Bozzoni, I. (2000) Identification of a novel element required for processing of intron-encoded box C/D small nucleolar RNAs in *Saccharomyces cerevisiae*. *Mol. Cell. Biol.*, **20**, 1311-1320.
- Vithana, E.N., Abu-Safieh, L., Allen, M.J., Carey, A., Papaioannou, M., Chakarova, C., Al-Magthteh, M., Ebenezer, N.D., Willis, C., Moore, A.T., Bird, A.C., Hunt, D.M. and Bhattacharya, S.S. (2001) A human homolog of yeast pre-mRNA splicing gene, PRP31, underlies autosomal dominant retinitis pigmentosa on chromosome 19q13.4 (RP11). *Mol. Cell*, **8**, 375-381.
- Wang, A., Forman-Kay, J., Luo, Y., Luo, M., Chow, Y.H., Plumb, J., Friesen, J.D., Tsui, L.C., Heng, H.H., Woolford, J.L., Jr. and Hu, J. (1997) Identification and characterization of human genes encoding Hprp3p and Hprp4p, interacting components of the spliceosome. *Hum. Mol. Genet.*, **6**, 2117-2126.
- Wang, B.B. and Brendel, V. (2004) The ASRG database: identification and survey of *Arabidopsis thaliana* genes involved in pre-mRNA splicing. *Genome Biol.*, **5**, R102.
- Watkins, N.J., Dickmanns, A. and Lührmann, R. (2002) Conserved stem II of the box C/D motif is essential for nucleolar localization and is required, along with the 15.5K protein, for the hierarchical assembly of the box C/D snoRNP. *Mol. Cell. Biol.*, **22**, 8342-8352.
- Watkins, N.J., Leverette, R.D., Xia, L., Andrews, M.T. and Maxwell, E.S. (1996) Elements essential for processing intronic U14 snoRNA are located at the termini of the mature snoRNA sequence and include conserved nucleotide boxes C and D. *RNA*, **2**, 118-133.
- Watkins, N.J., Segault, V., Charpentier, B., Nottrott, S., Fabrizio, P., Bachi, A., Wilm, M., Rosbash, M., Branlant, C. and Lührmann, R. (2000) A common core RNP structure shared between the small nucleolar box C/D RNPs and the spliceosomal U4 snRNP. *Cell*, **103**, 457-466.
- Weidenhammer, E.M., Ruiz-Noriega, M. and Woolford, J.L., Jr. (1997) Prp31p promotes the association of the U4/U6 x U5 tri-snRNP with prespliceosomes to form spliceosomes in *Saccharomyces cerevisiae*. *Mol. Cell. Biol.*, **17**, 3580-3588.
- Wersig, C. and Bindereif, A. (1992) Reconstitution of functional mammalian U4 small nuclear ribonucleoprotein: Sm protein binding is not essential for splicing *in vitro*. *Mol. Cell. Biol.*, **12**, 1460-1468.

6 References

- Wersig, C., Guddat, U., Pieler, T. and Bindereif, A. (1992) Assembly and nuclear transport of the U4 and U4/U6 snRNPs. *Exp. Cell Res.*, **199**, 373-377.
- Wilkie, S.E., Morris, K.J., Bhattacharya, S.S., Warren, M.J. and Hunt, D.M. (2006) A study of the nuclear trafficking of the splicing factor protein PRPF31 linked to autosomal dominant retinitis pigmentosa (ADRP). *Biochim. Biophys. Acta*, **1762**, 304-311.
- Will, C.L., Behrens, S.E. and Lührmann, R. (1993) Protein composition of mammalian spliceosomal snRNPs. *Mol. Biol. Rep.*, **18**, 121-126.
- Will, C.L. and Lührmann, R. (1997) Protein functions in pre-mRNA splicing. *Curr. Opin. Cell Biol.*, **9**, 320-328.
- Will, C.L. and Lührmann, R. (2001) Spliceosomal UsnRNP biogenesis, structure and function. *Curr. Opin. Cell Biol.*, **13**, 290-301.
- Will, C.L. and Lührmann, R. (2005) Splicing of a rare class of introns by the U12-dependent spliceosome. *Biol. Chem.*, **386**, 713-724.
- Williamson, J.R. (2000) Induced fit in RNA-protein recognition. *Nat. Struct. Biol.*, **7**, 834-837.
- Worton, R.G., Sutherland, J., Sylvester, J.E., Willard, H.F., Bodrug, S., Dube, I., Duff, C., Kean, V., Ray, P.N. and Schmickel, R.D. (1988) Human ribosomal RNA genes: orientation of the tandem array and conservation of the 5' end. *Science*, **239**, 64-68.
- Wozniak, A.K., Nottrott, S., Kühn-Hölsken, E., Schroder, G.F., Grubmuller, H., Lührmann, R., Seidel, C.A. and Oesterhelt, F. (2005) Detecting protein-induced folding of the U4 snRNA kink-turn by single-molecule multiparameter FRET measurements. *RNA*, **11**, 1545-1554.
- Wu, P., Brockenbrough, J.S., Metcalfe, A.C., Chen, S. and Aris, J.P. (1998) Nop5p is a small nucleolar ribonucleoprotein component required for pre-18 S rRNA processing in yeast. *J. Biol. Chem.*, **273**, 16453-16463.
- Xia, L., Watkins, N.J. and Maxwell, E.S. (1997) Identification of specific nucleotide sequences and structural elements required for intronic U14 snoRNA processing. *RNA*, **3**, 17-26.
- Yu, Y.T. and Steitz, J.A. (1997) Site-specific crosslinking of mammalian U11 and u6atac to the 5' splice site of an AT-AC intron. *Proc. Natl. Acad. Sci. U S A*, **94**, 6030-6035.

7. Appendix

7.1. Abbreviations

This section lists the abbreviations used in the present dissertation. Standard, internationally used abbreviations and physical units are not included.

3'-SS	3'-terminal splice site
5'-SS	5'- terminal splice site
α	anti or alpha
aa	amino acid
A	Ampere
Ac	Acetate
APS	Ammonium persulfate
ATP	Adenosinetriphosphate
BSA	Bovine serum albumin
bp	base pair
C	Cytidine
cpm	counts per minute
d	Deoxy
D	Dalton
DMEM	Dulbecco's Minimal Essential Medium
DMSO	Dimethyl sulfoxide
dNTPs	2-deoxynucleoside-5-triphosphates
DTE	Dithioerythrol
DTT	Dithiothreitol
EDTA	ethylene-diamine-tetraacidic acid
EtBr	ethidium bromide
EtOH	Ethanol
FBS	Fetal bovine serum
GTP	Guanosine-5'-triphosphate
h	Hour
HEPES	N-2-hydroxyethylpiperazine-N'-2-ethanesulfonic acid
hn	heterogeneous nuclear
kDa	Kilo

LB	Luria Bertani medium
M	molar
MW	molecular weight
m ₃ G	N2,N2,N7-Trimethylguanosine
m ⁷ G	N7-Monomethylguanosine
min	minutes
nt	nucleotide
OD	optical density
Oligo	oligonucleotide
P	phosphate
PAA	polyacrylamide
PAGE	polyacrylamide gel electrophoresis
PBS	phosphate-buffered saline
PCA	mixture of phenol, chloroform and isoamyl alcohol
PCR	polymerase Chain Reaction
PK	Proteinase K
PMSF	phenyl methane sulfonyl fluoride
pre-mRNA	precursor-mRNA
Pu	Purine
Py	Pyrimidine
R	Purine
RIPA	Radio Immuno Precipitation Assay
RNasin	RNase inhibitor
RNP	Ribonucleoprotein
RRM	RNA recognition motif
RT	room temperature
RT-PCR	Reverse transcription PCR
S	Svedberg-Unit (1 x 10 ⁻¹³ seconds)
sec	seconds
SDS	sodium dodecyl sulfate
SF	Splicing factor
sn	small nuclear
sno	small nucleolar

7 Appendix

snRNP	small nuclear ribonucleoprotein particle
SR	serin-(arginine)-rich
SSC	Standard sodium citrate buffer
TBE	Tris-Borate-EDTA
TEMED	N,N,N',N'Tetramethylethylendia mine
Tris/HCl	Tris-(hydroxymethyle)-aminomethane-Hydrochloride
U	Unit (Unit of enzyme activity)
U snRNP	uridine-rich small nuclear ribonucleoproteine particle
v/v	volume per volume
w/v	weight per volume
WT	wild-type
Y	Pyrimidine

7.2. Verzeichnis der akademischen Lehrer

Meine akademischen Lehrer waren Damen/Herren in Marburg

Aumüller

Beato

Besedovsky

Daut

Elsässer

Frenking

Habermehl

Junclas

Kaiser

Kirchner

Krieg

Lammel

Lill

Löffler

Lührmann

Müller

Schäfer

Schuchart

Seitz

Seitz

Voigt

7.3. Danksagung

An dieser Stelle möchte ich mich bei allen Personen bedanken, die mich in den letzten Jahren auf unterschiedlichste Weise unterstützt haben.

Mein besonderer Dank gilt hierbei Herrn Prof. Dr. Reinhard Lührmann dafür, dass er mir die Bearbeitung eines sehr interessanten Projektes ermöglicht und mich stets durch seine rege Diskussionsbereitschaft und zahlreiche Ratschläge unterstützt hat.

Klaus Hartmuth gilt mein besonderer Dank für das Korrekturlesen meiner Doktorarbeit, jedoch vor Allem für die gute und anregende Zusammenarbeit beim Paperschreiben und die Beantwortung vieler Fragen.

Nick Watkins möchte ich für seine Unterstützung zu Beginn meiner Doktorandenzeit danken.

Ping Li und Sunbin Liu möchte ich für den regen Austausch und die Diskussionen rund um das 15.5K Protein danken.

Nastaran Behzadnia und Regina Hecker möchte ich sehr für die schöne Atmosphäre in unserem kleinen Labor und ihre Freundschaft danken. Ich werde die Zusammenarbeit mit Euch sehr vermissen.

Den Mitgliedern des „Zellbiologischen Seminars“ Ira Lemm, Dierk Ingelfinger, Nick Watkins, Markus Hoßbach, Regina Hecker, Nina Schaffert und Patrizia Fabrizio möchte ich für rege Diskussionen und Anregungen danken.

Heike Behnecke, Claudia Schneider, Dierk Ingelfinger, Nick Watkins und Thomas Conrad möchte ich für die vielen schönen Abende mit und ohne Forschung danken.

Bei Cindy Will möchte ich mich für die kritische Durchsicht verschiedener Abstracts und für die Hilfe bei meinen Vortragsvorbereitungen bedanken.

Juliane Moses möchte ich ganz herzlich für die hervorragende Hilfe bei allen organisatorischen Fragen und so manches nette Plauderstündchen danken

Irene Öchsner, Gaby Heyne, Hossein Kohansal und Peter Kempkes möchte ich für ihre exzellente praktische Unterstützung danken.

Den übrigen ehemaligen und derzeitigen Mitgliedern der AG Lührmann danke ich für zahlreiche Tipps und Hilfestellungen sowie das nette Arbeitsklima.

Meinen Freundinnen Paula Vazquez, Birgit Mathes und Ute Schmidt möchte ich für die interessanten, horizonterweiternden Gespräche über das „Spleißen“ hinaus danken.

Meiner Familie möchte ich sowohl für ihre liebevolle Unterstützung während der letzten Jahre danken.

Zuletzt möchte ich meinem Mann Christopher und meiner Tochter Helena für ihre unglaublich große Geduld und ihre Unterstützung danken.